# A METALLOGENIC STUDY OF POLYMETALLIC, GRANOPHILE MINERALIZATION WITHIN THE EARLY PROTEROZOIC UPPER AILLIK GROUP, ROUND POND AREA, CENTRAL MINERAL BELT, LABRADOR

CRAIG S. MacDOUGALL

## NOTICE

The quality of this microform is heavily dependent upon the quality of the original thesis submitted for microfilming. Every effort has been made to ensure the highest quality of reproduction possible.

If pages are missing, contact the university which granted the degree.

Some pages may have indistinct print especially if the original pages were typed with a poor typewriter ribbon or if the university sent us an inferior photocopy.

Previously copyrighted materials (journal articles, published tests, etc.) are not filmed.

Reproduction in full or in part of this microform is governed by the Canadian Copyright Act, R.S.C. 1970, c. C-30.

## AVIS

La qualité de cette microforme dépend grandement de la qualité de la thèse soumise au microfilmage. Nous avons tout fait pour assurer une qualité supérieure de reproduction.

S'il manque des pages, veuillez communiquer avec l'université qui a conféré le grade.

La qualité d'impression de certaines pages peut laisser à désirer, surtout si les pages originales ont été dactylographiées à l'aide d'un ruban usé ou si l'université nous a fait parvenir une photocopie de qualité inférieure.

Les documents qui font déjà l'objet d'un droit d'auteur (articles de revue, tests publiés, etc.) ne sont pas microfilmés.

La reproduction, même partielle, de cette microforme est soumise à la Loi canadienne sur le droit d'auteur, SRC 1970, c. C-30.

Canada

A Metallogenic Study

of

Polymetallic, Granophile Mineralization
Within the Early Proterozoic Upper Aillik Group,
Round Pond area, Central Mineral belt, Labrador.

By

© Craig S. MacDougall, B.Sc. (Hons.)

A thesis submitted to the School of Graduate
Studies in partial fullfillment of the
requirements for the degree of
Master of Science

Department of Earth Sciences

Memorial University of Newfoundland

(September, 1988)

St. John's                                          Newfoundland

# Abstract

The Round Pond area, located within the coastal region of the Central Mineral Belt of Labrador, is underlain by Early Proterozoic, dominantly calc-alkaline felsic volcanic rocks of the Upper Aillik Group. The volcanic rocks were deposited during subduction-related volcanic activity, and have been subjected to at least two phases of deformation, metamorphism of upper greenschist - lower amphibolite facies, and a widespread synvolcanic soda metasomatic event.

Numerous post-tectonic granitoids intrude the rocks of the Upper Aillik Group in the coastal region, and two satellite stocks of the Monkey Hill Granite occur in the study area. The granitic stocks are highly differentiated, epizonal, leucogranitic intrusions which exhibit geochemical trends towards metallogenic specialization. Trace element and rare earth element evidence suggest that a metal-bearing volatile phase escaped into the surrounding country rock from the leucogranitic stocks.

The Round Pond area is characterized by widespread and varied Mo-(W)-base metal-U-F mineralization spatially associated with the contact margin of a satellite stock of Monkey Hill Granite. A crude metallogenic zonation is developed outwards from the granite ranging from proximal Mo-(W)-Cu-F mineralization, intermediate carbonate-hosted Zn-(Pb) mineralization, and distal U-Zn mineralization. Associated alteration mineral assemblages depict a typical calcic skarn mineral evolution.

Field relations, ore, accessory, and alteration mineral assemblages, as well as geochemical evidence suggest that the widespread and varied mineral occurrences in the Round Pond area have a common magmatic-hydrothermal origin related to the high level igneous activity of the Monkey Hill Granite. Ar/Ar age dating of alteration minerals reveals the mineralization is contemporaneous with the emplacement of the Monkey Hill Granite.

An epigenetic magmatic-hydrothermal model of origin is envisaged for the

polymetallic, granophile mineralization hosted by the felsic volcanic rocks of the Upper Aillik Group, in the Round Pond area.

## Acknowledgements

This study was made possible through the generous financial support received from Memorial Universtiy of Newfoundland in the form of a graduate fellowship and teaching assistantships; a grant from the Northern Science Training Program; funding from the Geological Survey of Canada; and a National Sciences and Engineering Research Council of Canada Operating Grant to Dr. D.H.C. Wilton. Welcomed logistical support was provided by Dr. R.J. Wardle, A. Kerr, M. Batterson, W. Tuttle and K. O'Quinn of the Newfoundland Department of Mines (NDM).

Capable field assistance and camp jokes were provided by C. Pumphrey. Fruitful discussions were held with Dr. R.J. Wardle, A. Kerr (NDM), Dr. D.F. Strong (MUN), and S.S. Gandhi (GSC).

The writer gratefully acknowledges the keen interest, guidance, continued encouragement, rum drinking ability and the poor *target* shooting of Dr. Derek Wilton who supervised this study throughout its development.

Thanks also go out to my fellow graduate students (and co-presidents of Ben Dover Gold Exploration) Len MacKenzie and Jon *Windsor* North for the numerous discussions, shared experiences and coffee ± rum sessions throughout this study.

Special thanks are also extended to my wife Karen who spent many hours drafting, typing, encouraging, and enduring the *thesis*.

# Table of Contents

# List of Figures

# List of Tables

# Chapter 1
# Introduction

## 1.1. Location and Access

The study area is located in the coastal region of central Labrador, approximately 210 km N-NE of Goose Bay near the small coastal village of Makkovik, and encloses two lakes known informally as Round Pond and Falls Lake. The area encompasses approximately 70 km$^2$ between latitudes 54° 58' N, and 55° 04' N, longitudes 59° 06' W, and 59° 12' W, and falls within an area of Labrador informally called (eg. Ryan, 1984) the Central Mineral Belt (see figure 1-1).

Access to the study area must be undertaken by air transport or coastal boat. Labrador Airways offers a year round scheduled service (Monday-Friday) to Makkovik from Goose Bay. C.N. Marine operates coastal passenger and freight service to Makkovik from Goose Bay, with similar service linking Goose Bay to Lewisporte, Newfoundland. The normal shipping season lasts from mid-June to late November. Float equipped fixed wing aircraft or helicopters flying out of Goose Bay offer convenient access to Round Pond or Falls Lake. Otherwise Round Pond can be reached by a 4 km muskeg trail from Makkovik.
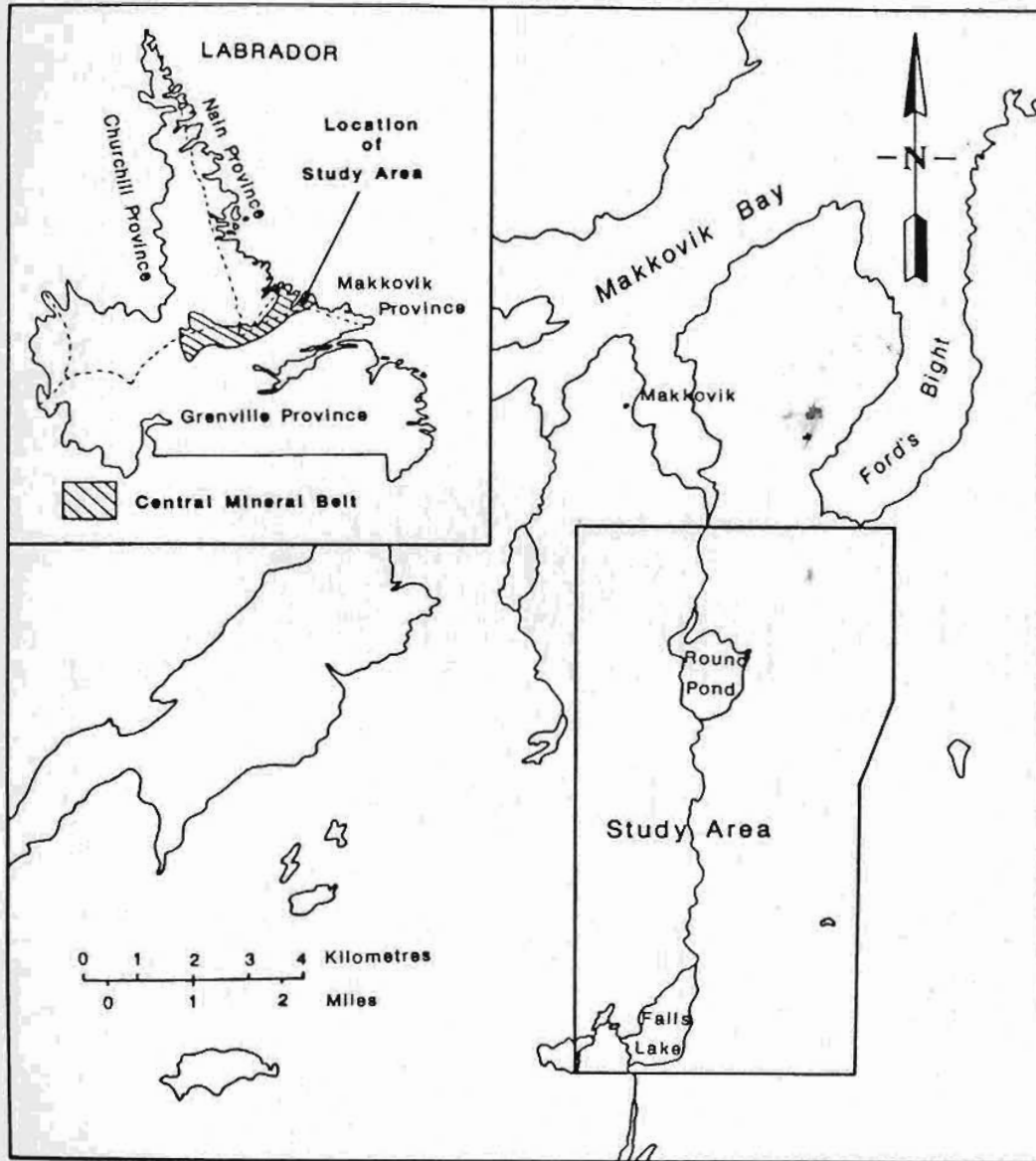
**Figure 1-1:** Location and extent of study area.

## 1.2. Physiography

The study area has been extensively glaciated, and exhibits moderate relief dominated by rounded hills averaging between 200 and 400 m above sea level. Monkey Hill dominates as the highest peak in the area with an elevation of 625 m, the northeastern spur of which falls within the study area.

Round Pond, with a surface elevation of 20 m, is situated in a narrow N-NE trending valley in the central portion of the study area. Located 1-2 km to the east and southeast of Round Pond is a rugged, poorly drained, raised plateau area consisting of discontinuous, subparallel, marshy draws with numerous scattered ponds. Local relief of 1-3 m is highlighted by discontinuous, N-NE trending linear outcrop ridges.

Falls Lake is located 5 km to the south of Round Pond, and with a surface elevation of 200 m, drains northward into Round Pond through the Makkovik Brook, a rather turbulent river characterized by numerous waterfalls and rapids. A 30 m high waterfall occurs in a gorge at the mouth of Falls Lake. The Makkovik Brook continues flowing from the north end of Round Pond and enters the coastal waters of the Makkovik Harbour 3 km north of Round Pond. Both Round Pond and Falls Lake have extensive sandy beaches along their S-SE margins suitable for float plane landings, and ideal for camp sites.

Vegetation is typical of a subartic type climate; dominated by stunted spruce, shrubs, moss, grass, and lichens on hill slopes and swampy areas. Stands of black spruce with abundant shrubs, alders, grass, and moss are found in the sheltered valley region along Makkovik Brook.

Outcrop exposure approaches 100% on elevated hill tops, but outcrops are generally encrusted with lichen. Snow is sometimes a problem in small, sun sheltered hollows and slopes. Outcrop exposure drops considerably on the stunted spruce slopes and swampy areas, and is very poor in the central valley region of the map area.

## 1.3. Regional Geological Setting of the Central Mineral Belt

The Central Mineral Belt defines an easterly to northeasterly trending linear belt of Proterozoic supracrustal volcanosedimentary and intrusive rocks in central Labrador (see figure 1-1, inset), occuping an area 260 km long, and up to 75 km wide (Ryan, 1984). The belt extends from Makkovik on the Atlantic coast southwest to the Smallwood Reservoir in central Labrador, and straddles the boundary between four structural provinces recognized by Taylor (1971), and Wardle et al. (1987) viz. : the Nain ( > 2560 Ma), the Makkovik (ca. 1850 Ma), the Churchill (ca. 1800 Ma), and the Grenville (ca. 1000 Ma) Provinces.

In the north, the supracrustal rocks of the Central Mineral Belt unconformably overlie the Archean gneisses and granites of the Nain Structural Province, the lower Proterozoic gneisses of the Churchill Province, and the middle Proterozoic Harp Lake anorthosite-adamellite Complex (Taylor, 1971; Greene, 1974; Marten, 1977; Ryan, 1984). In the south, the supracrustals are in fault contact with the gneisses of the Grenville Province, and intrusive and/or fault contact with granites of the Trans-Labrador batholith which forms a major linear belt of ca. 1650 Ma plutonism along the southern margin of the Makkovik province (Taylor, 1971; Gower et al., 1982; Gower and Owen, 1984; Ryan, 1984; Kerr, 1986, 1987).

The supracrustal rocks are formally divided into five volcanosedimentary sequences, which from west to east are: the Letitia Lake, the Seal Lake, the Bruce River, the Moran Lake, and the Aillik Groups. The supracrustals and associated intrusives are of considerable economic interest hosting numerous and varied base metal, uranium, molybdenum and other rare metal mineral occurrences.

The Aillik Group, which is the only sequence exposed in the Round Pond

study area, hosts the partially developed Kitts and Michelin uranium deposits, the subeconomic Aillik Bay molybdenite deposit, and over 70 smaller uranium prospects (see figure 1-2). In addition, a number of molybdenite, base metal sulphide, and fluorite occurrences are found within the Aillik Group, some of which have a common association with uranium mineralization. The recent report of anomalous gold values at Pomiadluk Point within the Aillik Group (Wardle and Wilton, 1985) adds to economic interest and potential of the Aillik Group in the Central Mineral Belt.

## 1.4. Previous Geological Work

The earliest geological studies in the area, by Steinhauer (1814), Leiber (1860), Packard (1891), and Daly (1902), involved purely reconnaissance surveys of scattered areas along the coast of Labrador. Daly produced the first detailed geological descriptions when he noted the sedimentary rocks at Pomiadluk Point and Aillik Bay, and the numerous dykes that intrude them.

The Geological Survey of Canada conducted a number of reconnaissance geological mapping surveys (Kranck, 1939, 1953; Christie et al. , 1953; Douglas, 1953) mostly along the coast of Labrador. Kranck (1939) introduced the term "Aillik Formation" to define the supracrustal sedimentary rocks at Makkovik and Aillik. He also recognized young volcanic rocks in the Makkovik-Aillik area as prospective sites of mineralization, and observed a high fluorine content in the Strawberry Granite, suggesting further, the possibility of mineralization in the surrounding rocks. Kranck (1953) released a regional geological map, and a comprehensive report that included results of theses work by McGill graduate students. Thesis work included petrological studies by Riley (1951) of supracrustal and granitoid rocks near Makkovik, Moore (1951) of mafic dykes at Cape Aillik, and Cooper (1951) of syenite and granite at Cape Strawberry and Dunn Island. Kranck (1953) further described the occurrence of fluorite and molybdenite near the contact of the Strawberry Granite with Aillik quartzites, and noted the presence of grossularite garnet with diopside in limestones and calcium-rich quartzites near Makkovik.

Christie et al. (1953) produced a geological compilation map of the coastal and interior regions of Labrador, with accompanying descriptive notes. Of interest is the mention of massive, perthitic leucogranites, exposed on the outer coast from Cape Smokey to Cape Aillik, and the occurrence of pyritic sulphide bodies along the coast.

Douglas (1953) presented descriptions of various localities in coastal Labrador. He noted that Monkey Hill is composed of granite, and that the geology of the Makkovik area is characteristic of an area near the roof of a granitic batholith. Douglas also noted the presence of pegmatites with pyrite and rare molybdenite, as well as a number of sulphide showings consisting of pyrite, chalcopyrite, and molybdenite. He went on to suggest that a molybdenite deposit may occur between Big Bight and Duck Island.

1:250,000 scale reconnaissance mapping of the region by the Geological Survey of Canada was completed by Stevenson (1970) south of latitude 55°00' N, and by Taylor (1975) north of latitude 55°00' N. Greene (1972) released a compilation geological map of Labrador.

The Central Mineral Belt has been the focus of sporadic mineral exploration activity since the late 1920's. However, in 1954, the discovery of uranium mineralization by M.J. Piloski of Brinex Ltd., 15 km south of Makkovik, initiated a period of extensive mineral exploration activity that spanned roughly 25 years. Much of the regional, as well as local geological features associated with the widespread uranium and molybdenite mineralization in the Central Mineral Belt have been described by Beavan (1958), Gandhi et al. (1969), Gandhi (1978, 1984, 1986), Gower et al. (1982), and Ryan (1984).
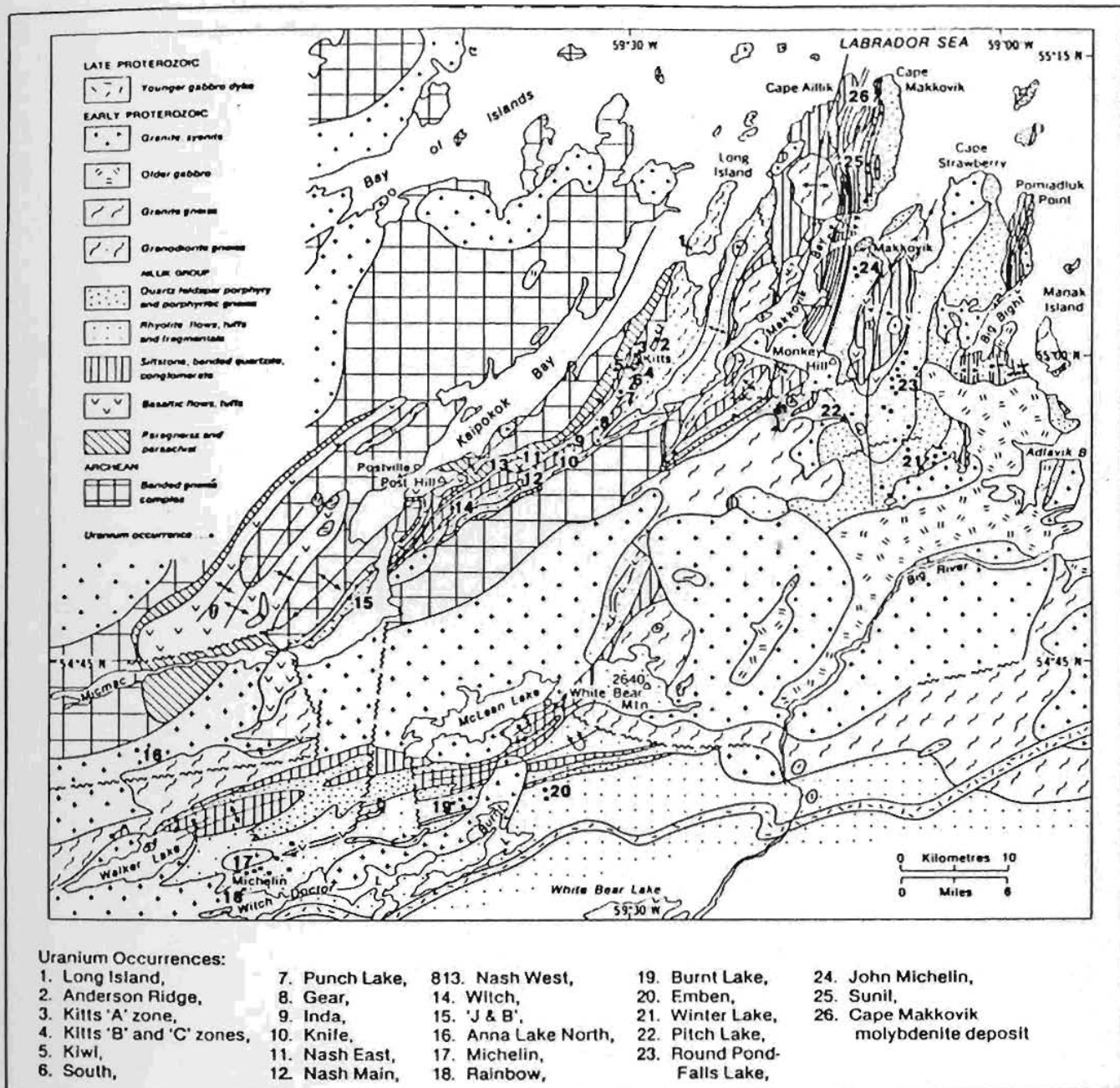
**Figure 1-2:** General geological map showing the Aillik
Group and associated uranium occurrences,
Kaipokok-Big River area, Labrador
(from Gandhi, 1986).

A number of undergraduate and graduate theses have been completed on the area (generally in concert with mineral exploration activity). Theses which centered on the study of mineral occurrences include: Gill (1966) on the petrology of molybdenite-bearing gneisses in the Makkovik area, Barua (1969) on the geology, mineralization, and geochemistry of rocks on the Cape Makkovik Peninsula, and Herrero (1970) on an integrated exploration program based on geophysical information for disseminated sulphides at Round Pond and Retreat Lake. Stratigraphic and structural studies which characterized the geology of the coastal area include: King (1963), Sampson (1966), Stoeterau (1970), Clark (1970, 1973), and Martin (1977). More recent graduate and research work has emphasized the geochemistry of uranium occurrences and associated host rocks, such as studies by: Minatidis (1976), White (1976), Kontak (1980), Evans (1980), and White and Martin (1980). Geochemical studies of Phanerozoic lamprophyres in the Aillik Bay area have been completed by Hawkins (1976), Foley (1982), and Malpas et al. (1986).

A number of geochronological studies have been undertaken on rocks in the area. Most involve K/Ar whole rock and mineral age dating, such as Lowdon et al. (1962), Leech et al. (1963), Gandhi et al. (1969), and Wanless et al. (1970, 1972, 1973, 1974, 1979). Rb/Sr age dating studies of felsic volcanic and granitic rocks include: White (1976), Gandhi (1978), Brooks (1979), and Kontak (1980). U/Pb dating of uranium occurrences has been carried out by Gandhi (1978), and Kontak (1979, 1980). Ar/Ar dating of the Walker Lake Granite has been reported by Archibald and Farrar (1979). Scharer et al. (in prep), report U/Pb zircon ages for the Upper Aillik Group.

Further government initiated work includes the geomorphological studies of Fulton et al. (1975), and Rosen (1980); economic mineral studies by Collerson et al. (1974), Ryan (1977), and Kontak (1980); mineral occurrence maps of the Newfoundland Department of Mines (NDM); and geochemical studies of felsic volcanic rocks by Payette and Martin (1986), and Gower and Ryan (1987).

Current research in progress involves a regional granitoid survey by Kerr (1986, 1987), and a metallogenic study of the Central Mineral Belt by Wilton et al. (1986, 1987), and Wilton and Wardle (1987).

## 1.5. History of Mineral Exploration

Information on the exploration is contained in unpublished exploration company reports (ie. Brinex, Brinex-Cominco, Brinex-Urangesellschaft, Placer-Brinex, etc.). A large number of these reports remain confidential, incomplete, or are not on file at the Newfoundland Department of Mines and Energy (NDM) library.

Piloski (1955) reported the first discovery of uranium mineralization at Pitch Lake (15 km south of Makkovik). In 1955, J.T. Cumberlidge and B. Chaulk, working for Brinex, discovered significant uranium mineralization in three zones east of Falls Lake (Piloski, 1955). These occurrences known as Showings No. 16, 17, and 18, were investigated by detailed mapping, trenching, and shallow drilling. Grades of uranium mineralization, although good in places (ie. $5.35\%$ $U_3O_8$ over 0.15 m), were generally low ($<1\%U_3O_8$), over only narrow core lengths, and laterally sporadic along strike (NDM Mineral Inventory File 13J/14/U017). Exploration was curtailed in 1956.

In 1959, geochemical orientation surveys for U, Cu, Zn, and Mo were conducted to thoroughly assess the mineral potential of the Brinex-Anglo-American Joint Venture Falls Lake-Shoal Lake area. Although numerous anomalies were detected, in general they did not correlate with known mineral occurrences (Hansuld, 1959).

In the 1960's, further exploration in the Round Pond area was fueled by the discoveries of the Kitts and Michelin uranium deposits, discovered in 1956 and 1968 respectively, and the Aillik Bay molybdenite deposit (Piloski, 1960).

Regional and detailed mapping of the study area was carried out by numerous exploration industry geologists working for Brinex Ltd. In 1963-64, detailed prospecting by B. Chaulk and J. Michelin revealed numerous occurrences of pyrite, chalcopyrite, molybdenite, and fluorite. The most promising showings were investigated by trenching and the shallow drilling of nine x-ray drill holes totalling 374 m (1246 ft). None of the showings proved to be economic at that time (the best intersections from the X-ray drill holes are listed in Table 1, and locations are shown on Map-1 in the back pocket). Many of the showings however, were not investigated beyond the original discovery, and not all the trenches were examined in detail due to a shortage of personnel and time.

**Table 1-1:** Best mineralized intersections
from drill holes in the Round Pond area.
(from Sutton, 1964).

| Hole No. | Depth (ft) | Core Length (ft) | Mo % | Cu % |
|---|---|---|---|---|
| 4-64 | 21.0-26.0 | 5.0 | 0.275 | – |
| 5-64 | 8.5-18.0 | 9.5 | 0.10 | – |
| " | 40.0-47.5 | 7.5 | 0.10 | – |
| 7-64 | 111.5-127.5 | 16.0 | – | 0.11 |
| " | 146.0-156.0 | 10.0 | – | 0.33 |
| 8-64 | 47.5-56.75 | 9.25 | 0.155 | – |
| 9-64 | 36.5-41.0 | 4.5 | 0.41 | – |

Extensive grid lines were cut through the area from immediately north of Falls Lake, to east of Fords Bight. Geochemical soil surveys for Mo and Cu were conducted over the entire grid in 1964, with subsequent followup surveys over selected areas in other years. Anomalies detected could generally be traced to known mineral occurrences (Newham, 1964). A variety of geophysical surveys including I.P., VLF-EM, and magnetic were run in areas of poor exposure from

1964 to 1969, and a number of drill targets were recognized to the northeast of Round Pond. These targets were subsequently drilled in 1970 in four diamond drill holes totalling approximately 600 m (2000 ft). Only sporadic, weak mineralization was encountered (Herrero, 1971).

· Although interest in the Mo-base metal showings in the Round Pond area waned, the discovery in 1967 of a radioactive zone on the southeast fringes of the Mo-base metal zone of mineralization, did create renewed interest (Gandhi, 1968). A 500 lb (230 kg) bulk sample was taken, but only returned a grade of 0.029% $U_3O_8$ (Gandhi, 1968). No further work appears to have been done, although further exploration was recommended.

Exploration in the area remained dormant until 1978, when the area became part of Placer-Brinex joint venture. This program attempted to re-evaluate many of the older showings. New grid lines were cut, and detailed geological mapping and prospecting carried out. In addition, VLF-magnetic surveys were conducted over uranium occurrences east of Falls Lake. No new showings of any significance were reported (NDM Mineral Inventory Files, 13O/03/Mo31, 13J/14/U017).

In 1984, R.J. Wardle and D.H.C. Wilton carried out a reconnaissance sampling program for precious metals in the Kaipokok-Big River area, and significant Au, Ag values were detected (Wardle and Wilton, 1985). This initiated a staking rush in coastal Labrador. Some limited exploration has since been undertaken by Maritec Exploration Ltd. (1985-1986), and Cuvier Mines Ltd. (1986-1987), involving re-evaluation of mineralized showings in the area, including a drill program to test Showings No. 7-11 at Winter Lake by Cuvier Mines in the fall of 1987.

## 1.6. Mo-U Metallogenesis

The felsic volcanic rocks of the Upper Aillik Group are host to numerous deposits, prospects, and showings of U, Mo, base metal, and fluorine mineralization that occur as dominantly *monometallic* (ie. Michelin and Kitts uranium deposits, Aillik Bay molybdenite deposit), or complex *polymetallic* (ie. Round Pond area, Shoal Bay No. 24 Prospect, Sunil prospect) ore mineral concentrations. The latter are spatially associated with high level, leucogranitic intrusions which host similar ore mineral assemblages in the form of mineralized pegmatites and local disseminations (in granitic rock).

The association of Mo and U, in a wide variety of deposit types, including pegmatites, base metal veins, skarns, pyroxenitic metamorphic rocks, Colorado Plateau uranium deposits, and porphyry deposits is well known (Soregaroli, 1975), and suggests that the behaviour of the two elements may be governed by similar geochemical parameters.

Strong (1980, 1981) suggests that among the various factors that control the behaviour of various elements in magmatic and hydrothermal systems, two of the most important are ionic radius, and ionic potential (see figure 1-3). Strongly lithophile elements (ie. Sn, W, Nb, Ta) tend to form tetrahedral complexes, and be strongly concentrated in silicic melts formed either by crystal fractionation or as partial melts. The strongly chalcophile element Cu can enter silicate lattices or form sulphides, and as a result tends to be randomly distributed in a cooling magma or during partial melting. The lithochalcophile elements (ie. Mo, U) form strongly covalent bonds with oxygen which exclude them from silicate lattices. Thus these elements are considered *incompatible*, and tend to be concentrated in residual, differentiated aqueous phases in crystallizing magmatic systems.

Element enrichment trends that would be predicted by these geochemical properties during cooling of a siliceous magma chamber have been documented by Hildreth (1979) from the Bishop Tuff of southern California. Wherein lithophile
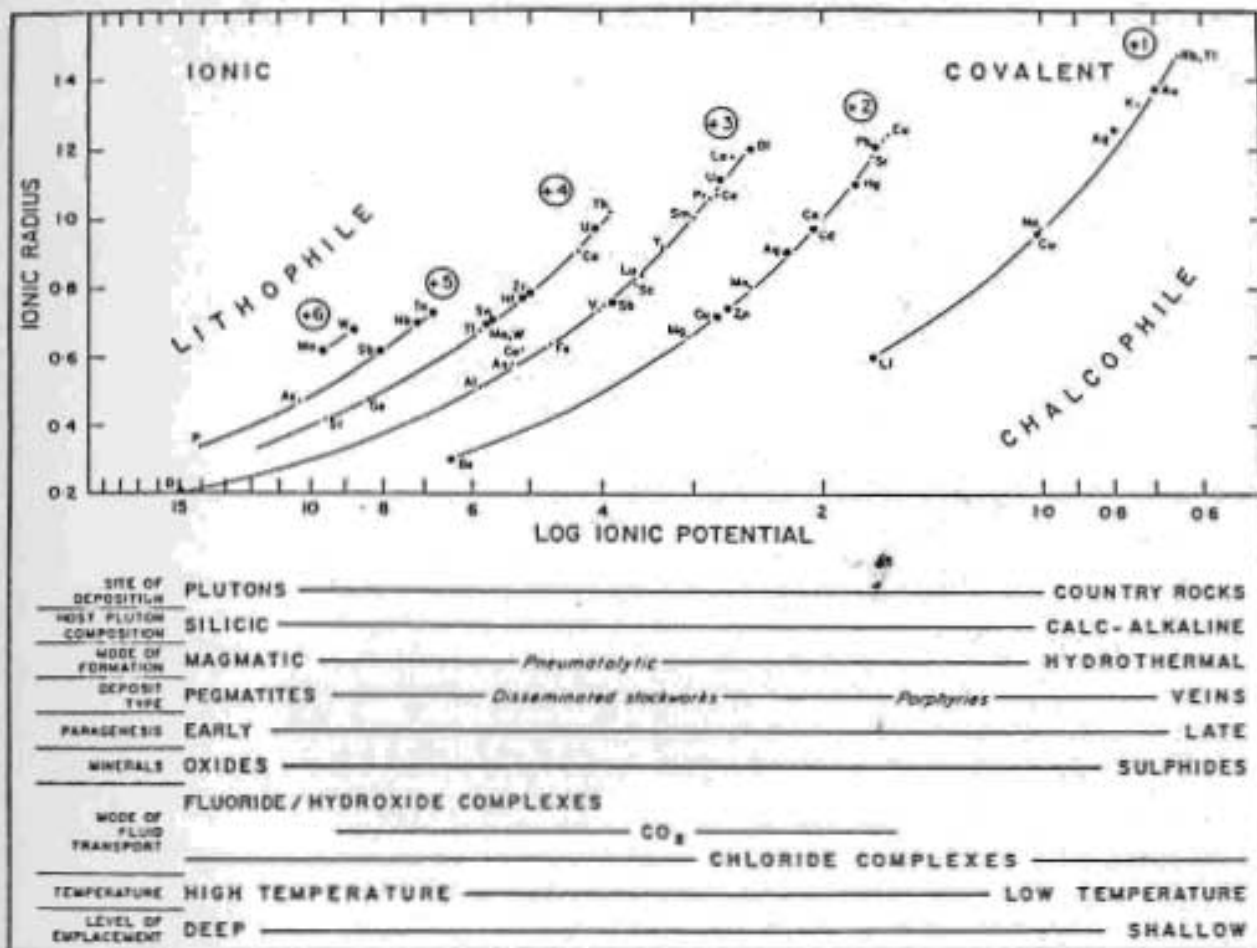
**Figure 1-3:** Schematic outline of the relationship between ionic radius and ionic potential of elements forming different types of granitoid mineral deposits (from Strong, 1980).

elements such as Mo, U, Sn, W, the heavy rare earths, and volatiles such as F and Cl were concentrated towards the top of the magma chamber. The chalcophile elements Fe, Cu, Au, and Co were concentrated in the lower (more primitive, less siliceous) portions.

Numerous studies have reported similar enrichment/depletion trends in granitoid rocks associated with mineral deposits (eg. Tischendorf, 1977; Mutschler et al., 1981; Westra and Keith, 1981; Wilson and Akerblom, 1982; Imeokparia, 1985; Ohlander, 1985; Ramsay, 1986; Du Bray, 1986; Tuach et al., 1986). Of particular interest is the association of lithophile elements with F in both plutonic and volcanic environments. This association has been described (eg. Rub, 1972; Bailey, 1977; Strong, 1980, 1981; Mutschler et al., 1981, Burt and Sheridan, 1981; Curtis, 1981; Cathelineau, 1982; Rice et al., 1985) as an important genetic link, with F acting either as a metal complexing agent, or as a network modifer of a crystallizing magma.

The association of U-Mo-F mineralization in a wide variety of volcanic to plutonic mineralizing environments ranging in age from Quaternary to Lower Proterozoic is illustrated in figure 1-4 (from Curtis, 1981). The genetic relationship between plutonic and volcanic environments has been emphasized by Sillitoe and Bonham (1984), and Hulen et al. (1987). Mineral deposits hosted by granitoid rocks are typically associated with either: 1) high level, calcalkaline plutons of intermediate composition which typically host porphyry (Cu-Mo) deposits that form by epigenetic, hydrothermal processes during sub-solidus cooling (eg. McMillan and Panteleyev, 1980); 2) leucogranitic plutons which typically form lithochalcophile (Sn, W, U, Mo) mineralized magmatic hydrothermal veins and pegmatites during crystallization as a result of magmatic concentration (Strong, 1980). The latter is of interest in this thesis.

Deposits associated with volcanic rocks may be hosted in the entire spectrum of volcanic, volcaniclastic, subvolcanic, and plutonic rocks. Mineralization may be syngenetic, or epigenetic with respect to the host rock, and related to various magmatic-hydrothermal, synvolcanic-exhalative, and supergene processes. Structural or stratigraphic (or a combination) factors may be important in localization of the mineralization. Source of the metals may be the associated
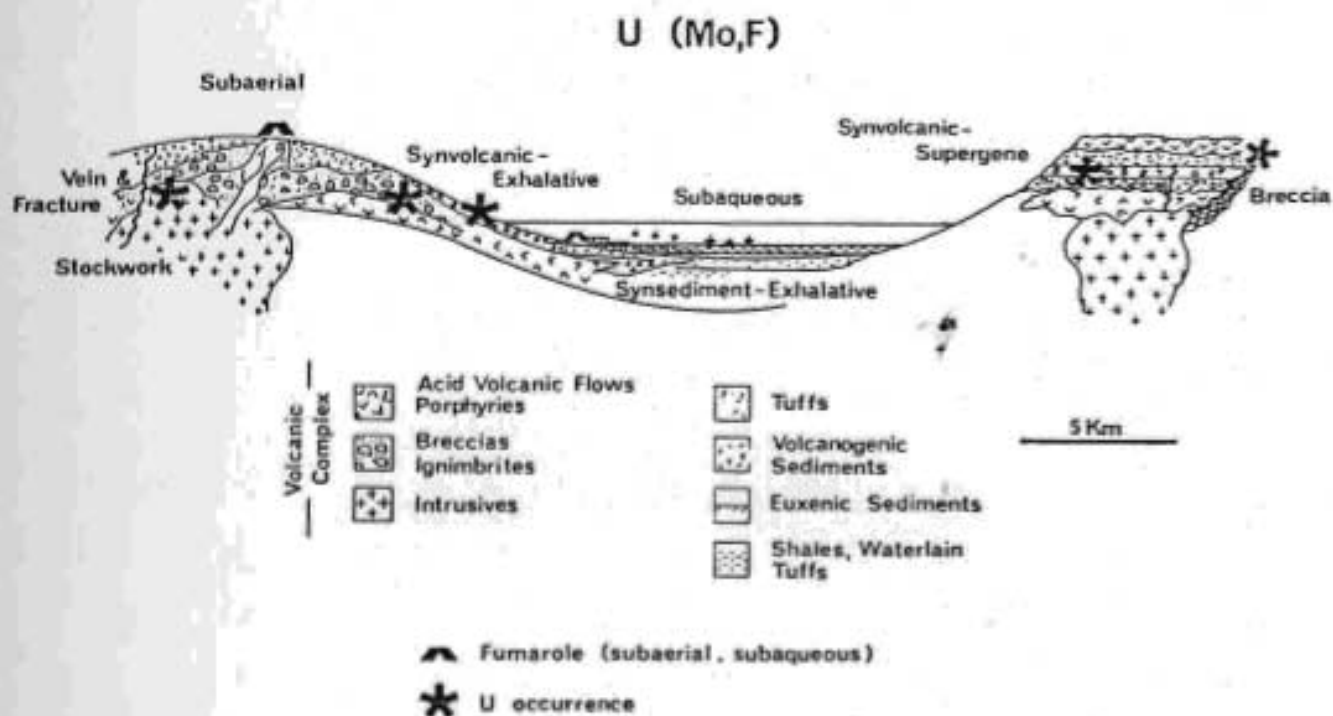
# U (Mo,F)



**Figure 1-4:** The spectrum of U-Mo-F deposits associated
with volcanic and volcanosedimentary
rocks (from Curtis, 1981).

intrusives which supply metal-bearing hydrothermal fluids, or the volcanic rocks,
from which the metals are mobilized by magmatic, volcanic, or meteoric fluids
and concentrated along favourable horizons or structures.

## 1.7. Purpose, Scope, and Methods of the Present Investigation

The Aillik Group consists of a sequence of Lower Proterozoic metavolcanic and metasedimentary rocks that form the eastern component of a uranium metallogenic district, termed the "Labrador Uranium Area" by Beavan (1958), and now referred to as the Central Mineral Belt (Ryan, 1984).

A number of important mineral deposits are hosted within the Aillik Group including the partially developed Kitts and Michelin uranium deposits, and the subeconomic Aillik Bay molybdenite deposit. In addition, over 70 smaller uranium prospects, and a number of molybdenite, base metal, and fluorite mineral occurrences occur.

Numerous genetic models have been proposed for the uranium mineralization (Gandhi et al., 1969; Gandhi, 1978, 1986; Evans, 1980; White and Martin; 1980, Gower et al., 1982), which vary in regard to the syngenetic or epigenetic character of individual deposits and the composition of the ore-forming fluids. Most, however, advocate broadly synvolcanic mineralizing events, and propose the source of the mineralization to be the felsic volcanic rocks, or associated synvolcanic plutons, of the Aillik Group. The leaching of uranium and molybdenum from felsic volcanic rocks to be concentrated in metallic deposits has been widely documented (ie. Zielinski, 1979; Haffty and Noble, 1972).

The felsic volcanic rocks of the Upper Aillik Group are exposed as two belts: i) a coastal belt that extends from Capes Aillik and Makkovik inland for 35 km, ii) and a 40 x 10 km inland area in which the Michelin uranium deposit is located. Compared to the inland belt, the rocks of the coastal belt are more intensely deformed and metamorphosed, have been intruded by numerous, high level, post-tectonic granite intrusions, and host a more complex metallogenic style of mineralization including U, Mo($\pm$U), and Pb-Zn. A question thus arises as to whether a genetic model advocating broadly synvolcanic mineralization can be extended to mineral occurrences hosted in both belts of Upper Aillik Group volcanic rocks?

This study has focused on the Round Pond area due to the spatial association of a number of molybdenite, base metal, and uranium mineral occurrences with post-tectonic granitic intrusions. The observed association suggests a different metallogenic history for mineral occurrences in the coastal area, than that (synvolcanic processes) proposed for mineral occurrences inland.

The present investigation of the Round Pond area is a metallogenic study of the Mo-base metal-U-F mineral occurrences in the area. This has been accomplished by: 1) Production of a 1:25,000 scale geological map involving a thorough petrological and geochemical (including analyses for major, trace, and rare earth elements) investigation of lithologies of the Upper Aillik Group exposed in the study area. 2) Study and documentation of the various styles of mineralization, ore mineralogy, and associated alteration. This included extensive geochemical analyses so as to determine compositional variations between mineralized and unmineralized samples, as well as provide absolute base metal, rare metal, and precious metal contents for mineralized samples. 3) Examination of the relationships between the ore mineralization, associated host rocks, and nearby granitic intrusions so as to provide a metallogenic model of origin for the mineralization in the Round Pond area. This involved the determination of the source of mineralization, establishing the nature of the mineralizing processes, identification of the favourable factors of concentration and localization of ore mineralization.

Methods employed in the present investigation include: general geochemical analyses (major and trace element analysis), REE analysis, precious metal analysis (done at commercial labratories), general petrology, detailed petrology of ore mineralization and associated alteration, XRD mineral identification, accessory and ore mineral identification using a Scanning Electron Microscope (SEM), microprobe analyses of alteration minerals, and Ar/Ar mineral dating performed for a fee at the University of Maine.

# Chapter 2
# Geology of the Round Pond Area

## 2.1. Geology of the Aillik Group

The Aillik Group proper, is an Early Proterozoic bimodal sequence of basaltic and rhyolitic volcanic rocks with interbedded volcaniclastic sediments. Thickness of the group has been estimated by Gandhi et al.(1969) as roughly 7600 m, and by Clark (1973) as 8500 m. First recognized by Daly (1902), early workers (eg. Beavan, 1958, Gandhi et al., 1969), originally described the Aillik Group as a quartzitic metasedimentary sequence. However, by the early 1970's, workers such as Sutton et al. (1971), and Watson-White (1976), began to recognize that the quartzitic metasediments were in fact the products of felsic volcanism.

Marten (1977) divided the Aillik Group into a lower sequence of metasedimentary schists, amphibolites, metabasalts, and pillow lavas termed the Lower Aillik Group; and an upper sequence of felsic volcanic, volcaniclastic, and derived sedimentary rocks; the Upper Aillik Group. The Lower Aillik Group structurally overlies reworked Archean gneisses of the Nain Province Craton; the actual contact is a ductile shear zone demarked by mylonites (Marten, 1977). The Lower-Upper Aillik contact is characterized by a zone of intense deformation, and has been suggested by Marten (1977) as disconformable, while Gandhi (1978) and Evans (1980) propose a transitional contact. Wardle and Bailey (1981), suggest an unconformity between the two subdivisions of the group based on differing structural styles and metamorphic grades.

The Upper Aillik Group underlies two areas in the eastern Central Mineral

Belt: a coastal belt which extends from Capes Aillik and Makkovik, inland for 35 km, in which the thesis area is located; and an inland zone roughly 40X10 km in size (Fig. 2-1). The two zones are separated by the Adlavik Brook Fault (Gower et al., 1982) and synkinematic to postkinematic granitoids. The Upper Aillik Group was deformed and metamorphosed to upper greenschist-lower amphibolite facies during the Hudsonian Orogeny ca. 1800-1600 Ma (Clark, 1973; Gower et al., 1982). Recent work by Wardle et al. (1986) has renamed the deformational event the Makkovikian Orogeny ca. 1800-1600 Ma. The most intense deformation and metamorphism was suffered by rocks along the coast, where complex polyphase deformational features are widespread. Rocks inland appear much fresher, and occasionally possess primary textures. Wilton and Wardle (1087) suggest further distinctions between the two belts of Upper Aillik Group rock, in that the rocks on the coast are intruded by abundant post-tectonic granites, and host a contrasting metallogenic style of mineralization.

Rhyolites of the Upper Aillik Group were dated by Rb/Sr whole rock isotopic techniques at between 1767 and 1676 Ma (White, 1976, Kontak, 1980). Kontak et al. (in press) believe these dates to be metamorphic. Recent precise U-Pb zircon dates by Scharer et al. (in press) have yielded concordant ages of 1855 Ma for rhyolites in the Michelin area, 1860 Ma for rhyolites in the Ranger Bight area, and 1810 Ma for a subvolcanic porphyry at White Bear Mountain.

Within the thesis area, two small, relatively undeformed, high level, granitic stocks intrude the rocks of the Upper Aillik Group (see Map-1, back pocket). The intrusions belong to the regionally extensive Monkey Hill Granite, and are interpreted (Kerr, 1986; Wilton et al., 1986; Wardle and Wilton, 1987; MacDougall and Wilton, 1987a) as satellite stocks and cupolas of the Trans-Labrador Batholith (ca. 1650-1600 Ma). A number of such satellite plutons intrude the rocks of the Aillik Group in the coastal areas, and several including those of the Monkey Hill Granite are spatially associated with mineralization. A more detailed discussion of the Monkey Hill Granite is presented in Chapter 3. In

addition, numerous pre- to post-tectonic amphibolite and diabase dykes cut all lithologies of the Upper Aillik Group.
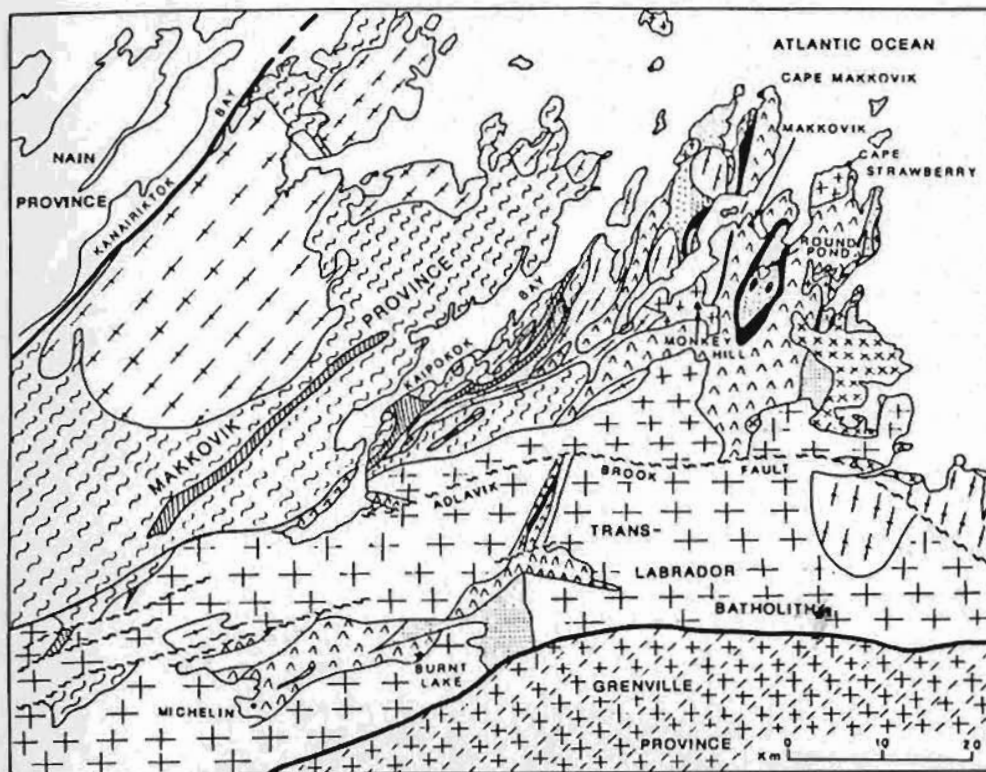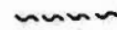


**Figure 2-1:** Simplified geology of the Makkovik Province (from Wilton and Wardle, 1987).

The tectonic setting of the Aillik Group has been interpreted by White (1976), Gandhi (1978, 1984), Evans (1980), and White and Marten (1980) as that of a nonorogenic, continental rift environment, based on lithological characteristics, particularly the abundance of rhyolitic volcanic rocks. However, Clark (1973), Wardle and Bailey (1981), and Gower et al. (1982), have suggested that the Lower Aillik Group was deposited in a transitional shelf environment, followed by the collision of two cratons (Clark, 1973). and that only the Upper Aillik Group was deposited in a rift environment. Payette and Marten (1986) reached a similar conclusion concerning the Upper Aillik Group.

## 2.2. Stratigraphy

Within the Round Pond-Falls Lake thesis area, the Upper Aillik Group consists of a thick sequence of subaerial, felsic volcanic rhyolite flows, and their subvolcanic equivalents, ash fall and ignimbritic tuffs, breccias and agglomerates, overlying a thin but persistent unit of amphibolitized basaltic volcanic rocks, which in turn overlies volcaniclastic conglomerate, tuffaceous sediments and lesser rhyolitic ash flow tuffs. The general stratigraphic sequence of the Upper Aillik Group in the Round Pond area is illustrated in figure 2-2. As suggested by Clark (1973), the supposed stratigraphic sequence in the Round Pond area is simply a product of the application of the law of superposition. Thus the oldest unit (unit 1) is found at the core of the domal anticline structure, and the units get progressively younger towards the fold limbs.
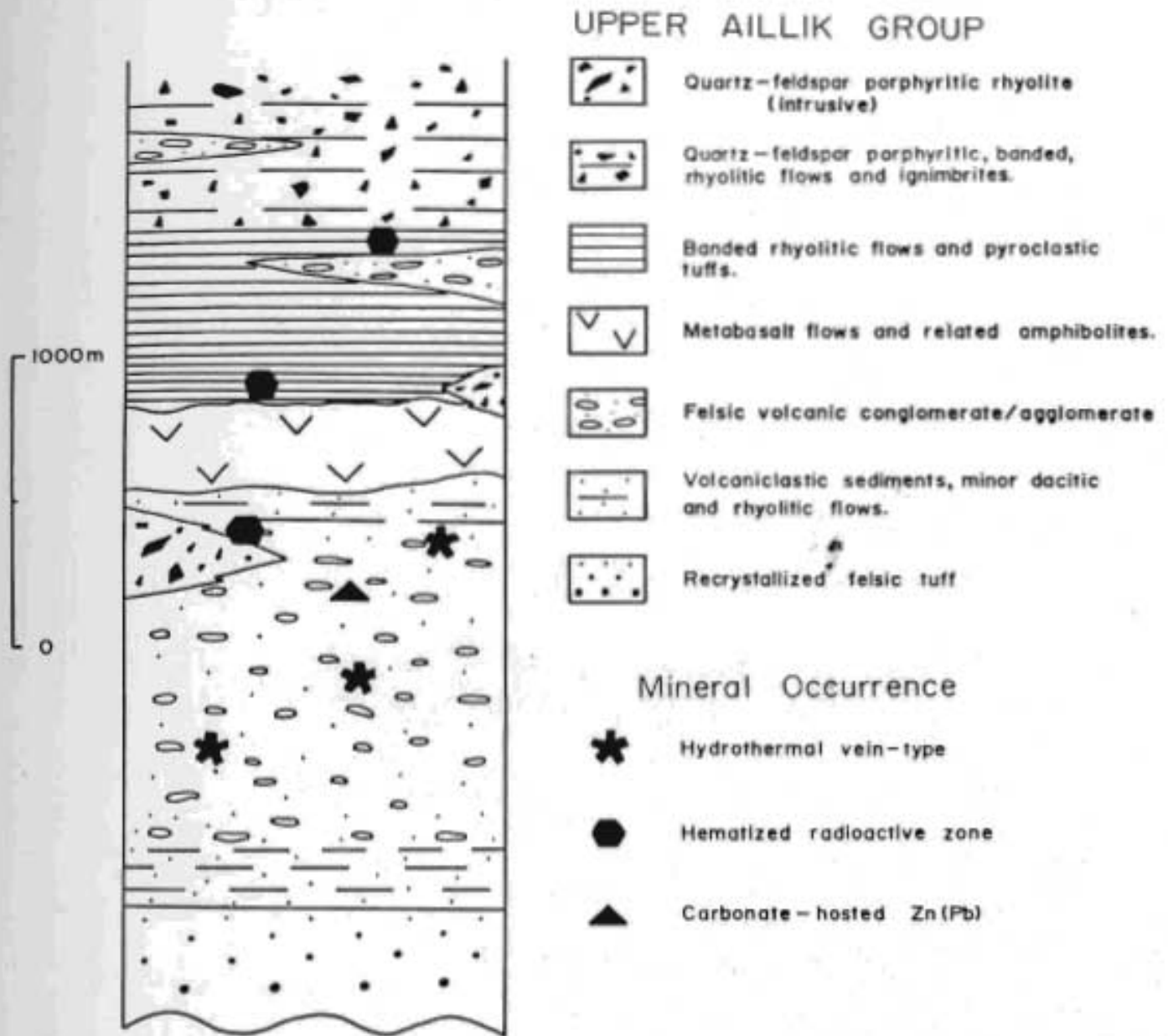
**Figure 2-2:** Simplified stratigraphic section of the Upper Aillik Group at Round Pond.

## 2.2.1. Unit 1: Recrystallized Felsic Tuff

Unit 1 is located in the central portion of the map area, at the core of the domal anticline structure. The unit is best exposed on the west side of Round Pond, but also occurs as sporadic outcrop along the Makkovik Brook north of Round Pond. No contact with the overlying lithology (unit 2) has been observed in the map area, and thus contacts are assumed. However, similarities with the overlying lithology suggest a transitional contact exists between the units.

In outcrop, the unit appears as a whitish to brownish grey, fine to medium-grained, equigranular rock, with minor relict 1-2 mm phenocrysts of quartz and feldspar, and ovoid clots of magnetite (up, to 1 cm). The unit is extensively recrystallized and possesses a sucrosic texture typical of the Aillik Group felsic volcanic rocks in the coastal exposures. Clark (1973), stated that the lithology possessed a weak gneissic foliation that parallels the schistosity of the Aillik Group.

In thin section, the unit possesses irregular to round phenocrysts of recrystallized quartz, and lesser ragged perthitic and feldspar phenocrysts, in a groundmass of polygonal, recrystallized quartz and feldspar (see figure 2-3). Clark (1973) stated that the major mineral proportions are 60% feldspar, primarily albite, oligoclase and andesine and 30% quartz, as has been observed in this study. Accessory minerals include abundant opaques (magnetite), microcline, hornblende, diopside, biotite, chlorite, sphene, garnet (andradite?) and fluorite. The garnet tends to be interstitial between major minerals, but also occurs as rims near large perthitic phenocrysts. Clots of magnetite intergrown with pyroxene, garnet and sphene are common, as are clots of euhedral sphene crystals.

Previous workers have had some difficulty in interpreting this unit. Gandhi et al. (1969), mapped this unit as a granoblastic, feldspathic quartzite, while Clark (1973), favoured a plutonic origin and mapped it as a granodiorite. Clark cited the presence of quartz and antiperthitic aggregates as indicating an igneous

glomeroporphyritic texture and thus, a plutonic origin. Gower et al. (1982), questioned Clark's identification, but lacked sufficient data to provide an unequivocal interpretation of the protolith. The lack of intrusive contact features, the apparent transitional nature of the contact with the overlying volcanic tuff (unit 2), and the presence of minor relict quartz-feldspar phenocrysts, suggest a volcanic origin for this lithology.

## 2.2.2. Unit 2: Volcanic Tuffs and Volcaniclastic Sediments.

Unit 2 is a variable lithology that ranges from a felsic to intermediate volcaniclastic to tuffaceous sedimentary unit. The unit is exposed as two, thin, incomplete annular rings in the Round Pond-Falls Lake area separated by a felsic-volcanic conglomerate unit. The unit which overlies the recrystallized felsic tuff (unit 1), grades into the overlying felsic volcanic conglomerate (unit 3), and in places reappears overlying the conglomerate, and a quartz-feldspar porphyritic rhyolite member (unit 7), in the south.

The presence of conglomeratic lenses and individual clasts within this unit, and tuffaceous lenses in the conglomerate serve to indicate the transitional nature between the two lithologies. This was further emphasized by previous workers such as Clark (1973) and Gower et al. (1982) who, although showing similar stratigraphic sequences, differed in the apparent thickness of the units.

In outcrop, the rock is a fine-grained, white to pink to grey, massive to poorly bedded, tuffaceous sediment, with minor interbedded rhyolitic to dacitic crystal tuffs and flows. Bedding is generally defined by magnetite-sphene and biotite-rich laminations and is restricted to grey varieties of the lithology (see figure 2-4).

**Figure 2-3:** Ragged perthitic phenocryst surrounded by a fine-grained, recrystallized, polygonal groundmass of quartz and feldspar. Unit 1: Recrystallized felsic tuff, CM-170 (mag. x10, x nicols).

**Figure 2-4:** Fine-grained magnetite-sphene (opague minerals) laminations in a recrystallized matrix of equigranular quartz and feldspar. Unit 2: Volcaniclastic tuffaceous sediment (mag. x10, plane polarized light).
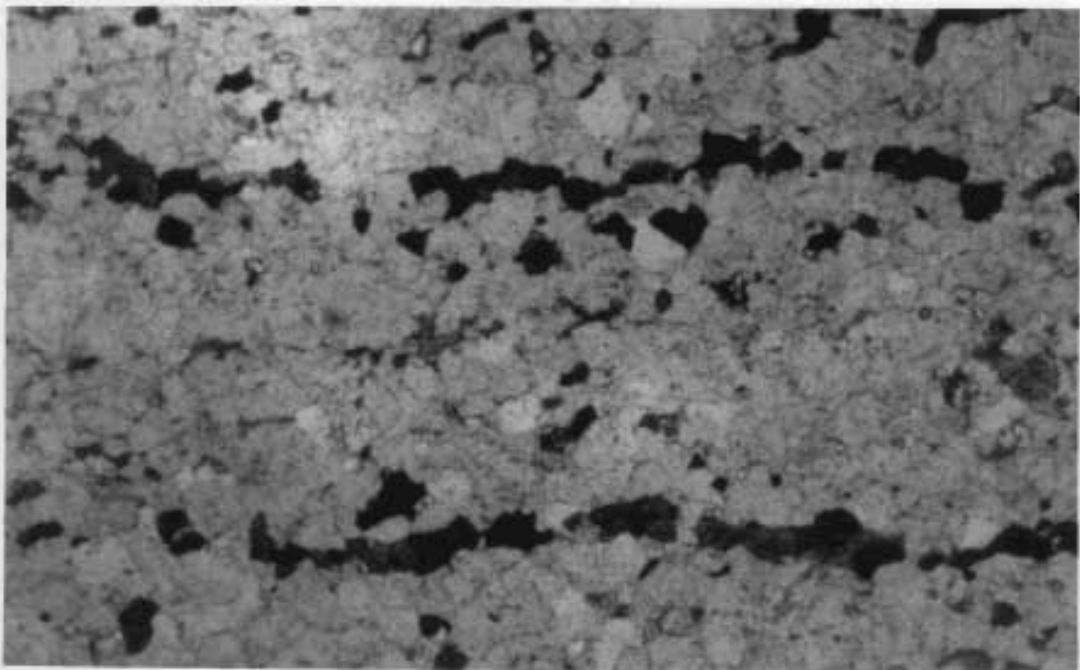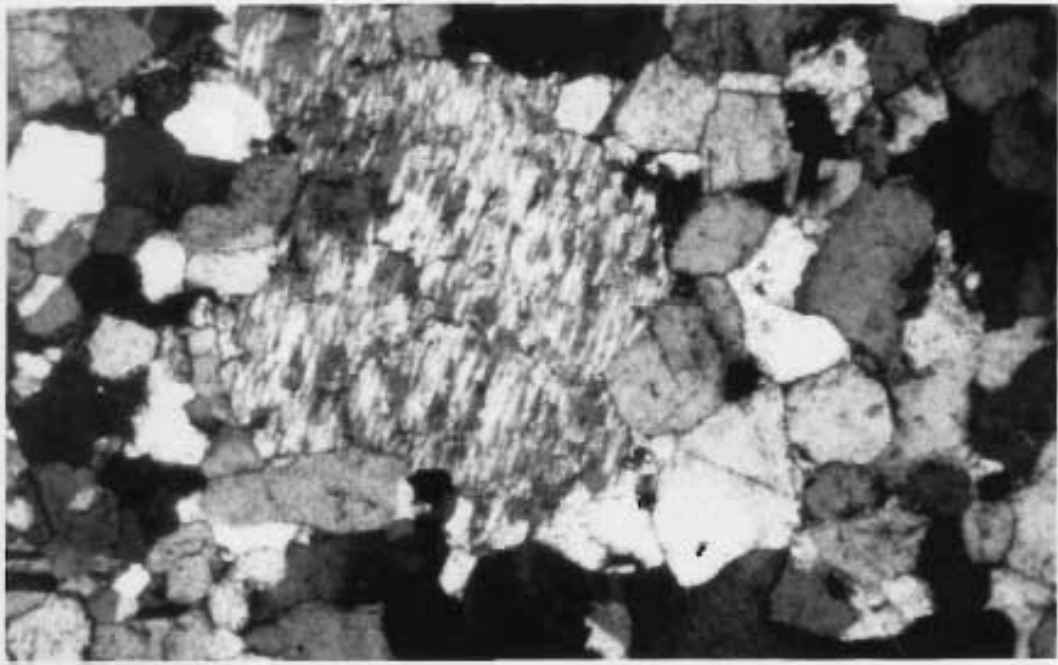
In thin section, the unit is composed of equigranular, polygonal to subrounded, twinned and untwinned feldspars (albite, oligoclase, sanidine), variable quartz, accessory biotite, epidote, diopside, sphene, magnetite, calcite, and pyrite.

### 2.2.3. Unit 3: Felsic Volcanic Conglomerate/Agglomerate

Unit 3 is a polymictic, felsic volcanic conglomerate to agglomerate that crops out extensively in the map area. The outcrop pattern forms a complete annular ring that clearly defines the regional anticlinal structure. Contacts with the underlying and overlying tuffaceous units are transitional. The widest exposure occurs east of Round Pond and ranges in thickness from 200 to 1000 m (Clark, 1973).

The unit is composed of tectonically deformed, ellipsoidal clasts set in a sucrosic, felsic tuffaceous matrix (see figure 2-5). Clasts range in size from less than 1 cm to almost 1 m in length, but generally exhibit a consistent length to width ratio of 5:1 along the fold limbs, while those near the fold axis have ratios up to 9:1. Larger clasts appear to be dominant in the central portions of the unit, while in stratigraphically lower and higher portions clasts are smaller in size. Quartz phenocrysts are locally abundant in the matrix towards the top of the unit. Clasts are stretched and oriented parallel to regional trends, and vary from prolate (cigar-shaped) on the hinge of the anticlinal structure, to oblate (discoidal) and steeply dipping on the fold limbs. Locally, brecciated and angular clasts occur (see figure 2-6), which appear to represent zones of shearing, or are the products of hydrothermal activity (ie. hydrothermal brecciation) and related gas explosions (ie. tuffisites).

**Figure 2-5:**   Tectonically deformed, ellipsoidal, felsic volcanic clasts set in a sucrosic, tuffaceous matrix. Unit 3: Felsic volcanic conglomerate, east of Round pond.

**Figure 2-6:**   Photomicrograph of hydrothermal breccia consisting of angular fragments of felsic volcanic rock set in a fluorite (dark) matrix. From drill core north of Round Pond. (mag. x10, plane polarized light).
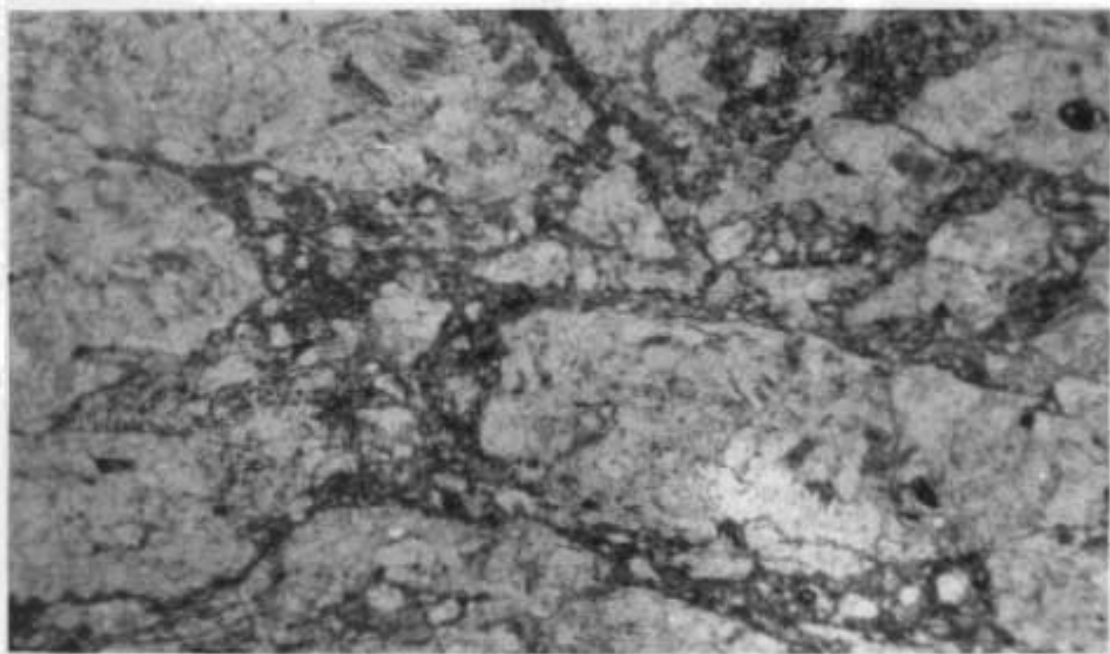
The most common clast type is a pink to white-grey, fine-grained felsic volcanic clast composed of finely recrystallized polygonal quartz and feldspar, with minor amounts of biotite, hornblende and magnetite. Clark (1973) stated that the major mineral portions of such clasts ranged from 20%-40% quartz, 30%-50% microcline and 40%-60% plagioclase, as estimated in this study. There are less common quartz-porphyritic felsic volcanic clasts, mafic amphibolite clasts and segregations, and rare granitic clasts. The granitic clasts which are not Monkey Hill Granite, appear as rounded clasts of white to grey, medium to coarse-grained granite. A thin section from one clast is composed of coarse-grained, subhedral albite phenocrysts, and lesser perthite, with medium to fine-grained euhedral orthoclase, and irregular quartz. Accessory minerals include diopside, sphene, and magnetite, with abundant carbonate replacement of the groundmass and embayment of the albite phenocrysts.

The matrix of the conglomeratic unit consists of medium to fine-grained sucrosic, felsic, tuffaceous material composed of polygonal, medium-grained albite, microcline, and quartz with minor calcite, diopside, hornblende, biotite and garnet (andradite). Locally, the matrix may be dominantly mafic (composed of amphibole, pyroxene and biotite), possessing a well defined foliation. On exposed surfaces, the matrix may weather out, preferentially leaving a "cobble-stone" weathering feature (see figure 2-5).

## 2.2.4. Unit 4: Metabasalt and Related Amphibolites

The metabasalt unit completely encircles the Round Pond anticlinal structure and is easily traced on air photos as a more or less continuous raised, annular ridge. The unit in the Round Pond area consists of mafic flows dominated by rocks of basaltic composition, with occasional minor andesitic flows. Best outcrop exposure occurs in the Falls Lake area where Clark (1973) recognised four thin, non-pillowed lava flows, each with a poorly developed autobrecciated base. The flows are intercalated with discontinuous felsic tuffaceous lenses (Gower et al., 1982). Maximum true thickness in the Round Pond area is estimated by Clark (1973) at approximately 300 m.

The sequence in the Round Pond area, is thought by Gower et al. (1982) to represent mafic tuffs and lavas of both subaqueous and subaerial origin. Pillows were not observed during this study, and have not been reported previously by either Clark (1973), or Gower et al. (1982). The unit contains relict vesicles and irregular calcite-biotite-hornblende blebs, possibly representing relict amygdules.

In outcrop, the unit varies from a dark green to grey to black, fine to medium-grained amphibole-rich rock, generally exhibiting a weakly developed tectonic fabric. Locally, coarse, "mottled" amphibole/feldspar textures are developed, as well as large 1-3 cm porphyroblastic aggregates identified by Stoeterau (1970) and Clark (1973) as scapolite. Optical examination of these porphyroblasts confirm the previous identification as scapolite, and the high birefringence noted by Clark (1973). The high birefringence indicates a high calcic composition of the scapolite, which is referred to as meionite (Deer et al., 1966). Porphyroblasts of hornblende and plagioclase also occur.

In thin section, the metabasalt exhibits a tectonic fabric formed by the alignment of hornblende and biotite. The rock is composed of fine to medium-grained hornblende and plagioclase, with minor to considerable amounts of metamorphic biotite, scapolite, epidote and carbonate, and accessory sphene, sericite and opaque minerals. Porphyroblasts are aggregates of medium-grained crystals of scapolite and plagioclase. Veinlets of epidote are common.

The andesitic member of this unit represents only a minor component, and appears as light to medium grey, medium-grained rock with vesicles and abundant coarse grained veinlets, pods and aggregates of hornblende and calcite. Similar descriptions were given by Gandhi (1978) for a lithology southeast of Round Pond which he termed as a massive to amygdaloidal andesitic flow, and by Stoeterau (1970), who described a calcite-and hornblende-rich rock northeast of Round Pond. Stoeterau (1970) however, thought that the lithology represented a metamorphosed intrusive dyke. Drill logs from north of Round Pond describe the calcite-hornblende-rich lithology as sheared metasediments (Sutton, 1964).

Interestingly, the lithology is similar to rock associated with radioactive showings to the south, and thus may be extensively altered.

In thin section, the andesites are composed of subhedral albite phenocrysts and abundant hornblende, as well as biotite and calcite, set in a polygonal groundmass of quartz, albite and sericite. Coarse pods of hornblende, biotite and calcite often occur with pyrite and rare molybdenite.

A number of mafic amphibolites are observed in the thesis area that are very similar to the metabasalt unit both in general appearance and petrography. The largest outcrop occurs east of Round Pond where it has been subsequently intruded by a stock of Monkey Hill Granite. Another small exposure occurs northwest of Round Pond. Both exposures lie stratigraphically below the metabasalt unit, and are concordant with regional trends. Another amphibolite to the east of Falls Lake lies stratigraphically above the metabasalt, but also appears concordant with regional trends. This amphibolite is characterized by secondary calcite-hornblende-biotite pods and fracture-fillings, not unlike the relict amygdules mentioned above. As well, calcsilicate pods and fracture-fillings are observed. Significant uranium mineralization is associated with this amphibolite as will be discussed later. The amphibolites possibly represent unrecognized basaltic flows, or are more likely subvolcanic intrusive sills related to the extrusive metabasalt.

## 2.2.5. Unit 5:  Banded Rhyolite

The banded rhyolite overlies the metabasalt, presumably conformably, although the contact relationships have not been observed. The unit is exposed both east and west of Round Pond, and is thin and discontinuous.

The lithology appears as a fine-grained, white to pinkish grey rock, exhibiting a generally well developed, fine, laminar banding, with minor, small ($<$ 1 mm) phenocrysts of quartz. The banding is 1-2 mm wide, and is defined by slight

colour differences. The bands are more or less continuous but are poorly developed in some places.

In thin section, the rhyolite is composed primarily of quartz, microcline and albite. Accessories include opaques, biotite and chlorite. The banding appears as medium-grained quartz-feldspar bands and aggregates exhibiting undulose extinction in a groundmass of fine-grained, polygonal, recrystallized, strain-free, quartz-feldspar (see figure 2-7).

The origin of the banding is not clear, previous workers referred to it as bedding (Gandhi et al., 1969), and flow banding (Clark, 1973). The extensive recrystallization of the groundmass surrounding strained phenocrysts and medium-grained bands suggests that the rocks have undergone a ductile recrystallization which has destroyed the primary features of the original banding. Thus, the origin of the banding is not clear. However, the fine grained nature of the lithology (despite recrystallization), and the fine laminar nature of the banding, suggest possibly an air fall ash origin for this unit.

Altered rhyolites also occur, and are generally distinguishable from unaltered rock. Rhyolites in the northeast corner of the map area, as well as a linear belt east of Falls Lake, appear to be altered. The altered rhyolite appears as a distinctive, bleached, white to light grey, banded to massive, sucrosic, quartz-albite porphyritic rhyolite. Some lithologies originally mapped by Clark (1973) as a transgresive arkose unit composed primarily of albite and quartz, may in fact be altered rhyolite. The altered rhyolite has undergone Na-metasomatism to be discussed below.

**Figure 2-7:** Coarse-grained, quartz-feldspar aggregates representing primary banding in a fine-grained, recrystallized, polygonal groundmass of quartz and feldspar. Unit 5: Banded rhyolite, CM-95 (mag. x10, X nicols).

**Figure 2-8:** Coarse quartz-microcline bands framing fine-grained, recrystallized, polygonal groundmass of quartz-microcline-albite. Unit 6: Quartz-feldspar porphyritic rhyolite (mag x10, x nicols).
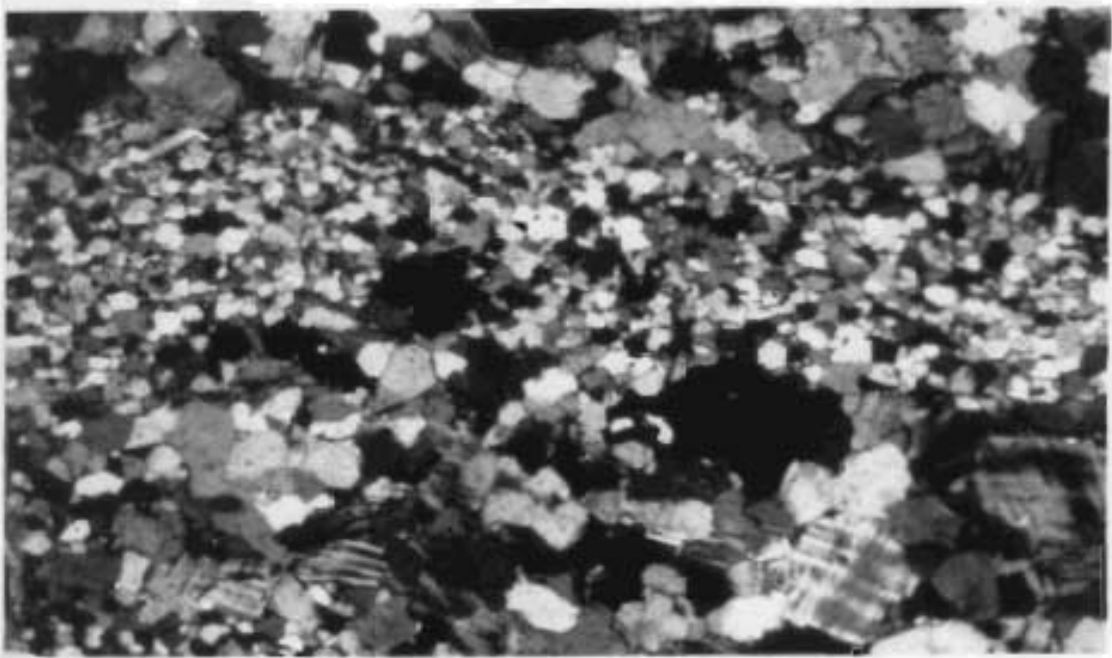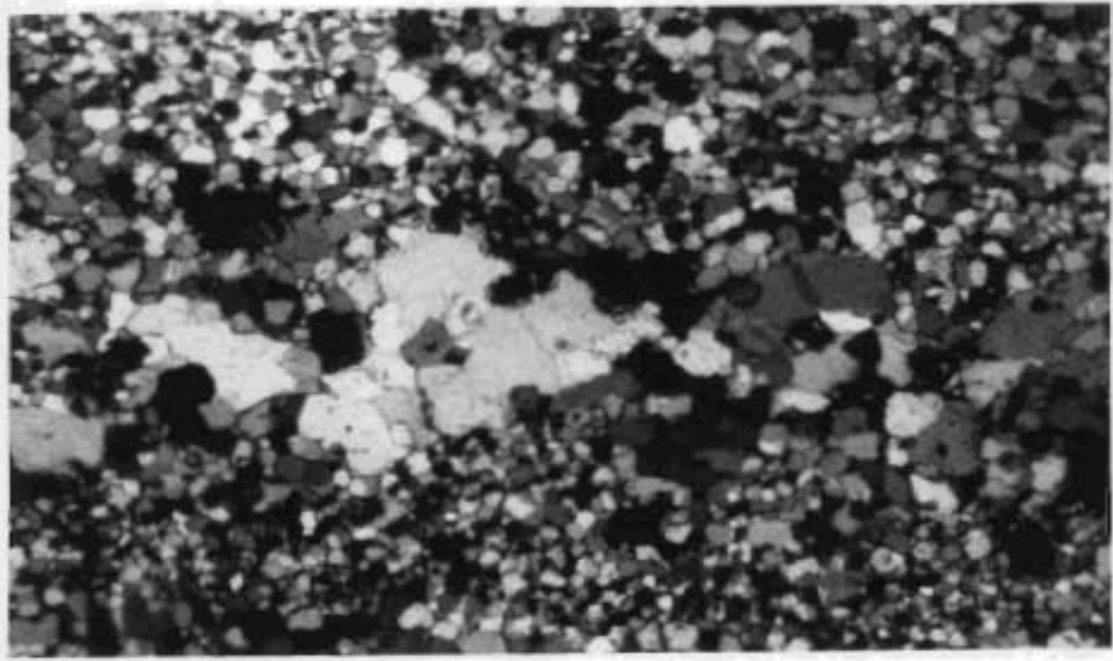
In thin section, the altered rhyolites are composed of numerous coarse aggregates of quartz and albitic phenocrysts (1-4 mm) set in a fine-grained groundmass of polygonal quartz, albite, minor microcline and calcite. Accessory minerals include streaks and pods of diopside, biotite, epidote and fluorite, which generally highlight any banding present.

## 2.2.6. Unit 6: Quartz-Feldspar Porphyritic Banded Rhyolite

The quartz-feldspar porphyritic banded rhyolite is best exposed in the eastern portions of the map area. The unit conformably overlies the lower banded rhyolite unit; contacts appear gradational but are complicated by interfingering of the two units. Lithic fragments and lenses of felsic volcanic agglomerate and tuff are common.

In outcrop, the rock appears as a grey to dark pink rhyolite with varying portions of quartz and feldspar phenocrysts ranging from 1-3 mm in size. Banding is generally evident but in some areas, it is poorly developed or absent all together. Banding appears as alternating grey to pink, discontinuous, coarse (1-2 mm) bands, that form resistant ridges on weathered surfaces.

In thin section, the unit is composed primarily of quartz and microcline, with minor albite. Accessories include biotite, chlorite, opaques such as magnetite and pyrite, and rare fluorite. Banding appears as discontinuous, linear streaks of medium-grained, strained, quartz-microcline, in a groundmass of fine-grained, polygonal, recrystallized, quartz-microcline-albite (see figure 2-8). Minor to abundant aggregates of quartz and coarse, subhedral microcline crystals representing relict phenocrysts are also present (see figure 2-9).

The banding was interpreted by Clark (1973) as normal igneous flow banding, and that the observed mineralogical differentiation between bands was due to syn- to post-volcanic migration of $Na_2O + CaO$ from $K_2O$ during spherulitic crystallization. The recrystallization indicates a ductile deformation as

mentioned above. Such recrystallization is commonly associated with mylonitic rocks (Bell and Etheridge, 1973). However, the rocks in Round Pond do not exhibit any evidence of translational movement characteristic of deformed mylonite zones. The banding thus represents a recrystallization of primary volcanic bands in response to ductile deformation of the rocks of the Upper Aillik Group.

The general lack of sorting with respect to phenocrysts, the discontinuous nature of the banding, and the association of lithic fragments, agglomerates, and banded ash tuffs, suggests an ignimbritic origin for this unit.

### 2.2.7. Unit 7: Quartz-Feldspar Porphyritic Rhyolite

The quartz-feldspar prophyritic rhyolite crops out on the southeast slopes of Monkey Hill, overlying the conglomerate unit. Clark (1973), who mapped the area as a plagioclase-porphyritic rhyolite, stated that the exposure covered an area of approximately 8 km$^2$. Gower et al. (1982), disagreed with Clark concerning this unit, stating that rocks in the area possessed good sedimentary structures and are in fact, arkosic sandstone. However, in the course of this study, a quick investigation of outcrop exposed in the area did not reveal any sedimentary structures but did confirm the presence of a quartz-feldspar porphyritic rhyolite. Areal distribution of the unit will remain as Clark (1973) has shown. In addition, a small exposure of the lithology occurs east of Round Pond as mapped by Stoeterau (1970).

The unit appears in outcrop as a fine-grained, pink to red-brown lithology with 1-10 mm in diameter phenocrysts of quartz, microcline and plagioclase. Quartz phenocrysts are dominant southwest of Round Pond and are locally exclusive. The outcrop east of Round Pond contains abundant K-feldspar phenocrysts 5-6 mm in diameter, that weather to conspicuous white "eyes".

**Figure 2-9:** Coarse aggregates of quartz exhibiting undulose extinction in a fine-grained, recrystallized, polygonal matrix of quartz-feldspar.
Unit 6: Quartz-feldspar porphyritic banded rhyolite (mag. x10, x nicols).

**Figure 2-10:** Coarse phenocryst of microcline in a finely recrystallized groundmass of polygonal quartz-feldspar.
Unit 7: Quartz-feldspar porphyritic intrusive rhyolite (mag. x10, x nicols).
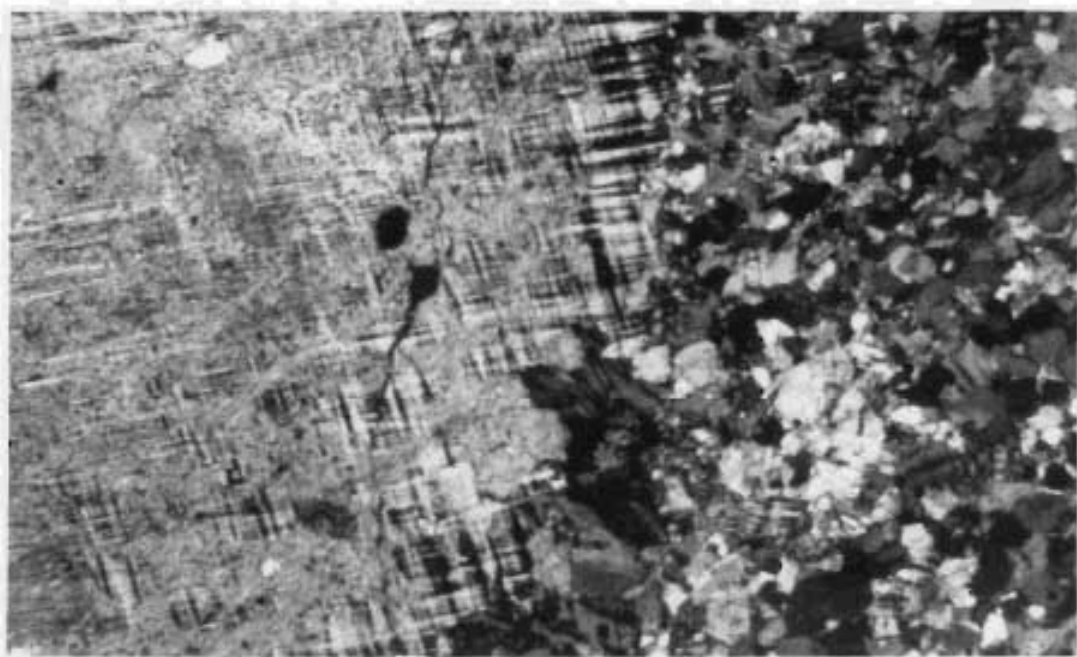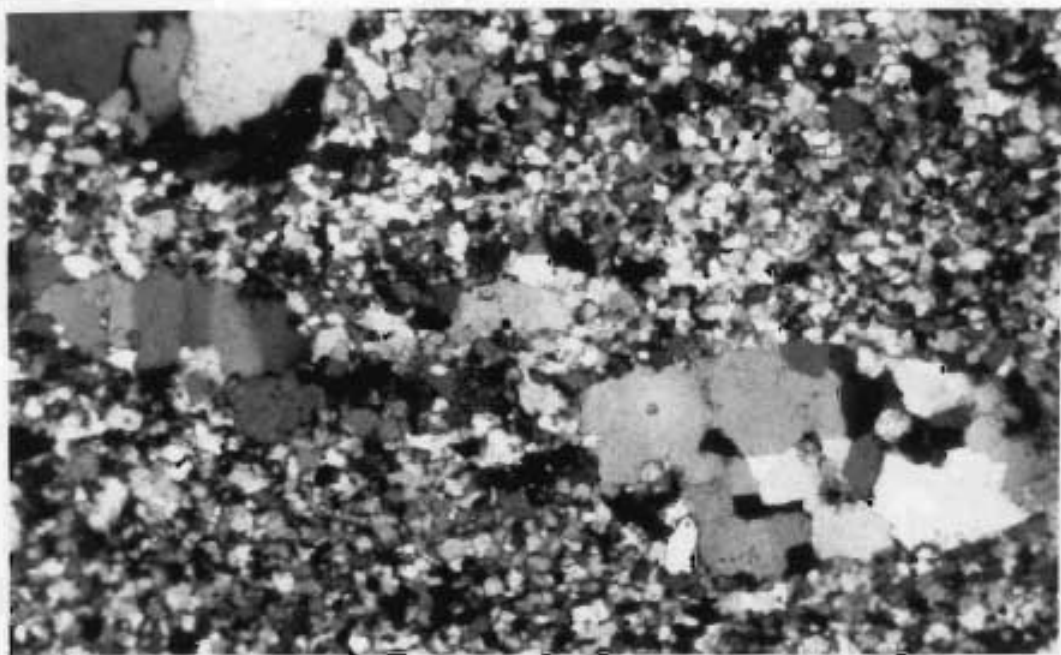
In thin section, the unit possesses a groundmass of finely recrystallized polygonal quartz and feldspar, with accessory hornblende, diopside, biotite, sphene, carbonate, fluorite and magnetite. Phenocrysts consist of recrystallized aggregates of quartz, microcline, and albite grains (see figure 2-10).

Clark (1973) favoured an extrusive origin for this unit based largely on the conformable nature of the unit, the lack of apophyses and the fact that no evidence of chilled-margins survived metamorphic recrystallization. However, the coarse grain size of feldspar phenocrysts (up to 10 mm) would tend to suggest an intrusive origin. An identical feldspar porphyry located east of Round Pond, occurs as a small dyke-like body clearly cross cutting several lithologies, and thus appears to be intrusive as suggested Stoeterau (1970). Geochemical evidence (discussed below) indicate compositions very similar to other stratigraphically higher rhyolites, suggesting that this unit may be a hypabyssal equivalent. An intrusive origin is thus favoured for this unit.

## 2.3. Structure

Early structural observations centered on the recognition of a few regional folds and faults, and a penetrative S-type fabric, all of which were interpreted by Gandhi et al. (1969) as representing a single cycle of orogenic deformation. However, complex polyphase deformational features are widespread in the study area, and have been interpreted by Clark (1973) as the result of at least four phases of Hudsonian (ca. 1800 Ma.(Stockwell, 1973)) deformation. The deformational event is now termed the Makkóvikian Orogeny (ca. 1800 Ma.) (Wardle et al., 1986). Clark (1973) described the four phases of deformation as follows: $D_1$ locally defined by relict mineral orientation of platy minerals; $D_2$ dominant, widespread deformational event which produced regional, upright, northeast trending folds and penetrative fabrics; $D_3$ and $D_4$ refolded $D_2$ fabrics and folds, and produced the regional interference fold patterns, but with no

associated fabrics. Gower et al. (1982) also suggested that the area exhibits features of polyphase deformation (similar to Clark, 1973) related to the Hudsonian Orogeny, and indicated as many as six phases of deformation may have occurred. Evidence from this study does not support Clark's (1973) designation of $D_1$ and $D_3$ as separate deformational events, and only two major deformational events are considered in this thesis.

The first deformational event described by Clark (1973) was defined on the basis of mineral orientation of biotite and hornblende preserved in scapolitic porphyroblasts within the metabasalt unit. Clark (1973) ascribes a pre to syn-$D_2$ origin for the porphyroblasts. Field observations and microscopic examination of the porphyroblasts suggests that they are post-$D_2$. There is no evidence of later deformation (ie. flattening), or the development of augen textures and pressure shadows, and the porphyroblasts appear to have overgrown metamorphic mineral assemblages which generally show a $D_2$ mineral orientation. The interpretation is further complicated however by possible hydrothermal mineral growth related the intrusion of post-tectonic granites.

The third deformational event described by Clark (1973) apparently resulted in only minor refolding of earlier folds and fabrics. In the Round Pond area, a small antiform considered by Clark (1973) to be southward plunging at 20° occurs southeast of Round Pond. Structural determinations in the field do suggest the presence of such a fold, but not enough determinations were gathered to confirm the plunge. The axial plane of this fold is parallel to an earlier regional anticlinal fold in the area, and no firm structural evidence was observed to suggest that it is in fact the result of a later deformational event. As a result the small fold southeast of Round Pond is considered to be related to same deformational event as the larger, regional anticline in the study area.

Evidence for only two deformational events is found in the Round Pond area. The two events which are referred to as $D_1$ and $D_2$ in this study correspond to Clark's (1973) $D_2$ and $D_4$ deformational events respectively.

## 2.3.1. $D_1$: First Deformational Event

The first apparent deformational event in the Round Pond area was widespread, producing penetrative fabrics and large, upright, N-NE trending folds (see Map-1, back pocket). Within the Round Pond area, the major structural feature developed during the first deformational event has been interpreted by previous workers (Gandhi et al., 1969, Clark, 1973) as a broad, open, upright, NE trending, doubly plunging, domal anticline fold, with a vertical axial plane, and a 40-60' dip on the fold limbs. Clark (1973) suggested that the observed variable axial plunge of the fold is the result of overprinting by a later $D_2$ east-west trending fold which resulted in large scale, open refolding, producing the observed interference fold pattern (ie. domal anticline). The interference pattern is consistent with theoretical patterns described by Ramsay (1967) for folds of similar orientation. A minor $F_1$ anticlinal fold also occurs to the southeast of Round Pond as discussed above. Extensive microfolding of banded lithologies and mafic dykes is observed throughout the area, and represent parasitic folds whose fold axis parallel the regional $F_1$ axial plane.

Lithological units within the study area exhibit subvertical, penetrative, S-type fabrics ($S_1$), and gently plunging lineations ($L_1$) that parallel the $F_1$ fold axes, and define the regional anticlinal structure. The felsic volcanic conglomerate is perhaps one of the most useful marker horizons. In the north part of the map area, the conglomerate exhibits prolate (cigar-shaped) clasts near the axial fold hinge demonstrating a lineation along the $F_1$ fold axis. A northerly shallow plunge of is observed within the clasts. On the fold limbs (ie. east of Round Pond) the clasts are oblate, striking parallel to the $F_1$ axial plane, and steeply dipping (see map-1, back pocket).

Figure 2-11 is a Flinn diagram which represents theoretical strain states of a strain ellipsoid, and illustates the fields of oblate versus prolate ellipsoids. Clasts near the fold hinge have undergone uniaxial extension along the fold axis ($K > 1$), while clasts on the fold limbs exhibit uniaxial flattening ($K < 1$) striking parallel to

the axial plane. Thus the value for K exhibits considerable variation within the study area. Clark (1973) observed a lack of consistency of in K values based on calculations made from deformed clasts, lithophysae, and phenocrysts from various lithologies in the area. He did not define the trend solely within a single lithology, thus introducing the possibility of variations due to rheological contrasts. Clasts observed solely within the conglomerate in this study verify his observations. Clark (1973) suggested that the second phase of deformation was the result of simple shear, with variations in K values due to modifications by pure shear. However, K variations may also reflect differing strain fields developed during folding related to fold geometry. Thus variations in clast deformation may be useful during field mapping to establish fold geometry.
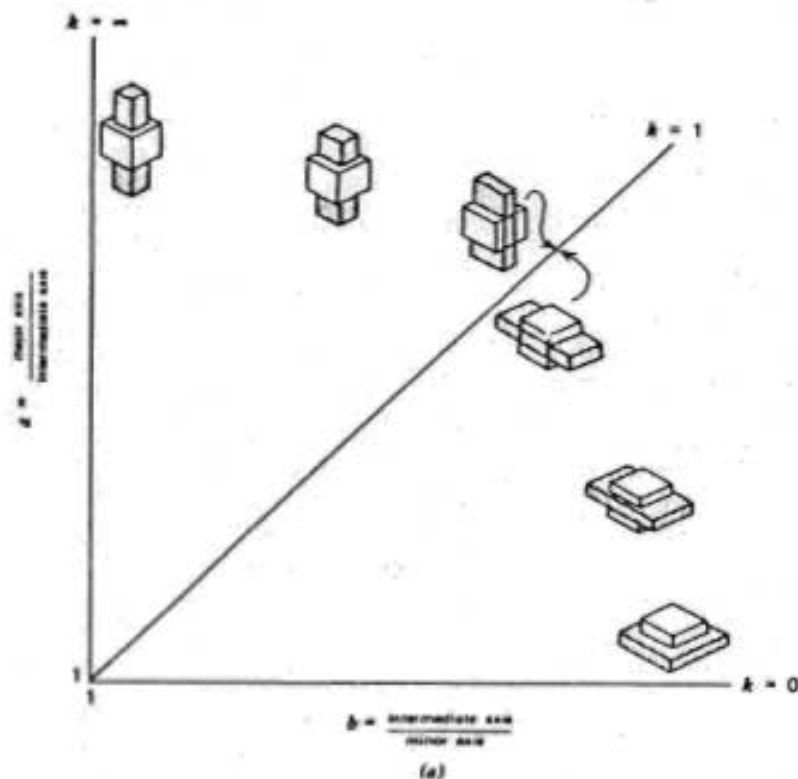


**Figure 2-11:**   Flinn diagram illustrating the fields
of oblate versus prolate strain ellipoids
(from Hobbs et al., 1976).

Banded rhyolites provide the only other lithology that exhibits widespread, macroscopic, structural features. The banded rhyolitic lithologies possess steeply dipping, northeast striking planar S-type fabrics, and gently plunging, northeast trending lineations, expressed as colour banding and deformed, flattened phenocrysts (see map-1 for trends). The banding parallels the northeast striking $F_1$ axial plane of the anticlinal structural and is clearly related to the $D_1$ structural deformation. As discussed above, the banding is the result of ductile recrystallization of original primary volcanic banding in response to deformation. Thus the banding represents a relict primary feature that has been modified by the $D_1$ deformational event.

Orientations of platy minerals such as biotite and hornblende are best observed on the metabasalt and related amphibolitic units, but are complicated by post-metamorphic mineral growth related to hydrothermal activity of post-tectonic granites.

### 2.3.2. $D_2$: Second Deformational Event

The most significant feature associated with the second deformational event $D_2$, (referred to by Clark, 1973 as $D_4$), is the development of an $F_2$ fold with an easterly trending, steeply dipping, fold axis, producing an interference dome with the earlier $F_1$ anticline in the Round Pond area (Clark, 1973). The outcrop pattern observed in the Round Pond area clearly suggests the presence of such a structure, as does the variable plunges observed on the $F_1$ fold axes. Amphibolitic dykes folded about an $F_1$ fold axis, were observed in the Round Pond area to be refolded about an easterly trending ($F_2$) fold axis (see figure 2-12). Less conclusive, is the elongate, ellipsoid nature of the granitic plugs which suggests elongation perpendicular to the $F_4$ fold axis. Similar interference pattern folds are found at showing #5 near Winter Lake (Wilton pers. com., 1987).

Post-$D_2$ deformational features include northwesterly to northeasterly trending faults and conjugate fracture sets. A northwestly trending fault has been
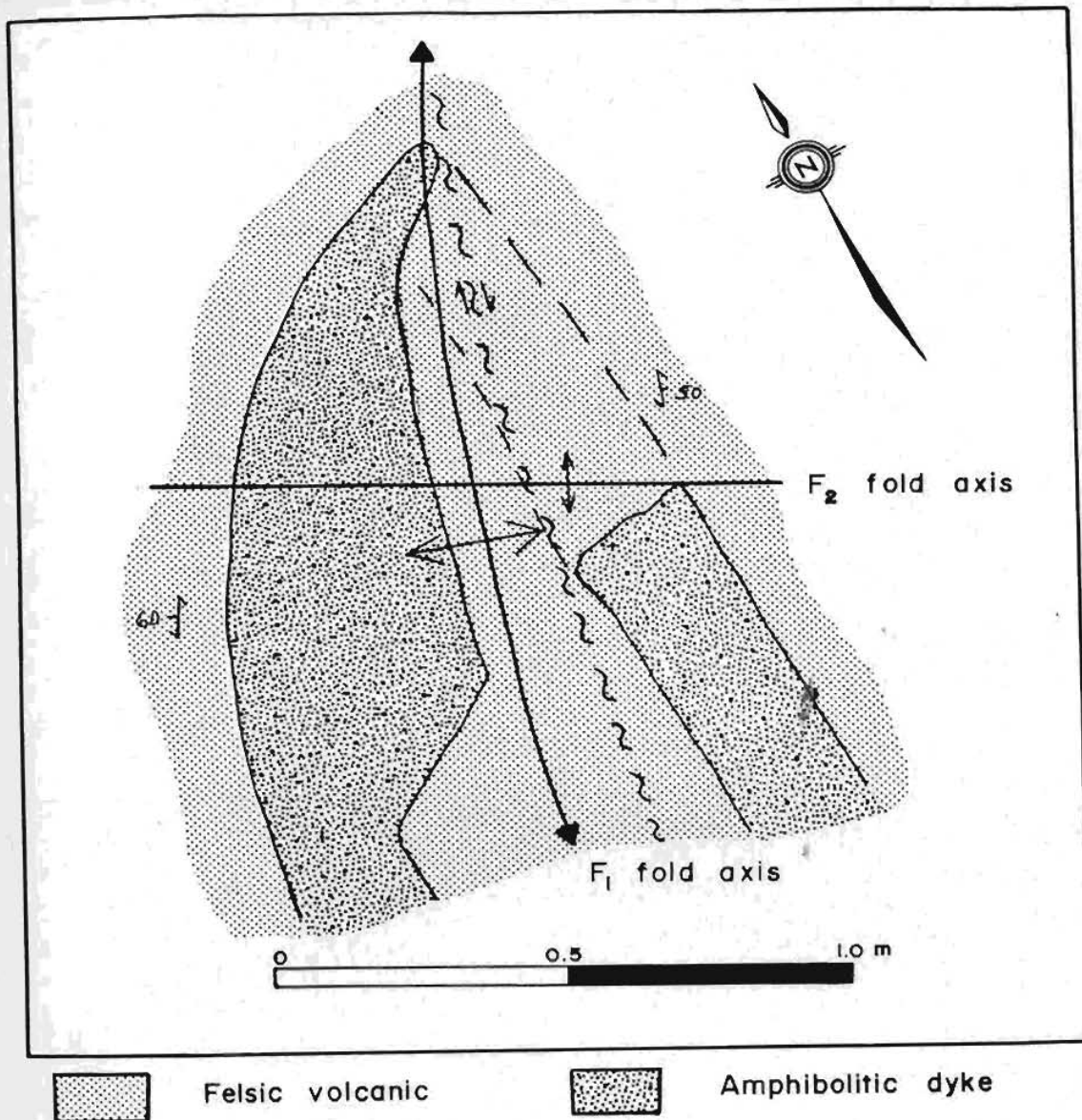
**Figure 2-12:** Amphibolitic dyke east of Round Pond exhibiting later $F_2$ folding superimposed on earlier $F_1$ recumbant folding.

assumed in the Round Pond to the northeast, with little or no significant displacement observed. Conjugate fracture sets are widespread. Many of the fractures are unfilled, but some contain quartz. Other fractures are observed to be pyritiferous and are rusty; these are related to a mineralizing event to be discussed later. No Grenvillian deformational features have been observed in the

Round Pond area, and previous workers (ie. Gower et al., 1982; Wardle et al., 1987; MacKenzie and Wilton, 1988), restrict Grenvillian deformation to rocks south of the Adlavik Brook Fault (ie. Michelin area).

## 2.4. Metamorphism

Metamorphism in the Round Pond-Falls Lake area is thought to have attained upper greenschist/lower amphibolite facies (Clark, 1973, Gandhi, 1978, Gower et al., 1982) during the Hudsonian Orogeny. Felsic volcanic rocks of the Upper Aillik Group have undergone extensive recrystallization which resulted in the destruction of primary textural features, and the development of coarse, sucrosic textures characterized by unstrained, polygonal recrystallization. Some lithologies locally possess garnet and diopside which appear to have nucleated and grown from triple point junctions, thus indicating they are later than polygonal recrystallization.

Metamorphism is best defined by amphibolitized basaltic volcanic rocks which exhibit metamorphic mineral assemblages of quartz, albite, hornblende, biotite, diopside and chlorite, which are overgrown by scapolitic and hornblende porphyroblasts. Contact metamorphic effects and hydrothermal alteration associated with the post-tectonic granitic stocks are discussed in   later sections (see section 4.4).

## 2.5. Geochemistry of the Upper Aillik Group

Major and trace element analyses were completed on approximately fifty unmineralized samples representative of the Upper Aillik Group in the Round Pond-Falls Lake area. Table 2-1 lists the average compositions of the various lithologies; complete analyses and analytical methods are given in Appendix I.

**Table 2-1:** Average chemical compositions of major lithologies of the Upper Aillik Group in the Round Pond area.

| Unit: | 1 | 2a | 2b | 3 | 4 | 4a | 5 | 5a | 6 | 7 |
|---|---|---|---|---|---|---|---|---|---|---|

Major Elements (wt.%)

| | 1 | 2a | 2b | 3 | 4 | 4a | 5 | 5a | 6 | 7 |
|---|---|---|---|---|---|---|---|---|---|---|
| SiO2 | 75.3 | 60.4 | 67.5 | 72.2 | 48.4 | 48.3 | 73.0 | 75.5 | 73.8 | 75.6 |
| TiO2 | 0.29 | 0.44 | 0.46 | 0.42 | 0.82 | 2.32 | 0.28 | 0.16 | 0.23 | 0.28 |
| Al2O3 | 11.8 | 18.7 | 13.5 | 12.3 | 17.0 | 14.1 | 12.4 | 11.9 | 12.2 | 12.1 |
| Fe2O3 | 3.83 | 3.67 | 4.34 | 3.46 | 11.3 | 15.7 | 2.80 | 2.58 | 3.15 | 2.63 |
| MnO | 0.10 | 0.14 | 0.18 | 0.13 | 0.19 | 0.29 | 0.05 | 0.12 | 0.03 | 0.04 |
| MgO | 0.09 | 1.33 | 1.21 | 1.29 | 7.80 | 4.10 | 0.36 | 0.49 | 0.11 | 0.20 |
| CaO | 0.69 | 2.20 | 2.78 | 2.68 | 7.79 | 6.41 | 0.53 | 0.98 | 0.36 | 0.43 |
| Na2O | 6.99 | 7.86 | 4.62 | 6.40 | 4.43 | 5.17 | 3.78 | 6.22 | 3.85 | 3.21 |
| K2O | 0.20 | 4.37 | 5.18 | 1.15 | 1.35 | 1.54 | 5.38 | 1.07 | 5.12 | 5.65 |
| P2O5 | 0.00 | 0.11 | 0.80 | 0.00 | 0.00 | 0.69 | 0.05 | 0.01 | 0.03 | 0.00 |
| LOI | 0.17 | 1.36 | 0.33 | 0.41 | 1.09 | 0.60 | 0.55 | 0.50 | 0.35 | 0.29 |

Total   100.53   100.48   99.23   99.53   100.72
  99.46   100.9   100.14   99.18   99.23

Trace Elements (ppm)

| | 1 | 2a | 2b | 3 | 4 | 4a | 5 | 5a | 6 | 7 |
|---|---|---|---|---|---|---|---|---|---|---|
| Pb | 17 | 28 | 21 | 28 | 43 | 44 | 25 | 32 | 39 | 29 |
| U | 1 | 1 | 2 | 1 | 0 | 8 | 5 | 6 | 2 | 9 |
| Th | 15 | 9 | 20 | 22 | 2 | 3 | 15 | 15 | 16 | 25 |
| Rb | 2 | 127 | 164 | 35 | 72 | 80 | 134 | 28 | 128 | 150 |
| Sr | 43 | 360 | 136 | 110 | 477 | 711 | 59 | 67 | 44 | 90 |
| Y | 64 | 18 | 58 | 36 | 24 | 67 | 40 | 63 | 67 | 67 |
| Zr | 339 | 83 | 333 | 240 | 48 | 229 | 409 | 399 | 454 | 495 |
| Nb | 22 | 5 | 19 | 19 | 5 | 16 | 24 | 22 | 25 | 36 |
| Ga | 24 | 21 | 19 | 20 | 18 | 22 | 21 | 25 | 24 | 28 |
| Zn | 121 | 72 | 162 | 181 | 261 | 870 | 13 | 57 | 105 | 13 |
| Cu | 5 | 7 | 9 | 3 | 11 | 76 | 9 | 6 | 6 | 6 |
| Ni | 0 | 0 | 9 | 2 | 57 | 1 | 0 | 0 | 0 | 0 |
| La | 72 | 7 | 79 | 27 | 0 | 7 | 33 | 53 | 77 | 52 |
| Ti | .22 | .42 | .40 | .43 | .83 | 2.24 | .28 | .16 | .25 | .27 |
| Ba | 119 | 2030 | 1613 | 361 | 692 | 2107 | 1478 | 145 | 647 | 585 |
| V | 0 | 111 | 15 | 29 | 202 | 143 | 24 | 4 | 2 | 2 |
| Ce | 137 | 40 | 109 | 47 | 29 | 89 | 103 | 46 | 73 | 67 |
| Cr | 0 | 17 | 13 | 5 | 41 | 0 | 2 | 0 | 0 | 0 |
| n | 3 | 2 | 2 | 5 | 8 | 3 | 3 | 5 | 15 | 2 |

n - number of analyses

Ti - wt.%

Geochemical analyses clearly indicate the bimodal nature of the Upper Aillik Group with respect to $SiO_2$ (see figure 2-13). Volcanic rocks of rhyolitic composition (> 70 wt% $SiO_2$) dominate the Upper Aillik lithologies in the thesis area, with basaltic rocks comprising the low $SiO_2$ compositions. The lack of rocks with intermediate compositions such as andesites is conspicuous, and has been noted by previous workers (eg. White, 1976; Gandhi, 1984).

In order to test the possibility that rocks of the Upper Aillik Group may have been subjected to synvolcanic, metamorphic, and/or hydrothermal alteration, geochemical data have been plotted on figure 2-14. The diagram, devised by Hughes (1973), uses the mobile alkalies $Na_2O$ and $K_2O$ to outline an area which represents the "igneous spectrum". This spectrum identifies rocks which are thought to exhibit only minimal disturbance of the alkalies from primary concentrations. Conversely, rocks which plot outside the "igneous spectrum" exhibit pronounced soda or potash metasomatism. However, it should be noted that rocks which lie within the "igneous spectrum" may still have undergone considerable change in $K_2O/Na_2O$ values, and thus a note of caution is mentioned. As can be observed from figure 2-14, a large proportion of rocks analyzed from the Upper Aillik Group exhibit pronounced soda metasomatism. The metasomatism is evident in all lith-ologies to some degree, except the uppermost rhyolite members, and is characterized by the enrichment of Na and depletion of K.

Barua (1969) recognized soda enriched rocks in the Aillik Bay area and suggested they were splitized lavas. White (1976), who was the first to recognize the soda enrichment as a metasomatic event within the felsic volcanic rocks, attributed the metasomatism to circulation of synvolcanic magmatic or meteoric fluids. Gower et al. (1982) suggest that stratigraphically lower portions of the Upper Aillik Group were deposited under shallow marine conditions, which gradually evolved into a subaerial environment. In such a case the observed soda metasomatism could result from interaction with sea water, as suggested by Evans (1980). The observed, widespread Na-metasomatism exhibited by the lower-most units of the Upper Aillik Group appears to represent a synvolcanic metasomatic event as suggested by previous workers (above). However, similar alkali metasomatism associated with many of the localized

uranium and molybdenite mineral occurrences hosted within the Upper
Aillik Group appear to be the result of later alkali leaching/enrichment
processes along discordant shear zones with which the mineralization is
associated (see Chapter5).
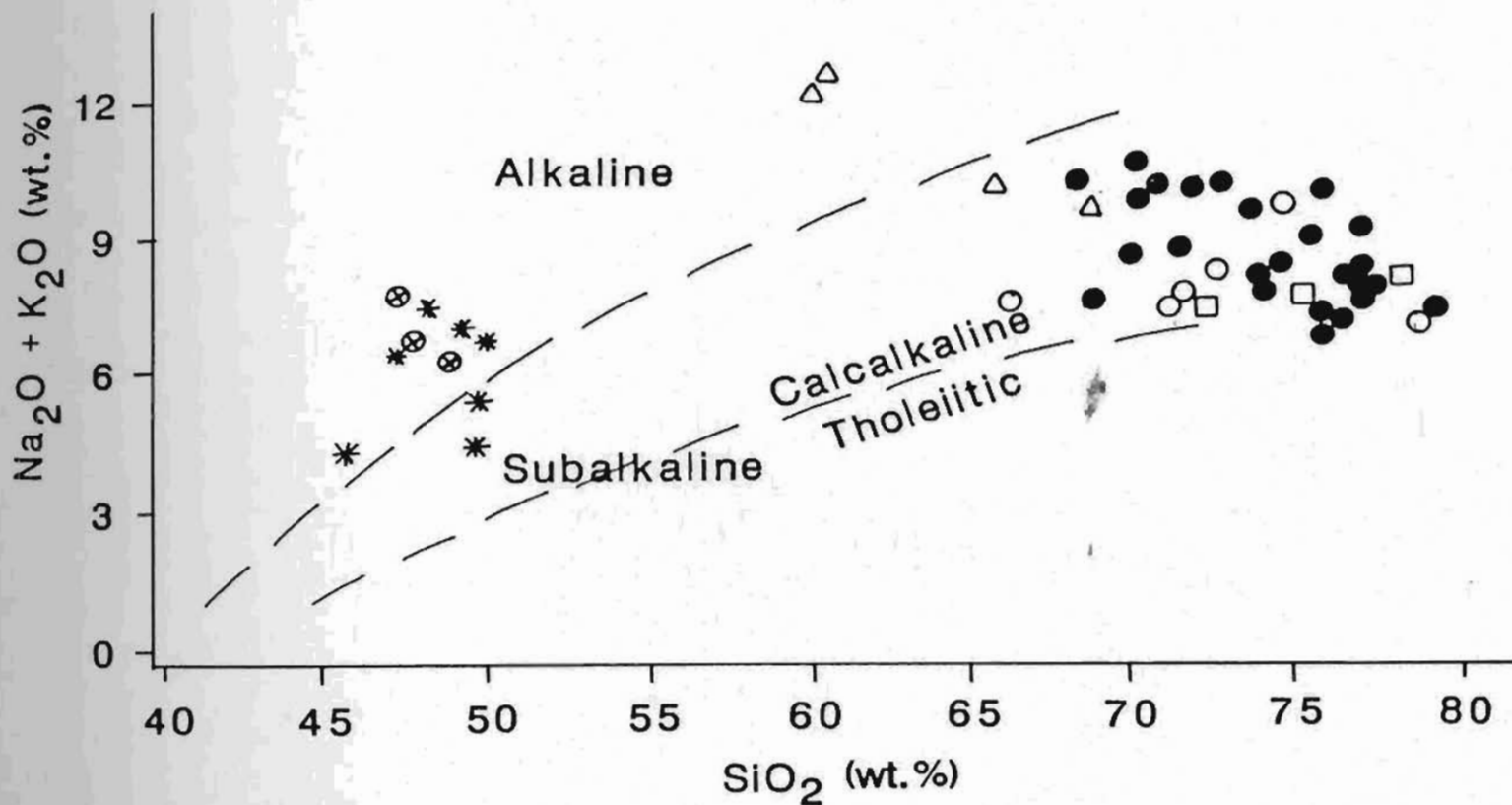


**Figure 2-13:** Total alkalies versus silica for the
Upper Aillik Group at Round Pond.

Symbols

● - Rhyolites (units 5, 6, 7)
⊗ - Amphibolites (unit 4A)
✳ - Basalts (unit 4)
○ - Felsic conglomerate (unit 3)
△ - Banded tuff (unit 2)
□ - Recrystallized tuff (unit 1)
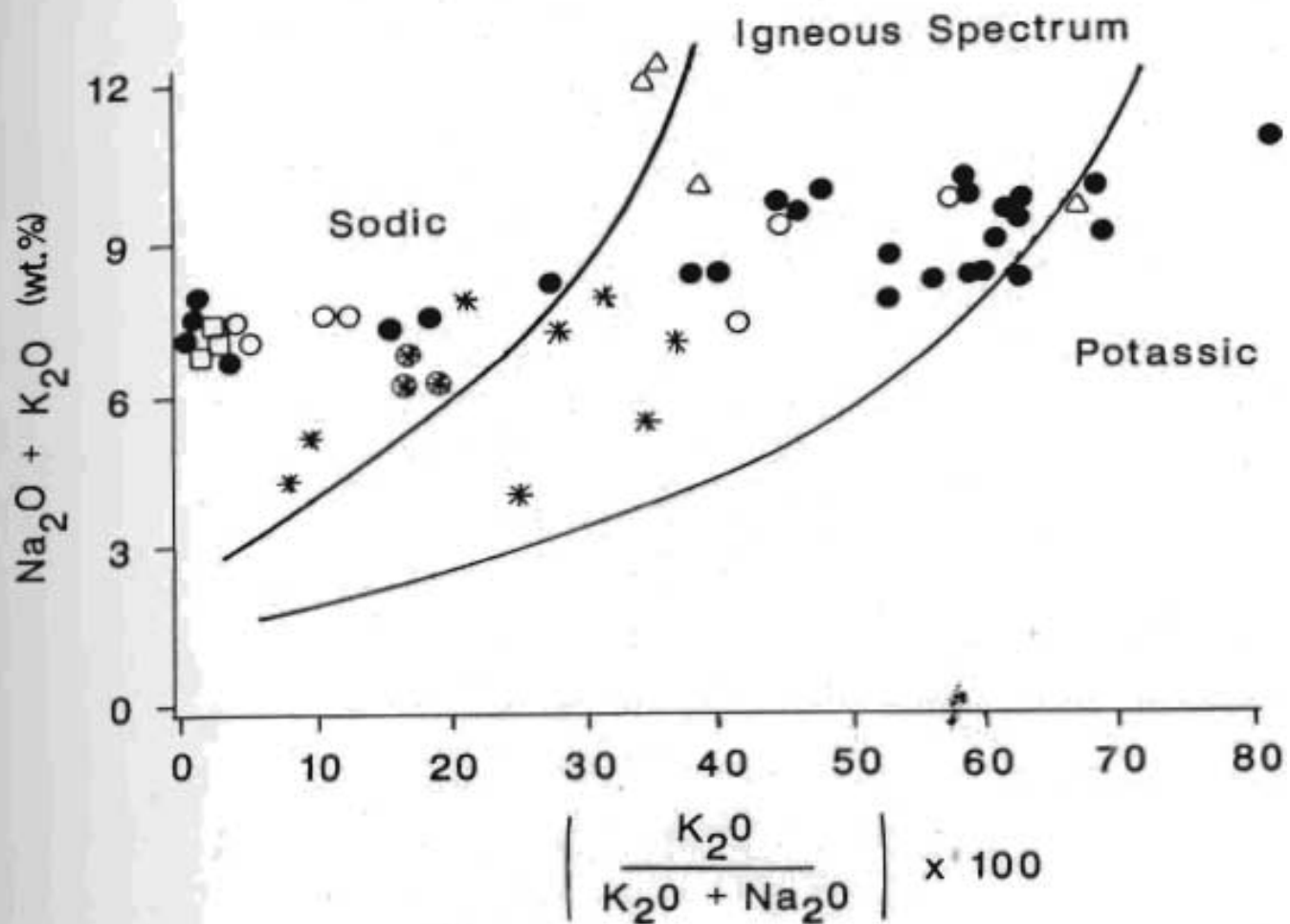
**Figure 2-14:** Upper Aillik Group volcanics in relation
to the "igneous spectrum" of Hughes (1973),
symbols same as above.

The Upper Aillik Group in the thesis area is dominated by calc-alkaline felsic volcanic rhyolites and related rocks, corresponding to the data of Evans (1980) for the inland portions of this group near the Michelin Deposit. Bailey (1979), Evans (1980), and Wardle and Bailey (1981) classified the rhyolites as calc-alkaline. This conclusion is supported by figure 2-13. Other workers (White, 1978; White and Marten, 1980; and Gandhi, 1978) suggest the rhyolites are alkaline to mildly peralkaline, and state that calc-alkaline trends observed are the result of the alkali metasomatism. From their published data however, it appears that only

altered rhyolites tend to exhibit peralkaline compositions. Payette and Martin (1986) also suggested an alkaline composition for the Upper Aillik based on the compositions of trapped melt inclusions from rhyolites in the Michelin area. Based on a recalculation of $SiO_2$ upwards to 73 wt.% to account for silica deposition on the inclusion walls, they suggest a composition of $Al_2O_3$ at 14.87 wt.%, $Na_2O$ at 3.18 wt. %, and $K_2O$ at 9.48 wt.% for the Upper Aillik Group. This most unusual composition clearly would not plot within Hughes (1973) "Igneous Spectrum", and suggests that the melt inclusions were susceptable to the alkali metasomatism suffered by the rhyolites of the Upper Aillik Group. From this study, unaltered rhyolites from the Round Pond area possess compositions which clearly suggest a high-K calc-alkaline trend.

## 2.5.1. Unit 1: Recrystallized Felsic Tuff

The recrystallized felsic tuff, for which there is no previous geochemical data, is characterized by high $SiO_2$ averaging >75 wt.%, enriched $Na_2O$ averaging nearly 7.00 wt.%, and depleted $K_2O$ averaging 0.20 wt.%. The unit clearly exhibits the effects of soda metasomatism, and use of the geochemical analyses to speculate the origin of this lithology is greatly reduced.

The unit, which has been mapped by previous workers as a quartzite (Gandhi et al., 1969), and as a granodiorite (Clark, 1973), does not bear any geochemical similarity to various analyses of quartzites from the Aillik Group, or syntectonic granitic bodies whose analyses are reported by White (1976), Evans (1980), Gower et al. (1982), and Gower and Ryan (in press). $SiO_2$ is too high for a granodioritic composition as suggested by Clark (1973), and is chemically similar to the soda enriched rhyolites higher in the stratigraphy; therefore suggesting a volcanic rather than plutonic origin.

### 2.5.2. Unit 2: Tuffs and Volcaniclastic Sediments

Banded tuffs and associated volcaniclastic sediments of unit 2 exhibit considerable geochemical variation. Two geochemically distinct groups of volcanic tuffaceous rocks are listed in Table 2-1. Variations in $SiO_2$, $Al_2O_3$, $Na_2O$, $K_2O$, and CaO are apparent. Analyses reported here are comparable to those reported by Gower et al. (1982), and Gower and Ryan (1987).

### 2.5.3. Unit 3: Felsic Volcanic Conglomerate

Geochemical data for the felsic volcanic conglomerate have not been described by previous workers. The unit averages > 72 wt.% $SiO_2$, enriched $Na_2O$ (> 6.00 wt.%), and depleted $K_2O$, (averaging just over 1.00 wt.%). All but one of the five samples analysed possessed a CaO content of $\geq$ 3.00 wt.% Only one sample (CM-119, see Appendix I) plotted within the "igneous spectrum" defined by Hughes (1973); the others exhibit soda metasomatism. Thus it might be reasonable to suggest that this particular sample may represent a reasonably close estimation of the original composition of this unit. The high $SiO_2$ contents and similar geochemical trends observed in other felsic volcanic rocks in the area support derivation from a felsic volcanic source.

### 2.5.4. Unit 4: Metabasalt and Related Amphibolites

Geochemical analyses of amphibolites and metabasalts from the Lower Aillik Group are abundant and have been described by White (1976), Evans (1980), and Gower et al. (1982). Only two analyses for the metabasalt from the Upper Aillik Group have been described (Gower et al., 1982), and these are from a metabasalt unit well to the west of the thesis area along the western shore of Makkovik Bay in the vicinity of Big Head (R. Wardle, pers. comm., 1987). Thus, the analyses reported here are the first for the metabaslt in the Round Pond-Falls Lake area. The average analysis in Table 2-1 is derived from eight analyses of the metabaslt unit and includes one analysis from the stratigraphically lower amphibolite east of Round Pond (sample 71, Appendix I). Three analyses for the stratigraphically

higher amphibolitic unit east of Falls Lake are listed separately due to obvious geochemical differences.

Table 2-2 lists previous analyses for various amphibolites and basalts in the area. The metabasalt in the Round Pond-Falls Lake area exhibit higher $Al_2O_3$ and $Na_2O$, and lower CaO, $TiO_2$ and $P_2O_5$ values than the analyses of the same unit provided by Gower et al. (1982). The metabasalt in the thesis area also exhibits some degree of soda metasomatism (see figure 2-15).

Compared to the basalts and amphibolites of the Lower Aillik Group, the metabasalt in the thesis area possesses higher $Al_2O_3$, MgO, $Na_2O$ and $K_2O$ contents, and lower $SiO_2$, $TiO_2$, and $Fe_2O_3$ $_T$. Systematic decreases in $Fe_2O_3$, and increases in MgO and CaO from Lower to Upper Aillik Group basalts noted by Gower et al. (1982), led them to suggest that successively less fractionated magmas were being tapped with time. Although these broad trends are observed, the metabasalt in the Round Pond area is geochemically distinct from Upper Aillik basalts at Makkovik Bay, and may represent an even less fractionated source magma for the basalts in the Round Pond area.

The basalts in this study exhibit alkaline to slightly subalkaline tendencies (see figure 2-13), but alkali enrichment as a result of alteration is probable. Figure 2-15 indicates that the basalts in the Round Pond-Falls Lake area are tholeiitic. Various trace element plots using trace elements generally regarded as immobile (ie. Zr, Ti, Y, Nb) confirm a tholeiitic classification for this unit (see figures 2-16, 2-17).

Analyses for the stratigraphically higher amphibolite (unit 4a) east of Falls Lake in Table 2-2 are the first descibed for this unit. The amphibolite is geochemically distinct from the metabasalt in that it possesses higher $Na_2O$, $P_2O_5$, and $TiO_2$, and lower CaO, $Al_2O_3$, $Fe_2O_3$ $_T$, and MgO. With respect to trace elements, the unit is enriched in U, Zr, Y, Nb, Zn, Cu, Ba and depleted in Cr and Ni. This could indicate a more highly fractionated source magma,

Table 2-2:Chemical compositionof basalts and
amphibolites of the Aillik Group.

| Basalt: | 1 | 2 | 3 | 4 | 5 | 6 |
|---|---|---|---|---|---|---|
| $SiO_2$ | 50.16 | 51.92 | 47.50 | 47.16 | 48.30 | 48.30 |
| $TiO_2$ | 2.23 | 1.13 | 1.10 | 2.14 | 0.82 | 2.32 |
| $Al_2O_3$ | 13.96 | 14.28 | 15.98 | 17.84 | 17.00 | 14.10 |
| FeO | 15.65 | 11.72 | 11.42 | 12.70 | 10.14 | 14.14 |
| MnO | 0.14 | 0.13 | 0.23 | 0.21 | 0.19 | 0.29 |
| MgO | 3.33 | 6.02 | 7.14 | 7.05 | 7.80 | 4.10 |
| CaO | 8.04 | 8.85 | 10.31 | 8.17 | 7.79 | 6.41 |
| $Na_2O$ | 3.36 | 3.39 | 2.71 | 3.20 | 4.43 | 5.17 |
| $K_2O$ | 0.79 | 0.96 | 1.26 | 0.69 | 1.35 | 1.54 |
| $P_2O_5$ | - | - | 0.16 | - | - | 0.69 |
| LOI | - | - | 1.82 | - | 1.09 | 0.60 |
| Total | 97.66 | 98.40 | 99.62 | 99.16 | 98.91 | 97.66 |

1 - Post Hill Amphibolite (White, 1976)
2 - Kitts Pillow Lava (Evans, 1980)
3 - Upper Aillik Metabasalt (Gower et al., 1982)
4 - Seal Lake Group Basalts (Barager, 1977)
5 - Meatbasalt Round Pond (this study)
6 - Amphibolite Falls Lake (this study)

reversing the trend observed earlier between basalts of the Lower and Upper
Aillik, and corresponding to the eruption of highly differentiated felsic volcanic
rocks. However, not all the features observed can easily be accounted for by
differentiation. Indeed, the enriched total Fe, slightly enriched soda, $Al_2O_3$
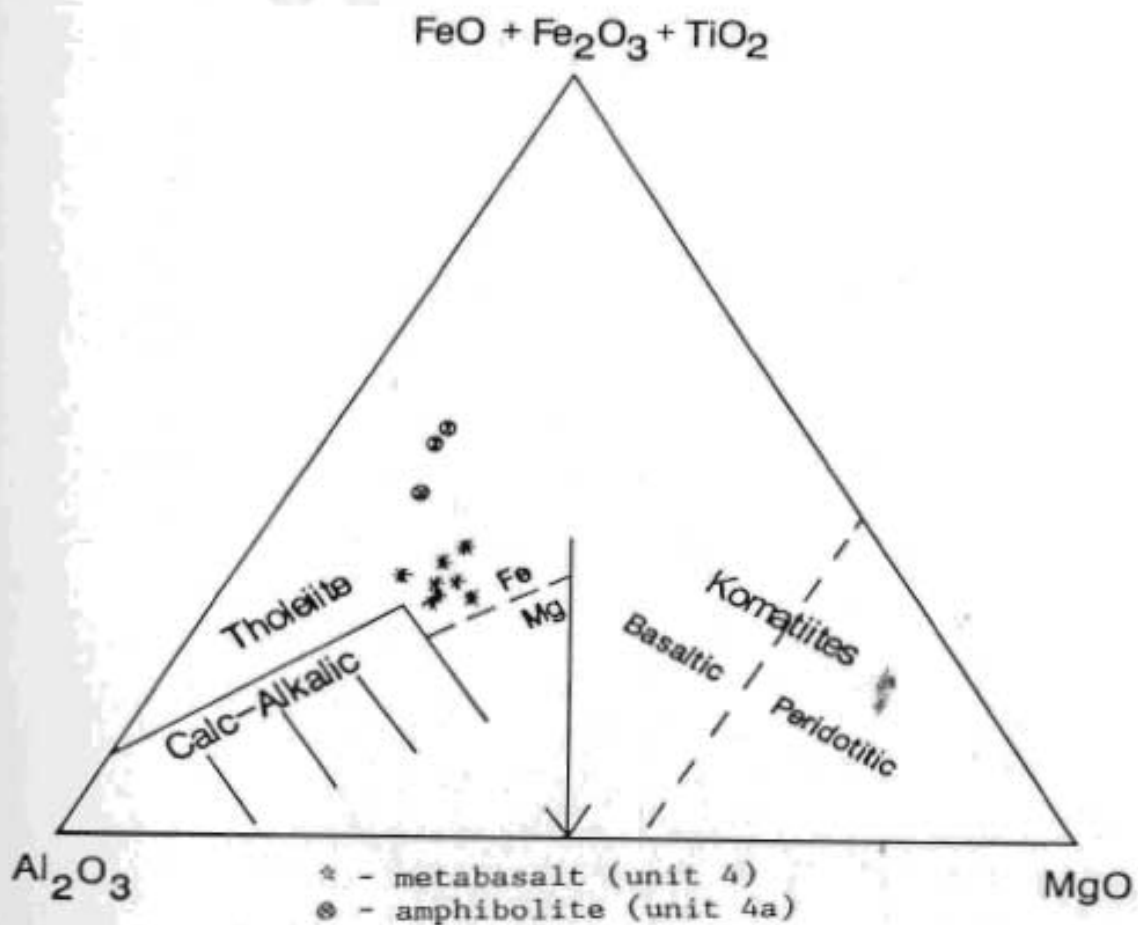
**Figure 2-15:** Jensen (1977) cation plot of the basalts and related amphibolites of the Upper Aillik Group, in the Round Pond area.

depletion, and Ti mobility are similar to alteration observed by Evans (1980) at the Kitts Deposit for the Lower Aillik pillow lava basalt. The enriched Zr, Ti, Y, Nb, U, and Ba probably reflects a secondary enrichment associated with a uranium mineralizing event.
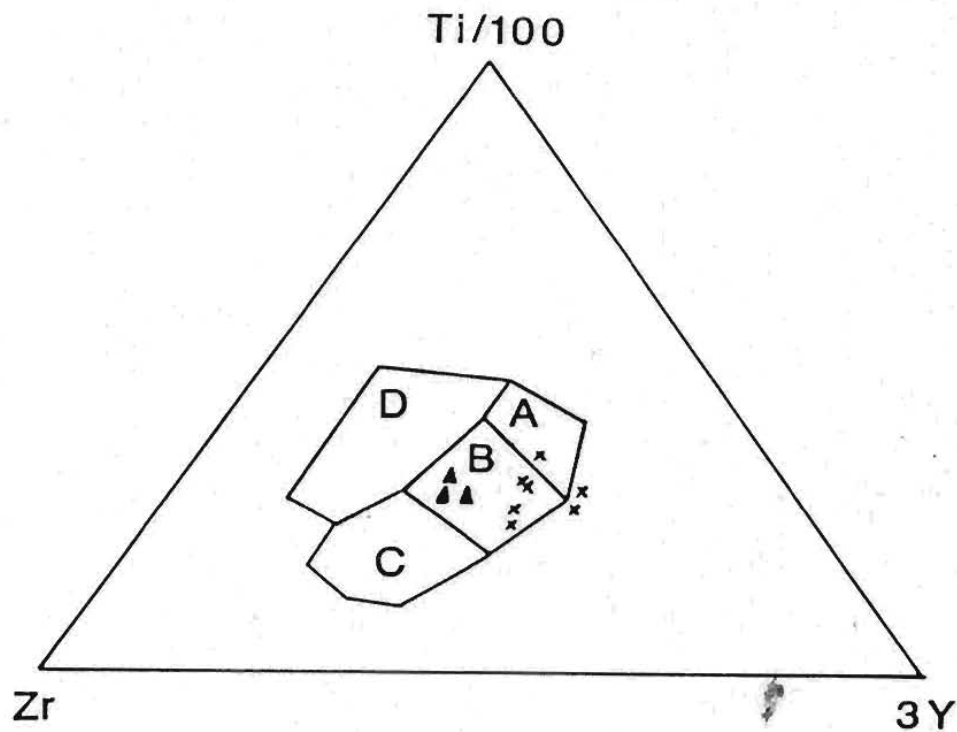
**Figure 2-16:** Lithotectonic Ti-Zr-Y discrimination
diagram (after Meschede, 1986) with data
from the basalts and related amphibolites
from the Upper Aillik Group in
the Round Pond area.

```
Fields: Within plate basalt: D
        Ocean floor basalt: B
        Low K tholeiite : A,B
        Calcalkaline Basalt: c, B

Symbols: X - basalts; ▲ - amphibolite
         (unit 4)        (unit 4a)
```
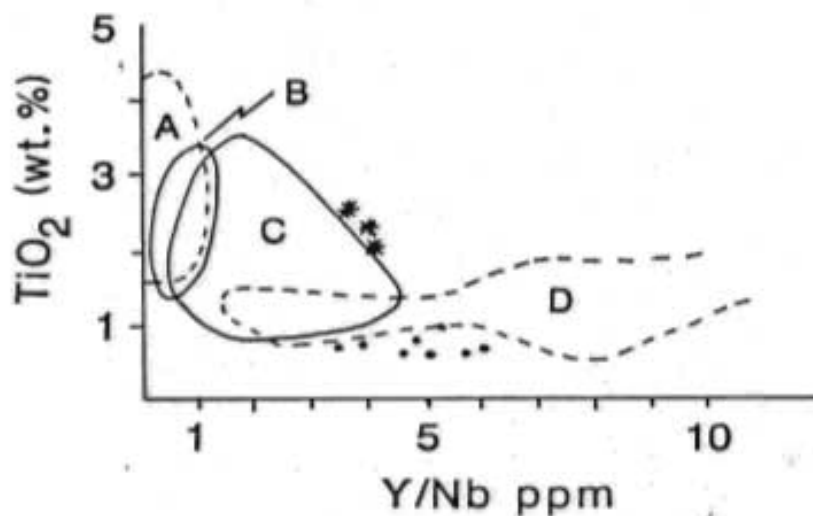
**Figure 2-17:** Lithotectonic discrimination diagram
(from Floyd and Winchester, 1975) with data
from of the basalts and related amphibolites
of the Upper Aillik Group, in the
Round Pond area.

Fields: A - ocean alkaline basalt
B - continental alkaline basalt
C - continental tholeiitic basalt
D - ocean tholeiitic basalt

Symbols: • - basalt; * - amphibolite
(unit 4)        (unit 4a)

### 2.5.5. Rhyolites

The unaltered composition of the various rhyolitic members are all very similar with no significant geochemical distinction between lithological units. As a result, all the rhyolites will be discussed in one section. The analyses in Table 2-1 are similar to those provided by White (1976), Evans (1980), Gower et. al. (1982), and Gower and Ryan (1987) for various rhyolites of the Upper Aillik Group.

The rhyolites in the Round Pond-Falls Lake area are the product of a highly fractionated source magma, and are characterized by high $SiO_2$, and low MgO and CaO. The rhyolites are generally potassic in nature with $K_2O$ greater than $Na_2O$. The rhyolites are calc-alkaline as suggested by previous workers (Bailey, 1979; Evans, 1980; Wardle and Bailey, 1981). Peralkaline affinities suggested by other workers (White, 1976; Marten and White, 1980; Gandhi, 1978) could not be substantiated in this study.

Some samples exhibit metasomatism characterized by the enrichment of $Na_2O$ and depletion of $K_2O$. First recognized by White (1976), the metasomatism is thought to be the result of synvolcanic magmatic of meteoric fluids, with later metasomatism along shear zones.

## 2.6. DISCUSSION

The recognition and study of ancient tectonic enviroments is based largely on the knowledge of relatively recent and modern day environments such as island arcs and active continental margins, and the successful extrapolation of this knowledge to ancient rock suites. This task is greatly complicated by deep erosion and the effects of later deformation and metamorphism suffered by many of these ancient rock suites, including those of the Aillik Group.

Various tectonic models have been postulated for the Aillik Group by different workers. Gandhi et al. (1969) recognized that the structural, metamorphic and intrusive events preserved within the Aillik Group resembled an

orogenic cycle, termed the Hudsonian Orogeny. Watson-White (1976), Ghandi (1978), Evans (1980) and White and Martin (1980) suggested that the abundance of rhyolite volcanic rocks indicated a nonorogenic, continental rift enviroment. Clark (1973), Wardle and Bailey, (1981) and Gower et al. (1982) proposed contrasting tectonic enviroments between the Lower and Upper Aillik. They suggested that the Lower Aillik Group was deposited in a transitional, marine enviroment. The Upper Aillik Group, in contrast was the result of major volcanism related to the collision of two continents (Clark, 1973), or a continental rift environment (Wardle and Bailey, 1981; Payette and Martin, 1986). Ryan (1984) advocated an ensialic extensional basin or accumulation along a rifted, subsiding continental margin for the Lower Aillik Group, and continental backarc spreading resulting from initiation of a subduction zone as the cause of the Upper Aillik volcanism.

The Aillik Group consists of a bimodal sequence of basaltic and rhyolitic volcanic rocks overlying an Archean basement of refoliated gneisses. Rhyolite greatly predominates over basalt, and andesitic volcanic rocks are virtually absent. The Round Pond area is underlain by rhyolitic volcanic rocks and associated volcaniclastic sediments of the Upper Aillik Group, with only a minor basaltic component. The lack of andesitic volcanic rocks has been noted by previous workers (White, 1976 and Ghandi, 1978) and is in sharp contrast to that typically associated with earlier Archean volcanism, where rocks of andesitic composition are significant components of Archean volcanic assemblages (ie. greenstone belts; Goodwin, 1977), as well as many modern day volcanically active areas.

Volcanic assemblages associated with the Great Bear Batholith (ca. 1800 Ma) in the Western Bear Province of the Canadian Shield are observed to consist of a basal, bimodal volcanic assemblage of trachybasalt lava flows and rhyolites overlying basement (Hoffman and McGlynn, 1977). Above this bimodal assemblage, are cyclic sequences of andesite and dacite - rhyolite volcanics, dominated by dacite to

rhyolite ignimbrites. Realizing the effects of deep erosion, one could easily postulate that the lack of andesites in the Upper Aillik Group is a function of erosion and thereby, does not represent profound implications with respect to tectonic environment, as suggested by Gandhi (1978). Indeed, younger Proterozoic volcanic sequences observed further inland in Labrador, such as the Bruce River Group, do consist of thick, cyclic sequences of andesite-dacite-rhyolite (Ryan, 1984).

The Upper Aillik Group, however, represents a high level volcanic-subvolcanic environment consisting of a bimodal basalt-rhyolite assemblage, dominated almost exclusively by rocks of silicic compositions such as rhyolites. Similar bimodal basalt-rhyolite assemblages occur in the Snake River Plain, Yellowstone National Park, where early basaltic extrusions give way to voluminous rhyolitic pyroclastic eruptions that produced calderas (Williams and McBirney, 1979; Best, 1982). Such areas of volcanic activity occur in areas of continental extension and rifting. The Tonga-New Zealand arc represents a much different tectonic enviroment but similar volcanic assemblages. The island of Tonga, which rests upon oceanic crust, is characterized by volcanic assemblages of monotonous tholeiitic basalts and andesites. New Zealand which overlies continental crust, is characterized by a much more diverse volcanic assemblage, consisting of only minor andesitic and basaltic volcanics but voluminous rhyolite volcanic rocks (Ewart et al., 1977).

It thus appears that the presence of diverse, voluminous, volcanic assemblages dominated by silicic rocks, is not as much a function of tectonic environment, as an apparent intimate association with continental crust. Jakes and White (1971, 1972) and Hildreth (1970, 1981) note that more felsic and diverse magmas are founded on continental crust, in contrast to more restricted mafic magmas that are associated with oceanic crust. McBirney (1970) suggests that no other process other than melting of sialic crust can adequately explain the highly silicious composition of such felsic rocks, their great volume and virtual restriction to areas

underlain by continental crust. Hoffman and McGlynn (1977) propose that magmatic evolutionary trends towards granite of the Great Bear Batholith reflects progressively greater contributions from melts derived by crustal anatexis. Thus, the dominance of silicic volcanic rocks over mafic basaltic volcanic rocks in the Aillik Group, suggests an intimate relationship with silicic continental crust from which the Aillik Group was probably derived as partial melts, and on which the Aillik Group overlies.

Trace element tectonic diagrams for the rhyolites (see Figure 2-18) suggest a "Within Plate" environment thus supporting the idea of a significant continental crustal influence on the generation of the Aillik Group rhyolites. Ryan (1984) postulated that the bimodal volcanism of the Upper Aillik Group was generated within a continental backarc spreading center as a result of initiation of subduction. Such an environment would clearly account for the high volume of silicic volcanic rocks of the Upper Aillik Group, as well as the observed high K calc-alkaline trends. Hoffman and McGlynn (1977) suggest that the basal bimodal basalt-rhyolite assemblage they observe was initially the result of an ensialic rift, based on the alkaline (potassic) nature of the basalt. The basalts of the Upper Aillik Group in the Round-Pond area similarily possess alkaline tendencies, but again this must be viewed with caution in view of the apparent alkali mobility exhibited by these rocks.
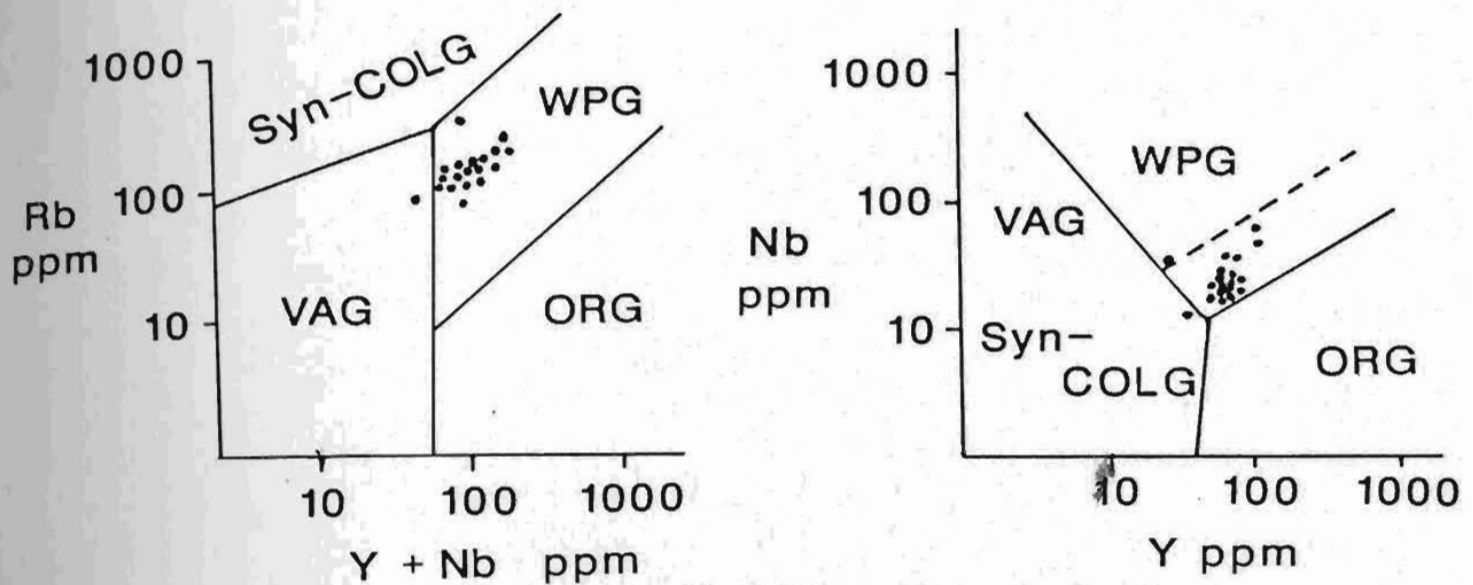
**Figure 2-18:** Tectonic discrimination diagrams for the rhyolites of the Upper Aillik Group at Round Pond (after Pearce et al., 1984).

VAG-volcanic arc granite
WPG-within plate granite
ORG-orogenic granite
Syn-Colg-syncollisional granite

The tectonic trace element discrimination diagrams for the basalts proved to be puzzling and perhaps reflect an excessive degree of alteration which limits the use of such diagrams. Commonly used discrimination plots (see figures 2-16, 2-17) consistently pointed to rocks of tholeiitic compositions with no discrimination between tectonic enviroments. The diagram (figure 2-16) by Meschede (1986) suggested that the basalts of the Round Pond area are low-K tholeiites, although $K_2O$ is generally high. Interestingly, the fields of low-K tholeiites generally overlap with those of calc-alkaline basalts.

Figure 2-19 by Pearce et al., (1977) uses relatively immobile elements to characterize the basalts in terms of possible tectonic environments. The bulk of the metabasalts plot along the boundary between orogenic, oceanfloor and continental enviroments, with a concentration towards the oceanfloor environment. The stratigraphically higher amphibolites plot within the continental field, suggesting a higher degree of differentiation or greater influence by continental crust. The pattern of distribution in both the continental and oceanic fields was observed by the authors for Archean rocks and lead them to suggest a possible analogy with present day "within plate" volcanism. Figure 2-20 by Gale and Pearce (1982) illustrates an evolution of the lower metabasalts from arc lavas to the stratigraphically higher amphibolites to "within plate" basalts.

A tectonic model for the Upper Aillik Group based on the above discussion is best summarized as modified from Ryan (1984) (figure 2-21). The Lower Aillik Group was deposited in a totally ensialic trough or on a rifted continental margin. Bimodal volcanism of the Upper Aillik Group began in a continental backarc basin resulting from the initiation of subduction. The observed basalt/amphibolite compositional evolution suggests that a more primitive initial source magma (derived from partial melting of oceanic crust) gave way to a more diverse, evolved source magma as a result of increased contributions from partial melts of sialic continental crust. Hudsonian deformation, which began shortly after the initiation of subduction, resulted in thickened crust and subsequent continetal crustal anatexis, giving rise to continued outpourings of felsic volcanic rocks of the Upper Aillik Group. This crustal melting also resulted in diapiric rise of syn-to post-tectonic granitic intrusions, related to above volcanism.
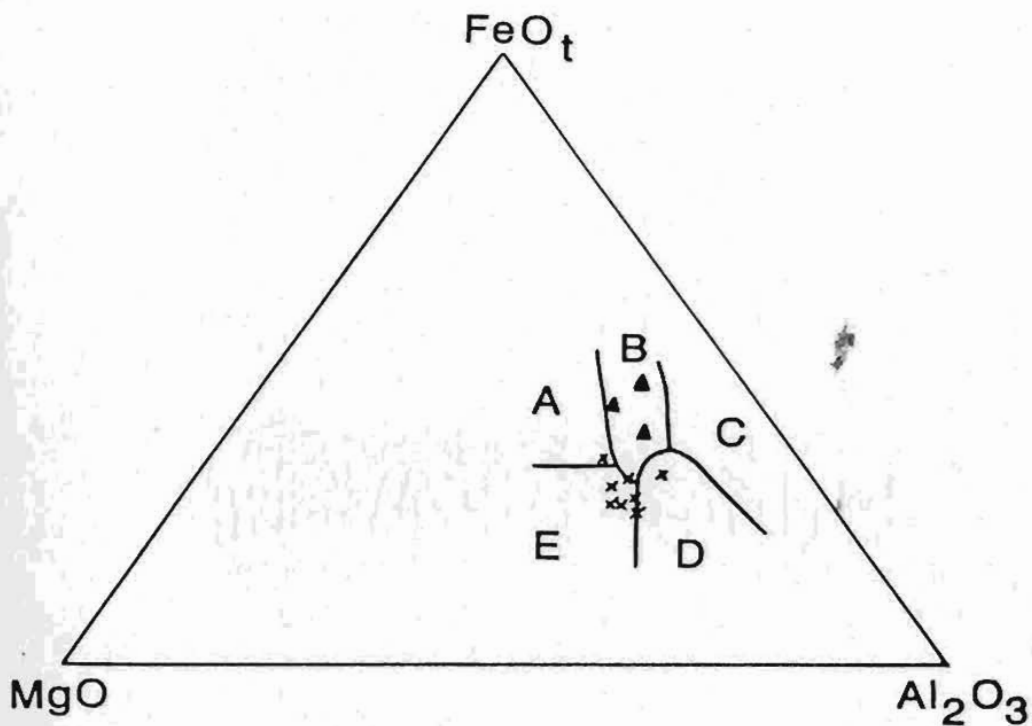
**Figure 2-19:** FeO-MgO-Al$_2$O$_3$ tectonic discrimination
diagram of basalts and amphibolites from the
Upper Aillik Group, in the Round Pond area
(after Pearce et al., 1977).

Fields: A - ocean island
        B - continental
        D - orogenic
        E - ocean ridge

Symbols: x - basalt;  ▲- amphibolites
            (unit 4)        (unit 4a)
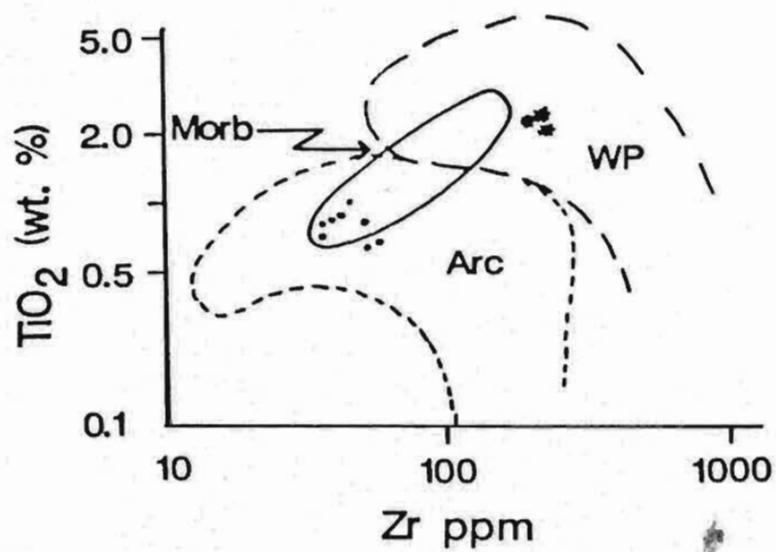
**Figure 2-20:** Tectonic discrimination diagram for basalts and amphibolites of the Upper Aillik Group, in the Round Pond area (after Gale and Pearce, 1981).

WP - within plate
  • - basalts;  * - amphibolites
    (unit 4)        (unit 4a)
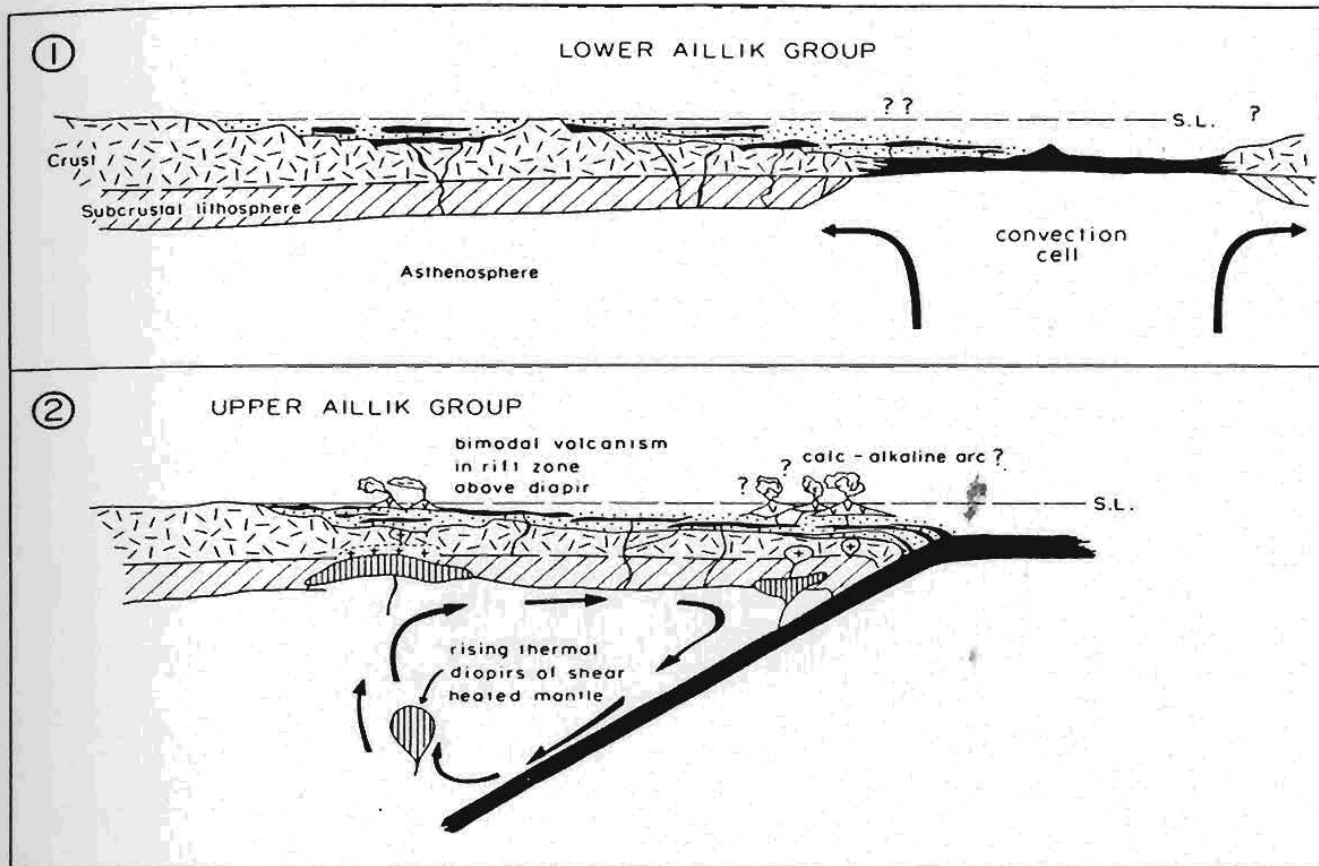
**Figure 2-21:** Schematic diagram representing the tectonic
evolution of the Aillik Group during an
Aphebian subduction-island arc environment
(after Ryan, 1984).

Stage ı - deposition of the Lower Aillik
Group on stretched Archean crust.
Stage 2 - subduction-related bimodal volcanism
of the Upper Aillik Group.

# Chapter 3
# Monkey Hill Granite

## 3.1. Introduction

The Upper Aillik Group in the Round Pond area was intruded by two small, post-tectonic, high level, leucogranitic stocks. The intrusions are part of the regionally extensive Monkey Hill Granite, a small irregular pluton exposed on Monkey Hill (just west of the study area). The main body and related satellite stocks are homogeneous, displaying little textural or grain size variation and consist mostly of a quartz-rich, fine to medium-grained, pink to pinkish grey granite. The stocks in the Round Pond area are satellite intrusions of the main pluton; the east stock is also spatially associated with exocontact Mo-base metal-U-F mineralization.

The Monkey Hill Granite has been dated by K-Ar isotope techniques on biotite at $1620 \pm 60$ Ma (Wanless et al., 1970), and is interpreted as a post-tectonic granitic intrusion produced during the Hudsonian Orogeny (ca. 1850-1700 Ma). Recent work by Wardle et al. (1987) indicates that the Monkey Hill Granite belongs to an intrusive event which resulted in the emplacement of the Trans-Labrador Batholith, defined as the Labradorian Orogeny (ca. 1650-1600 Ma). A composite Rb/Sr isochron for the TLB indicates an age of 1600 Ma (A. Kerr, pers. comm., 1988).

## 3.2. Field Relations and Petrology

The two satellite stocks of Monkey Hill Granite exposed in the thesis area are a homogeneous, white to pink, fine to medium-grained, equigranular leucogranite (see figure 3-1). The plugs are small (< 2 km) elliptical intrusive stocks of similar size, which parallel the axial plane of the regional anticlinal structure. Previous workers (Clark, 1973; Gower et al., 1982) also mapped a third, smaller intrusive plug due south of Round Pond. Field work in the area failed to confirm the presence of this plug, although numerous granitic and pegmatitic dykes were observed. Associated with the granitic intrusions are numerous granitic, pegmatitic and aplitic dykes, which often contain minor pyrite, fluorite, molybdenite and anomalous radioactivity (see chapter4, section 4-3).

Clark (1973), described the Monkey Hill Granite as a post-tectonic intrusion, although the elongate shape of the stocks suggested a possible synintrusional structural overprint related to $F_2$ folding. The granite-country rock contact is generally covered by overburden, but is exposed along the northeast margin of the eastern stock, where the contact can be traced discontinously for several hundred metres as a sharp, discordant intrusive contact (see figure 3-2). The nature of the contact, and the isotropic internal fabric of the stocks support a post-tectonic emplacement. These features together with country rocks which exhibit only weak contact-metamorphism, and are locally intensely mineralized suggest that the granitic stocks in the Round Pond area are high level, epizonal intrusions.

The two plugs differ slightly, in that the western plug is finer grained and possesses a slightly recrystallized appearance compared to the eastern stock. In addition, the western stock is characterized by the presence of "simple" pegmatitic pods (up to 1-2 m in length) and irregular miarolitic cavities (1-5 mm, with euhedral quartz crystals) within the stock, and numerous pegmatitic veins in the surrounding country rock. The eastern stock, in contrast, is spatially associated with numerous hydrothermal Mo-base metal-U-F showings, and small, pyrite and molybdenite-bearing aplitic veins. These features are evidence of the high level of emplacement of the intrusive stocks in the Round Pond area.

Clark (1973) describes modal mineral proportions in the granite (including the stocks at Round Pond) as 30-40% quartz, 30-40% albite and 20-30% microcline. Thus, the Monkey Hill Granite falls within the "monzogranite" field according to the I.U.G.S. modal classification scheme for granitoid rocks (Streckeisen, 1976) (see Figure3-3). Normative calculations performed for this study confirm this classification. Petrographic studies indicate the presence of albite and microcline as euhedral to subhedral grains (some with kinked twins), and quartz as anhedral grains (exhibiting undulose extinction). Coarse, stringy, perthitic textures are abundant. The presence of perthitic feldspar, and the general lack of hydrous mineral phases such as muscovite and biotite suggest that the satellite stocks of Monkey Hill Granite in the Round Pond area were initially dry granitic melts. Abundant granophyric mantles on euhedral feldspars, suggest the presence of water late in the crystallization history of the stocks (see figure 3-4). The presence of biotite as a distinctly late, hydrous mineral phase (see figure 3-5), as well as the irregular miarolitic cavities and pegmatitic pods described earlier, clearly supports this conclusion.

The most abundant accessory minerals include biotite (often replaced by chlorite), fluorite, pyrite, magnetite and sphene, with lesser apatite, zircon and monazite. In addition, very rare flakes of molybdenite and grains of scheelite have been observed within the granitic stocks in the Round Pond area (see Figure 3-6). Previous workers (Gandhi et al., 1969; Clark, 1973; Gower et al., 1982) also observed hornblende and epidote within the granite, and fluorite, pyrite, arsenopyrite, molybdenite and anomalous radioactivity in associated veins and pegmatites. All but arsenopyrite has been observed in veins or pegmatites in this investigation.

Figure 3-1: Two samples of the typically fine
to medium-grained, quartz-feldspar
leucogranite. Left - east stock;
right - west stock.

Figure 3-2: Sharp intrusive contact (marked by
hammer) between the stock of Monkey
Hill Granite (left) and felsic
conglomerate (right), east of Round Pond.
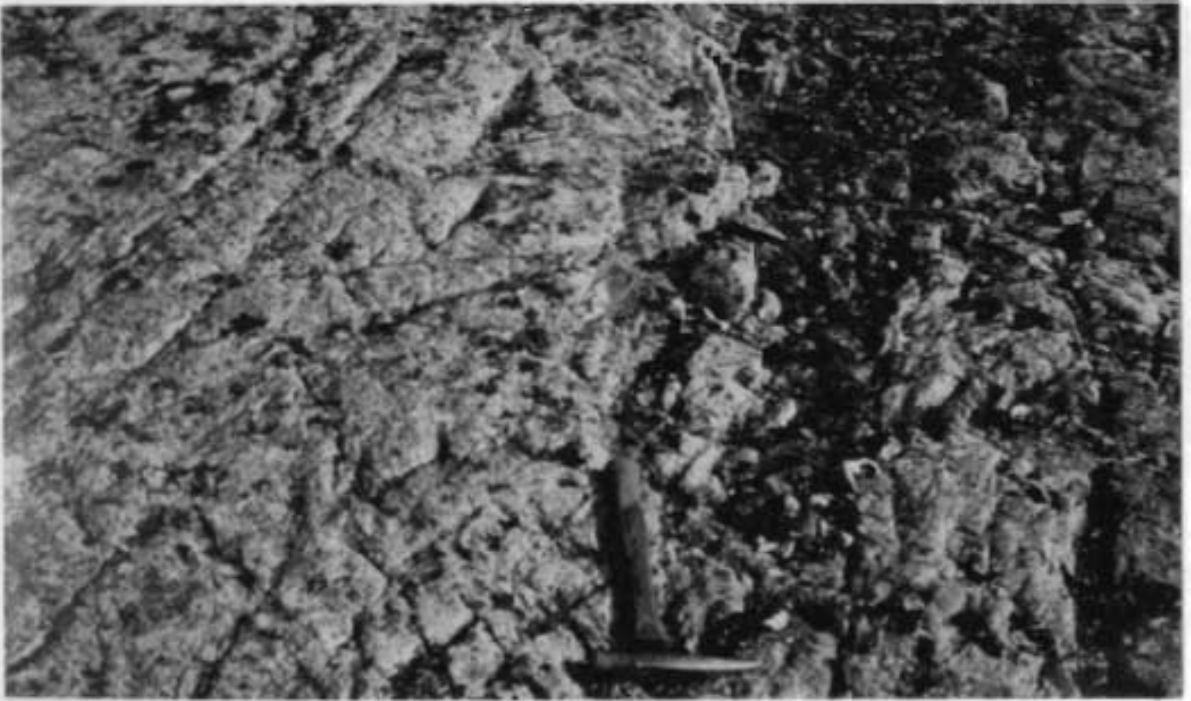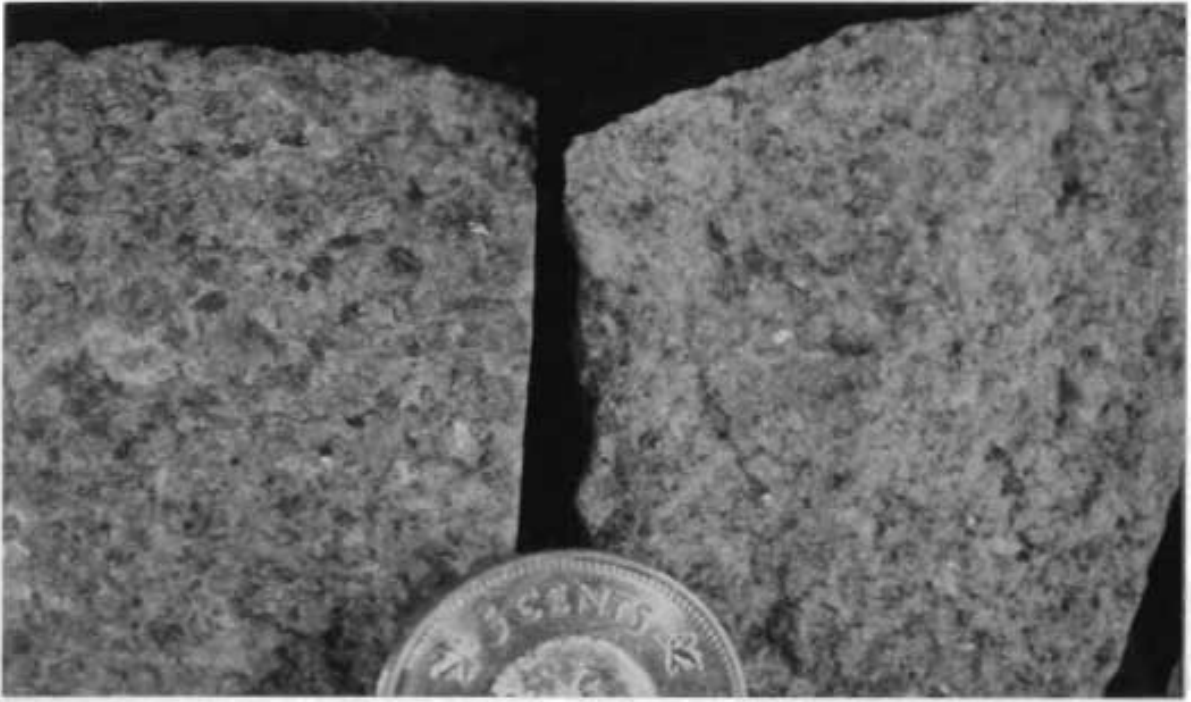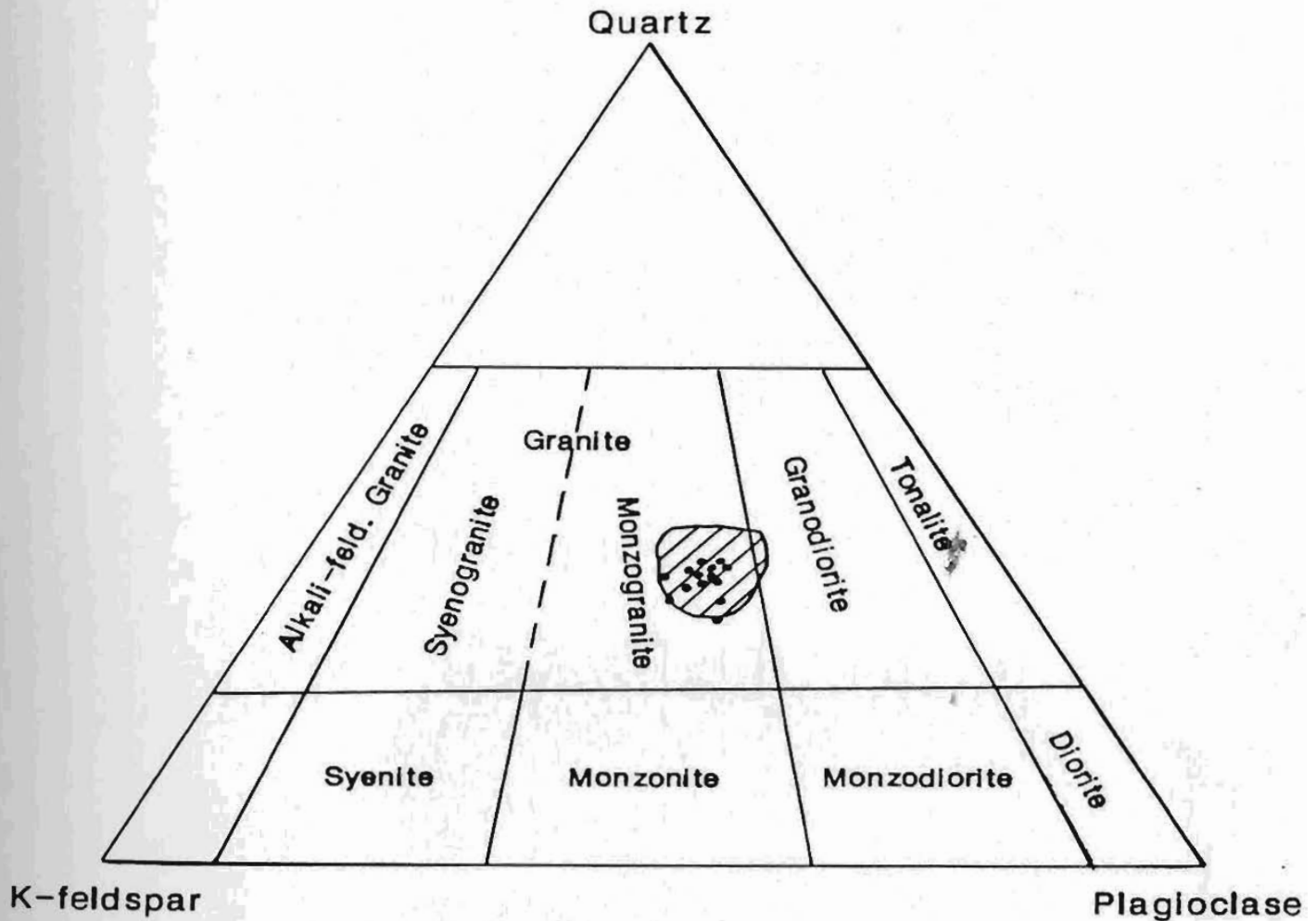
**Figure 3-3:** Modal and normative classification of the Monkey Hill Granite in the Round Pond area.

The hatched field is Clark's (1973) modal classification.

• - CIPW normative composition (this study).

**Figure 3-4:**   Granophyric mantle on euhedral feldspar
from the Monkey Hill Granite
(mag. x10, x nicols).

**Figure 3-5:**   Irregular, interstitial biotite (dark),
and fluorite (high relief) between
euhedral feldspar and quartz,
in the Monkey Hill Granite
(mag. x 20, plane polarized light).
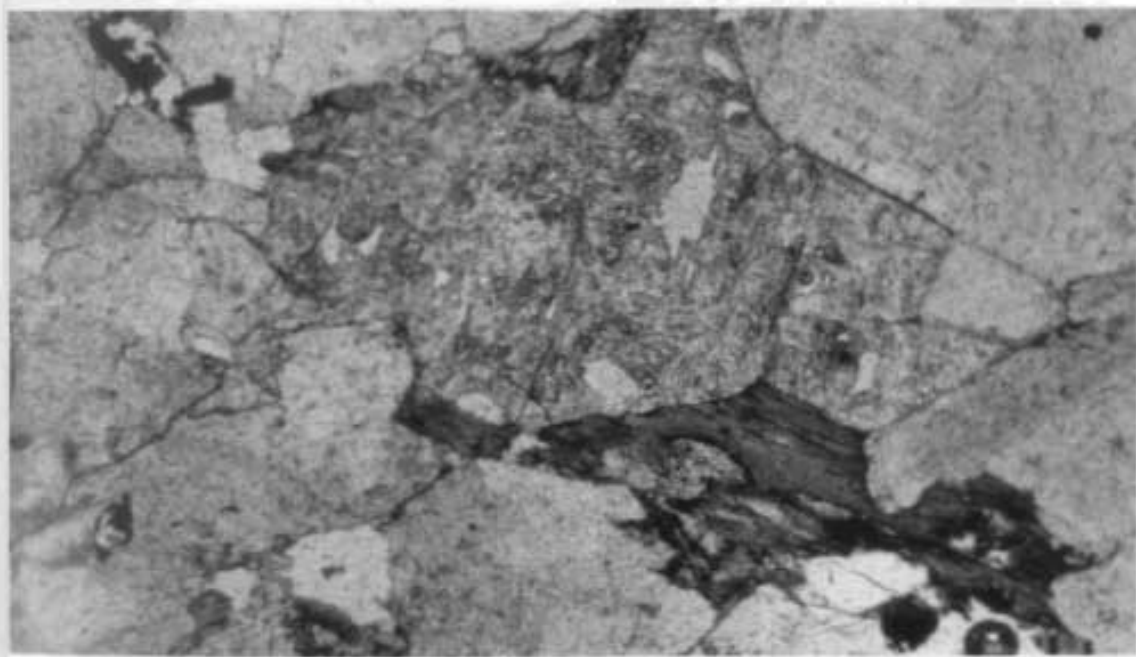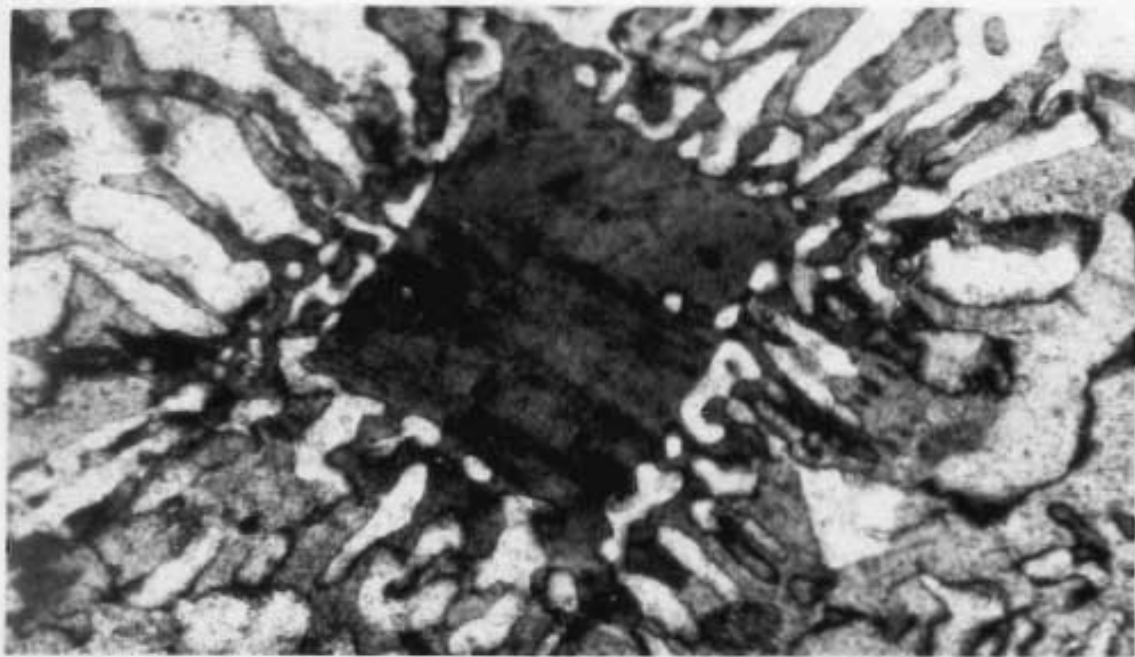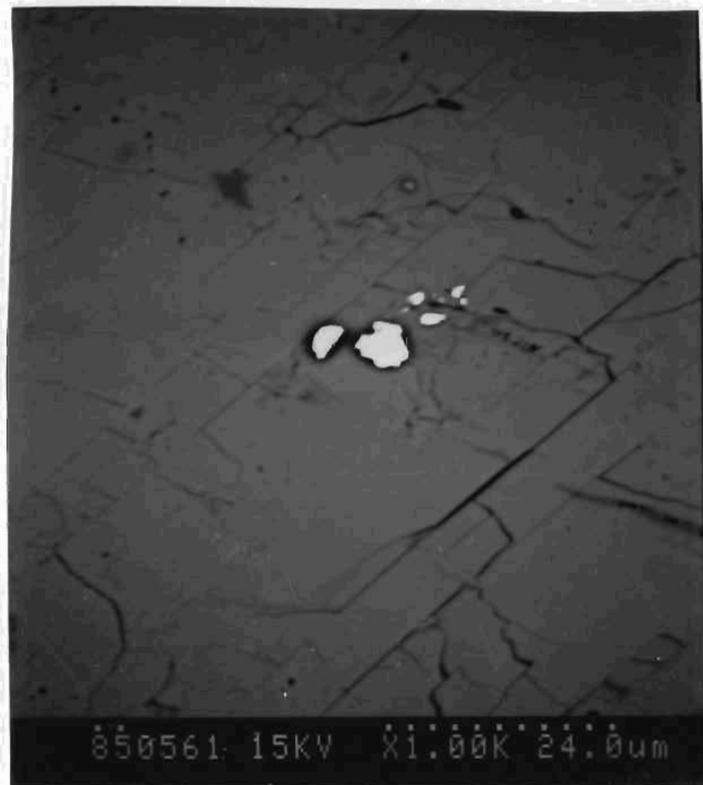
**Figure 3-6:** SEM backscatter photograph of small grains of scheelite (white) within a K-feldspar crystal from the Monkey Hill Granite, Round Pond area.

A general mineral paragenetic sequence appears to have developed, ranging from feldspars and quartz, ending with granophyric mantles on euhedral feldspar, and interstitial biotite and fluorite; indicating that the Monkey Hill Granite was initially water undersaturated. Eutectic crystallization of anhydrous feldspar and quartz led to water-saturated conditions, and subsequent development of a volatile-rich phase, marked by granophyric mantles, late interstitial biotite and fluorite, miarolitic cavities, and pegmatites. Hydrothermal alteration possibly related to this late, volatile-rich phase is minor, marked by the occasional "reddening" of feldspar.

## 3.3. Geochemistry of the Monkey Hill Granite

Geochemical analyses were carried out on 15 samples from the Monkey Hill Granite stocks, and three associated granite pegmatite veins in the Round Pond area. The data are listed in Table 3-1. Analytical procedures are described in Appendix I. Average data for the main pluton of Monkey Hill Granite to the west of the study area are from Kerr (1987).

### 3.3.1. Major Elements

The satellite stocks of the Monkey Hill Granite are high-silica, averaging 76.0 wt%, highly differentiated, mildly peraluminous to metaluminous granitic intrusions. CIPW normative compositions are plotted on figure 3-3. The plutons have low CaO contents (averaging 0.51%), and $K_2O$ dominates slightly over $Na_2O$, averaging 4.64 and 4.16 wt% respectively. Combined total Fe as $Fe_2O_3$, and MgO average 0.96 wt%, and $TiO_2$ is similarly low at 0.06 wt%. The western stock is generally more differentiated than the eastern stock, possessing higher $SiO_2$ and lower CaO contents. This may indicate a slightly higher level of intrusion is exposed in the west stock. The finer grain size associated with the west stock would tend to support this.

## Table 3-1: Chemical composition of the Monkey Hill Granite, and associated pegmatites, in the Round Pond area.

f

| Sample | CH-18 | CH-19 | CH-28 | CH-39 | CH-53 | CH-56 | CH-121 | CH-122 | CH-171 | CH-171a | CH-180 | CH-181 | RP-4G | RP-6 | RP-7 | CH-107 | CH-135 | CH-176 |
|---|---|---|---|---|---|---|---|---|---|---|---|---|---|---|---|---|---|---|
| SiO2 | 76.4 | 76.4 | 73.5 | 75.4 | 77.4 | 76.1 | 77.8 | 73.8 | 72.4 | 75.8 | 76.6 | 76.8 | 76.9 | 76.7 | 77.4 | 76.4 | 78.0 | 75.5 |
| TiO2 | 0.08 | 0.08 | 0.12 | 0.04 | 0.00 | 0.04 | 0.00 | 0.08 | 0.08 | 0.04 | 0.04 | 0.04 | 0.08 | 0.08 | 0.04 | 0.04 | 0.04 | 0.00 |
| Al2O3 | 12.8 | 12.5 | 13.6 | 13.2 | 12.5 | 13.3 | 12.7 | 14.1 | 14.1 | 13.1 | 12.7 | 13.0 | 12.8 | 12.6 | 12.7 | 13.3 | 12.5 | 12.6 |
| Fe2O3 | 0.58 | 0.67 | 1.53 | 0.95 | 0.63 | 0.71 | 0.39 | 1.65 | 1.60 | 0.81 | 0.61 | 0.53 | 0.44 | 0.71 | 0.62 | 0.59 | 1.55 | 1.87 |
| MnO | 0.01 | 0.01 | 0.04 | 0.01 | 0.00 | 0.01 | 0.01 | 0.06 | 0.06 | 0.02 | 0.01 | 0.01 | 0.00 | 0.00 | 0.00 | 0.08 | 0.02 | 0.01 |
| MgO | 0.05 | 0.04 | 0.36 | 0.21 | 0.04 | 0.08 | 0.04 | 0.40 | 0.40 | 0.14 | 0.06 | 0.05 | 0.03 | 0.06 | 0.03 | 0.02 | 0.01 | 0.00 |
| CaO | 0.38 | 0.18 | 0.82 | 0.64 | 0.32 | 0.54 | 0.34 | 0.84 | 1.08 | 0.52 | 0.40 | 0.46 | 0.38 | 0.38 | 0.36 | 0.36 | 0.18 | 0.18 |
| Na2O | 3.96 | 3.80 | 4.39 | 3.88 | 4.19 | 4.16 | 4.34 | 4.39 | 4.34 | 3.99 | 3.98 | 4.30 | 4.10 | 4.26 | 4.36 | 5.60 | 6.66 | 4.96 |
| K2O | 4.79 | 5.06 | 4.58 | 5.20 | 4.40 | 4.50 | 4.28 | 4.49 | 4.56 | 4.87 | 4.63 | 4.25 | 4.77 | 4.80 | 4.40 | 3.36 | 1.04 | 3.68 |
| P2O5 | 0.01 | 0.02 | 0.03 | 0.02 | 0.00 | 0.00 | 0.00 | 0.03 | 0.02 | 0.01 | 0.00 | 0.00 | 0.01 | 0.01 | 0.00 | 0.00 | 0.00 | 0.00 |
| LOI | 0.41 | 0.53 | 0.76 | 0.66 | 0.42 | 0.39 | 0.32 | 0.44 | 0.90 | 0.54 | 0.30 | 0.11 | 0.40 | 0.30 | 0.280 | 0.26 | 0.23 | 0.27 |
| Total | 99.47 | 99.29 | 99.73 | 100.21 | 99.90 | 99.83 | 100.22 | 100.28 | 99.54 | 99.84 | 99.33 | 99.55 | 99.91 | 99.90 | 100.19 | 99.25 | 100.23 | 99.07 |
| **(ppm)** | | | | | | | | | | | | | | | | | | |
| F | 90 | 140 | 580 | 610 | 400 | 160 | 540 | 540 | 750 | 970 | 110 | 140 | nd | nd | nd | nd | nd | nd |
| Li | 6 | 3 | 18 | 8 | 4 | 9 | 8 | 33 | 27 | 7 | 9 | 8 | nd | nd | nd | nd | nd | nd |
| Pb | 20 | 24 | 22 | 22 | 68 | 39 | 34 | 30 | 33 | 23 | 28 | 30 | 13 | 10 | 16 | 81 | 53 | 23 |
| U | 9 | 7 | 1 | 1 | 4 | 10 | 11 | 7 | 8 | 4 | 0 | 3 | 3 | 1 | 6 | 13 | 67 | 4 |
| Th | 22 | 9 | 17 | 15 | 32 | 16 | 19 | 10 | 24 | 22 | 14 | 16 | 2 | 0 | 9 | 19 | 89 | 59 |
| Rb | 175 | 177 | 184 | 184 | 200 | 176 | 214 | 174 | 183 | 188 | 175 | 178 | 179 | 229 | 225 | 412 | 29 | 149 |
| Sr | 53 | 103 | 197 | 136 | 22 | 87 | 17 | 227 | 212 | 62 | 73 | 62 | 38 | 12 | 18 | 16 | 32 | 19 |
| Y | 11 | 12 | 22 | 15 | 17 | 15 | 16 | 29 | 29 | 23 | 11 | 17 | 22 | 28 | 32 | 61 | 142 | 41 |
| Zr | 71 | 92 | 121 | 101 | 82 | 68 | 86 | 124 | 132 | 88 | 77 | 56 | 78 | 102 | 103 | 67 | 1038 | 69 |
| Nb | 15 | 12 | 16 | 13 | 19 | 12 | 18 | 18 | 20 | 12 | 12 | 8 | 17 | 23 | 32 | 36 | 145 | 43 |
| Ga | 19 | 17 | 21 | 19 | 22 | 20 | 22 | 20 | 19 | 19 | 13 | 19 | 21 | 23 | 23 | 36 | 54 | 35 |
| Zn | 0 | 0 | 8 | 0 | 59 | 0 | 0 | 34 | 11 | 0 | 0 | 0 | 0 | 33 | 0 | 1 | 31 | 0 |
| Cu | 6 | 11 | 5 | 27 | 38 | 12 | 12 | 5 | 6 | 17 | 6 | 5 | 6 | 6 | 1 | 2 | 0 | 3 |
| La | 0 | 0 | 2 | 7 | 0 | 0 | 0 | 23 | 20 | 2 | 0 | 0 | 0 | 0 | 0 | 0 | 0 | 0 |
| Ti | .02 | .08 | .13 | .09 | .00 | .05 | .00 | .13 | .13 | .05 | .02 | .01 | .02 | .00 | .00 | .00 | .04 | .01 |
| Ba | 66 | 333 | 438 | 307 | 0 | 185 | 0 | 482 | 466 | 133 | 75 | 48 | 40 | 0 | 0 | 0 | 64 | 58 |
| V | 0 | 0 | 1 | 0 | 0 | 0 | 0 | 0 | 3 | 0 | 0 | 0 | 0 | 0 | 0 | 0 | 0 | 0 |
| Ce | 38 | 0 | 63 | 36 | 65 | 16 | 48 | 99 | 31 | 84 | 50 | 74 | 63 | 89 | 38 | 68 | 0 | 33 |
| Mo | 2 | 2 | 2 | 2 | 3 | 4 | 2 | 2 | 2 | 3 | 2 | 2 | nd | nd | nd | nd | nd | nd |
| Rb/Sr | 3.3 | 1.7 | 0.9 | 1.4 | 9.1 | 2.0 | 12.6 | 0.8 | 0.9 | 3.0 | 2.4 | 2.7 | 4.7 | 19.1 | 12.5 | 25.5 | 0.9 | 7.8 |
| K/Rb | 227 | 237 | 207 | 235 | 183 | 212 | 166 | 214 | 207 | 215 | 220 | 208 | 221 | 174 | 162 | 68 | 299 | 206 |
| **Norm** | | | | | | | | | | | | | | | | | | |
| Qtz | 34.2 | 34.5 | 28.6 | 31.3 | 35.4 | 33.4 | 35.4 | 28.8 | 26.9 | 32.7 | 34.8 | 34.5 | 34.0 | 32.8 | 34.4 | | | |
| Or | 28.3 | 29.9 | 26.5 | 30.7 | 26.0 | 26.6 | 25.3 | 26.5 | 27.0 | 28.8 | 27.4 | 25.1 | 28.2 | 28.4 | 26.0 | | | |
| Ab | 33.5 | 32.2 | 37.2 | 32.8 | 35.5 | 35.2 | 36.7 | 37.2 | 36.7 | 33.8 | 33.7 | 36.4 | 34.7 | 36.1 | 36.9 | | | |
| Cor | 0.43 | 0.49 | 0.11 | 0.07 | 0.26 | 0.60 | 0.31 | 0.56 | 0.11 | 0.34 | 0.41 | 0.49 | 0.23 | 0.00 | 0.11 | | | |

Note: Samples CH-53, CH-121, RP-6, RP-7 from west granitic stock.
Samples CH-107, CH-135, CH-176 are pegmatitic veins.
nd - not determined.

Harker diagrams illustrate (fig. 3-7) typical differentiation trends with respect to increasing $SiO_2$ (also shown in the diagrams are an average for the main pluton of Monkey Hill Granite from Kerr (1987), and three associated granite-pegmatite veins from the Round Pond area). Of interest is the increase in $Na_2O$ with increasing $SiO_2$ within the stocks and a dramatic increase in the pegmatite veins. Mineralized showings in the Round Pond area exhibit a similar enrichment in $Na_2O$.

The major element contents are typical of evolved granites and suggest the possibility of "specialization" based on criteria outlined by Tischendorf (1977) Specialized granites generally possess high silica contents ($> 72\%$), low CaO ($< 0.50$) with extreme depletion of MgO and total Fe. These trends are clearly evident in this study.

### 3.3.2. Trace Elements

Despite the highly differentiated nature of the granitic plugs, trace element data do not have highly evolved contents (see figure 3-8). There is only minor to no enrichment in large ion lithophile (LIL) trace elements (Rb, U, Pb, Th) compared to average values for low-Ca granites as reported by Turekian and Wedepohl (1961), and Li is well below average. Rb enrichment is positively correlated with increasing $SiO_2$, while Pb, U and Th distributions are erratic (see Figure 3-8). The granite is not noticeably enriched in Mo, as contents are generally below the detection limit.
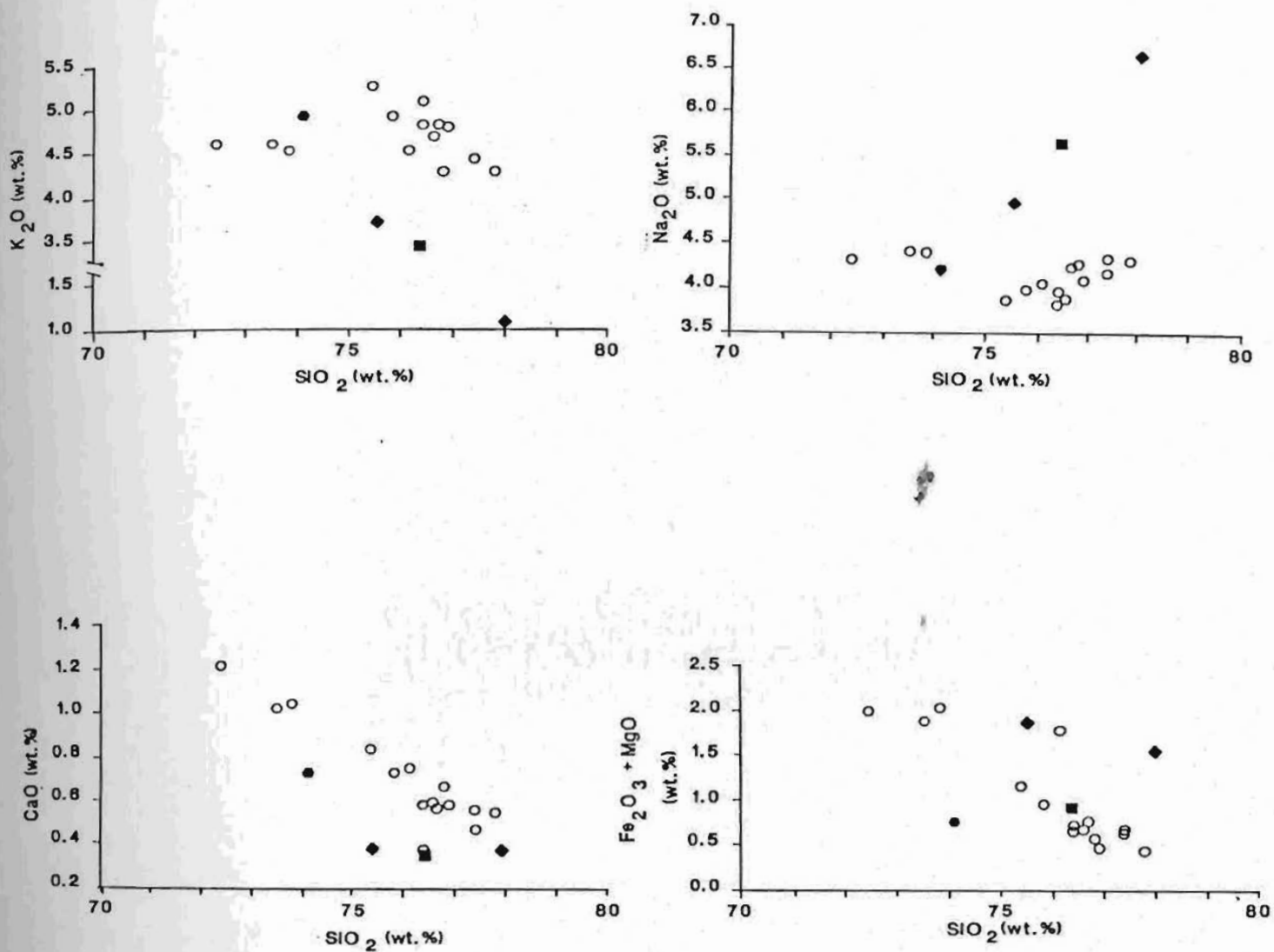
**Figure 3-7:** Harker diagrams plotting various major elements versus silica for the Monkey Hill Granite.

Symbols

○ - Monkey Hill Granite (Round Pond)
◆ ■ - Pegmatites (Round Pond)
⬢ - Main MHG pluton (Kerr, 1987)

High field strength (HFS) elements (ie. Zr, Y, Nb and Ga) range from average (Nb and Ga), to below average (Zr and Y) compared to low-Ca granites (Turekian and Wedepohl, 1961). Zr and Y decrease with increasing $SiO_2$, while Nb and Ga show no particular trends. Low contents of compatible elements (Cr, Ni, V) typical of felsic rocks, are observed. LIL elements such as Ba and Sr, which behave as compatible elements due to incorporation in feldspar, similarly suggest evolved rocks. Ba is well below average compared to typical values for low-Ca granites (Turekian and Wedepohl, 1961), while Sr ranges from average to below average but shows progressive depletion with increasing $SiO_2$. Rb/Sr ratios show a wide range from 0.77 to 19.1 but generally average less than 5.0.

Fluorine averages 435 ppm, ranging from a low of 90 ppm to a high of 970 ppm and is below average for low-Ca granites (Turekian and Wedepohl, 1961; Bailey, 1977). No variation with $SiO_2$ is observed (see Figure 3-8). This is apparently contradictory in view of the highly differentiated nature of the granite indicated by major elements, and the occurrence of fluorite as an accessory mineral within the granite. In addition, numerous mineralized, hydrothermal, fluorite veins occur in the country rock adjacent to the eastern granitic stock. These will be dicussed later.

Comparisons with average data from the main Monkey Hill Pluton (Kerr, 1987), suggest that satellite stocks in the Round Pond area are more highly differentiated, exhibiting slightly higher LIL contents, and lower contents of compatible elements and Sr and Ba. Interestingly, Zr is also noticeably lower.

### 3.3.3. Granite-Pegmatite Veins

Three analyses of granitic-pegmatite veins within country rock adjacent to the granitic stocks are listed in Table 3-1. The veins are coarse-grained, simple pegmatites, and consist of quartz and feldspar, with magnetite, pyrite, and fluorite; one possesses anomalous radioactivity. CM-107 possesses elevated Pb values as indicated by the presence of amazonite feldspar. All are associated with pyritiferous, rusty gossans.
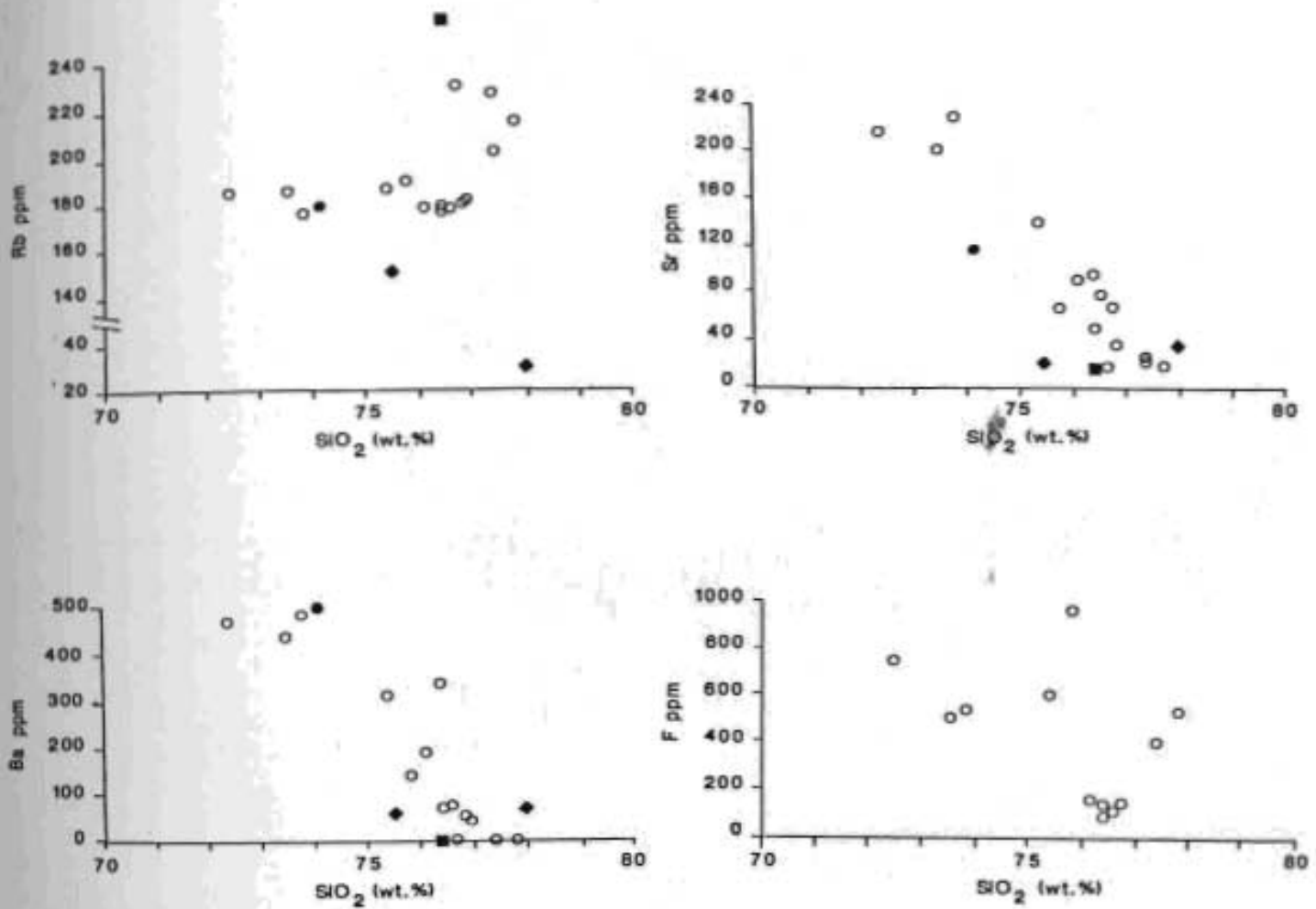
**Figure 3-8:** Harker diagrams plotting various
trace elements versus silica for
the Monkey Hill Granite
(symbols as above).

Major element analyses differ from those of the granitic plugs in that $Na_2O$ is greater than $K_2O$, and in the case of sample CM-135, appears enriched. Trace element contents for sample CM-176 suggest similarities with the granitic stocks but do exhibit enrichments in Nb and Ga. Other trends are the same as mentioned above. Sample CM-135 in contrast exhibits considerable enrichment in the LIL elements U, Th and Pb, and extreme enrichment in the HFS elements Zr, Y, Nb and Ga. Oddly enough, Rb does not exhibit any enrichment. Compatible elements and LIL elements (Ba, Sr) show typical depletion trends observed within the granites.

### 3.3.4. Rare Earth Elements

Analytical procedures for rare earth element (REE) analysis are given in Appendix I, and data are listed in Table 3-2. Chondrite-normalized REE plots (see figure 3-9) for Monkey Hill Granite plugs show typical granitic patterns at lower $SiO_2$ contents, with HREE depleted relative to LREE and a negative Eu anomaly. With increasing $SiO_2$ (ie. differentiation), several features are observed; first, the overall REE contents decrease and REE profiles become flatter, changing from steep, negative, LREE-enriched profiles, to nearly flat profiles (indicating a LREE depletion). This is a typical feature observed in granitic rocks (Hansen, 1980) and has been observed in numerous studies (Muecke and Clark, 1981; Miller and Mittlefehldt, 1982; and Chatterjee and Strong, 1984). Trends typically associated with the reduction in LREE abundances include 1) a drop in Eu/Eu* (observed Eu/Eu value predicted by a smooth chondrite-normalized REE pattern), 2) progressive depletion in REE with decreasing atomic number (resulting in slightly enriched to slightly depleted HREE). The former trend, which is attributed to removal of feldspar into which Eu is partitioned , is not clearly developed in this case. The latter trend however is evident. and results in the observed saucer-shaped profiles with increasing differentiation.

In addition to the general flattening of REE profiles and overall REE depletion with increasing $SiO_2$, significant depletions in Sm and Gd are observed.

**Table 3-2:** REE contents for the Monkey Hill
Granite, Round Pond area.

| sample | CM-171 | CM-28 | CM-122 | CM-171a | CM-56 | CM-180 | CM-19 | CM-181 | CM-53 | CM-121 |
|---|---|---|---|---|---|---|---|---|---|---|
| SiO2 (ppm) | 72.4 | 73.5 | 73.8 | 75.8 | 76.1 | 76.1 | 76.4 | 76.8 | 77.4 | 77.8 |
| La | 50.1 | 57.4 | 48.6 | 26.0 | 6.4 | 14.1 | 11.2 | 18.7 | 10.5 | 8.2 |
| Ce | 99.4 | 114.2 | 98.8 | 46.3 | 16.9 | 25.7 | 33.6 | 32.9 | 21.8 | 22.0 |
| Pr | 9.4 | 9.7 | 9.0 | 4.6 | 0.7 | 2.6 | 1.1 | 3.2 | 1.9 | 1.2 |
| Nd | 39.4 | 31.0 | 37.3 | 15.5 | 4.6 | 7.8 | 7.3 | 9.6 | 6.9 | 6.5 |
| Sm | 6.4 | 2.4 | 4.0 | 0.9 | 0.8 | 0.3 | 1.0 | 1.2 | 0.2 | 0.0 |
| Eu | 0.6 | 0.4 | 0.2 | 0.1 | 0.0 | 0.1 | 0.4 | 0.0 | 0.0 | 0.0 |
| Gd | 5.1 | 2.7 | 3.5 | 1.1 | 1.2 | 0.3 | 1.1 | 0.9 | 0.7 | 1.5 |
| Dy | 4.9 | 4.2 | 4.6 | 2.6 | 1.7 | 1.5 | 2.7 | 2.0 | 1.7 | 2.1 |
| Er | 2.2 | 3.0 | 2.7 | 2.1 | 1.4 | 1.8 | 2.1 | 2.0 | 2.2 | 1.8 |
| Yb | 2.1 | 3.1 | 2.4 | 2.0 | 1.1 | 0.8 | 1.6 | 0.9 | 1.6 | 1.6 |
| Total REE | 219.6 | 228.1 | 211.1 | 101.2 | 34.8 | 55.0 | 62.1 | 71.4 | 44.9 | 44.9 |
| Eu/Eu* | 0.35 | 0.48 | 0.15 | 0.47 | - | 1.60 | 1.26 | - | - | - |

This, together with decreasing Eu abundances, suggests an overall depletion of the MREE with differentiation. This is not a usual trend observed in felsic igneous rocks and appears to account for the lack of a drop in Eu/Eu* mentioned above and suggests that another process other than feldspar fractionation was operative in the case of the MREE.

REE, and in particular the LREE (characterized by larger radii), have generally been considered incompatible (except Eu) and thereby, would be

## MONKEY HILL GRANITE
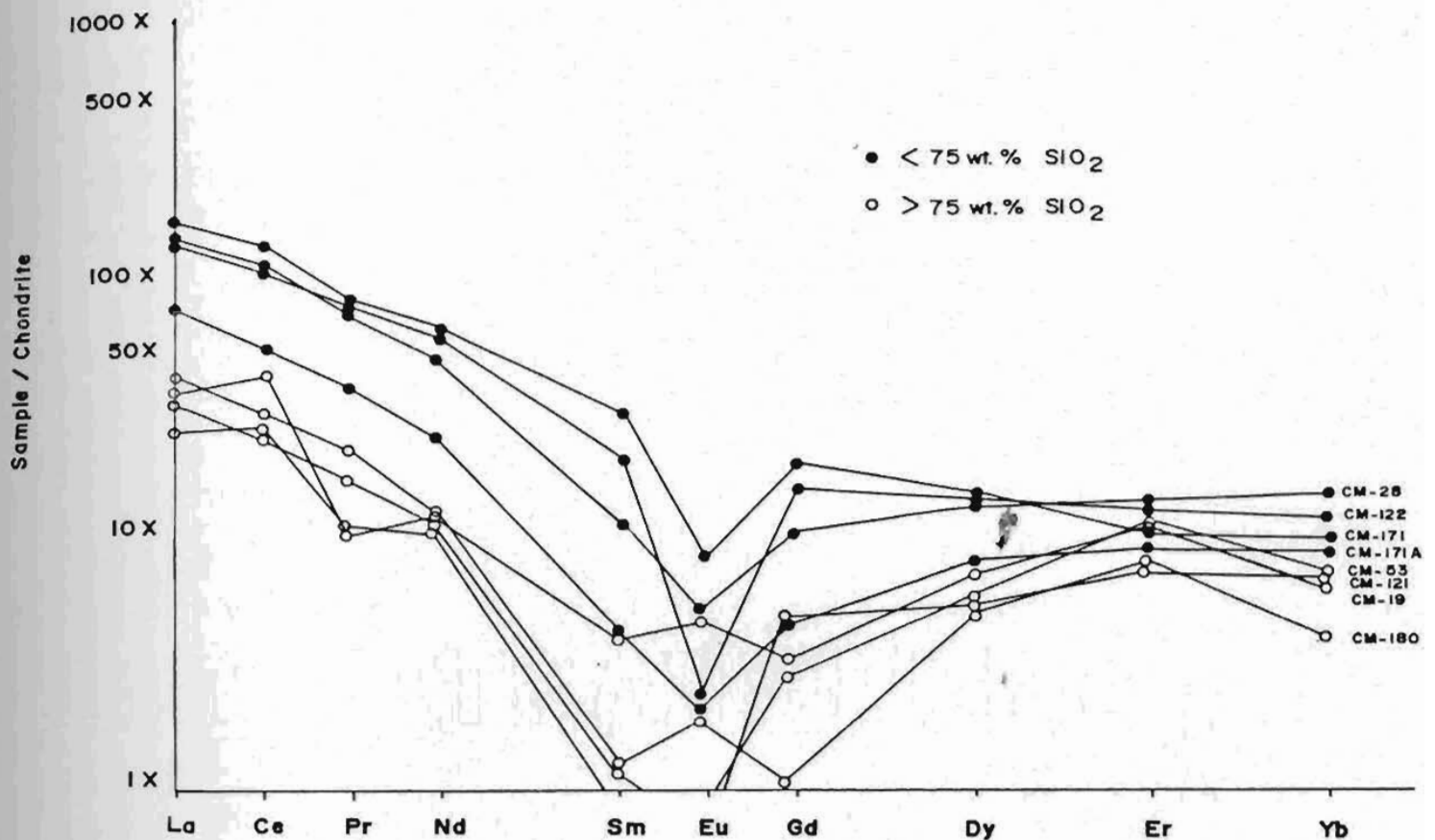


**Figure 3-9:** Chondrite-normalized REE plot for
the Monkey Hill Granite,
Round Pond area.

partitioned into the magma preferentially compared to coexisting crystals. Thus, one would expect that igneous processes such as crystal fractionation should result in progressive enrichment of REE in residual liquids. As stated above this is not the case. Miller and Mittlefehldt (1982) and Cullers and Graf (1984) suggest that LREE are not incompatible and that the observed LREE depletion is due to the fractional crystallization of minute LREE-rich accessory minerals such as

monazite or allanite. By analogy then, the depletion of MREE observed in this study, could result from fractional crystallization of accessory minerals such as apatite and sphene which have a strong affinity for the MREE (Simmons and Hedge, 1978). A decrease in $P_2O_5$, $TiO_2$ and $CaO$ with increasing $SiO_2$ observed in this study, does lend support to this idea. However, the presence of REE-enriched accessory minerals such as monazite, apatite, sphene and zircon within the stocks of Monkey Hill Granite indicate that a significant separation of these accessories from the magma as a result of fractional crystallization did not occur. Thus, this could not have been an effective mechanism to account for the magnitude of REE depletions observed, and that the decreases in the elements mentioned above are not entirely related to fractional crystallization of these accessory minerals.

Loss of REE in an exsolved volatile-rich vapour phase has been suggested as a viable mechanism to account for REE depletion in highly differentiated granitic rocks (Muecke and Clark, 1981; Fourcade and Allegre, 1981). Experimental evidence (Flynn and Burnham, 1978) together with the empirical studies (McLennon and Taylor, 1979; Taylor and Fryer, 1982, 1983) have indicated that in general, Cl complexes and transports LREE, while F and $CO_3$ complexes and transports the HREE. Realizing that apatite has a strong affinity for MREE (Simmons and Hedge, 1978; Hanson, 1980), it may be reasonable to suggest that a phosphate-rich volatile phase (ie. $PHO_4$) could effectively complex and transport the MREE.

Compelling evidence (see section 4.5) to support depletion of REE, in particular the MREE, due to the loss of a REE-enriched volatile phase is found in the mineralized hydrothermal veins distal to the granitic stocks in the adjacent country rock. The veins exhibit overall enriched, flat to saucer shaped REE profiles, with Eu anomalies that range from small, negative to slightly positive. Compared to unmineralized country rock, the mineralized veins have had a significant addition of Eu (Wilton and Wardle, 1987), which correlates with the pronounced MREE depletion exhibited by the granites. The mineralization is

associated with fluorite, apatite and carbonate, as well as a pronounced Na-metasomatism, indicating a relationship to a mixed volatile-rich fluid as suggested above.

The observed depletions in MREE, along with lesser depletions in LREE and HREE suggest that more than one anionic species was probably present in the exsolved volatile-rich phase. The saucer-shaped profiles mentioned above, have been interpreted as indicating the presence of a $F^-$ and/or $CO_2^{2-}$ volatile-rich phase (Taylor et al., 1981). The loss of such a phase would result in the depletion of HREE. The observed depletion in the MREE along with the LREE suggests that P and Cl anionic species were also involved. Thus a mixed volatile-rich phase consisting of $CO_2^{2-}$, $F^-$, $Cl^-$, and $HPO_4^{2-}$ anions could effectively concentrate and remove REE as complexes from a granitic melt, resulting in the observed depletions.

## 3.4. Petrogenesis

Field and petrographic evidence indicate that the satellite stocks of the Monkey Hill Granite in the Round Pond area are shallow, epizonal intrusions. The emplacement of the stocks to such a high level implies that the magma must have been water undersaturated, at least initially. This is supported by the observed order of crystallization from . quartz and feldspar to late interstitial biotite. Water saturation late in the magma evolution is marked by the appearance of . biotite, granophyric mantles on euhedral feldspar, irregular miarolitic cavities and pegmatitic pods and veins associated with granophile mineralization. The occurrence of pegmatitic veins and mineralized hydrothermal fluorite veins in the adjacent country rock suggest that an exsolved fluid phase eventually escaped from the crystallizing stocks, resulting in volatile loss.

Geochemical data indicate that the leucogranite stocks in the Round Pond area are highly differentiated granitic intrusions typical of high level, apical

portions or cupolas of batholiths at depth. The observed major-element and trace-element trends must ultimately be the result of long-lived magmatic processes such as fractionational crystallization (Groves and McCarthy, 1978 ; Miller and Mittlefehldt, 1984) or liquid-state thermogravitational diffusion (Hildreth, 1981). The granitic stocks in the Round Pond area by themselves do not allow a subjective evaluation of these two processes, which would require a much more regional study of a scale far larger than the present study (eg. Tuach et al., 1986; Kerr, 1987). Of greater importance to this study are processes that develop late in the history of magma evolution which ultimately result in divergent chemical trends and the possible generation of mineralization.

As high level, apical portions of a batholith at depth, the granitic stocks in the Round Pond area are favourable sites for the accumulation of metal-bearing volatile-rich phases. Such volatile-rich phases have important implications regarding the history of crystallization and degree of differentiation, as well as the level of emplacement. As can be seen from figure 3-10, the presence of volatiles, such as F and P within a crystallizing magma, lower the solidus (ie. crystallization occurs at lower temperatures), thus prolonging differentiation and promoting intrusion to higher levels (Bailey, 1977; Strong, 1981). The occurrence of fluorite as a vein mineral in mineralized hydrothermal veins adjacent to the granitic stocks, and as a minor mineral phase within the granitic stocks, strongly suggests that fluorine-rich aqueous fluids played an important role in the late-stage magmatic evolution of the satellite stocks of Monkey Hill granite. Bailey (1977) states that the presence of F promotes quartz and feldspars above biotite in the order of crystallization, as is observed in this study. F would, as a result, migrate to upper portions of the magma chamber to be concentrated in residual and interstitial melts.

Interestingly, the expected enrichment in F is not observed in the granitic stocks at Round Pond. F contents are generally low and well below average for low-Ca granites. Bailey (1977) has pointed out that during differentiation towards
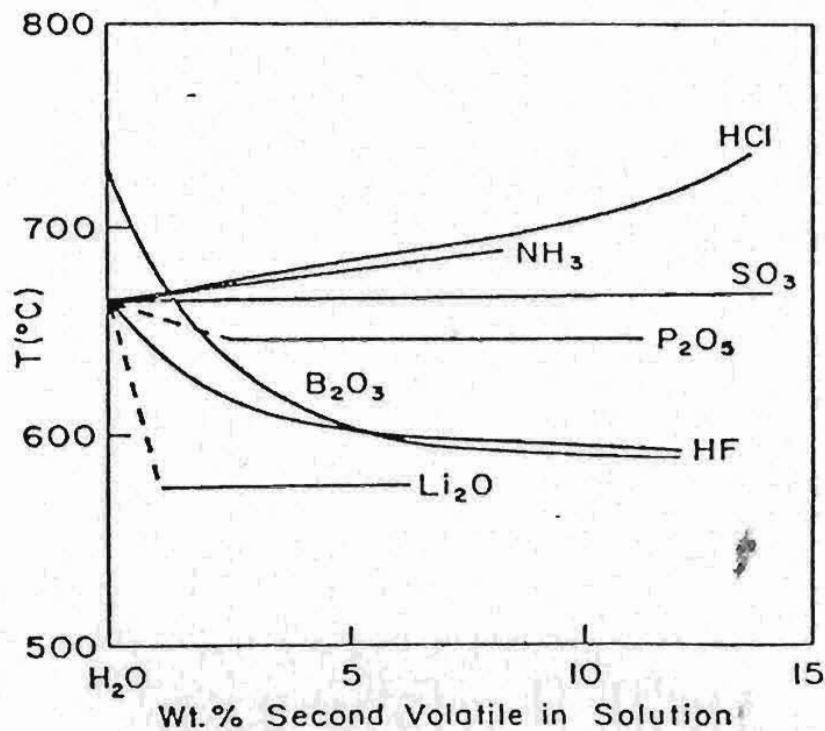
**Figure 3-10:** The effects of different elements
or compounds on the melting temperature
of granitic magmas at 2.5 kbar
(from Strong, 1980).

more siliceous melts (ie. differentiation), there is an increasing loss of F to a
vapour phase. At shallow levels of emplacement, such phases may readily escape
once volatile pressures exceed confining pressures as a result of retrograde boiling
and failure of the confining rock. The occurrence of numerous fluorite-bearing
pegmatite veins and mineralized hydrothermal veins in the adjacent country rock
of the Round Pond area (MacDougall and Wilton, 1987a) clearly suggest that such
a volatile-rich phase escaped from the crystallizing stocks. Degassing (volatile-
separation) of a F-rich residual magma would result in F contents of 400-600 ppm

in the granite, with enrichments in pegmatites and mineralized veins (Bailey, 1977), as observed in this study (see figure 3-11).
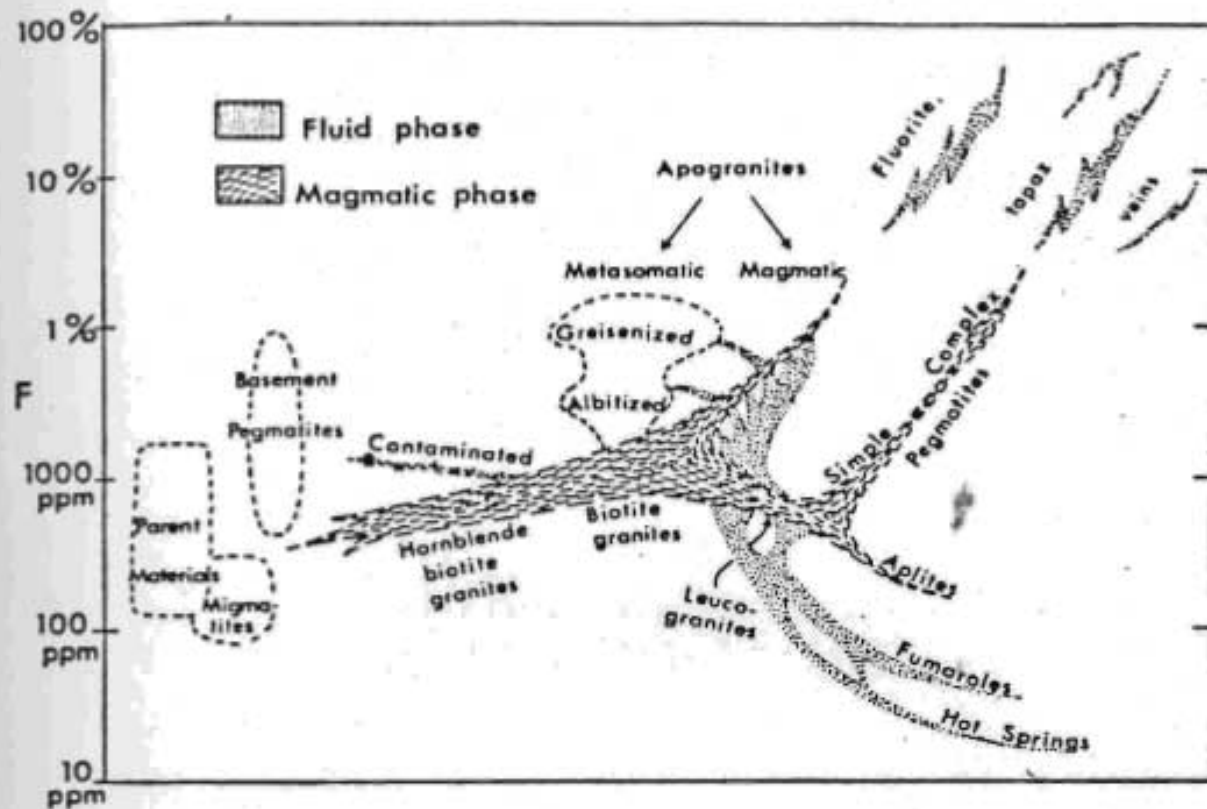


**Figure 3-11:**   Schematic diagram of F variation
in a calc-alkaline granitic system
(from Bailey, 1977).

The escape of a volatile-rich phase would also result in the loss of other elements represented by an apparent depletion or lack of enrichment. A logical extension of this is that the below-average contents of HFS elements and lack of significant granophile elements (Sn, W, U, Mo) may be linked to the loss of the volatile-rich phase envisaged above. The close association of granophile elements with F and other solidus-lowering volatiles with mineralized showings in the

Round Pond area provides compelling evidence for such a case. The enrichment/depletion trends of other elements (ie. Rb, Ba, Sr) can be explained by normal magmatic differentiation trends and are widely observed in other studies. REE patterns discussed previously similarly suggest the presence of a mixed ($CO_2^{2-}$, $F^-$, $PHO_4^{2-}$, $Cl^-$) volatile-rich phases within the highly differentiated granitic stocks and that the escape of such a volatile-rich phase may account for the observed depletion of REE.

### 3.4.1. Classification of the Monkey Hill Granite

A popular classification scheme for granitic rocks involves genetic subdivisions based on the source materials from which the granites were derived as partial melts. Subdivisions are based on a range of criteria, but centre on geochemical compositions of the granitic rocks. Chappell and White (1974) demonstrated that granites of eastern Australia can be classified as either I-type, derived from the partial melting of an igneous source, or S-type, derived from a sedimentary source. Under this classification scheme, the stocks of Monkey Hill Granite would be classed as I-type granites, based on low molecular ratios of $Al_2O_3/(Na_2O + K_2O + CaO) < 1.05$, with only small amounts of normative corundum $< 1\%$.

Since this initial classic work, tectonic factors have been implied which suggest that I-type granites are produced in post-orogenic, uplift, regimes; and S-type granites are the product of continental collisions (Beckinsale, 1979; Pitcher, 1983). A further genetic-tectonic granite subdivision was introduced by Loiselle and Wones (1979), referred to as the A-type (anorgenic) granite, produced by second stage, post-tectonic melting of anhydrous lower crust from which an orogenic granite magma had been previously extracted. A-type granites are characterized by high $SiO_2$, total alkalies, Fe/Mg ratios, and trace elements such as F, Zr, Nb, Ga, Sn, Y, and REE, with low CaO and trace elements Ba and Sr (Loiselle and Wones, 1979; Collins et al., 1982; White and Chappell, 1983).

The Monkey Hill Granite appears to be an A-type granite, or at least represents a transition between I-type and A-type (see figure 3-12). Classification as an A-type granite is consistent with the interpretation as a post-tectonic granite intrusion. Similar, subalkaline, A-type, and transitional A-type granites have been identified in New Brunswick and Newfoundland, which are associated with granite-related Sn, W, Mo, F mineralization (Whalen, 1986; Tuach et al., 1986).
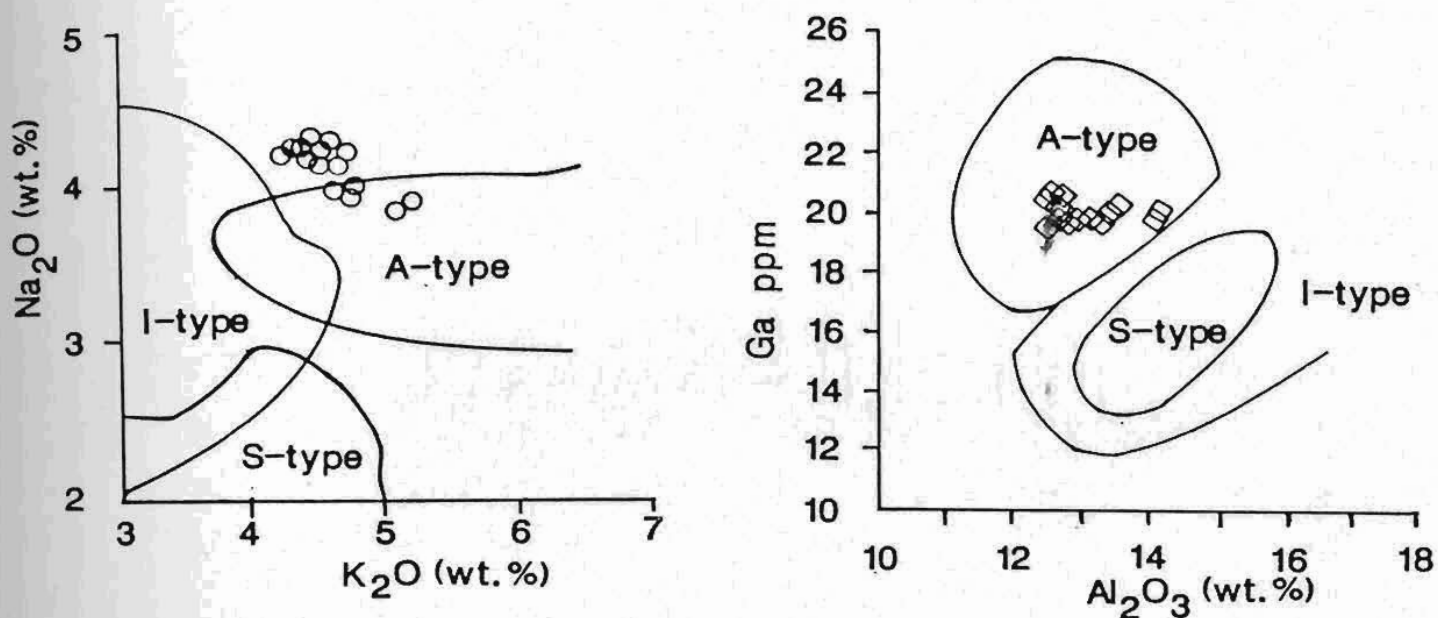


**Figure 3-12:** Genetic-tectonic classification of the Monkey Hill Granite.

(after White and Chappell, 1983)

## 3.5. Discussion

Field relations and geochemical data suggest that the satellite, granitic stocks in the Round Pond area are shallow, epizonal intrusions that represent highly differentiated, apical portions of a large granitic batholith (ie. Trans-Labrador batholith) present at depth (MacDougall and Wilton, 1987a). Kerr (1986, 1987)

reached a similar conclusion based on preliminary results of a regional granite study. Such intrusions are considered to be favourable sites for the accumulation of metal-bearing, volatile rich phases (Mutschler et al., 1978; Stemprok,1980) which can ultimately result in the formation of mineral deposits. The occurrence of mineralized hydrothermal fluorite veins in the Round Pond area, that are commonly associated with shallow seated plutons, clearly lends support to this interpretation.

The characteristics of granitoid rocks associated with a variety of "granophile" mineral deposits have been discussed by numerous authors (ie. Tischendorf, 1977; Strong, 1981; Stemprok, 1980; Mutschler et al., 1981; Westra and Keith 1981; White et al., 1981, etc.). Among the various concepts to emerge, one of the most significant is the recognition of "specialized granites". Tischendorf (1977) broadly defined "specialized granites" as a metallogenically specialized granitoid rock series spatially and genetically associated with ore deposits of rare elements (Sn, Li, Rb, Cs, Be, Nb, Ta, W, Mo, F, U). Such metallogenically specialized granites exhibit similar geochemical, petrographical and geotectonical features, as outlined in table 3-3. Specialized granites can be distinguished by the sum of their characteristics in Table 3-3. More recent studies (ie. Chatterjee et al., 1983) have attempted to refine this concept so as to recognize the specialization with respect to specific economic elements such as Sn, W and U.

**Table 3-3:** Comparison between Monkey Hill
Granite and "Specialized Granites"
as defined by Tischendorf, (1977).

| Specialized Granites | Monkey Hill Granite |
|---|---|
| | |

### Geo-tectonic Features

| | |
|---|---|
| - Mid to late stages of orogeny | - Post-tectonic, A-type granite |
| - True intrusive character | - Discordant, intrusive contacts |
| - High level of emplacement | - Epizonal stocks |
| - Apical portions of batholith | - Apical portions of TLB |

### Chemical Features

| | |
|---|---|
| - High $SiO_2$ (> 72%), extreme depletion of CaO, MgO, total Fe. | - High $SiO_2$ (avg. >76%), low CaO, MgO, total Fe. |
| - Enrichment in LIL elements (Rb, Pb, U, Th), and sometimes HFS elements (Zr, Y, Nb, Ca). | - LIL element enrichment based on regional geochem. background (Kerr, 1987), Depletion of HFS elements. |
| - Depletion in Sr, Ba, and Compatible elements (Cr, Ni, V). | - Depletion in Sr, Ba, and Cr, Ni, V. |

### Other

| | |
|---|---|
| - Evidence of volatile activity, hydrothermal alteration, high volatile content ie. enrichment in F, B, Cl. | - Miarolitic cavities, pegmatitic pods and veins, fluorite accessory mineral and as exocontact veins. |
| - associated with granophile (Sn,W,U,Mo) mineralization. | - associated with exocontact Mo,U, (W),base metal mineralization. |

Based on the criteria established by Tischendorf (1977), the satellite stocks of Monkey Hill Granite in the Round Pond area appear to represent metallogenic specialized granites (see Table 3-3) possessing most of the criteria. However, as mentioned earlier, trace element contents, especially the degree of enrichment of LIL is of a lesser magnitude compared to highly specialized compositions reported from many studies (Tischendorf, 1977; Mutschler et al., 1981; Imeokparia, 1985; Ramsay, 1986). Kerr (1987) similarly noted the low absolute abundances of lithophile elements from highly differentiated granites of the TLB, and concluded that regional granites representative of deeper, non-specialized portions of the Trans-Labrador Batholith were depleted in these elements relative to the average contents reported by Turekian and Wedepohl,(1961) for low Ca granites. Thus the overall low abundances in LIL elements reflects ultimately the nature of the Archean source material and subsequent degree of partial melting. Based on this, Kerr (1987) stated that such highly differentiated satellite intrusions of the TLB, although possessing low absolute abundances, exhibit LIL enrichment trends of specialized granites in relation to their own local geological and geochemical background. Wilton et al., (1986), and MacDougall and Wilton (1987a) similarly suggested enriched trace element contents.

Recognition of the Monkey Hill Granite satellite stocks as specialized granites is further complicated by the separation and loss of a metal-bearing, volatile-rich phase. Lack of enrichment in granophile elements (ie. Mo, U, F, etc.), low abundances in HFS elements (Zr, Y, Nb, Ga) and REE has been shown to reflect the loss of such a phase, and that these elements are found to be enriched in mineralized hydrothermal veins hosted in the adjacent country rock.

Thus the concept of "specialized granites" must be used with caution, and not be based solely on comparisons of absolute elemental abundances between various metallogenically specialized granitic provinces.

# Chapter 4
# Mineralization

## 4.1. Introduction

The Upper Aillik Group hosts numerous, monometallic uranium, and polymetallic Mo-base metal $\pm$ U mineral occurrences, including the partially developed Michelin uranium deposit, and the subeconomic Aillik Bay molybdenite deposit.

Genetic models for the widespread uranium and molybdenite mineralization (based largely on the monometallic Michelin and Kitts uranium deposits), have generally advocated broadly synvolcanic hydrothermal processes, and propose the source of the mineralization to be the felsic volcanic rocks, or associated synvolcanic plutons of the Upper Aillik Group (Gandhi et al., 1969; Gandhi, 1978, 1986; Evans, 1980; White and Martin, 1980; and Gower et al., 1982). Mineralization in the Round Pond area, however, is dominated by polymetallic (Mo, U, Cu, Zn, Pb, F) magmatic-hydrothermal veins as well as hematized radioactive zones spatially associated with the intrusive contact zone of a high level, post-tectonic leucogranite.

## 4.2. Regional Metallogeny of the Aillik Group

Table 4-1 summarizes information concerning grade and ore reserves of the more important mineral deposits and prospects, and figure 4-1 (after Gower et al., 1982) shows locations of the mineral occurrences discussed.

Most of the mineral occurrences hosted by the metasedimentary and

metavolcanic rocks of the Aillik Group may be grouped into three geographic metallogenic districts, each of which exhibit a distinctive style of mineralization (see figure 4-1). Similar metallogenic or stratigraphic - structural belts have been suggested by Gandhi (1978), Gower et al. (1982), and Wilton and Wardle (1987); and districts discussed in this section are modified from those previous workers. The three metallogenic districts are: i) Kitts - Post Hill, ii) Michelin - White Bear Mountain, iii) Aillik - Makkovik Coastal districts.

Mineral occurrences in the Kitts - Post Hill district are hosted in metasedimentary rocks of the Lower Aillik Group, while occurrences in the other two districts are hosted by felsic volcanic rocks of the Upper Aillik Group. Fundamental differences, however, exist between the two later areas concerning the degree of deformation and metamorphism, nature of the post-tectonic granitic intrusions (see section 2.1), and metallogenic characteristics (see below).

### 4.2.1. Kitts - Post Hill District

In the Kitts - Post Hill metallogenic district, a number of stratabound uranium mineral occurrences are hosted in metasedimentary rocks of the Lower Aillik Group. The most significant of these are the high grade Kitts deposit, and similar lower grade Inda, Nash, and Gear prospects (Gandhi, 1978).

Mineralization is associated with argillaceous and tuffaceous metasedimentary rocks which occur near the top of the Kitts pillow lava formation, close to the contact with the overlying felsic volcanic rocks of the Upper Aillik Group (Gandhi, 1978; Gower et al., 1982). The mineralized zone at the Kitts deposit has been delineated along strike for 364 m, with an average thickness of 1.5-2.0 m. Mineralization occurs as thin, discordant to concordant veinlets of pitchblende, and as coatings on fracture and shear surfaces (Gandhi, 1978).

**Table 4-1:** Tonnage, grade, and reserves
for important mineral deposits hosted
by the Aillik Group
(from Gower et al., 1982).

| Deposit (District) | Approximate tonnage (tonnes) | Grade | Reserves (approximate) x 1,000,000 kg |
|---|---|---|---|
| Kitts deposit (Kitts-Post Hill) | 207,150 | 0.73% U | 1.36 |
| Inda prospect (Kitts-Post Hill) | 550,000 | 0.155% U | 0.8 |
| Nash prospect (Kitts-Post Hill) | 238,000 | 0.20% U | 0.45 |
| Gear prospect | <80,000 | 0.145% U | <0.1 |
| Michelin deposit (Michelin-White Bear Mountain) | 7,000,000 | 0.13% U | 8.3 |
| Rainbow prospect (Michelin-White Bear Mountain) | <300,000 | 0.10% U | <0.12 |
| Burnt Lake prospect (Michelin-White Bear Mountain) | <150,000 | 0.082% U | <0.12 |
| Aillik Bay Deposit (Aillik-Makkovik) | 2,000,000 | 0.25% Mo local U <0.05% | N/A |
| Sunil prospect (Aillik-Makkovik) | <350,000 | 0.102% Mo 0.028% U | <0.33 <0.1 |
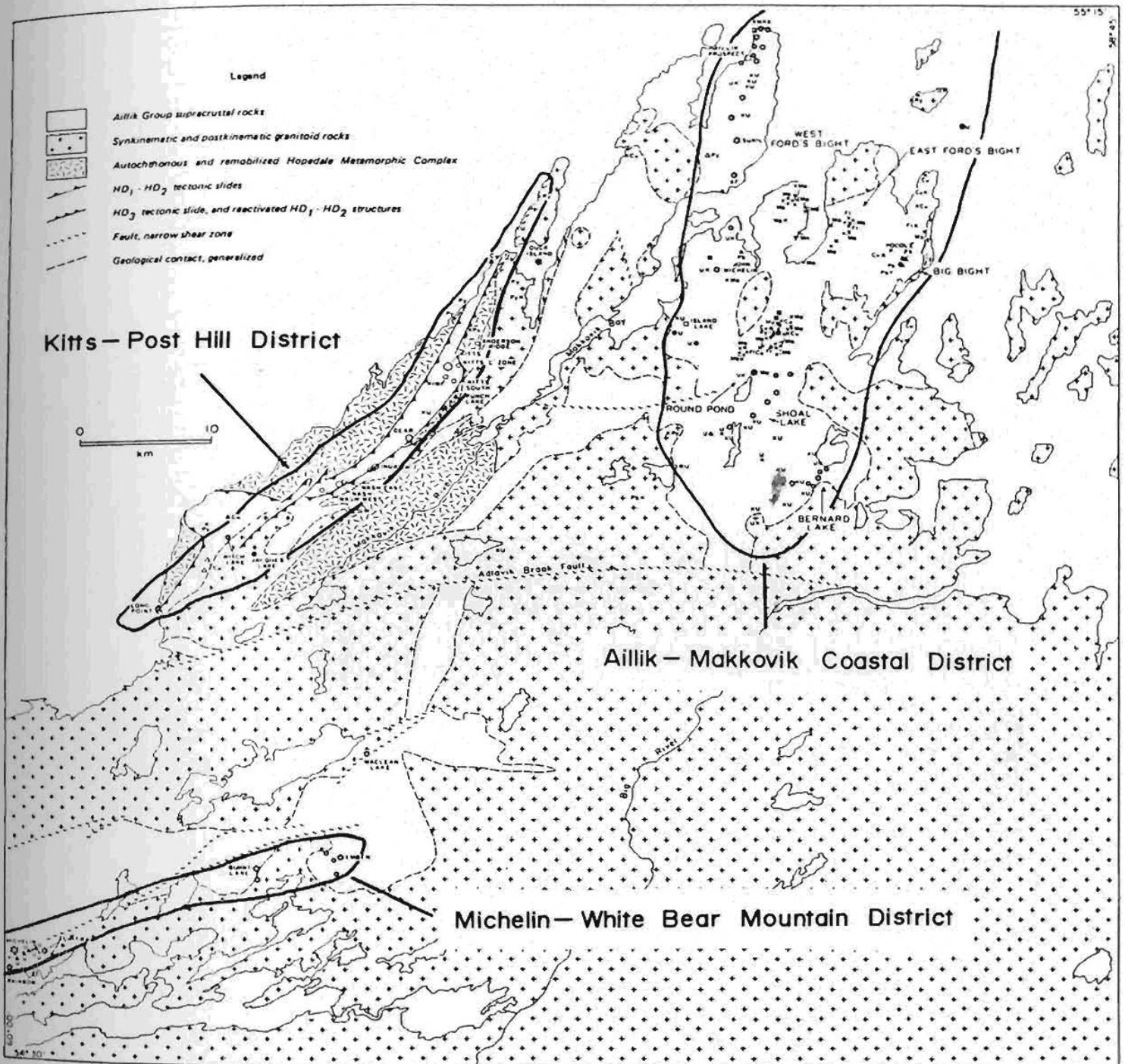
**Figure 4-1:** Summary of mineral occurrences and
metallogenic districts in the
Kaipokok Bay - Big River area
(modified from Gower et al., 1982).

Visible wall rock alteration is generally lacking or poorly developed, although calcite veining is widespread (Gower et al., 1982). Geochemical data from Evans (1980) suggest the presence of a Na-metasomatic halo.

Gandhi (1978) described the mineralization as syngenetic with the host reduced sediments of the Lower Aillik Group; later, Gandhi (1986) stated that the host unit is actually the lower portion of the Upper Aillik Group.

### 4.2.2. Michelin - White Bear Mountain District

The Michelin - White Bear Mountain metallogenic district is characterized by numerous uranium mineral occurrences hosted in rhyolites of the Upper Aillik Group. The Michelin Deposit is the largest known uranium deposit hosted in the Aillik Group, with drill proven reserves of 7,000,000 tonnes of ore grading 0.13 % $U_3O_8$ (Gower et al., 1982). Several smaller uranium prospects, notably the Rainbow, Burnt Lake, and Emben prospects, occur nearby. '

The Michelin deposit ore zone consists of numerous, thin, lenticular mineralized zones distributed en echelon over a total strike length of 1200 m, with individual lenses up to 5 m thick (Gandhi, 1978, Gower et al., 1982). Mineralization is associated predominantly with a coarse porphyritic rhyolite unit, and occurs as finely disseminated pitchblende associated with pyroxene, amphiboles, sphene, andradite, and Fe-Ti oxides (Gandhi, 1978; Gower et al., 1982). The Burnt Lake prospect also contains traces of sphalerite, galena, and silver, which may represent a later superimposed base metal mineralizing event (MacKenzie and Wilton, 1987).

Wall rock alteration consists of visible red hematization associated with ore zones, and a wider, pronounced zone of Na-metasomatism and oxidation (White, 1976; Gandhi, 1978; Evans, 1980; White and Martin, 1980; Gower et al., 1982).

## 4.2.3. Aillik - Makkovik Coastal district

The Aillik - Makkovik Coastal metallogenic district exhibits a more complex metallogenic style of mineralization compared to the Michelin-White Bear Mountain district (Gower et al., 1982; Wilton et al., 1986; Wilton and Wardle, 1987; MacDougall and Wilton, 1987a; MacKenzie and Wilton, 1987). The district is characterized dominantly by molybdenite $\pm$ low grade uranium mineralization, uranium mineralization without molybdenite, and minor base metal (Pb-Zn) mineralization. Wilton et al. (1986), have suggested a $Mo\underset{}{.}Ag\pm U$ association exists in this district. In addition to more complex metallic mineral associations, complex alteration mineral assemblages are observed (Beavan, 1958; Wilton et al., 1986; MacDougall and Wilton, 1987a, 1988; Wilton and Wardle, 1987). Figure 4-2 shows locations of some of the more significant mineral occurrences in the district.

The most important mineral occurrence is the Aillik Bay molybdenite deposit (Piloski, 1960; Gandhi, 1978; Gower et al., 1982), hosted in recrystallized felsic volcanic rocks of the Upper Aillik Group. A mineralized zone extending 2300 m along strike, with a maximum width of 25 m has been outlined, containing 2,000,000 tonnes of ore material grading 0.2-0.3% $MoS_2$.

Mineralization consists of molybdenite-pyrite disseminations, fracture-fillings, and quartz veins, subparallel to the planar fabric of the host rock, locally resembling a typical stockwork style of mineralization (Wilton et al., 1986; Wilton and Wardle, 1987). Previous workers (Gandhi, 1968, Ryan, 1977, Gower et al., 1982) described the mineralization as parallel to the host rock foliation. Minor uranium mineralization is occassionally present, generally grading $< 0.05\%$ $U_3O_8$. Uranium mineralization at the north end of the Aillik Bay molybdenite deposit is associated with pyritiferous, fluorite-bearing metavolcanic rocks, and occurs as intergrown amphibole, uraninite, and sphene fracture- fillings (Wilton et al., 1986). Morse (1961), Barua (1966), and Gandhi (1969) reported anomalous quantities of albite and enriched Na contents in the host rock, suggesting Na-metasomatism similar to that observed at the Kitts and Michelin uranium deposits.
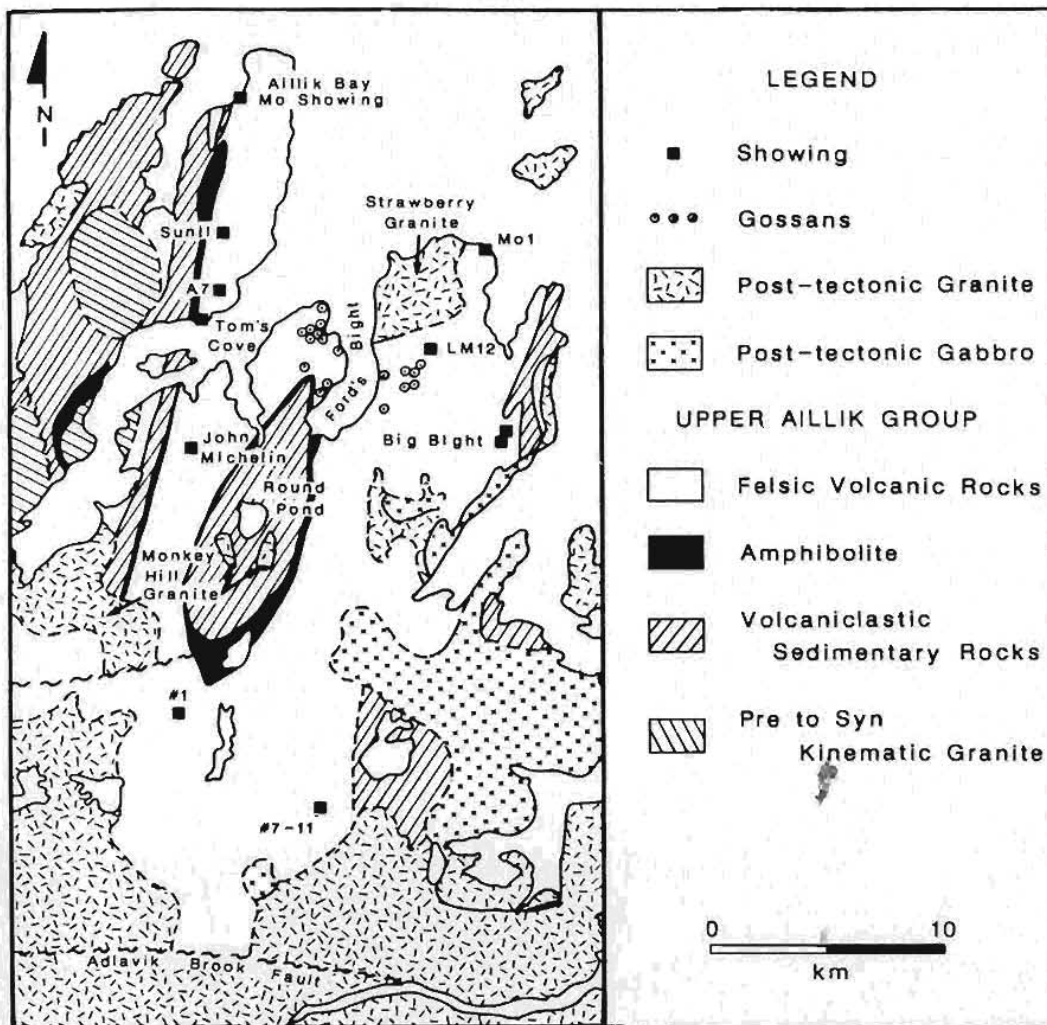
**Figure 4-2:** Location of important mineral
occurrences, post-tectonic granitoids,
and gabbroids in the Aillik-Makkovik
Coastal District (from Wilton and
Wardle, 1987).

Numerous Mo and Mo-Base Metal-U-F mineral occurrences also occur in the
Round Pond and Ford's Bight areas. Those in the Round Pond area are discussed
in detail below (see section 4-3).

The most important uranium mineral occurrences in the Aillik - Makkovik
Coastal district occur in a discrete stratigraphic level within the Upper Aillik
Group (Gower et al., 1982), and include the Sunil and A-7 prospects, and the

John Michelin showing. The Sunil prospect is hosted in felsic metavolcanic rocks interbedded with minor metasedimentary horizons, and contains an estimated 350,000 tonnes with an average grade of 0.03% $U_3O_8$ and 0.1% $MoS_2$ (Gower et al., 1982). The mineralized zone consists of a stratiform, sheetlike body 350 m long and 5 m thick. Mineralization occurs as a pyritiferous gossan containing disseminated molybdenite, sphalerite, and radioactive fluorite, with minor chalcopyrite rare galena, and traces of Ag and Au (Wilton et al., 1986, 1897b). Small concordant to discordant veinlets of fluorite carrying disseminated uraninite also occur.

The A-7 prospect is similar to the Sunil Prospect and contains a reported average grade of 0.19% $U_3O_8$ (Gower et al., 1982). Mineralization consists of small (< 3.0 cm) skarnoid zones (consisting of carbonate, garnet, fluorite, amphibole, and biotite), carrying sphalerite, and pyrite mineralization. The zones are associated with uraninite-amphibole fracture-fillings (Wilton et al., 1986).

The John Michelin showing consists of a 200 m zone exhibiting weak radioactivity with local high-grade spots. Mineralization occurs as disseminated uraninite intergrown with andradite, sphene and amphibole in fracture-fillings within metavolcanic rock. Skarnoid patches of carbonate, garnet, epidote, and quartz are also present (Wilton et al., 1986; Wilton and Wardle, 1987).

Further to the southeast, a number of significant uranium occurrences occur in the Shoal Lake - Falls Lake, and Bernard Lake - Winter Lake areas. Occurrences in the Falls Lake area are discussed in detail below (see section 4-3). Of particular note is the uranium showing known as Showing # 1 near Shoal Lake, which represents a different style of mineralization than has been discussed in this review. Mineralization occurs as pitchblende and specular hematite in a shear zone cutting the contact between an amphibolite of the Upper Aillik Group and a dyke of Monkey Hill Granite. The mineralization has been concentrated by a later Grenvillian period of remobilization (Beavan, 1958; Gandhi, 1978; Wilton et al., 1986).

## 4.3. Mineralization in the Round Pond Area

### 4.3.1. General Features

The Round Pond area is characterized by numerous, widely distributed, zones of Mo-(W)-base metal-U-F mineralization, and linear radioactive zones (which locally attain economic grades), and exhibit considerable diversity with respect to form. Although the mineralization is widely distributed (see Map-1, back pocket), there appears to be a dominant litho- structural control with respect to the localization of mineralization (see figure 2-2, Chapter 2). Mo-(W) base metal-U-F mineral showings are heavily concentrated as exocontact mineralization along the contact zone of the east stock of Monkey Hill Granite. The mineralization is hosted in the felsic volcanic conglomerate/agglomerate (unit 3) and appears to be associated with N-S trending fractures and shear zones, slightly discordant with regional trends. The fractures and shear zones are presumably related to the intrusion of the post-tectonic Monkey Hill Granite. Similar mineralization located northwest of Falls Lake is also hosted in the felsic volcanic conglomerate.

The intrusive granitic stock to the west intrudes a recrystallized felsic tuff unit, and does not appear to be associated with any significant mineralization. This suggests that the felsic volcanic conglomerate was a favourable lithologic unit for the localization of mineralization, due to a greater permeability resulting from structural weakness (compared to other lithologies) which induced fracture/shear channelways allowing the migration of mineralized fluids.

Linear radioactive zones, in contrast, are predominantly restricted to rhyolitic lithologies. One occurrence, however, is hosted in felsic volcanic conglomerate northwest of Falls Lake. Uranium mineralization is generally associated with slightly discordant fractures and shear zones concentrated along lithologic contacts (ie. zones of structural weakness).

Mineral occurrences in the Round Pond area are spatially associated with the intrusive contact zone of a high level, post-tectonic, leucogranitic stock, which has been interpreted to represent the apical portions of a batholith at depth. A crude metallogenic zonation is observed with respect to the east satellite stock of Monkey Hill Granite. Mineralization varies from Mo-Cu-F hydrothermal veins and stockwork mineralization proximal to the granite, spatially intermediate Zn-Pb bearing carbonate vein mineralization, and finally distal U-Zn mineralization. A similar metallic zonation was reported in the Strawberry Granite pluton to the north, by Wilton and Wardle (1987).

### 4.3.2. Types of Mineralization

Mineralized samples were analyzed for base metal (Cu, Pb, Zn) and U contents by X-ray fluoresence; Mo and Ag by ICP-MS at a commercial labratory; and Au by fire assay preconcentration, with atomic absorption finish also at a commercial labratory (see Appendix I).

Gandhi et al. (1969) recognized three types of mineralization in the Round Pond area: i) disseminated pyrite-molybdenite zones; ii) disseminated suphide mineralization at the contacts of "metadiorite dykes"; iii) hydrothermal veins containing massive pyrite, with lesser molybdenite, chalcopyrite, pyrrhotite, and fluorite. Small, stratiform radioactive zones were also reported in the southeastern portion of the study area (Piloski, 1955; Gandhi, 1967). In the course of this investigation, these basic types have been further defined, and several important new types are described.

### 4.3.3. Pyritiferous Gossan Zones

Rusty pyritiferous gossan zones hosted in recrystallized felsic tuffs, rhyolites, and volcanic conglomerate represent the most abundant type of mineralization in the Round Pond area (see figure 4-3). The gossans which are a product of secondary surface oxidation of disseminated sulphide mineralization, appear as lightly to moderately rusted, linear zones up to hundreds of metres in length. Mineralization

is generally low grade ($< 0.1\%$ $MoS_2$), dominated by disseminated, fine to coarse pyrite, with occassional flakes and stringers of molybdenite, and minor disseminated chalcopyrite, sphalerite, fluorite and rare galena. Similar mineralization is described by Gower et al. (1982), Wilton et al. (1986), and Wilton and Wardle (1987) scattered throughout the metavolcanic rocks on the Cape Strawberry and Ford's Bight Peninsulas (see figure 4-2).

The gossan zones are generally localized in zones of shearing and fracturing (see figure 4-4), and are occassionally cut by sulphide-bearing quartz veins (which may represent the foci of ore fluid influx as suggested by Wilton et al., 1986), and/or mineralized pegmatites carrying disseminated pyrite, molybdenite and fluorite. Where gossan zones are intruded by diabase dykes, mineralization appears to be concentrated towards the intrusive contacts. The dykes themselves are unmineralized, suggesting that the concentration represents a secondary redistribution of mineralization within the gossans.

### 4.3.4. Hydrothermal Veins

Discordant hydrothermal veins in the Upper Aillik Group represent the most significant mineralization in the Round Pond area. Most occur proximal to the eastern stock of Monkey Hill Granite, but one vein system occurs northwest of Falls Lake, and may be related to the main intrusive pluton of Monkey Hill Granite that occurs west of the study area. Vein-type mineralization described in this section correspond to Veins 1 through 14 listed in the NDM Mineral Inventory Files.

**Figure 4-3:** Intensely rusted, pyritiferous gossan
hosted within felsic volcanic conglomerate.
Coarse pyrite mineralization occurs in the
tuffaceous matrix surrounding ellipsoidal
(less rusted) felsic volcanic clasts.

**Figure 4-4:** Outcrop of pyritiferous gossan with
intense pyrite (rusted) mineralization
localized in N-S trending fractures.
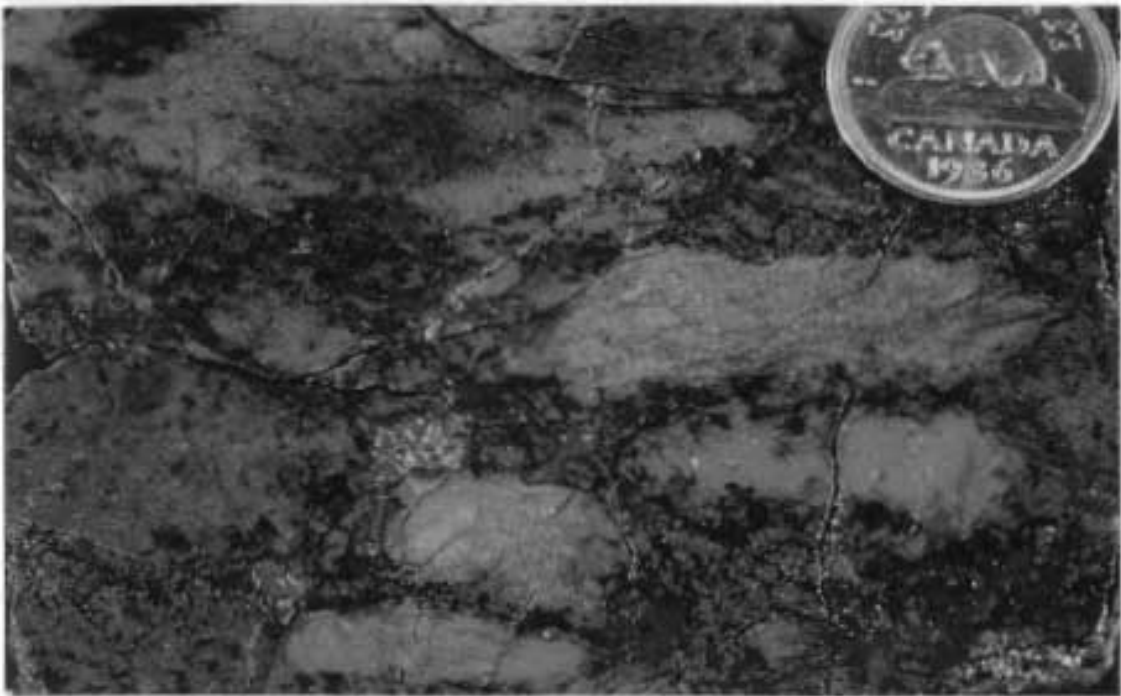
The vein systems are small, ranging from tens of centimetres to several metres wide, with lengths up to 100 m. Often veins disappear under low, swampy, grassy areas, suggesting that they might extend farther along strike. The vein systems appear to be associated with zones of shearing, and locally brecciation is developed. Similar brecciation has been observed with other styles of mineralization (see below) as well as in drill core which intersected weak molybdenite mineralization north of Round Pond (see figure 2-6, Chapter 2). The brecciation is hydrothermal in nature, and is typically associated with fluorite and carbonate. Calcic skarn alteration mineral assemblages are generally developed in country rock adjacent to the veins (see section 4-4).

Mineralization within the the hydrothermal veins is often spectacular, and reflects a hydrothermal ore metal assemblage of Fe-Mo-(W)-Cu-Zn-Pb-U-F-Ba, with minor enrichments in Co, Ag, Bi, Te, and Au. Gossan zones are always associated with hydrothermal veins, which suggests that other gossan zones distributed throughout the Round Pond area are the result of hydrothermal activity, and may be closely related to vein systems not presently exposed.

Primarily three types of mineralization are recognized as hydrothermal veins: i) massive and stockwork sulphides, ii) mineralized fluorite veins, iii) quartz-molybdenite veins. A paragenetic sequence is developed from early massive sulphides, to later crosscutting mineralized fluorite and quartz veins.

### i) Massive and Stockwork Sulphide Mineralization

Mineralization within massive and stockwork sulphide zones is dominated by pyrite, pyrrhotite, magnetite, chalcopyrite, with minor molybdenite, fluorite, and barite, intergrown with quartz, feldspar and andraditic garnet (see figure 4-5, 4-6). Scheelite has also been identified, and occurs as rare, discrete grains ($< 20$ um) in pyrite (see figure 4-7). The pyritiferous sulphides also host a variety of Bi, Ag, and Pb tellurides (see figure 4-8), and rare Ag sulphides (argentite ?). The presence of

Ag tellurides and sulphides is reflected by anomalous Ag values which range from between 1 and 10 ppm. Geochemical analyses also reveal occassional enrichment in Co (up to 5520 ppm), reflecting a substitution of Co for Fe in pyrite. Analysis for Au returned values ranging between 10-50 ppb.

### ii) Mineralized Fluorite Veins

Mineralized fluorite veins are found as both fracture-fillings, and as slightly discordant veins within massive sulphide and rusty pyritiferous zones in recrystallized felsic volcanic rocks. The veins consist of finely crystalline, deep purple fluorite, with local quartz and adularia, minor zircon and apatite, and carry variably disseminated to massive pyrite and pyrrhotite, disseminated molybdenite and minor chalcopyrite (see figures 4-9, 4-10). All of the fluorite veins possess anomalous radioactivity (up to 1129 ppm U), with enrichments in Zn, Pb, and Ag. The uranium mineralization occurs as pitchblende in the form of either small individual grains (< 20 um), or as rims on zircon (see figure 4-11), and is easily observed under the microscope as small, dark purple metamict patches in fluorite. The observed mineralogical association clearly suggests a hydrothermal origin from fluids of a magmatic derivation.

A unique fluorite-amphibole vein occurs at the contact of the metabasalt and rhyolite southeast of Round Pond (see figure 4-12). Several metres to the west of the vein, a red hematized radioactive zone with associated sphalerite, pyrite, and minor fluorite mineralization occurs. The vein is 10-15 cm wide and consists of large (10 cm in length) euhedral hornblende crystals with abundant fluorite and lesser feldspar, andradite garnet, and biotite. Minor zircon, sphene, and apatite also occur. The vein is highly radioactive (> 5000 ppm U), and contains molybdenite, chalcopyrite, galena, and sphalerite mineralization, with significant Ag enrichment (> 10 ppm Ag). The uranium mineralization occurs as disseminations of individual pitchblende grains throughout the vein. Energy dispersive spectra for pitchblende grains reveal the presence of U, Pb, and

Y. Figure 4-13 shows a magmatic-hydrothermal metallic mineral association, and clearly suggests a common source for the molybdenite and uranium occurrences in the Round Pond area.

### iii) Quartz-molybdenite Veins

Quartz-molybdenite veins have provided some of the most spectacular molybdenite mineralization in the Round Pond area. The veins are generally 2-10 cm wide, and appear to crosscut earlier hydrothermal mineralization. The veins consist of quartz with coarse "booklets" of molybdenite, minor pyrite and chalcopyrite (see figure 4-14). The coarse molybdenite mineralization is generally concentrated at the vein margins, with finer, randomly oriented flakes permeating the country rock, or occurring as spectacular concentrations along fracture planes.

Associated wall rock alteration is characterized by pyritiferous, skarnoid, alteration zones immediately adjacent to the quartz veins. The alteration zones grade into weaker mineralized and altered, pyritiferous gossans. The mineralized alteration zones consist of intensely rusted, pyritiferous zones with extensive coarse calcsilicate-fluorite alteration mineral assemblages (see section 4-4), localized in zones of shearing and brecciation. Mineralization consists of abundant pyrite, coarse flakes of molybdenite, with minor chalcopyrite (see figure 4-15).

**Figure 4-5:** Extensive coarse, euhedral pyrite
mineralization in a siliceous (black) matrix.

**Figure 4-6:** Pyrite-quartz stockwork mineralization
in felsic volcanic, typically associated
with minor, finely disseminated molybdenite.
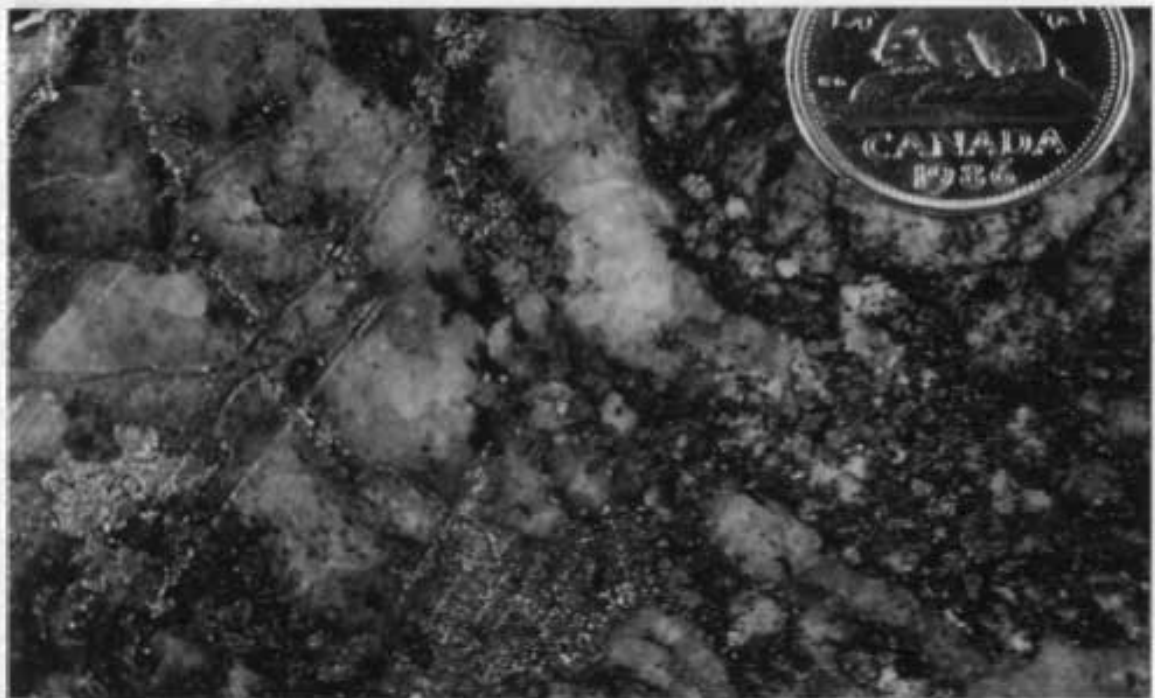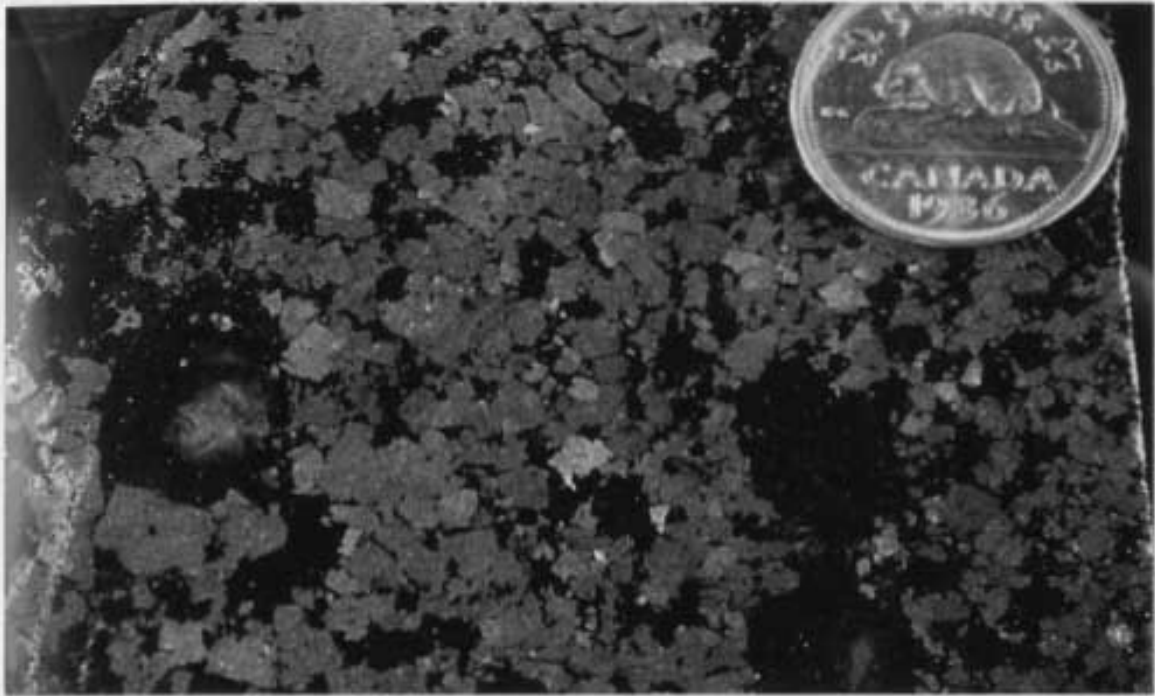
**Figure 4-7:**  A SEM back scatter image of a
large fractured grain of scheelite
(white), with pyrite (med. grey), and
quartz (dark grey).

**Figure 4-8:**  A SEM back scatter image of an
irregular grain of pyrite (grey),
with two small inclusions of Bi-telluride
(white) in the upper portion of the grain,
and an elongate flake of molybdenite
(white) in the lower area.

080302 15KV X250 96um

851112 15KV X35.0 .69mm
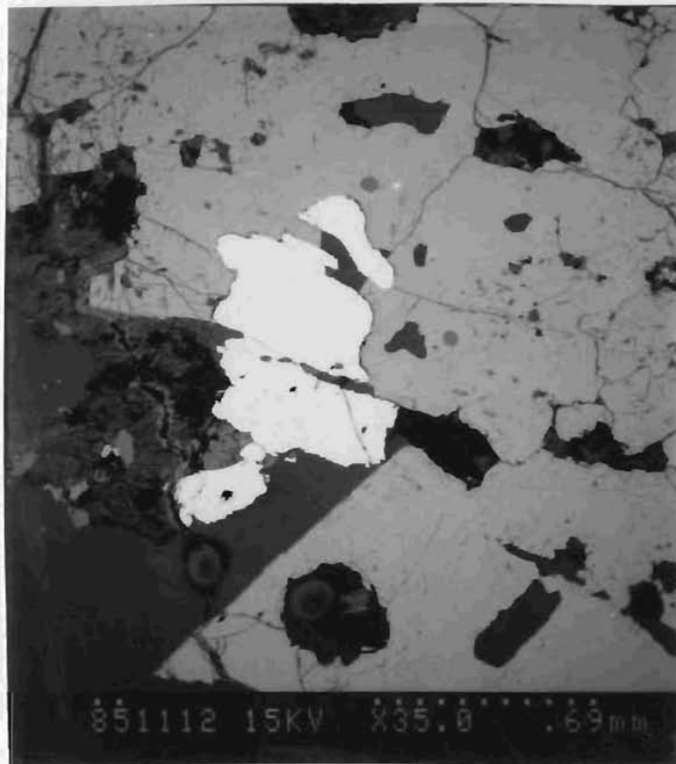
**Figure 4-9:** Hydrothermal vein with extensive dark purple, radioactive fluorite (black) hosting flakes of molybdenite (pale grey), associated with recrystallized quartz (lower center), and adularia (upper right).

**Figure 4-10:** Dark purple fluorite (black) with extensive coarse pyrrhotite (bronze) and lesser pyrite (yellow) mineralization.
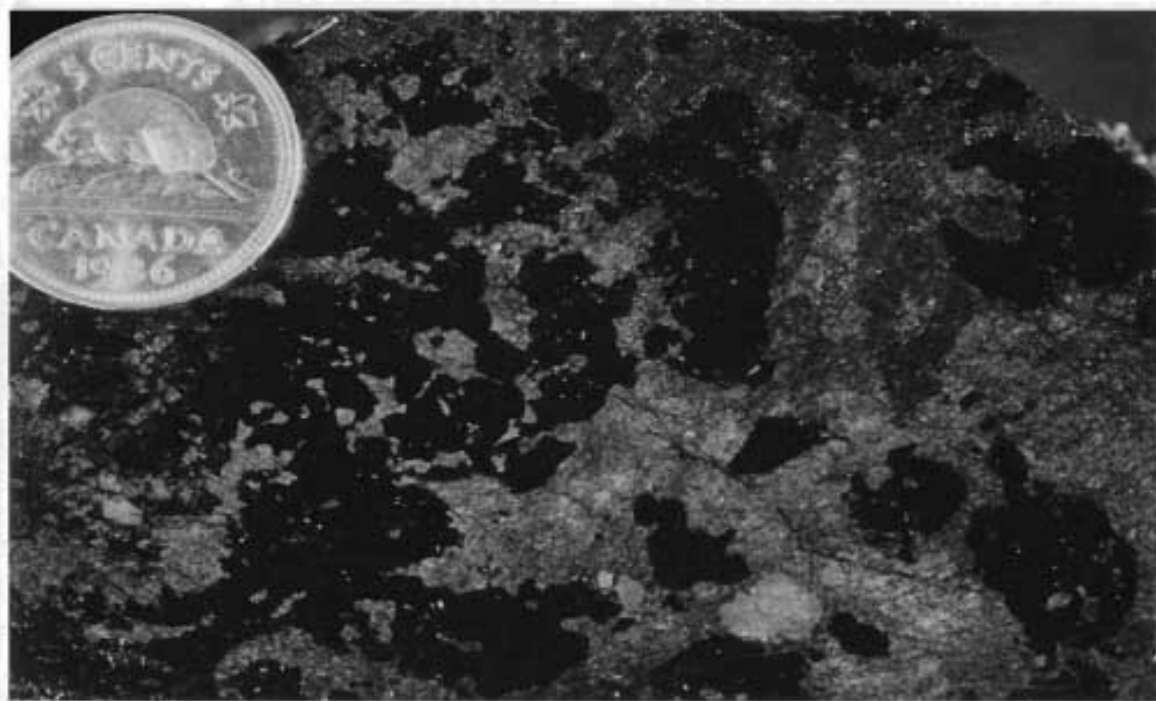
**Figure 4-11:** A SEM back scatter image of a
zircon crystal (grey) with a pitchblende
core and rim (white), from a fluorite
vein. Pitchblende also occurs as
individual grains (white) associated
with flakes of molybdenite (med. grey).

**Figure 4-12:** A cut section through a highly radioactive hydrothermal vein consisting of coarse-grained hornblende (dark green), irregular patches of albite-quartz-fluorite (white), and coarse flakes of molybdenite (pale grey).

**Figure 4-13:** A SEM back scatter image of a flake of molybdenite (med. grey) from a hydrothermal vein, with small inclusions of pitchblende (white), and zircon (dark grey). From figure 4-12.
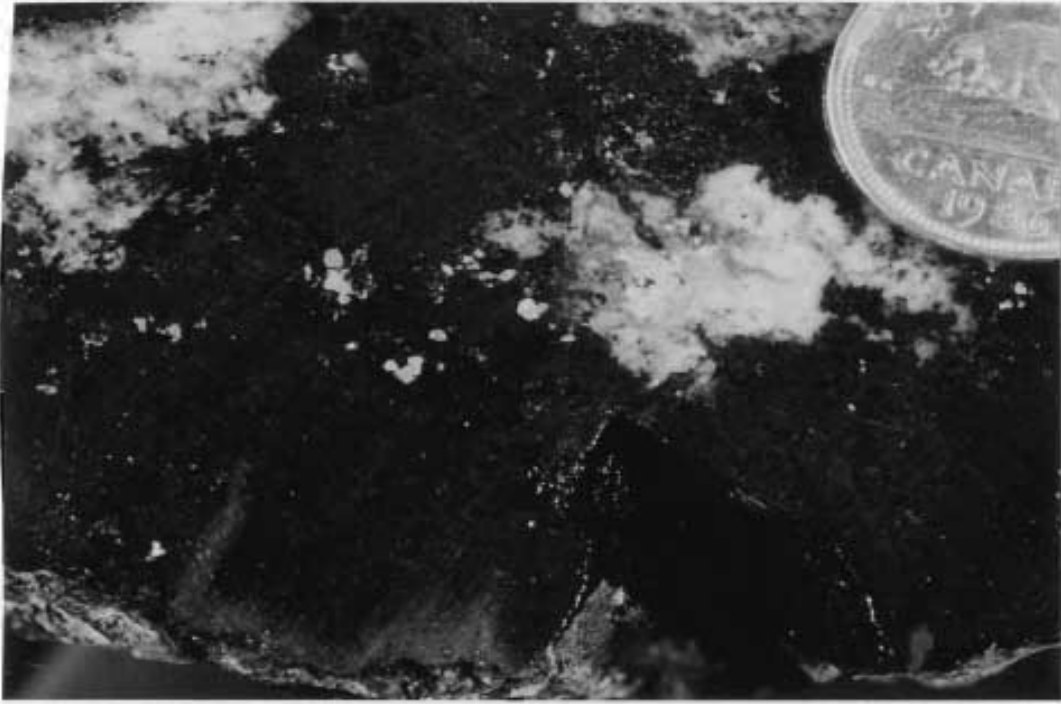
**Figure 4-14:** Coarse booklets of molybdenite (silver) within and along the rusted contact of a rusty quartz vein in felsic volcanic country rock. Note calcsilicate (salite) alteration mineral lower right.

**Figure 4-15:** Rusted, pyritiferous, skarn alteration zone with coarse flakes of molybdenite (silver) mineralization. Alteration dominated by coarse salite (dark green).
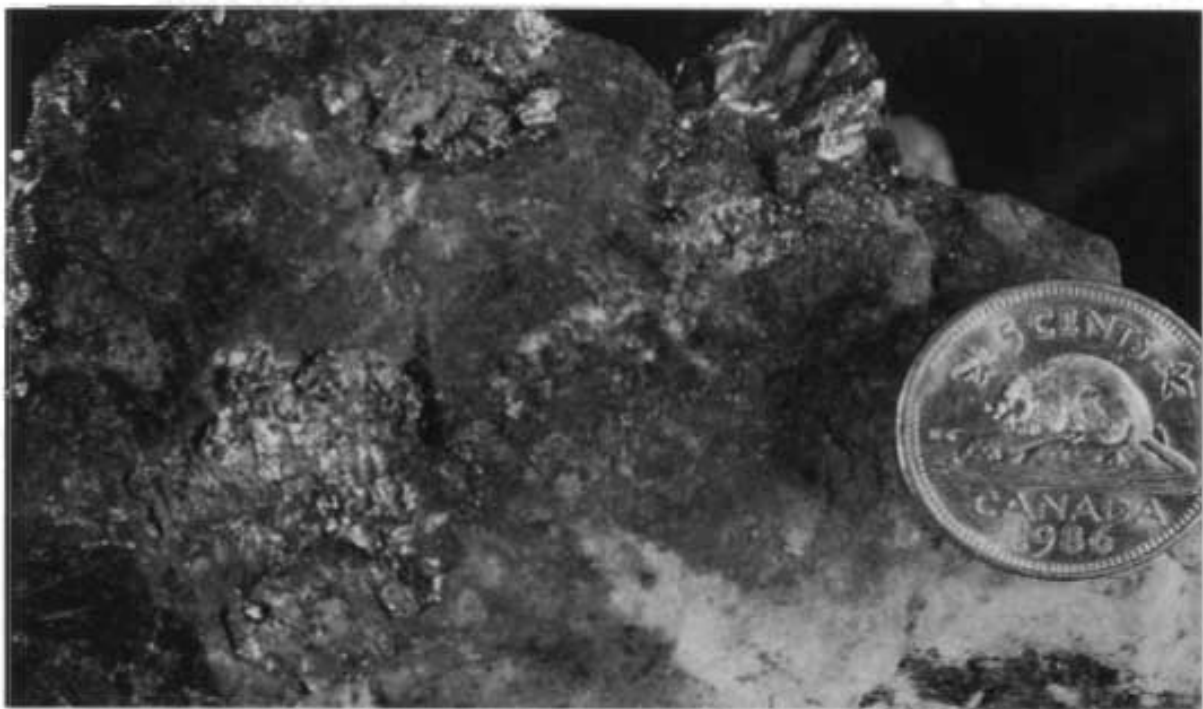
## 4.3.5. Carbonate Vein-hosted Zn(Pb)

Significant sphalerite, with minor pyrite, galena, chalcopyrite, and fluorite mineralization has been observed within a 2.0-2.5 m carbonate vein system cutting sheared volcanic conglomerate east of Round Pond (Wilton et al., 1986; MacDougall and Wilton, 1987a, b). The showing is a new mineral occurrence in the area, and occurs distally from the east granitic stock.

Mineralization consists of abundant, coarse grained (up to 1 cm), dark grey sphalerite, hosted in a white to pale pink carbonate vein (see figure 4-16). Minor disseminated pyrite, galena and purple fluorite are associated. Reported grades of mineralization range from 3.85 - 7.40 wt% Zn, with generally low Pb, Cu, Mo, and U values. Highest Au values were 55 ppb, while Ag reached a high of 6.6 ppm (MacDougall and Wilton, 1987b). Mineralization is also observed in the sheared and brecciated country rock adjacent to the mineralized veins, and consists of minor chalcopyrite, pyrite, and molybdenite intergrown with calcite-fluorite fracture-fillings, and as disseminations (see figure 4-17). Anomalous Au and Ag values are associated (up to 820 ppb and 3.0 ppm, respectively). The country rock possesses a distinctive "red-brown" alteration which is accompanied by abundant calcite and fluorite fracture-fillings typical of a hydrothermal breccia.

The showing is similar to the galena-sphalerite bearing carbonate veins at the Big Bight showing 10 km to the northeast. Grades up to 10.8% Pb, 6.0% Zn, 1700 g/t Ag, and 3 g/t Au have been reported (Gower et al., 1982; Wardle and Wilton, 1986; Wilton et al., 1987b).

Figure 4-16: Extensive medium-grained sphalerite (dark grey-brown) mineralization hosted in a white to pale pink, medium-grained calcite vein.

Figure 4-17: Hydrothermally brecciated felsic volcanic conglomerate with extensive calcite (white), minor fluorite, disseminated pyrite (brass coloured), and molybdenite (pale grey) mineralization.
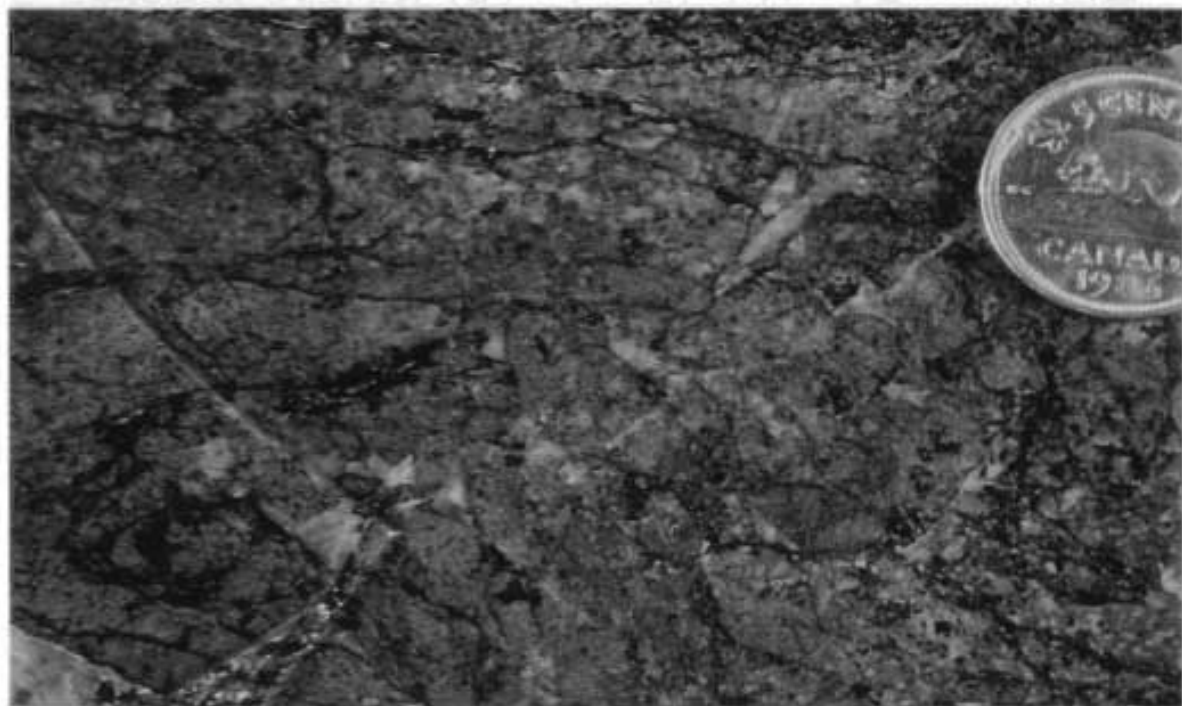
### 4.3.6. Linear Radioactive Zones

, Linear radioactive zones represent the only significant (ie. in terms of extent of mineralization) style of uranium mineralization in the study area. The radioactive zones occur primarily in the south-southeast portion of the study area, distal from the the satellite stocks of Monkey Hill Granite (see Map-1, backpocket). The most significant zones are referred to as Showing's # 16, 17, and 18 (Piloski, 1956),and are located immediately east of Falls Lake. Several other important mineral occurrences were also examined, and individual descriptions are given below.

Generally, the zones extend several hundred metres along strike, are <1.0-5.0 m wide, and are associated with rhyolitic volcanic rocks. The mineralized zones are quite distinctive with red to pink colour resulting from hematization (see figure 4-18). Mineralization is generally sporadic along strike, and is localized in one of the following ways:i) in fractures and breccia zones along lithologic contacts; ii) fractures and zones of shearing and brecciation within rhyolite and amphibolite; iii) discordant zones within permeable felsic volcanic conglomerate (MacDougall and Wilton, 1988).

Uranium mineralization occurs as discrete grains of pitchblende (< 20 um), and as inclusions or intergrowths with sphene, Fe-Ti oxides, apatite, and amphibole, that are disseminated throughout hematized zones, or concentrated with hornblende-calcite in discordant, tension veinlets and fracture fillings (see figure 4-19). Similar mineral associations are also reported by Gandhi (1978), Gower et al. (1982), and Wilton et al. (1986). Energy dispresive spectra for individual grains of pitchblende indicate the presence of U, Pb, and occassionally Y (see figure 4-20). Significant sphalerite mineralization (up to 1.9% Zn), with minor pyrite, chalcopyrite, molybdenite, galena, fluorite, and anomalous Ag values (1.0-6.8 ppm Ag) is typically associated.

Figure 4-18:   Pink hematized radioactive zone (left of hammer) immediately adjacent to unmineralized felsic volcanic rhyolite from Showing # 16 North.

Figure 4-19:   A SEM back scatter image of finely disseminated pitchblende (white) mineralization in a hematized (med. grey wispy streaks) rhyolite.

860100 15KV X110 218um
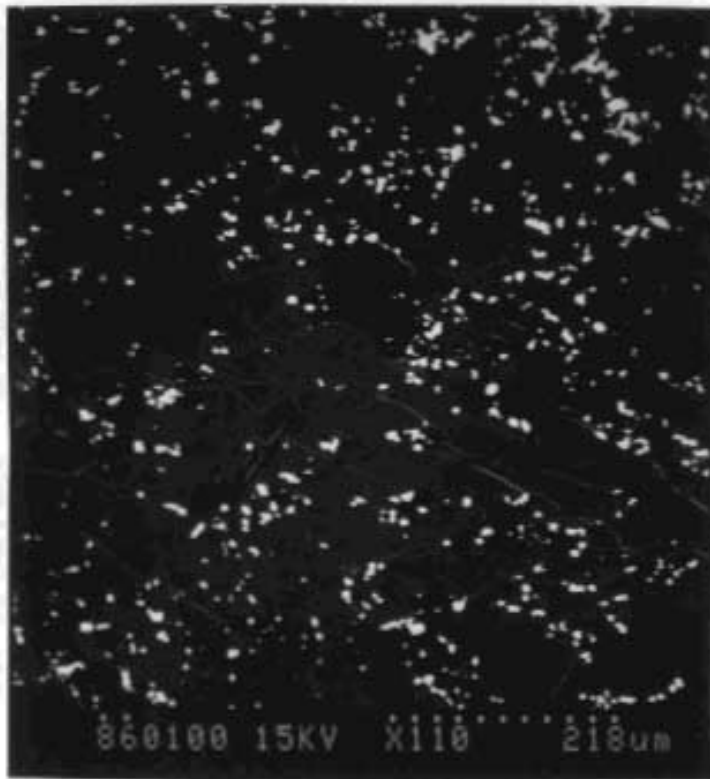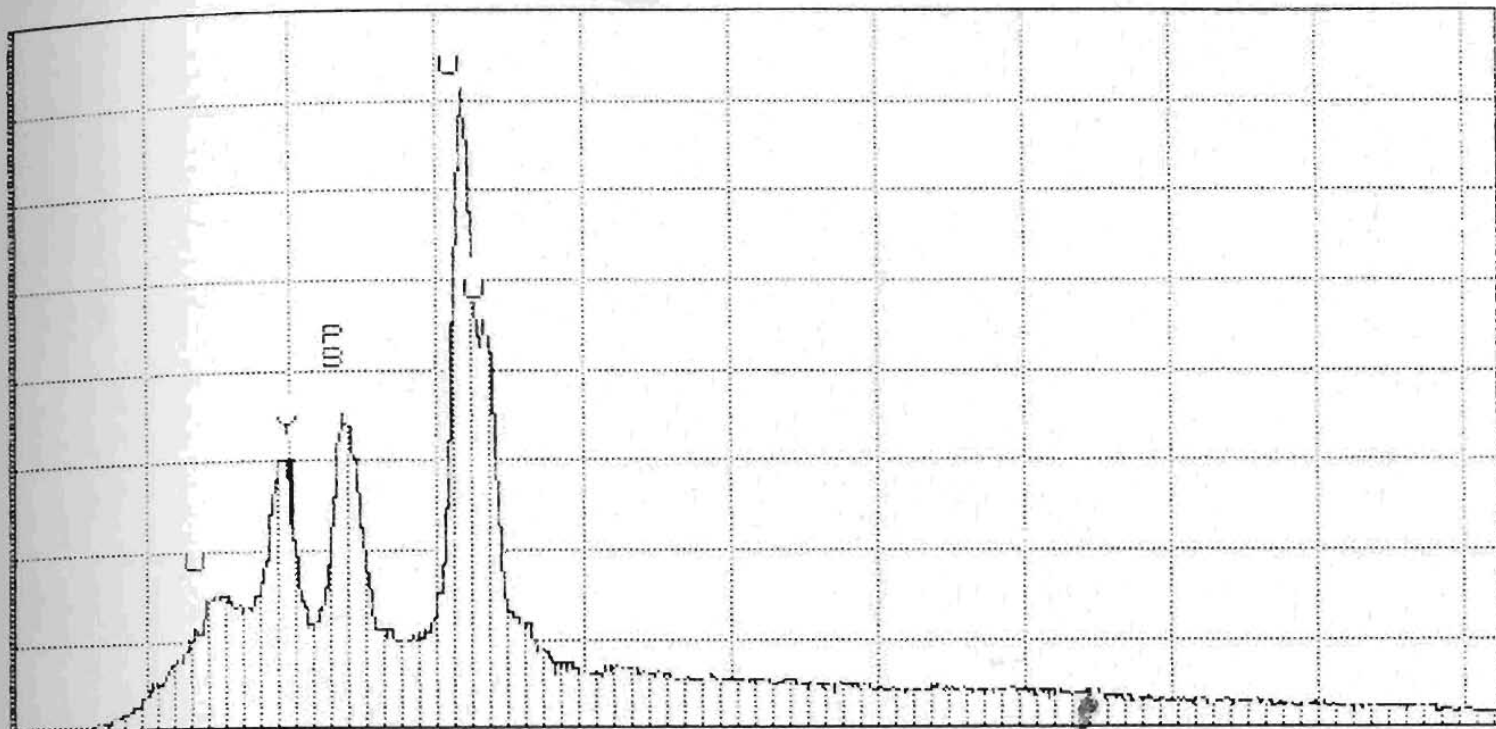
**Figure 4-20:** Energy dispersive X-ray spectra for pitchblende mineralization from hematized rhyolites in the Round Pond area.

Showing # 16

Showing # 16 consists of a discontinuous, moderately radioactive zone, 0.30 to 2.0 m wide, and roughly 600 m long. Mineralization is concentrated along the contact between a felsic porphyritic to equigranular, banded rhyolite and a dark, fine-grained mafic amphibolite of probable subvolcanic to volcanic origin. The contact zone commonly exhibits evidence of brecciation and extensive fracturing, suggesting that it is a zone of structural weakness (see figure 4-21). Zones of radioactivity are typically associated with a red to pink hematitic staining within the rhyolite. The uranium mineralization occurs as pitchblende concentrated in steeply dipping hornblende-calcite veinlets and fracture fillings at a low angle to the contact zone, and as individual pitchblende grains disseminated throughout

red hematized zones in rhyolitic rocks. Yellow uranophane staining is common. Significant sphalerite mineralization (up to 1.1% Zn, from grab samples), and minor pyrite, chalcopyrite, galena, and fluorite mineralization occur, associated with radioactive veinlets and fracture fillings and as disseminations (see figure 4-22). Numerous small (<1 - 3 cm) carbonate veins consisting of white calcite carrying minor galena mineralization, typically crosscut the mineralized zone.

Reported uranium grades were generally low (<0.1% $U_3O_8$), over narrow widths (< 1.0 m), and laterally discontinuous (Piloski, 1955). Similar grades were detected from grab samples in this study. Diamond drilling verified the generally low grades found on surface. Best intersection was reported as 0.498% $U_3O_8$ over 0.07 m.

## Showing # 16 North

A series of trenches not located on mineral occurrence maps were found several hundred metres north of Showing # 16, and appear to represent a northward extension of that showing. Thus the total strike length of Showing # 16 may be close to 1.0 km. Showing # 16 North is very similar to the original Showing # 16. The mineralized zone is thin, 0.3 to 0.5 m wide, about 30-40 m long, and occurs at the contact of rhyolite and a thin, amphibole-rich mafic lithology. Extensive hematization and yellow uranophane staining occur along the contact, together with low angle, steeply dipping, amphibole-carbonate veinlets, fracture fillings, and associated brecciation (see figure 4-23). Uranium mineralization occurs as pitchblende intergrown in veinlets and fracture fillings (above), and as disseminations associated with minor galena, sphalerite, chalcopyrite, and pyrite. Grab samples from this study returned grades as high as 3.3% U.

Figure 4-21: Moderately hematized rhyolite at Showing
# 16 exhibiting extensive brecciation
with infillings of hornblende and biotite.

Figure 4-22: A SEM back scatter image of finely
disseminated pitchblende (white) associated
with coaser sphalerite (light grey) and
pyrite (med. grey) mineralization.

051002 15KV  X150      160um
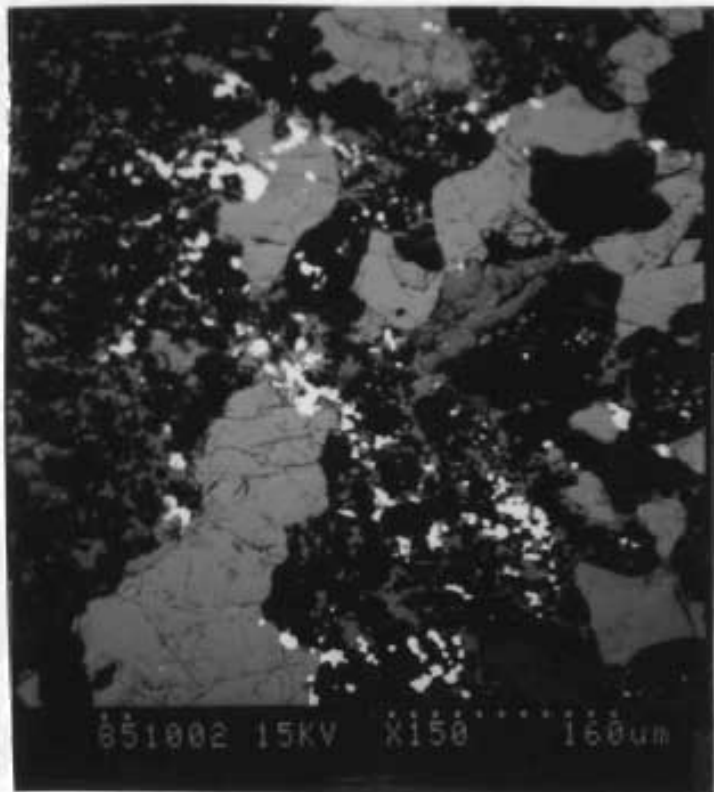
### Showing # 17

Showing # 17 consists of sporadic uranium mineralization in a zone 5.0 m wide, and over 275 m long. The zone is located several hundred metres east of Showing # 16, and is hosted in mafic amphibolite. Mineralization reportedly consists of visible pitchblende hosted in a number of narrow, short, steeply dipping fractures, that are slightly discordant with the regional trend of the host lithology (Piloski, 1955). Narrow (<1.0 m), rusty, radioactive breccia zones, containing minor disseminated pyrite and chalcopyrite were also observed in this study. Calcsilicate (diopside-hedenbergite) and carbonate veinlets and pods appear to be associated with the mineralization. Abandoned drill core nearby, was observed to contain similar calcsilicate-carbonate veinlets carrying molybdenite and chalcopyrite mineralization (see figure 4-24). Similar alteration mineral assemblages are observed in molybdenite skarn mineralized zones east of Round Pond.

Grades of mineralization are generally < 1.0% $U_3O_8$ (Piloski, 1955), over narrow widths, with only local high spots. Best surface values reported include 5.3% over 0.18 m, 1.4% over 1.8 m, and 1.48 % over 0.15 m. Drilling confirmed the narrow, low grade nature of the mineralization, but did return a high of 5.35% $U_3O_8$ over 0.15 m.

**Figure 4-23:** Pink hematized radioactive rhyolite localized along contact with amphibolite dyke. Note low angle, hematized, radioactive, amphibole-rich fracture cutting contact.

**Figure 4-24:** Tension fracture in amphibolite (from drill core) filled with salite (black), feldspar (white), molybdenite (grey), and chalcopyrite (yellow) mineralization. Note the calcsilicate alteration halo along fracture.
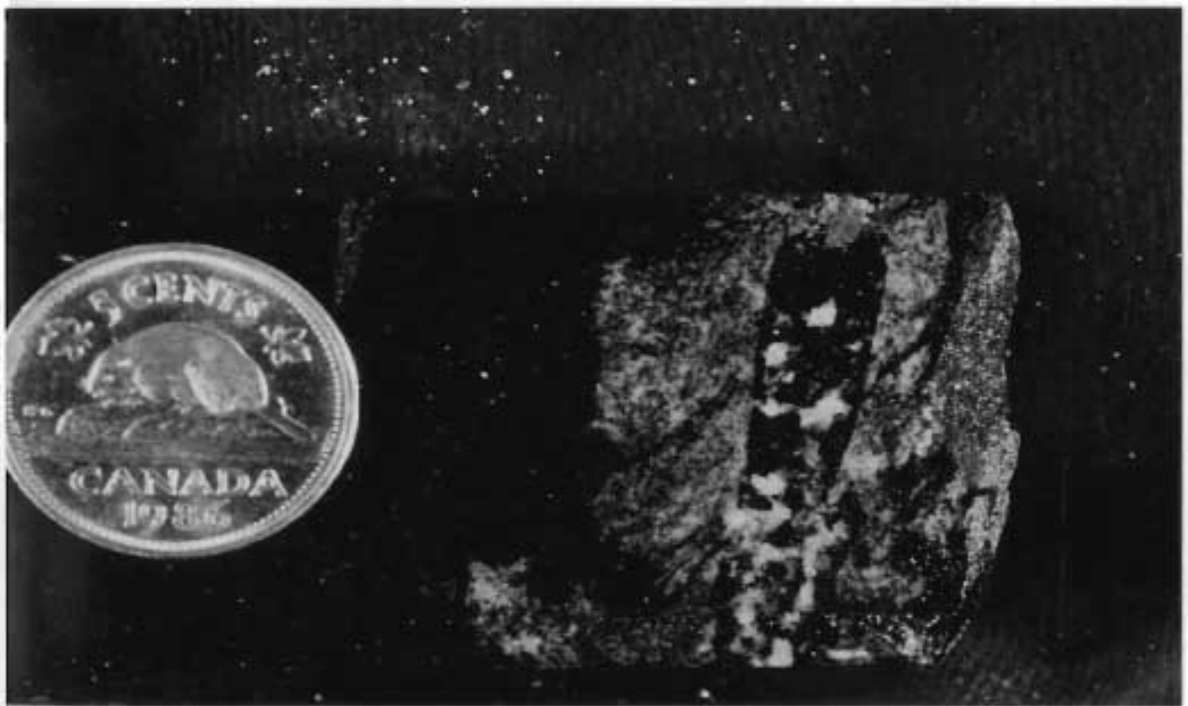
## Showing # 18

Showing # 18 consists of a moderately radioactive zone, 0.3 to 2.0 m wide, with a minimum length of 600 m, reported by Piloski (1955) to be open to the south. The rhyolitic rocks exhibit the characteristic red hematitic alteration, but the amphibolite associated with earlier showings is not present. Piloski (1955), reported that mineralization was concentrated within weak fractures along bedding planes in sandy quartzites. Radioactive fractures are, however, slightly discordant to the regional foliation within the host rhyolites. Reported uranium grades were generally below 0.06% $U_3O_8$, although local grades as high as 0.13% and 0.299% were obtained over narrow widths (ie. < 0.6 m). Yellow uranophane staining commonly occurs with areas of moderate radioactivity. Minor pyrite, chalcopyrite, malachite staining, fluorite, and rare molybdenite are observed, typically associated with carbonate (see figure 4-25).

## Showing # 19

Showing #. 19, located northwest of Falls Lake, consists of a small, 0.3 to 1.0 m wide, 10 m long radioactive zone, hosted in a felsic volcanic conglomerate. The showing exhibits the characteristic red hematitic staining and amphibole-carbonate alteration assemblage associated with the other rhyolite-hosted radioactive showings. The mineralized zone is discordant with the regional orientation of conglomeratic clasts in the area. Uranium mineralization is associated with abundant chalcopyrite (up to 2.3% Cu), malachite, pyrite, minor bornite, sphalerite, molybdenite and fluorite mineralization (see figure 4-26). Geochemical analysis reported by Wilton et.al. (1986, 1987), indicate a significant enrichment in Ag (68 ppm), and Au (1600 ppb). Similar mineralization occurs at showing # 7-11 at Winter Lake (Beavan, 1958; Wilton et al., 1987a, 1987b).

**Figure 4-25:** Pink. hematized, radioactive rhyolite with minor pyrite-chalcopyrite (yellow) mineralization associated with fluorite (black) and irregular blebs of carbonate (white), at Showing # 18.

**Figure 4-26:** Pink hematized radioactive conglomerate with extensive chalcopyrite mineralization, and malachite staining at Showing # 19.
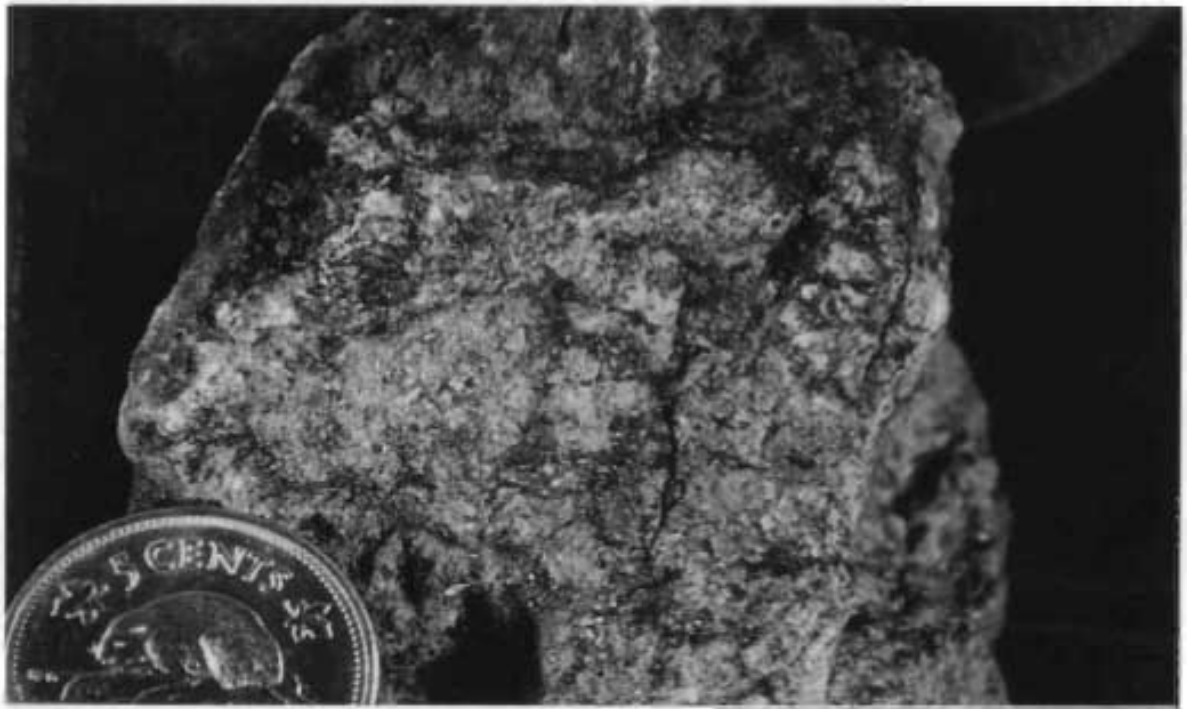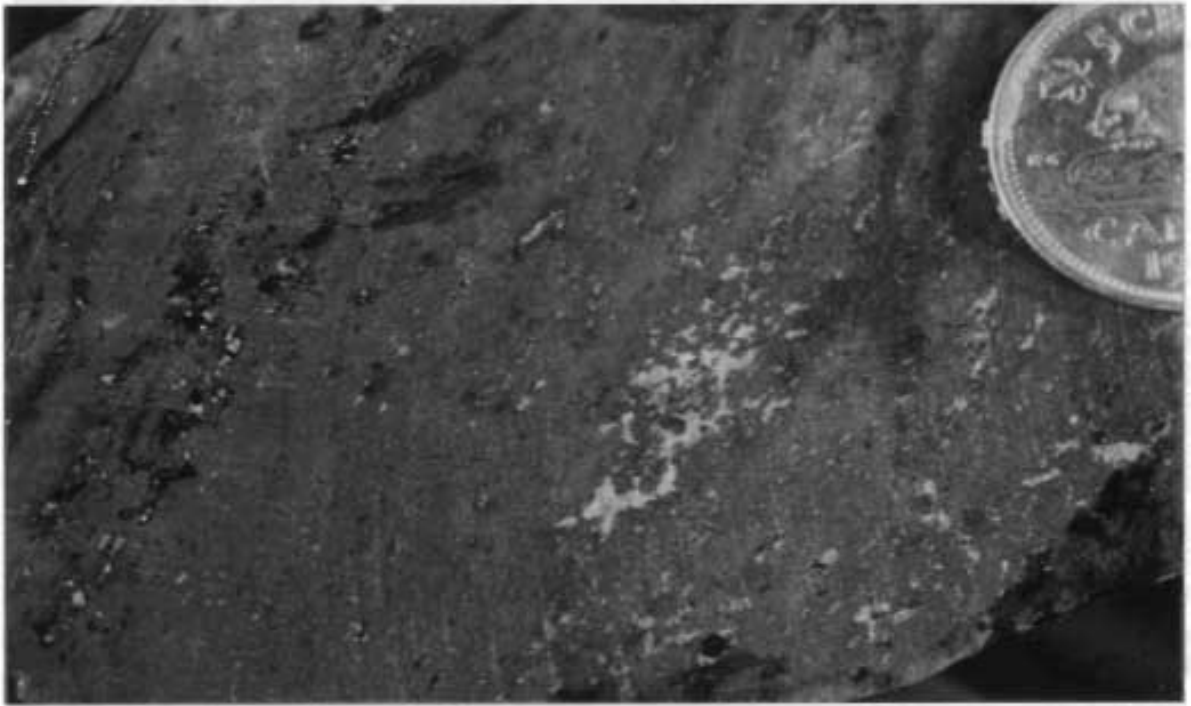
Along strike from the mineralized zone to the south, a radioactive, hematitic, felsic volcanic boulder was observed with extensive molybdenite mineralization (see figure 4-27). Assays from a grab sample returned 2816 ppm U, and > 1.0 % Mo, along with 3.0 ppm Ag. Mineralization occurs as individual grains of pitchblende disseminated throughout the hematized rock, and as inclusions in coarser flakes of molybdenite (see figure 4-28). A similar association is described from a hydrothermal fluorite vein above (see figure 4-14). The occurrence of such extensive Mo-U mineralization in hematized felsic volcanic rock is rare amoung the Upper Aillik Group mineral occurrences. Spatially associated with this mineral occurrence, are numerous pyritiferous, molybdenite-bearing veins and gossans. Gandhi (1970), also reported the occurrence of a radioactive pegmatite with associated minor pyrite, chalcopyrite, molybdenite, and fluorite mineralization near this showing.

### Northeast Falls Lake

The uranium mineral occurrence located northeast of Falls Lake was originally referred to as the Round Pond radioactive zone. Gandhi (1968), stated that the zone was continuous for more than 350 m, with a width of 15 m. Mineralization is however, very sporadic and discontinuous, and thus the zone is not easily traced. Uranium mineralization occurs as fine disseminations in a grey, fine grained, feldspathic quartzite, associated with aggregates of calcite, hornblende, and biotite (Gandhi, 1968). Gandhi (1978) later referred to this unit as a massive to amygdaloidal andesitic flow. A 230 kg (500 lb) bulk sample, taken from a stream cut, returned an assay of 0.029% $U_3O_8$. The site of the bulk sample could not be located with any confidence, but a sample taken from an anomalously radioactive outcrop near the stream is very similar to previous descriptions, and returned a similar assay value for uranium mineralization. In addition, a small red hematitic radioactive patch occurring in a quartz porphyritic rhyolite was examined along the apparent trend of the radioactive zone. Gandhi (1978) reported notable amounts of Ag and Se from a fairly high grade sample found in quartzite (now mapped as rhyolite) from the zone.

## Southeast Round Pond

The showing southeast of Round Pond consists of a small, red hematized, moderately radioactive zone, hosted in a quartz porphyritic rhyolite. The zone may represent an along strike northest extension of the "Round Pond radioactive zone" disscussed above. Mineralization consists of disseminated pitchblende, pyrite, sphalerite, minor chalcopyrite, and anomalous Ag. An assay of a grab sample returned 229 ppm U, 1.9% Zn, and 3.2 ppm Ag.

### 4.3.7. Granite-hosted Mineralization

Numerous radioactive pegmatites have been reported in the Aillik-Makkovik region, including the Round Pond area (Gandhi, 1969; Gower et al., 1982; Wilton et al., 1986, MacDougall and Wilton, 1987a, Kerr, 1987). Generally, the pegmatites are simple quartz-feldspar pegmatites, exhibiting anomalous radioactivity, and minor disseminated pyrite, chalcopyrite, molybdenite, and fluorite (Gandhi, 1969).

In the Round Pond area, pegmatitic, granitic, and aplitic dykes occur carrying minor, disseminated, pyrite, molybdenite, fluorite and occassionally exhibiting anomalous radioactivity (see figure 4-29). Pegmatitic dykes in the western portion of the study area are commonly associated with rusty, pyritiferous gossans carrying rare molybdenite-fluorite mineralization (see figure 4-30). A similar association has been observed at a small molybdenite mineral occurrence southeast of the main outcrop of the Strawberry Granite at Strawberry Point (Wilton et al., 1986; Wilton and Wardle, 1987).

Figure 4-27: Pink, hematized, radioactive felsic volcanic boulder with extensive coarse molybdenite (grey) mineralization, and associated calcsilicate (salite, dark green) alteration.

Figure 4-28: A SEM back scatter image of a flake of molybdenite (grey) with numerous pitchblende (white) inclusions.
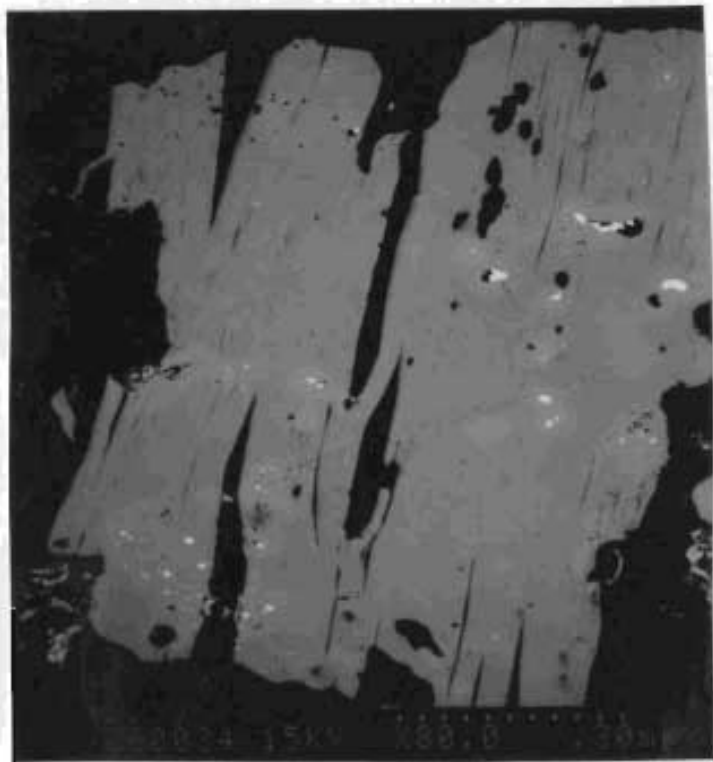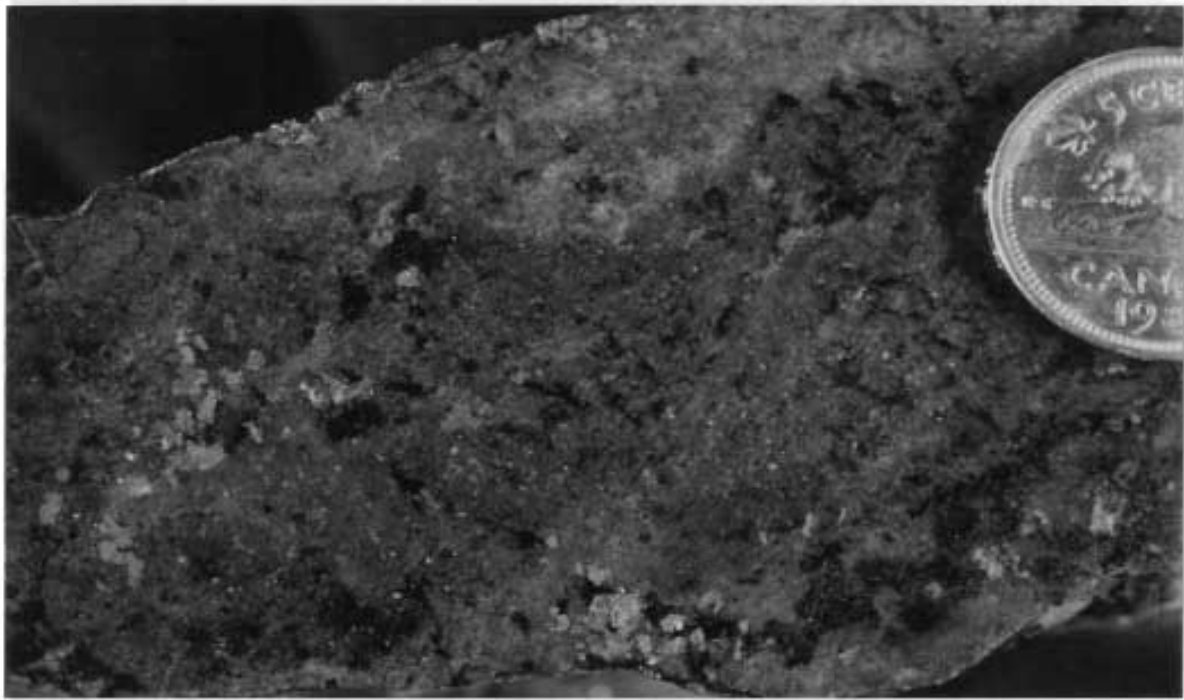
**Figure 4-29:** Aplitic dyke sample containing minor coarse flakes of molybdenite (grey).

**Figure 4-30:** Pegmatitic dyke with associated pyritiferous gossan intruding felsic volcanic rocks west of Round Pond.

Mineralization hosted within granite plutons is relatively uncommon compared to the numerous mineral occurrences hosted within the Upper Aillik Group. However, in the course of this investigation, disseminated pyrite, fluorite, and very rare flakes of molybdenite, as well as rare grains of scheelite have been observed within the small, satellite stocks of Monkey Hill Granite in the Round Pond area (see figure 3-6, Chapter 3). Similar mineralization consisting of heavily disseminated molybdenite, associated with pyrite, chalcopyrite, and rare bornite has been observed in a leucogranite resembling the Monkey Hill Granite on Duck Island (Kerr, 1987; Wilton and Wardle, 1987), located 20 km to the northwest. Locally, high grade molybdenite mineralization occurs along the contact of the Burnt Lake Granite with volcanic rocks of the Upper Aillik Group (MacKenzie and Wilton, 1987). Invariably, these mineralized granites have been interpreted as small epizonal satellite intrusions representing the apical portions of granitic batholiths at depth, which are considered favourable sites for the accumulation of granophile metals (ie. Sn, W, U, Mo).

Although the granite-hosted mineralization appears to be of limited economic importance, it does provide an important genetic link regarding the source of mineralization in the Aillik-Makkovik area, and in particular the Round Pond area. The potential exists for further mineralization hosted within unexposed contact zones of the Monkey Hill Granite, as well as other high level, post-tectonic plutons.

## 4.4. Alteration Mineral Assemblages

Identification of alteration assemblages was carried out using standard petrographic, X-ray diffraction, and microprobe mineral analysis techniques (see Appendix II for microprobe technique and data).

Alteration assemblages associated with the mineralized hydrothermal veins are restricted to areas immediately adjacent to the veins. A wider, less

prounounced, pyritiferous, calc-soda alteration halo or "gossan" is typical, characterized by the presence of albitized feldspar, abundant calcite, minor fluorite and calcsilicate minerals (ie. andradite garnet, salite pyroxene, hornblende, epidote).

Alteration adjacent to the mineralized veins is more intense, and is dominated by coarse grained, calcsilicate minerals, primarily olive green salitic pyroxene ($Hd_{34-53}$ - mole % hedenbergite), and black to brownish red andradite garnet ( $Ad_{78-96}$ - Mole % andradite) (see figures 4-31, 4-32). Salitic pyroxene is dominant, and the two minerals are generally mutually exclusive in occurrence. Abundant quartz, calcite, epidote, fluorite, sphene, and lesser biotite, hornblende, actinolite and magnetite also occur. Locally, silicic, chloritic, and sericitic alteration is developed, and scapolitic porphyroblasts are often observed in nearby mafic dykes.

The alteration assemblage is typical of that observed in classic "calcic skarn" type environments, and has been observed with a number of molybdenite mineralized skarns (ie. Einaudi et al, 1981; Hellingwerf and Baker, 1985; Barton, 1987). Similar "skarnoid" alteration assemblages have been described by Beavan (1958), Wilton et al. (1986), and Wilton and Wardle (1987) for a number of molybdenite, uranium, and calcsilicate mineral occurrences in the Aillik-Makkovik coastal region. The formation of calcic skarn mineral assemblages in the Round Pond area is favoured by the presence of a calcareous (potentially reactive) volcanic conglomerate host rock.

Figure 4-31:  Salitic calcsilicate alteration (dark green) of the tuffaceous matrix surrounding felsic volcanic clasts.

Figure 4-32:  Coarse pods and disseminated andradite garnet (black-brown), with minor salite (dark green) within felsic volcanic conglomerate.
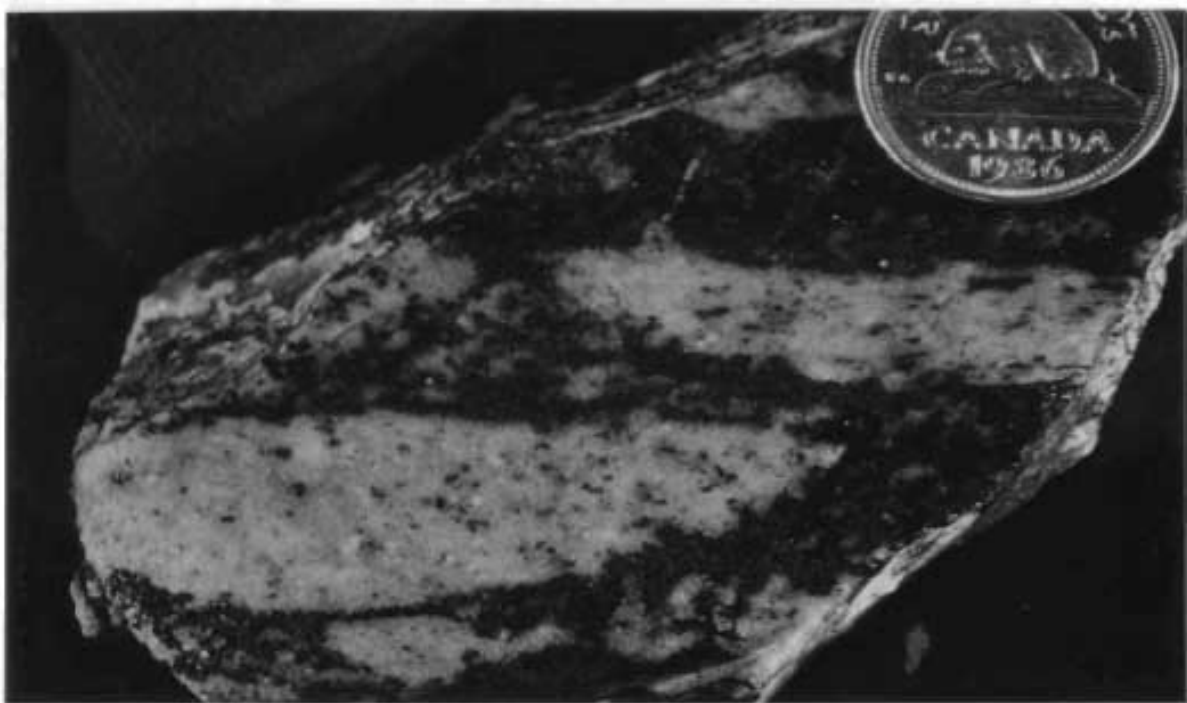
Alteration associated with linear radioactive zones is dominated by a distinctive red hematization accompanied by albitization of feldspar which results in a pronounced Na-metasomatism (see section 4-5). This is typical of many of the uranium mineral occurrences hosted within the Upper Aillik Group (White,1976; Gandhi, 1978; White and Martin, 1980; Gower et al., 1982; Wilton et al., 1987a). Abundant amphibole (hornblende), biotite, epidote, calcite, quartz, sphene, lesser zircon, apatite, and minor fluorite, actinolite and salitic pyroxene are typically associated, and are most intensely developed along the contact of an amphibolitic unit with rhyolite. Cross cutting calcite-biotite-amphibole and quartz-carbonate veinlets with minor galena are common. Morse (1961) also reported the presence of soda-rich amphibole and pyroxenes. However, mineral analyses of amphiboles and pyroxenes have only indicated the presence of calcic-rich varieties of hornblende, and salitic pyroxene (see Appendix II), although they do exhibit slightly higher Na contents than alteration minerals associated with the hydrothermal veins discussed above.

The alteration assemblage is similar to that observed with the hydrothermal veins mentioned above, and with other uranium mineral occurrences in the Aillik-Makkovik region. Hellingwerf and Baker (1985) describe an identical mineral assemblage in plagioclase-amphibole dominated skarns associated with scheelite mineralization in Sweden. Skarn zones (garnet-epidote-diopside) are also associated with uranium mineralization in Northern Sweden (Smellie and Laurikko, 1984).

Skarn formation is typically characterized by an evolution of associated mineral assemblages (Einaudi et al., 1981). Early skarn development is dominated by prograde mineral growth of anhydrous Ca-rich calcsilicate mineral assemblages such as andradite-salite, at temperatures of 650-400°C. Late retrograde reactions lead to replacement of Ca-rich calcsilicate minerals by an assemblage of hydrous Ca-depleted silicates (ie. hornblende, epidote), iron oxides or sulphides, carbonate, and albitic plagioclase. These reactions are typically lower temperature, 450-300°C,

and often crosscut and extend beyond earlier skarn patterns. This stage is generally the main stage of sulphide deposition. The final stage in skarn evolution is marked by low temperatue 300-100°C quartz-carbonate mineralization typically hosting Pb-Zn mineralization.

The similarities between the alteration associated with the mineralization in the Round Pond area and the typical skarn evolution of mineral assemblages is striking. The proximal, and thus early mineralized hydrothermal veins are characterized by anhydrous Ca-rich calesilicate alteration mineral assemblages. These are typically associated with broader, pyritiferous ±Mo gossans exhibiting albite, calcite, hornblende, epidote,and crosscutting quartz veins representing retrograde mineral growth. The distal, hematized radioactive zones represent late mineralization and are dominated by hydrous, calcium depleted (relative to andradite and salite) minerals such as hornblende, and epidote, and exhibit extensive albitization of feldspar and thus represent a lower temperature, retrograde mineralizing fluid. The cross-cutting quartz-carbonate-galena veinlets associated with the hematized radioactive zones, and the carbonate-sphalerite veins located east of Round Pond represent the final lower temperature quartz-carbonate stage of mineralization.

The presence of salitic pyroxene (low $Fe^{+2}$), andraditic garnet (high $Fe^{+3}$), and epidote are diagnostic of a relatively oxidized-type skarn (see figure 4-33) typically formed in noncarbonaceous or hematitic host rocks and/or at shallow depths (Einaudi et al., 1981). Pyrite is generally the dominant iron sulphide over pyrrhotite, and abundant hematite and magnetite are typically associated with such skarns. The occurrence of iron sulphides and oxides suggests a wide range of $fO_2$, $fS_2$, and pH conditions during mineralization probably related to physico-chemical changes in the ore-forming fluid as a result of wall rock interaction and decreasing temperature and pressure resulting in various retrograde reactions.

Studies reviewed by Einaudi et al. (1981) involving field, petrographic, and analytical information, as well as fluid inclusion and isotopic data have yielded
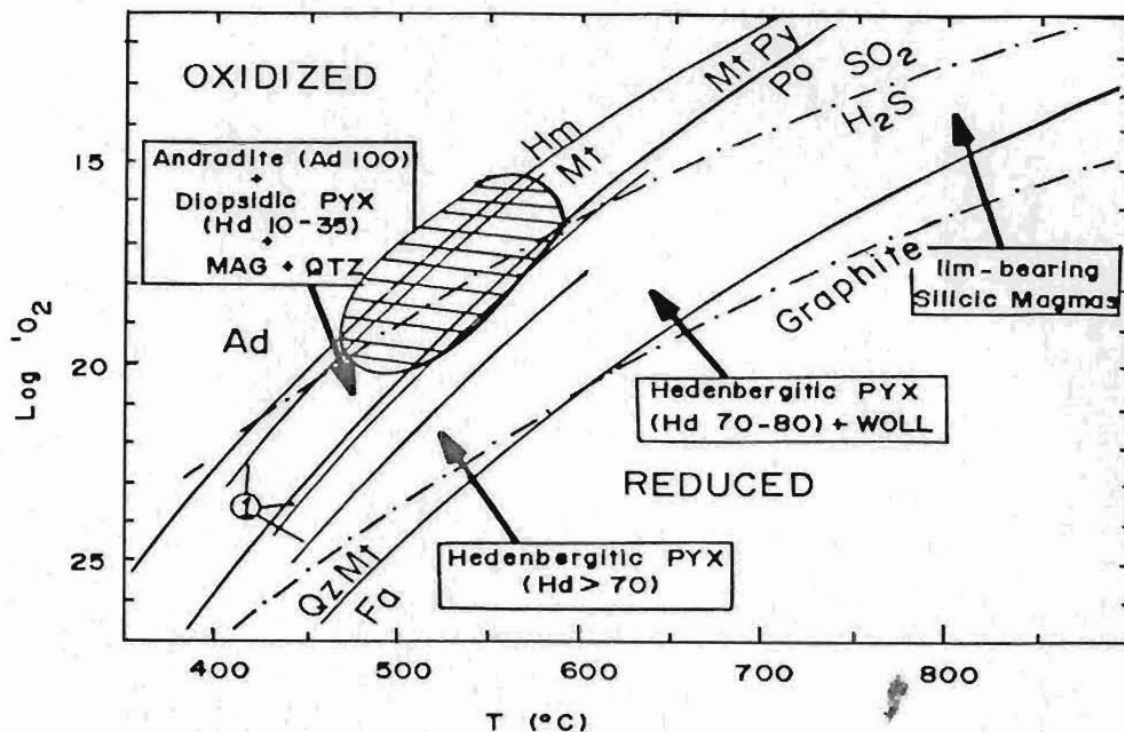
**Figure 4-33:** Oxygen fugacity versus temperature relations for silicic magmas and skarn-forming environments at approximately 1kb. Ruled field represents conditions estimated from this study (modified from Einaudi et al., 1981).

Curve 1 :

   hedenbergite + $O_2$ = andradite + magnetite +
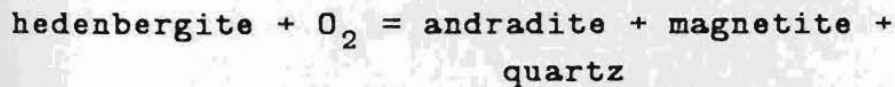
                   quartz

Ad-andradite; Fa-fayalite; Hm-hematite;
Mt-magnetite; Qz-quartz; Py-pyrite;
Po- pyrrhotite

estimates concerning P-T-X conditions during skarn formation. The observed salite-andradite alteration assemblage is typical of relatively high temperature hydrothermal systems, with an estimated temperature of initial skarn formation at between 325-650°C. Late crosscutting retrograde mineral assemblages represent lower temperatures of formation. Field relations and geochemical

evidence from this study indicate a shallow, epizonal environment (ie. 0.3-1 kb) in which boiling is a typical feature. The hydrothermal fluid is usually characterized by moderate salinities (10-15 % NaCl). The source of sulphur (and metals) is generally proposed to be magmatic, and the origin of $H_2O$ varies from magmatic during early stages, to mixed magmatic-meteoric in later retrograde stages.

## 4.5. Geochemistry

The mineralization in the Round Pond area is characterized by a diverse polymetallic mineral association. Geochemical trends exhibited by different styles of mineralization, however, bear similarities as indicated by the observed alteration mineral assemblages.

A number of mineral occurrences were analyzed for major, trace, and REE concentrations (see Appendix I), including pyritiferous ($\pm$Mo) gossans, hematized radioactive zones hosted in felsic volcanic conglomerates and rhyolites, and intensely calcsilicate-altered wall rock adjacent to mineralized hydrothermal veins. Samples were chosen so as to represent the alteration typically associated with mineralization, while at the same time, minimizing the effect of extensive metallic mineralization on major element concentrations (ie. apparent decreases). Thus, some analyses of intensely mineralized rock (recognized by high metallic element and $Fe_2O_3$ concentrations) are not considered in the general discussion. Similarly, altered rocks whose analyses reveal high LOI are not considered in a general sense in this section.

Regional background geochemical analyses for lithologies of the Upper Aillik Group in the Round Pond area have been reported and discussed in chapter 3. One of the important features to emerge was the widespread, possibly synvolcanic, Na-metasomatism exhibited by many of the stratigraphically lower lithologies of the Upper Aillik Group. The stratigraphically higher rhyolite lithologies do not exhibit the effects of a pronounced widespread alkali

metasomatism. As will be discussed below, the mineral occurrences in the Round Pond area are associated with a pronounced sodic metasomatism localized in post-tectonic, discordant shear zones which are associated with the mineralization. Thus, attempts to define the alteration associated with mineral occurrences hosted within the felsic volcanic conglomerate are complicated by the widespread regional metasomatism exhibited by the lithology. Similar mineral occurrences hosted within the rhyolites, however, can be directly compared geochemically to an unaltered host rock, and much of the following discussion will be based on comparisons with rhyolite-hosted mineralization (see Table 4-2).

### 4.5.1. Major and Trace Elements

Numerous workers have documented extensive sodic-metasomatism characterized by the enrichment of Na, and depletion of K, associated with many of the uranium (to a lesser extent molybdenite) mineral occurrences hosted by the Aillik Group. Morse (1961) reported the presence of albite, soda-rich amphiboles and pyroxenes associated with uranium mineral occurrences in the Falls Lake-Winter Lake area. Barua (1969) reported high $Na_2O$ (4.5-6.5 wt%), accompanied by low $K_2O$ (<0.3 wt%), in host rhyolites associated with uranium and molybdenite mineral occurrences on Cape Aillik. He regarded the rhyolites as the products of spilitized lavas. White (1976), and Gandhi (1978), reported similar alkali enrichment/depletion trends for rhyolites hosting the Michelin uranium deposit, and suggested that the observed metasomatism was the result of circulating, synvolcanic magmatic or meteoric fluids.

White and Martin (1980) recognized differing intensities of metasomatism, and suggested that relatively mildly metasomatized rock evolved by simple Na for K ion exchange, while intensely metasomatized rocks evolved by a Na±Al-metasomatism. Evans (1980), similarily recognized increasing intensity of metasomatism characterized by progressive depletion of K and Si, and enrichment of Al, Na, $Fe_2O_3$, Zr and U towards ore zones. He suggested that the observed metasomatism was caused by the interaction of an oxidized ore fluid with a potassic rhyolite host rock. Similar alkali metasomatism associated with uranium mineralization related to hydrothermal fluids have been reported in other studies (ie. Kish and Cuney, 1981; Smellie and Laurikko, 1984).

The rhyolitic rocks in the Round Pond area host numerous hematized radioactive zones and pyritiferous (±Mo) gossans which exhibit alkali metasomatism involving the enrichment of Na and depletion of K (see figure 4-34). $Na_2O$ values vary from 4.58 to 10.2 wt% in hematized radioactive zones, and from 6.75 to 10.75 wt% in pyritiferous gossans. $K_2O$ values range from 1.77 to 0.12 wt%, and 0.39 to 0.07 wt % respectively. Unmineralized rhyolites generally possess $Na_2O$ values of 3.0 to 5.0 wt%, and $K_2O$ values of 4.0 to 6.0 wt%.

Increased CaO values are also commonly associated with the observed Na-metasomatism (see figure 4-35). CaO varies from 0.9 to 9.56 wt% in mineralized rhyolite, compared to <1.0 wt% in unmineralized rhyolite. Highest values are generally associated with rhyolites along the contact of an amphibolite. Similar enriched CaO values are observed immediately adjacent to mineralized hydrothermal veins hosted in calcareous volcanic conglomerate. Values range from < 3.00 wt% in unmineralized rock to a high of > 12.0 wt% immediately adjacent the veins. Associated pyritiferous gossans generally show a corresponding depletion in CaO.

## Table 4-2: Major and trace element data for various rhyolite-hosted mineral occurrences in the Round Pond area.

| Sample | RP-1 | CM-59 | CM-100 | CM-99 | RP-11a | CM-139b | CM-146 | CM-24 | CM-26 |
|---|---|---|---|---|---|---|---|---|---|
| Major Elements (wt.%) | | | | | | | | | |
| $SiO_2$ | 62.1 | 57.9 | 55.5 | 75.4 | 50.0 | 57.0 | 59.0 | 63.5 | 65.0 |
| $TiO_2$ | 0.48 | 0.48 | 2.08 | 0.08 | 2.16 | 0.48 | 0.68 | 0.42 | 0.44 |
| $Al_2O_3$ | 16.4 | 14.9 | 14.8 | 10.9 | 12.6 | 11.1 | 15.7 | 17.3 | 17.1 |
| $Fe_2O_3$ | 6.45 | 6.72 | 10.05 | 2.66 | 15.24 | 10.7 | 7.75 | 5.22 | 4.84 |
| MnO | 0.09 | 0.45 | 0.32 | 0.04 | 0.27 | 0.13 | 0.09 | 0.04 | 0.03 |
| MgO | 1.23 | 1.81 | 1.96 | 0.05 | 3.59 | 2.28 | 1.64 | 0.08 | 0.32 |
| CaO | 3.14 | 5.20 | 4.38 | 2.46 | 7.66 | 6.26 | 1.58 | 0.54 | 0.92 |
| $Na_2O$ | 9.10 | 8.02 | 7.64 | 6.05 | 4.94 | 5.48 | 8.33 | 10.75 | 9.60 |
| $K_2O$ | 0.36 | 0.14 | 0.33 | 0.16 | 1.29 | 0.58 | 1.02 | 0.39 | 0.15 |
| $P_2O_5$ | 0.03 | 1.24 | 0.48 | 0.03 | 0.92 | 0.15 | 0.27 | 0.07 | 0.02 |
| LOI | 0.69 | 2.31 | 0.62 | 1.14 | 0.26 | 4.65 | 2.38 | 2.07 | 1.93 |
| Total | 100.07 | 99.17 | 98.16 | 98.97 | 98.93 | 98.81 | 98.44 | 100.38 | 100.35 |
| Trace Elements (ppm) | | | | | | | | | |
| Pb | 385 | 131 | 164 | 303 | 1754 | 424 | 284 | 20 | 22 |
| U | 218 | 229 | 520 | 301 | 6041 | 481 | 154 | 0 | 5 |
| Th | 1 | 37 | 11 | 17 | 0 | 28 | 163 | 21 | 16 |
| Rb | 8 | 2 | 10 | 5 | 106 | 38 | 116 | 4 | 2 |
| Sr | 333 | 474 | 424 | 75 | 480 | 154 | 176 | 84 | 108 |
| Y | 45 | 241 | 139 | 35 | 105 | 103 | 45 | 72 | 14 |
| Zr | 747 | 982 | 2263 | 436 | 767 | 1531 | 1787 | 1049 | 681 |
| Nb | 24 | 20 | 24 | 19 | 20 | 21 | 46 | 54 | 35 |
| Ga | 40 | 33 | 34 | 28 | 23 | 6 | 22 | 40 | 33 |
| Zn | 271 | 19171 | 11802 | 20 | 499 | 1404 | 237 | 0 | 7 |
| Cu | 44 | 258 | 1012 | 33 | 0 | 22723 | 10 | 24 | 14 |
| Ni | 0 | 10 | 5 | 0 | 0 | 1 | 3 | 0 | 0 |
| La | 63 | 4 | 0 | 66 | 18 | 23 | 0 | 23 | 0 |
| Ti | .46 | .42 | 1.89 | .10 | 2.06 | .38 | .89 | .53 | .58 |
| Ba | 183 | 233 | 560 | 0 | 1111 | 124 | 725 | 162 | 95 |
| V | 108 | 27 | 194 | 6 | 158 | 33 | 21 | 6 | 7 |
| Ce | 112 | 82 | 0 | 131 | 123 | 0 | 1513 | 0 | 140 |
| Cr | 0 | 0 | 2 | 0 | 0 | 13 | 0 | 0 | 0 |
| Mo | <1 | 48 | 5 | 11 | <1 | 166 | 7760 | 25 | 325 |

RP-1, CM-59, CM-99, CM-100 rhyolite-hosted hematized radioactive zones. RP-11a amphibolite-hosted radioactive zone. CM-139a conglomerate-hosted hematized radioactive zone. CM-24, CM-26 rhyolite-hosted pyritiferous gossan. CM-146 conglomerate-hosted radioactive pyritiferous gossan.
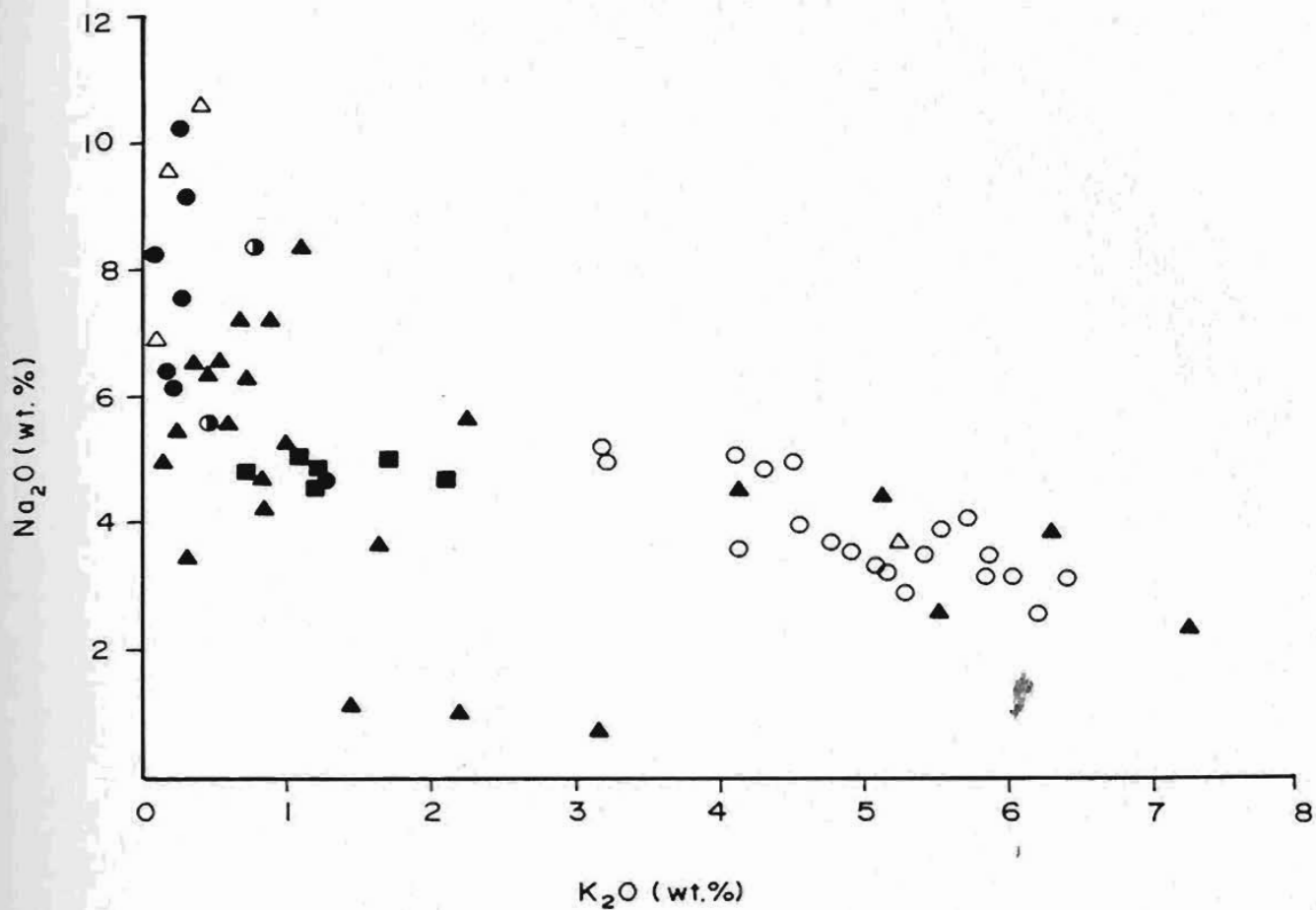
**Figure 4-34:** Na$_2$O versus K$_2$O for mineralized
samples, and unmineralized rhyolites in
the Round Pond area.

(Symbols)

○ – unmineralized rhyolite
● – hematized radioactive rhyolite
◑ – hematized radioactive conglomerate
△ – pyritiferous gossan in rhyolite
▲ – pyritiferous gossan in conglomerate
■ – radioactive amphibolite
▽ – gossan associated with pegmatite
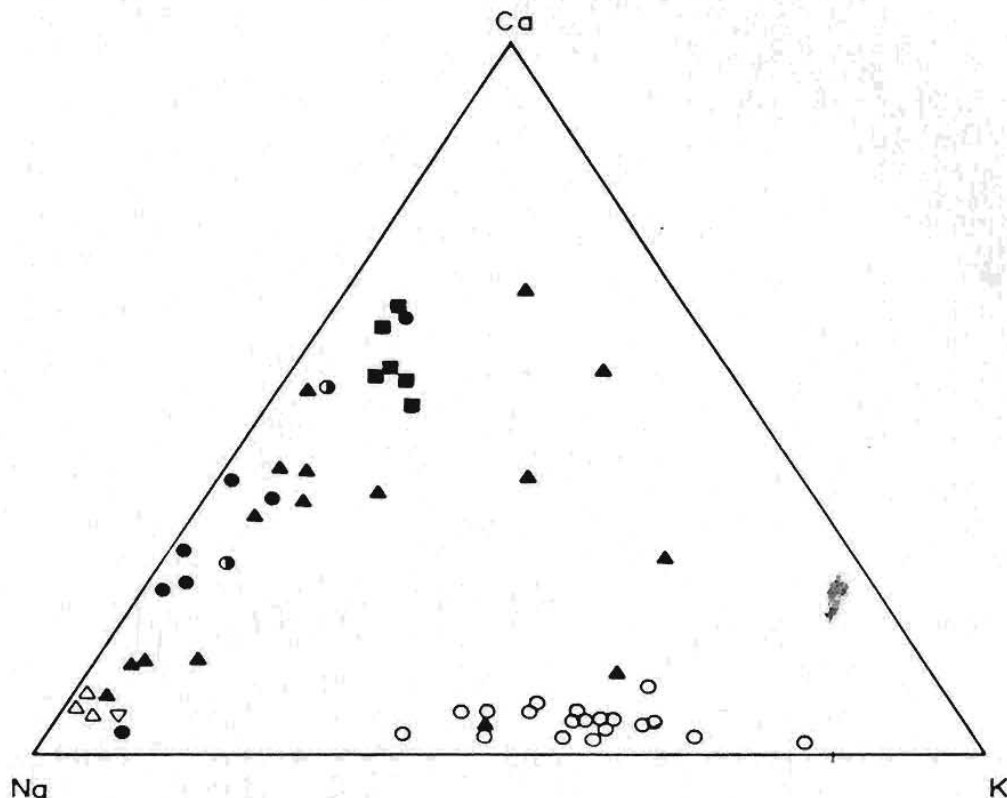
**Figure 4-35:** Ca-Na-K (wt.%) ternary plot for mineral
ocurrences and unmineralized rhyolite
in the Round Pond area (symbols as above).

The hematized radioactive rhyolites exhibit varying intensities of metasomatism as suggested by White and Martin (1980), and Evans (1980). The least metasomatized rhyolites are characterized by pronounced disturbance of the alkalies (above), and minor addition of CaO. This is typified by Showing # 18 (samples CM-99, RP-8, Appendix I). Increasing intensity of metasomatism is characterized, in addition to the alkali disturbance, by further increased CaO contents, as well as increases in $Al_2O_3$, $Fe_2O_3$, $TiO_2$, MgO, $P_2O_5$, LOI, and decreases in $SiO_2$ (<60.0 wt.%). Figure 4-36 illustrates the fields for unaltered, weakly metasomatized, and strongly metasomatized rhyolites. Radioactive mineral occurrences, and rhyolite-hosted pyritiferous gossans generally exhibit intense

metasomatism (except for samples from Showing # 18). No relationship appears to exist between the concentration of uranium mineralization and intensity of metasomatism. Other mineral occurrences (ie. conglomerate-hosted pyritiferous gossans and skarn-altered molybdenite mineralized rock) exhibit similar but more variable intensities of metasomatism, and span the complete range of intensity of metasomatism. The overall similarity exhibited by these various mineral occurrences with respect to their major element geochemistry suggests that they are related to the same ore-forming fluids.
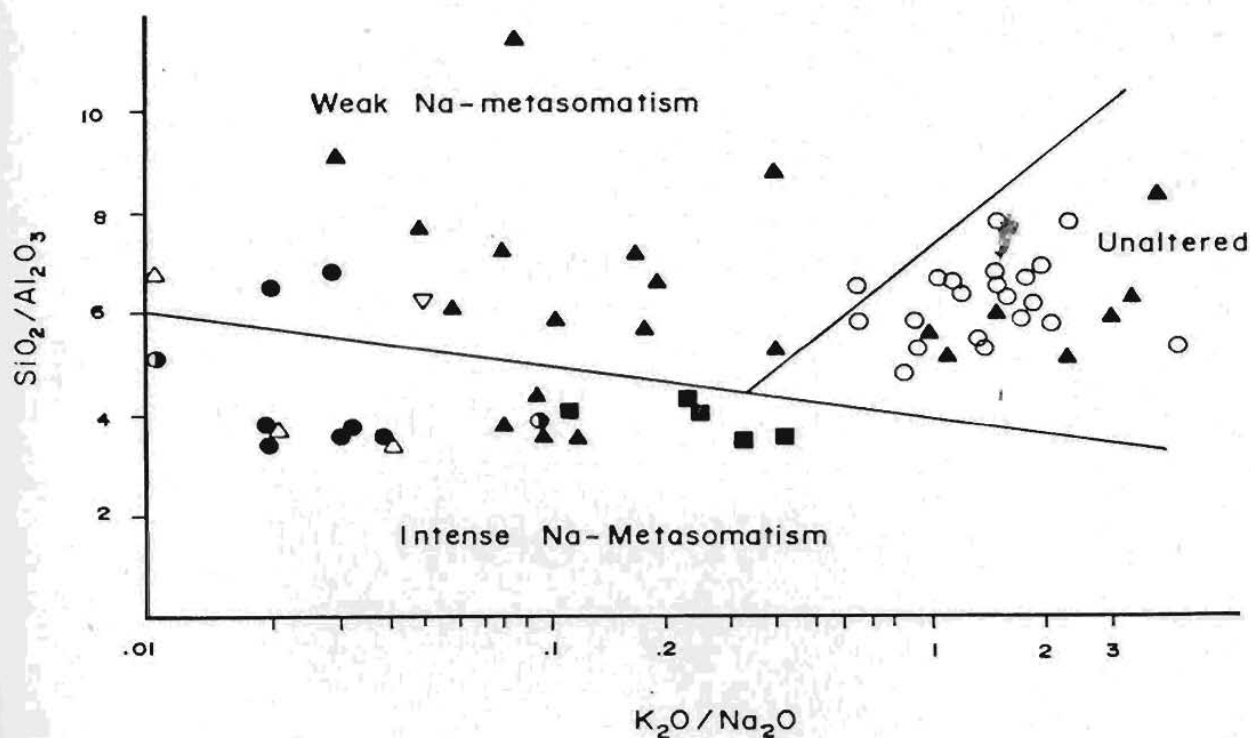


**Figure 4-36:**  $SiO_2/Al_2O_3$ versus K/Na illustrating fields of varying intensity of metasomatism (symbols as above).

Minor enrichments of $K_2O$ have been observed accompanied by decreases in $Na_2O$ and $CaO$ (see figures 4-35, 4-36). In three instances, the samples were associated with late stage crosscutting mineralized quartz veins, or the carbonate-hosted sphalerite mineralization. Thus this feature may be the result of compositional variations of the hydrothermal fluid late in the mineralizing event.

The observed major element trends are consistent with the observed alteration mineral assemblages associated with the mineralization. Enriched Na and depleted K, along with desilicification, are related to the albitization of K-feldspar. Increased Fe, Ti, and Ca, correspond to the presence of hematite, Fe-Ti oxides, sphene, calcic amphiboles and pyroxenes and abundant calcite. Increased volatile content is indicated by the presence of P as apatite, lesser F as fluorite, and overall increased LOI. In contrast, mineralized hydrothermal fluorite veins proximal to the granitic stocks are dominated by F with lesser P.

Trace element enrichment/depletion trends are generally more widely developed in hematized radioactive zones which exhibit the most intense degree of metasomatism among the various types of mineralization. Trace element analyses reveal depletion/enrichment trends in Rb/Sr related to the albitization of feldspar, along with variable enrichments in U, Th, Pb, Zn. Cu, Mo, Zr, Y, V, and occassionally Ba. Zr values vary from 566 to 2263 ppm in intensely metasomatized rhyolite, compared to an average of <500 ppm in unmineralized rhyolite. Interestingly, Zr values associated with mineralization hosted in amphibolite are enriched up to 5471 ppm, while enrichments of up to 333 ppm have been detected in radioactive hydrothermal fluorite veins. Minor enrichments of Y in radioactive zones and fluorite veins correspond to its variable presence in pitchblende as indicated by x-ray energy dispersive analysis (see Appendix III). Enrichments in Ba and V are sporadic, ranging from average values to enrichments > 31,000 ppm, and 623 ppm respectively. Barite has been identified as a common gangue mineral; however, the enriched vanadium is not as easily explained. Vanadium-rich garnets have been reported by some workers (ie. Gandhi, 1986) associated with some uranium occurrences, but no garnets have as yet been observed with hematized radioactive zones in the Round Pond area. The presence of enriched vanadium may indicate the presence of secondary, complex U-V oxides such as carnotite.

Figure 4-37 compares trace and ore element enrichment factors between

hematized rhyolite versus unmineralized rhyolite, and mineralized hydrothermal veins versus the Monkey Hill Granite. The greatest enrichments are Mo ($>$1000x) and U ($>$ 200x). The similarity of enrichment factors exhibited by the two styles of mineralization is striking and provides further evidence supporting the supposition of a common ore-forming fluid. Furthermore, the Monkey Hill granite is implicated as the source of the metal-bearing hydrothermal fluid.

The observed enrichments outlined above suggest widespread mobility and introduction of Ca, $Fe^{+3}$, Mg, Ti, Zr, Y, Mo, base metals, and U associated with Na-metasomatism related to oxidized, volatile-rich ($F^-$, $P^{5-}$, $CO_3^{2-}$, $Cl^-$) hydrothermal fluids of probable magmatic origin. The observed enrichment in relatively immobile elements such as Zr and Ti suggest relatively high temperatures were involved. Geochemical and mineralogical variations observed between various types of mineralization reflect the varying geochemical parameters and reducing nature of the host rocks, the intensity of metasomatism, and the ever changing physico-chemical nature of the ore-forming fluid.

## 4.5.2. Rare Earth Elements

In recent studies, it has been demonstrated that REE may serve as sensitive indicators of alteration and mineralization in hydrothermal systems, providing insight into the nature and activity of the dissolved anionic species involved in metal complexing and subsequent transport (see review by Taylor and Fryer, 1983). It is generally thought that LREE are most effectively transported by Cl-rich fluids, while HREE are transported by F- and $CO_3$-rich fluids (McLennon and Taylor, 1979; Muecke and Clarke, 1081; Taylor and Fryer, 1982, 1983; Chatterjee and Strong, 1984; Strong et al., 1984). MREE may be transported by P-rich fluids as suggested by the strong affinity of the MREE for apatite (Simmons and Hedge, 1978; Hanson, 1980), as well as by F-rich fluids (Strong et al., 1984).
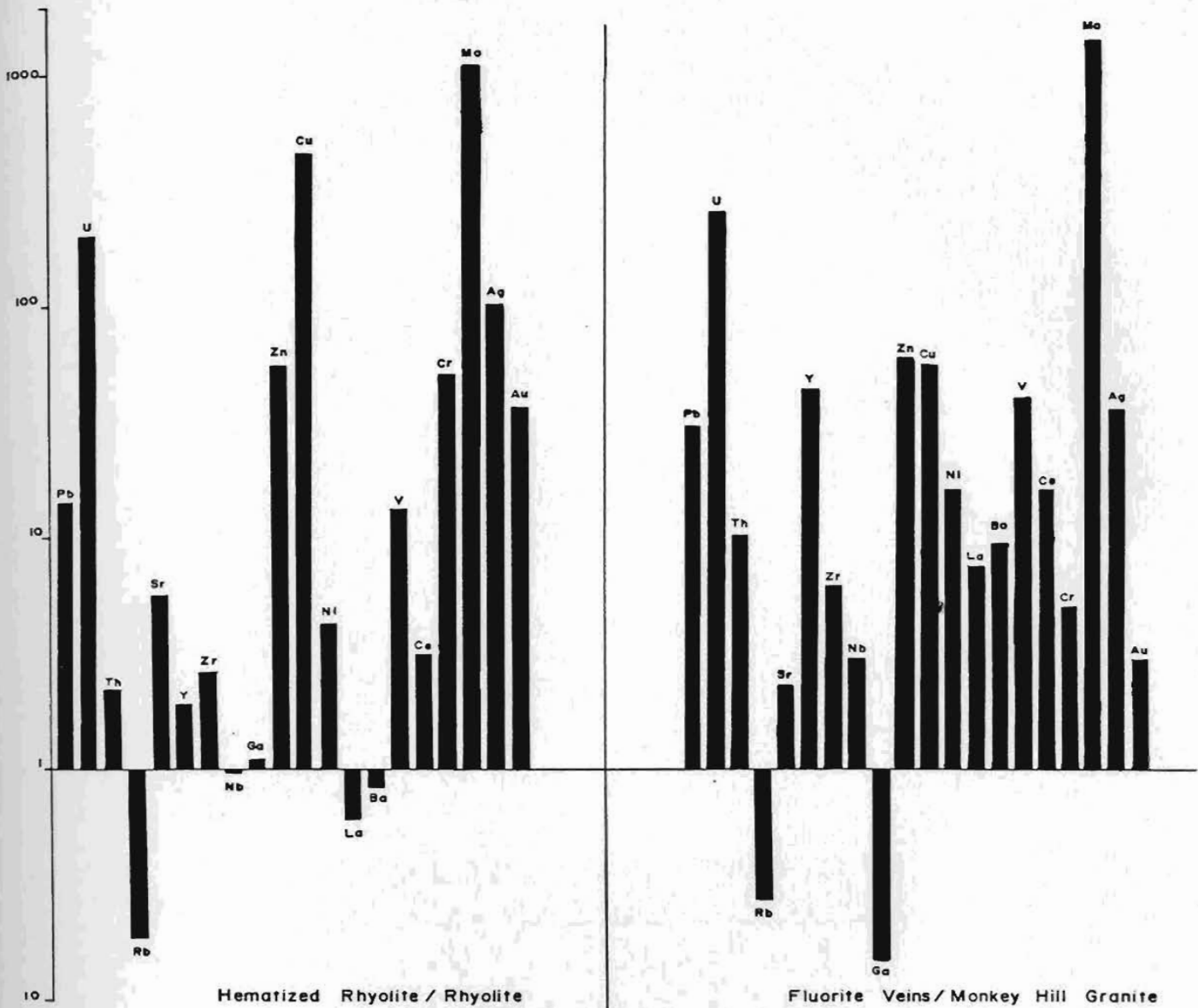
**Figure 4-37:** Enrichment factors calculated for
mineralized rock relative to host rock
for hematized radioactive rhyolite versus
unmineralized rhyolite, and hydrothermal
fluorite veins versus Monkey Hill
Granite.

(Note: Au and Ag contents for the Monkey
Hill Granite were assumed to be 5 ppb
and 0.1 ppm respectively.)

REE studies of mineral deposits hosted in the Aillik Group are relatively
rare, generally involving limited studies on "inland" (ie. Michelin area) uranium

occurrences (ie. White and Martin, 1980; Taylor and Fryer, 1982). Recently, more detailed studies have been undertaken on a variety of mineral occurrences throughout the Aillik Group (Wardle and Wilton, 1987; MacKenzie and Wilton, 1987; MacDougall and Wilton, 1987).

REE analyses, using the thin film XRF technique outlined by Fryer (1977) (see Appendix I), were carried out on various types of mineralization in the Round Pond area, including pyritiferous ($\pm$Mo) gossans, carbonate-hosted sphalerite mineralization, hydrothermal fluorite veins, and hematized radioactive zones.

Analyses of unmineralized Upper Aillik Group rhyolites have been reported by Wilton et al. (1987a), MacKenzie and Wilton (1987), and Wilton and Wardle (1987) (see figure 4-38). Analyses of two unaltered, unmineralized rhyolites from the Round Pond area have been carried out during this study, and are also shown in figure 4-38. Unmineralized Upper Aillik Group felsic volcanic rocks possess overall enriched REE contents (up to x500 chondrite), LREE enriched relative to HREE, and a pronounced negative Eu anomaly.

REE patterns exhibited by altered volcanic rock associated with uranium mineralization are typically much flatter (reduced LREE contents and/or enriched HREE contents) resulting in a saucer-shaped profile, with normal to slightly enriched HREE relative to LREE, and a much reduced negative to slightly positive Eu anomaly (see figure 4-39). These features are most pronounced in intensely metasomatized samples (discussed above), with more subtle variations observed with mildly metasomatized samples (ie. RP-1, RP-8). An interesting point to be noted is that showings which exhibit profiles similar (ie. negative Eu anomalies) to unmineralized rhyolites (which exhibit the least degree of metasomatism) possess the lowest enrichments in $P_2O_5$, thus supporting the concept of complexing and transporting the MREE as phosphate complexes.

Sample CM-58 (figure 4-39) is a radioactive, hydrothermal, amphibole-fluorite vein. Enrichment in overall REE contents characterized by extreme enrichment in

# UPPER AILLIK GROUP
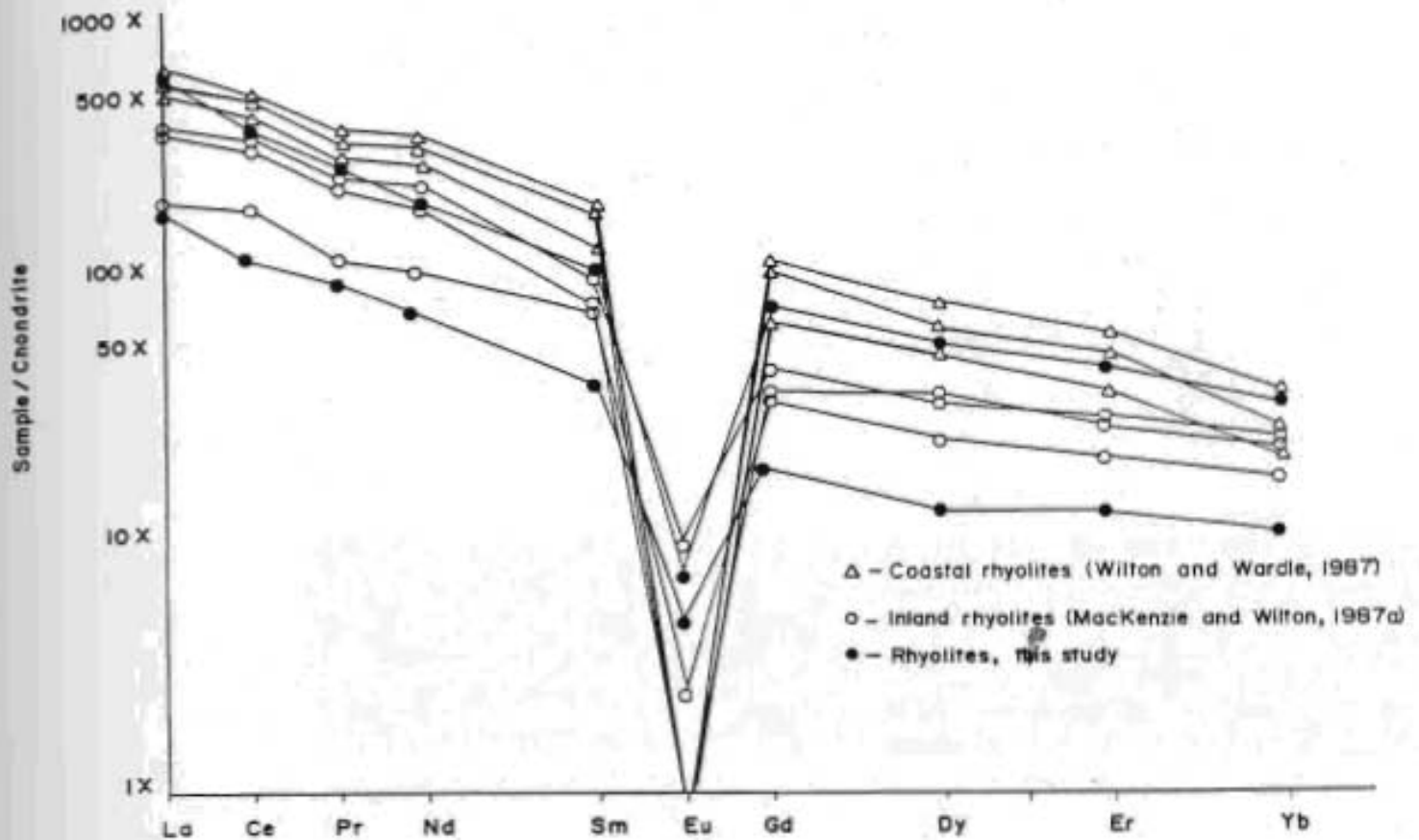


**Figure 4-38:** Chondrite normalized REE profiles for the Upper Aillik Group rhyolites.

HREE and MREE is observed. A mineralized hydrothermal fluid with similar REE contents would account for the enrichment trends observed in mineralized versus unmineralized rhyolites in the Round Pond area.

The same REE patterns are exhibited by pyritiferous ($\pm$Mo) gossans, carbonate-hosted sphalerite mineralization, (see figure 4-40). Wardle and Wilton (1987) reported similar REE patterns associated with mineral occurrences hosted within the Upper Aillik Group along the coast. Mineralized hydrothermal fluorite veins also show similar, but more variable patterns (see figure 4-41). The similarity of REE patterns exhibited by different types of mineralization hosted in
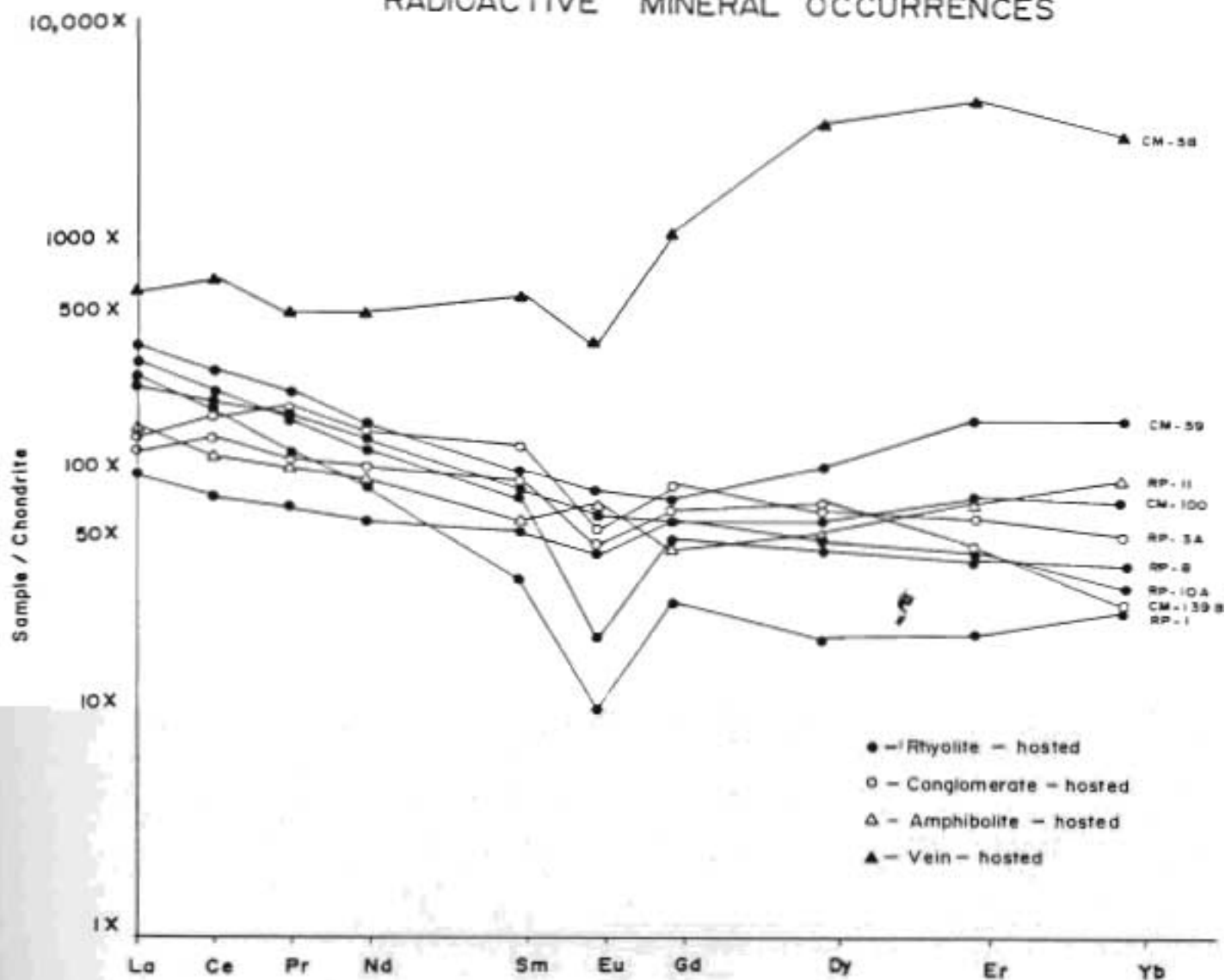
**Figure 4-39:** Chondrite normalized REE profiles
for various radioactive mineral occurrences
in the Round Pond area.

the Upper Aillik Group in the Round Pond area, provides further evidence supporting a common ore-forming fluid.

The saucer-shaped REE patterns which exhibit positive HREE fractionation relative to LREE, and a reduced negative to slightly positve Eu anomaly indicate that HREE and MREE were enriched and/or LREE depleted as a result of
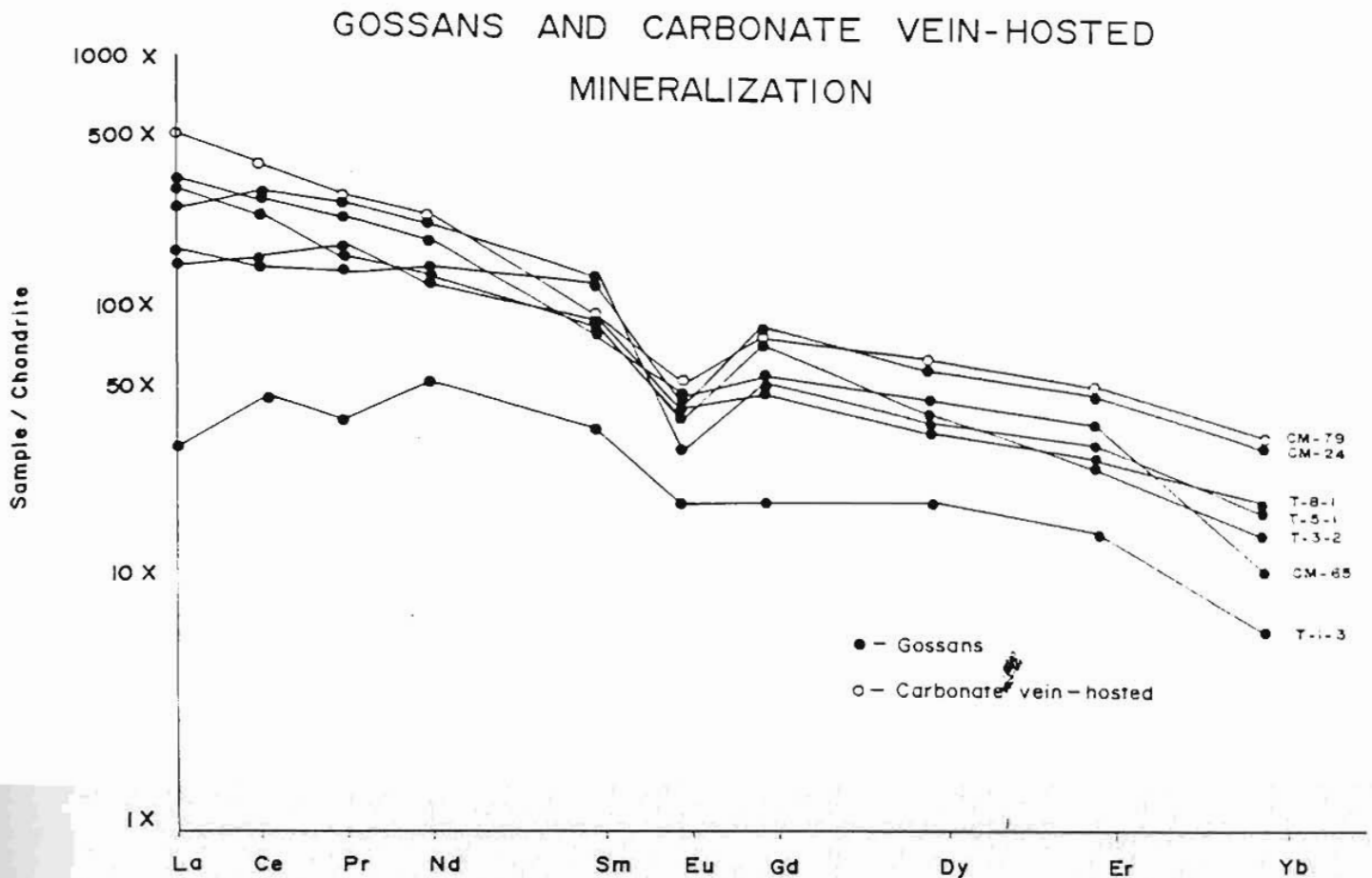
**Figure 4-40:** Chondrite normalized REE profiles for
pyritiferous gossans and carbonate
vein-hosted mineralization in the
Round Pond area.

mineralization. The mineralizing fluids were thus dominated by $F^-$ and $CO_3^{2-}$ anions (HREE deposition), $PO_4^{2-}$ (MREE deposition), and $Cl^-$ (LREE leaching). The presence of abundant hydrothermal albite (ie. Na-metasomatism), fluorite, carbonate, and apatite associated with the mineral occurrences in the Round Pond area lends strong support to the mineralizing fluid having such a composition.

The observed REE enrichment trends, in particular the MREE, associated

MINERALIZED FLUORITE VEINS
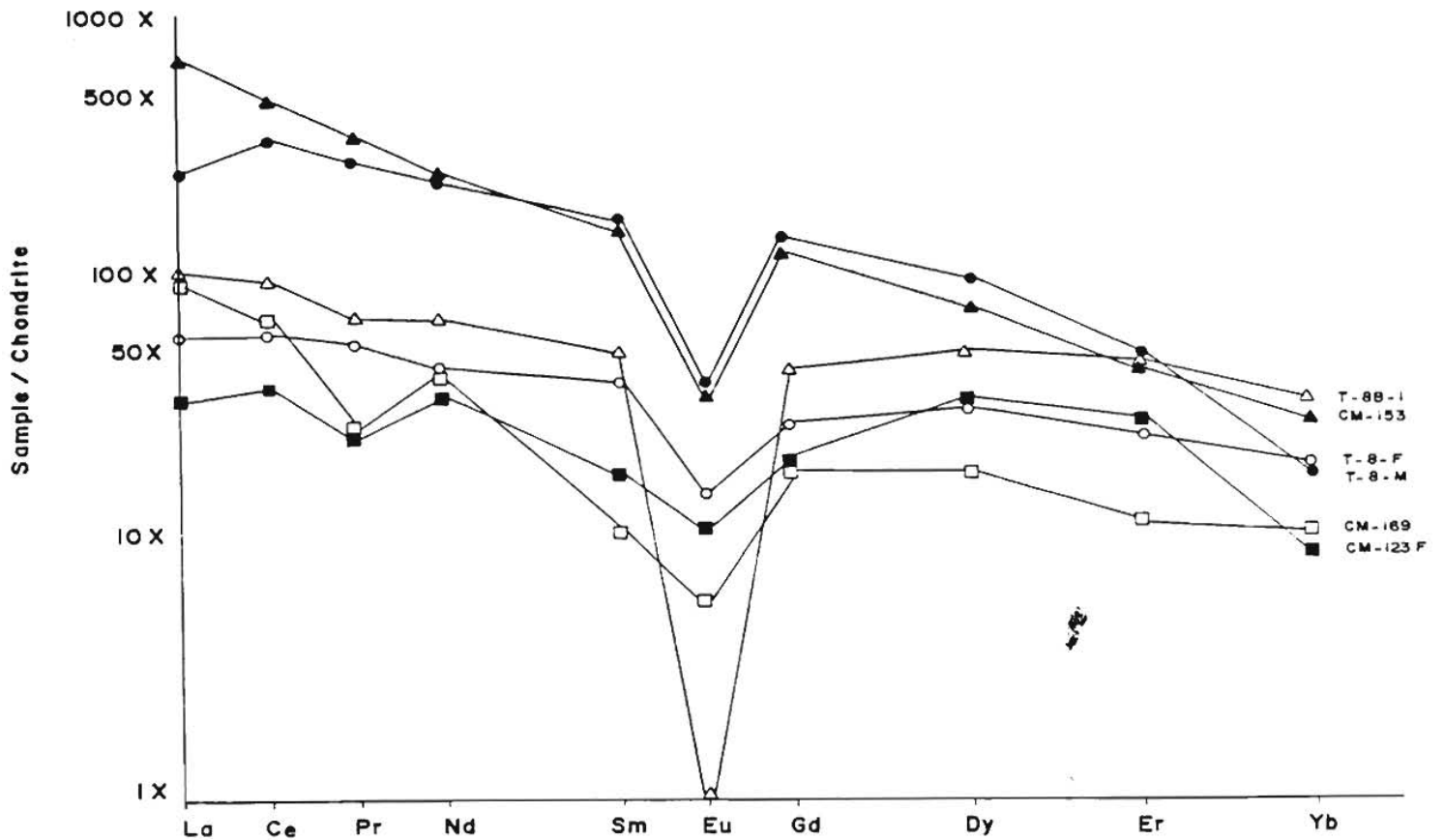


**Figure 4-41:** Chondrite normalized REE profiles for
hydrothermal fluorite veins in the
Round Pond area.

with the mineralization correspond to coincident depletion trends observed in the satellite stocks of Monkey Hill Granite. As has been previously discussed (see section 3-3), the granitic stocks appear to have suffered REE and other element depletions as a result of the escape of a mixed $CO_3$, F , $PO_4$, Cl volatile-rich phase.

## 4.6. Ar/Ar Mineral Dating

Two Ar/Ar mineral dates have been obtained from amphibole mineral separates associated with the mineralization in the Round Pond area (see Appendix IV). A hornblende mineral separate was collected from sample CM-58, a highly radioactive pyroxene-fluorite-andradite hydrothermal vein carrying abundant molybdenite, and lesser chalcopyrite and galena mineralization. A hornblende mineral separate was also collected from sample CM-70, a small vein of disseminated molybdenite mineralization with associated pyroxene alteration minerals.

Ar/Ar age dating techniques yielded plateau ages of 1603 $\pm$27, and 1564 $\pm$15 Ma (see figure 4-42). These compare well with a Pb isotope date reported by Wilton and Wardle (1987) of 1529 for galena mineralization from Big Bight. The dates suggest that the mineralizing event in the Makkovik area was contemporaneous with emplacement of high level, satellite stocks of the Monkey Hill Granite dated by Wanless et al.,(1970) at 1620 $\pm$60 Ma. This supports other evidence (discussed above) which suggests an intimate relationship between the Monkey Hill Granite and mineralization in the Round Pond area.
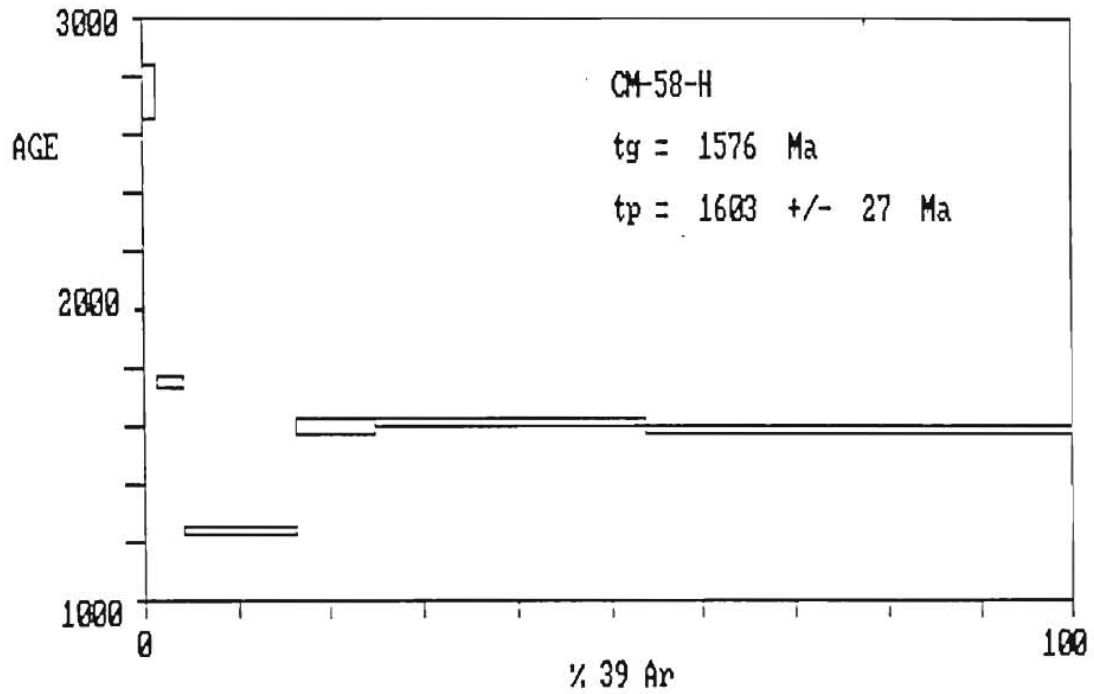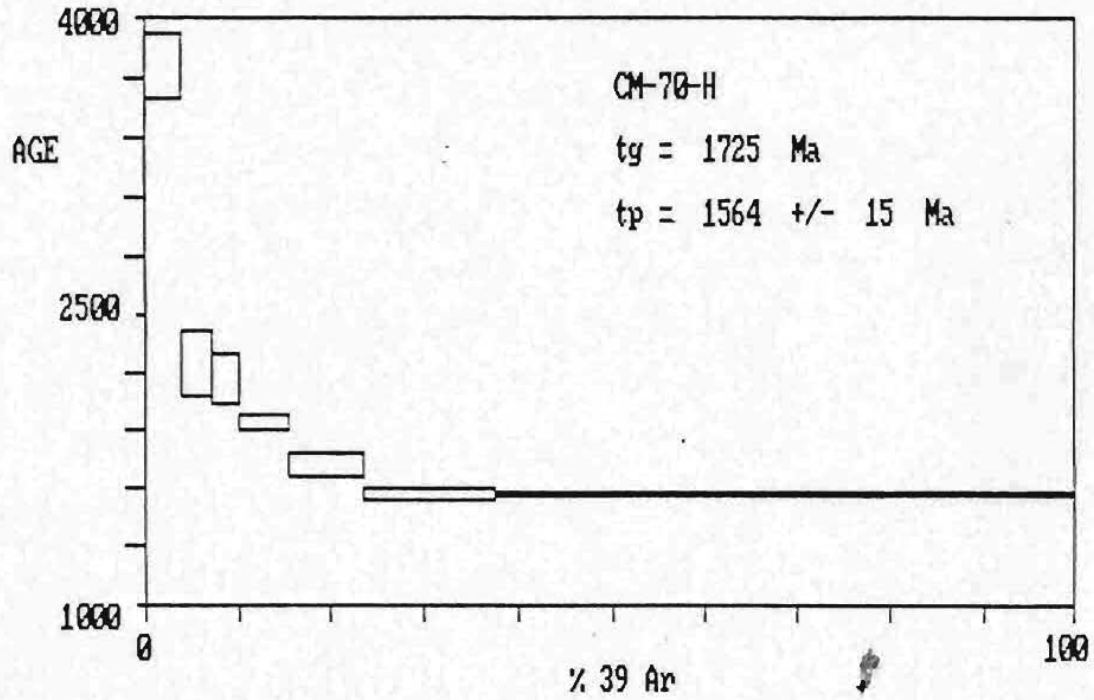
**Figure 4-42:** Ar/Ar age plateau's (tp) determined from amphibole alteration mineral separates associated with mineralization in the Round Pond area.

## 4.7. Discussion

Previous genetic models for uranium mineralization in the Aillik Group have advocated broadly synvolcanic mineralizing processes in which uranium was leached from the felsic volcanic rocks of the Upper Aillik Group, or associated synvolcanic plutons, by various hydrothermal fluids and concentrated along favourable horizons or structures.(ie. Gandhi, 1978, 1984; Evans, 1980; White and Martin, 1980; Gower et al., 1982). The models were based on information drawn largely from the "monometallic" Michelin and Kitts uranium deposits. Figure 4-43 illustrates the genetic model envisaged by Gower et al. (1982).
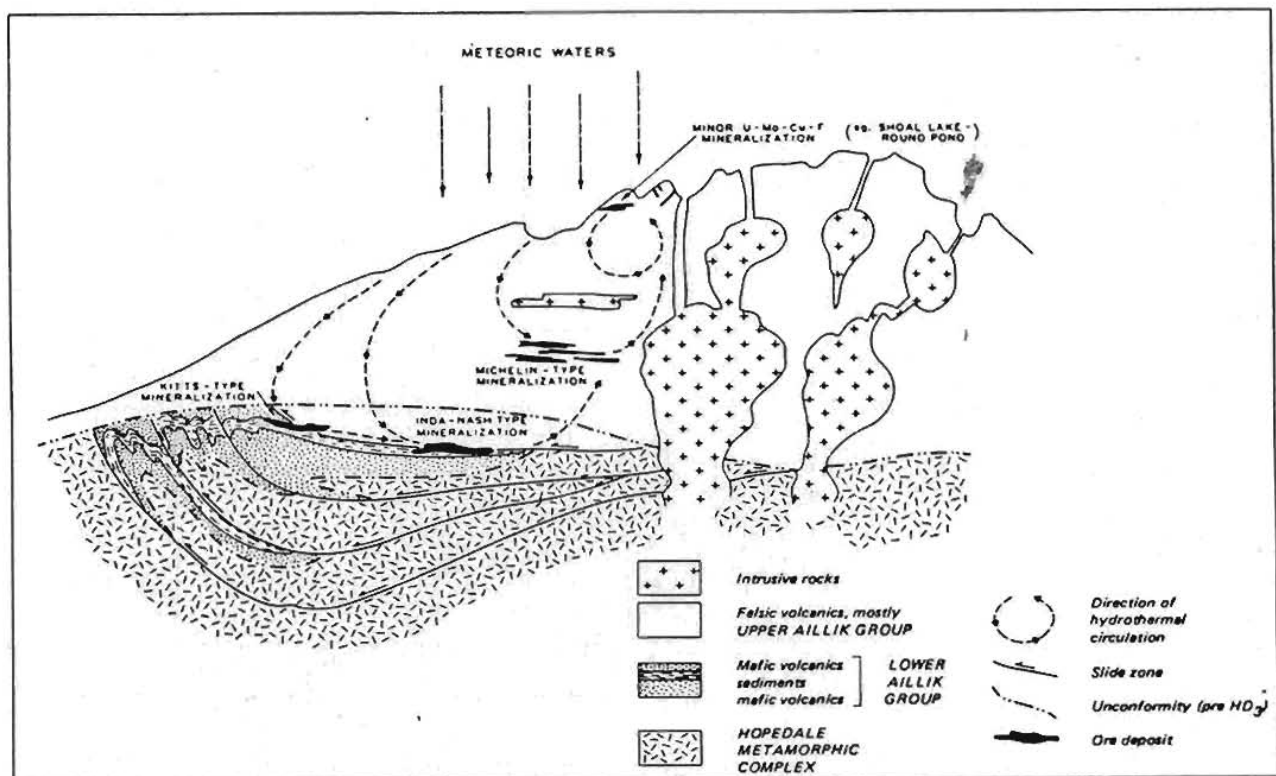


**Figure 4-43:**  Synvolcanic genetic model envisaged
for the widespread uranium and Mo-base
metal-F mineralization hosted within
the Aillik Group
(from Gower et al., 1982).

The mineralization observed in the Round Pond area exhibits a much more complex metallic mineral association (ie. Mo-U-base metal-(W)-F), as well as a more complex associated alteration assemblage. This complex metallic mineral

association was considered "coincidental" by Gandhi (1968), as he suggested the association was the result of the random superposition of "different epochs of mineralization." Gower et al., (1982) suggested that the observed polymetallic mineral association observed along the coast reflected differing degrees of mobility of uranium versus molybdenite in the hydrothermal system, thus restricting molybdenite proximal to the source of the metals rather than penetrating to deeper levels like the uranium at the Kitts and Michelin uranium deposits.

Various workers (ie. Sampson, 1966; Ryan, 1977; Gower et al., 1982; Wilton and Wardle, 1987; MacDougall and Wilton, 1987) have, however, suspected that the numerous, post-tectonic granitic intrusions which intrude the rocks of the Upper Aillik Group along the coast, may have played an important role in the metallogeny of the area. Evidence gathered throughout the course of this study clearly points to the small satellite stocks of Monkey Hill Granite as the source of the widespread and varied Mo-(W)-base metal-U-F mineralization in the Round-Pond area.

Mineralization is dominated by exocontact, hydrothermal veins, pyritiferous ($\pm$Mo) gossans, and linear radioactive zones which display a spatial association with the east stock of Monkey Hill Granite. A crude metallogenic zonation outward from the granite is defined, from dominantly Mo-Cu-F mineralization proximal to the stock, Zn-Pb spatially intermediate, and U-Zn-(Pb) mineralization as linear radioactive zones located distally from the stock. Similarities exhibited between the different types of mineralization with respect to ore mineral associations, alteration assemblages, major element geochemistry, geochemical enrichment factors, as well as evidence supplied by REE data indicate that the various types can be traced to the same mineralizing fluids.

The mineralization is characterized by Fe-Mo-(W)-Cu-Zn-Pb-U-F ore metal associations that exhibit minor enrichments of Ag, Co, Bi, Te, and Au, and thus represent a classic hydrothermal ore mineral assemblage. The abundance of fluorite, zircon, and apatite, typically associated with Na-metasomatism suggests a

dominantly magmatic character of the hydrothermal fluids, related to the Monkey Hill Granite. Gower et al. (1982) described the hydrothermal veins as showing "pegmatitic affinities", and similarily suspected a relation to the Monkey Hill Granite.

Alteration mineral assemblages associated with the hydrothermal veins and, to a lesser extent, the linear radioactive zones, are dominated by calcsilicates typical of that observed in calcic skarn environments. Such environments are thought to be related to magmatic-hydrothermal systems generated by granitic intrusions which are the source of the metals. Suggested temperatures of skarn formation are consistent with a magmatic source for the hydrothermal fluids.

The mineralization is generally localized in shear zones, fractures, stockworks and breccia zones (which are hydrothermal in nature), that are discordant with the regional trends, indicating a post-tectonic origin. The satellite stocks of Monkey Hill Granite are similarly post-tectonic and have been dated by K/Ar techniques at $1620 \pm 60$ Ma (Wanless et al., 1970). Ar/Ar dating of alteration minerals associated with the mineralization carried out in this study returned dates of $1603 \pm 27$ and $1564 \pm 15$ Ma. Recent Pb isotope dating of galena mineralization from Big Bight, located 10 km northeast of Round Pond, similar to carbonate-hosted sphalerite-galena mineralization discussed in this study, returned an age of mineralization of $1529 +112/-56$ Ma for a secondary isochron (Wilton and Wardle, 1987). These dates of mineralization are contemporaneous with the emplacement of the high-level, satellite stocks of the Monkey Hill Granite.

Minor fluorite, and rare molybdenite, and scheelite mineralization have been observed in the stocks of Monkey Hill Granite. Geochemical analysis from this study reveal that granitic stocks are more enriched in U relative to the rhyolitic volcanics (averaging 5 ppm and 3 ppm respectively), and thus are a more favourable source. Numerous pegmatitic, granitic, and aplitic dykes are observed in the adjacent country rocks which carry significant pyrite, molybdenite, chalcopyrite, and fluorite mineralization, occassionally associated with anomalous

radioactivity. These dykes are often directly or spatially associated with pyritiferous ($\pm$Mo) gossans or hematized radioactive zones which carry similar mineralization. The pegmatites also exhibit enriched Na contents similar to that associated with the other types of mineralization.

Geochemical evidence and field relations suggest that the small granitic stocks of Monkey Hill Granite in the Round Pond area represent highly differentiated (ie. specialized), shallow, epizonal intrusions that are interpreted to represent the apical portions of the Trans-Labrador Batholith at depth. Such intrusions are considered favourable sites for the accumulation of metal-bearing volatile-rich phases. It has been suggested in this study, that the granitic stocks successfully exsolved a Na$\pm$Ca metal-bearing, mixed (F, P, $CO_3^{2-}$, Cl) volatile-rich phase which escaped to form the observed exocontact mineralization in the Round Pond area. The presence of mineralized pegmatites and hydrothermal fluorite veins carrying granophile ore mineral associations of Mo-(W)-U associated with "granitic" accessory minerals such as fluorite, zircon, apatite, and sphene, provide compelling evidence that such an interpretation is possible. However, direct evidence has been supplied by REE data. The granitic stocks exhibit a pronounced MREE depletion, while the various types of mineralization in the Round Pond area exhibit a corresponding MREE enrichment relative to host rocks.

The weight of evidence discussed above clearly implicates the Monkey Hill granite as the source of the widespread, Mo-(W)-base metal-U-F mineralization in the Round Pond area. Thus the mineralization is epigenetic with respect to the Upper Aillik Group, and is related to the magmatic-hydrothermal processes of the post-tectonic satellite intrusions of the Monkey Hill Granite.

# Chapter 5
# Metallogeny

## 5.1. Introduction

As discussed in the preceeding chapter, the widespread, and varied Mo-(W)-base metal-U-F mineralization in the Round Pond area appears to have a common magmatic-hydrothermal origin related to the high level igneous activity of the post-tectonic Monkey Hill Granite, and is, thus, epigenetic with respect to the felsic volcanic rocks of the Upper Aillik Group. A similar epigenetic model for a variety of mineral occurrences in the Aillik-Makkovik area, related to the post-tectonic granites intruding the Upper Aillik Group in the coastal region has been suggested by Wilton and Wardle (1987). This represents a significant departure from previous genetic models which proposed the source of the uranium and molybdenum metals to be the felsic volcanic rocks of the Upper Aillik Group or associated synvolcanic plutons.

## 5.2. Epigenetic magmatic-hydrothermal model

The epigenetic magmatic hydrothermal model of mineralization as envisaged for the Mo-(W)-base metal-U-F mineralization in the Round Pond area is illustrated in figure 5-1. The deformed felsic volcanic rocks of the Upper Aillik Group were intruded by the post-tectonic Monkey Hill Granite marking an intrusive event referred to as the Labradorian Orogeny, during which the Trans-Labrador Batholith was emplaced.

The intrusions in the Round Pond area are small, highly differentiated, epizonal stocks, that represent the higher levels or apical portions of larger granitic batholiths at depth. Emplacement to such shallow depths was possible due to initial low water content, and high solidus-lowering volatile content. These small satellite stocks were favourable sites for the accumulation of oxidized, alkali and metal-bearing, volatile phases during differentiation and crystallization of the granitic magma.

The shallow emplacement of the granitic stocks and subsequent boiling of the volatile phase produced structural weaknesses in favourable or incompetent lithologies (ie. volcanic conglomerate, and lithologic contact zones). The induced structural weaknesses produced fractures, and zones of shearing and brecciation that were concentrated adjacent to the contact margin of the granitic stock, providing permeable channel-ways for the escape of the metal-bearing, volatile phase as an oxidized hydrothermal fluid.

The movement of hot, oxidized, alkali-rich, hydrothermal fluids through the cold country rock resulted in disequilibrium reactions which produced the associated alkali metasomatism, as well as the observed calcsilicate alteration so typical of calcic skarn-type environments. The Ca necessary for the skarn-type alteration was in part supplied by the hydrothermal fluids, but mostly was derived from calcareous country rocks such as the volcanic conglomerate and mafic amphibolites. Retrograde mineral growth occurred in response to decreasing temperature and changing physicochemical characteristics of hydrothermal fluid.

U,Zn,Cu

Mo,Zn,U

U,F

Mo,(W),Cu

Present Erosional
Surface

Metallogenic Zone
Boundary

Na

U,Mo,(W),Cu,Zn
F, P, CO₃, Cl

Granite Stock

UAG

UAG

| | |
|---|---|
| + + | Fine-grained Chill Margin and Granitic Dykes |
| · · · | Metal-bearing Volatile-rich Hydrothermal Phase |
| ⌇ ⌇ | Zone of Fracturing & Sites of Metal Deposition |
| ▲ | Migration Direction of Mineralized Hydrothermal Fluids |
| UAG | Upper Aillik Group |
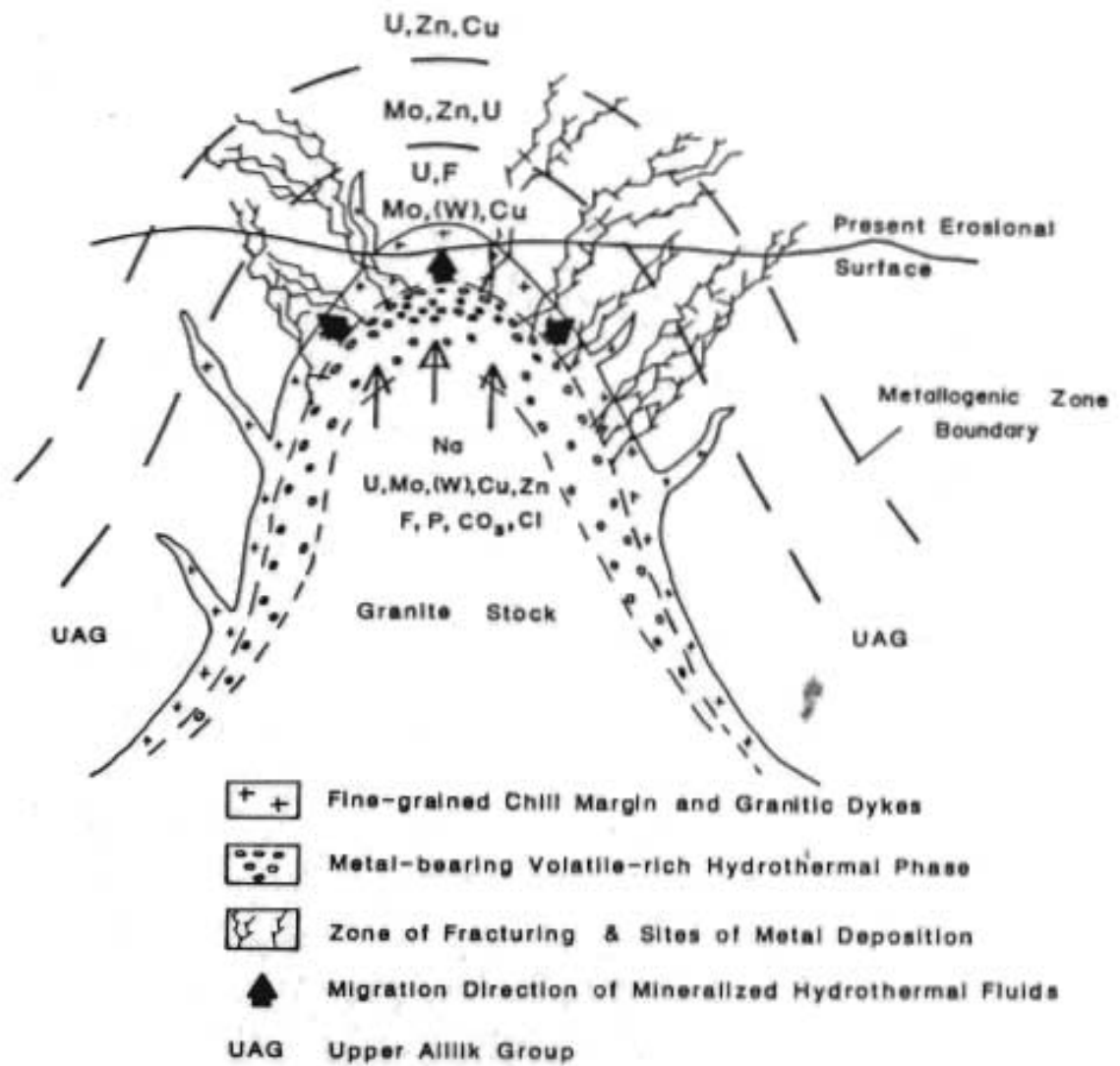
**Figure 5-1:** Schematic diagram representing an
epigenetic magmatic-hydrothermal genetic
model for the Mo-(W)-base metal-U-F
mineralization hosted within the
Upper Aillik Group in the Round
Pond area.

The metals were transported within the fluid as various fluoride, carbonate, phosphate and chloride complexes as suggested by the presence of abundant fluorite, calcite, apatite, and the observed Na-metasomatism associated with the metallic mineralization. Numerous workers (ie. Holland, 1972; Bailey, 1977; Strong, 1980, 1981; Mutschler et al., 1981; Romberger, 1984; Eugster, 1985; etc.) have suggested that such anions are important complexing agents for metal transportation in hydrothermal systems. The dominant complexing agent depends primarily on concentration of the various complexing anions, which is further influenced by temperature, pressure, and pH of the hydrothermal fluid (Romberger, 1984). These variables change during the physicochemical evolution of the hydrothermal fluid. Assuming a constant temperature (ie. $200^{\circ}$ C) at which all of these complexing anions may be active, chloride and fluoride complexes are favoured at low to neutral pH, phosphate complexes at neutral pH, and carbonate at high pH (Langmuir, 1978; Romberger, 1984).

The dominance of fluorite over apatite in hydrothermal fluorite veins proximal, and apatite over fluorite in hematized radioactive zones distal to the granitic stock observed in this study, may reflect differing pH levels at which the anionic complexes are stable during the evolution of the hydrothermal fluid. Holland (1972) states that the quench pH of aqueous solutions equilibrated with granitic melts is generally between 1.4 and 2.2. Thus metal-bearing fluoride and chloride complexes would be favoured early in the fluid evolution, with other complexes becoming important in later stages in response to increasing pH. This may account for the observed spatial metallogenic zonation as discussed below.

Uranium is complexed and transported in a hexavalent ($U^{6+}$) state (Langmuir, 1978; Romberger, 1984), and is insoluble in the tetravalent ($U^{4+}$) state. Candela and Holland (1984) report that hexavalent molybdenum is much more abundant than tetravalent molybdenum in aqueous phases, although both are stable. Thus an oxidized, ore-forming fluid is necessary for the transportation of both U and Mo.

Deposition of pitchblende, and by anology molybdenite, may result from the reduction of U (and Mo) from a hexavalent to a tetravalent oxidation state as a result of oxidation of reductants such as $Fe^{+2}$, sulphur and carbonaceous material. Gower et al. (1982) suggest such a mechanism was involved in the precipitation of uranium in the Aillik Group, and accounts for the observed association of hematite and calcite with many of the mineral occurrences. Gandhi (1978, 1986) has suggested that precipitation of uranium was a result of reactions with Ti- and Fe-bearing minerals such as sphene, pyroxene, and hornblende. These minerals however, appear to have been introduced along with uranium in the mineralizing fluid, and often uranium occurs as inclusions within these minerals.

Romberger (1984), however, has suggested that changes in pH may be even more important than reduction for the precipitation of uranium. Deposition of metals as various sulphides (Fe, Mo, Cu, Pb, Zn) and oxides (U, Fe) would occur in response to increasing pH (and destabilization of the complexing anions) as a result of fluid-wall rock reactions, and/or loss of volatiles during boiling of the hydrothermal fluid. In addition, the alkali metasomatism and precipitation of fluorite, calcite, and apatite as a result of wall rock reactions and decreasing solubility due to decreasing temperatures would reduce the activity of Cl, F, $CO_3$, and P as complexing agents, and thus promote further metal deposition. All of the mechanisms were probably interrelated and occured in combination.

The association of Na-metasomatism and calcite with all types of mineralization in the Round Pond area suggests that ore-bearing hydrothermal fluids existed under a wide range of pH values. The association of abundant fluorite with molybdenite mineralization and abundant apatite with uranium mineralization suggests that Mo was transported predominantly as a fluoride complex, while U was transported predominantly as a phosphate complex. Thus the distribution of proximal molybdenite-bearing hydrothermal fluorite veins and distal hematized radioactive zones, may reflect differences in the activity of the two complexing agents in the hydrothermal system due to increasing pH, resulting in the observed metallogenic zonation.

## 5.3. Conclusions

The Round Pond area in coastal Labrador is underlain by the dominantly calcalkaline felsic volcanic rocks of the Upper Aillik Group which are hypothetically suggested to have been deposited during subduction related volcanic activity ca. 1855 Ma. The volcanic rocks were subjected to intense polyphase deformation and metamorphism of upper greenschist - lower amphibolite facies during the Makkovikian Orogeny (ca.1800 Ma). Numerous post-tectonic granitoids intrude the Upper Aillik Group rocks in the coastal region marking the Labradorian intrusive event (ca. 1600 Ma). In the Round Pond area, two satellite stocks of the regionally extensive Monkey Hill Granite (1620 ± 60 Ma) occur.

The granitic stocks are highly differentiated, epizonal, leucogranitic intrusions which exhibit geochemical trends towards metallogenic specialization. The satellite stocks are interpreted as representing apical portions of the Trans-Labrador batholith at depth. Such sites are considered favourable sites for the accumulation of metal-bearing, volatile-rich fluids which may ultimately escape to form associated granophile ore mineral (Sn, W, U, Mo) deposits. Trace and rare earth element analyses suggest that such a metal-bearing, volatile phase has escaped, resulting in the observed depletion and/or lack of enrichment in granophile, volatile, and rare earth elements.

The Round Pond area is characterized by widespread and varied Mo-(W)-base metal-U-F mineralization spatially associated with contact margin of satellite stock of Monkey Hill Granite. A crude metallogenic zonation is developed outwards from the granite. Field relations, ore mineral and alteration mineral assemblages, and geochemical evidence suggest that widespread, and varied mineral occurrences in the Round Pond area are related to a common magmatic-hydrothermal origin related to the high level igneous activity of the Monkey Hill

Granite. Ar/Ar age dating of alteration minerals with mineralization return ages of 1603 ±27, and 1564 ±15 Ma, and thus support an epigenetic magmatic-hydrothermal model of origin for the mineralization in the Round Pond area.

# Bibliography

Archibald, D., and Farrar, E., 1979. $Ar^{40}/Ar^{39}$ mineral ages from the Walker Lake - Benedict Granodiorite, Central Mineral Belt, Labrador. Unpublished report to NDME, 12 p.

Bailey, D.G., 1979. Geology of the Walker-McLean Lake area, 13K/9, 13J/12, Central Mineral Belt, Labrador. NDME Report 78-3, p. 17.

Bailey, D.G., 1981. Kaipokok Bay - Big River, Labrador. NDME, Map 81-18, 1:100,000.

Bailey, J.C., 1977. Fluorine in granitic rocks and melts: a review. Chem. Geol., vol. 19, pp. 1-42.

Baragar, W.R.A., 1977. Volcanism of the stable crust. in Volcanic Regimes in Canada, eds. W.R.A. Barager, L.C. Coleman, J.M. Hall. Geol. Assoc. of Canada, Special Paper 16, pp. 377-405.

Barton, M.D., 1987. Lithophile-element mineralization associated with late Cretaceous two mica granites in the Great Basin. Geology, vol. 15, pp. 337-340.

Barua, M.C., 1969. Geology of uranium-molybdenite bearing rocks of the Aillik-Makkovik Bay area, Labrador. Unpub. M.Sc. thesis, Queen's University, Kingston, Ont., 76 p.

Beavan, A.P., 1958. The Labrador uranium area. Proceedings of the Geol. Assoc. of Canada, vol. 10, pp. 137-145.

Beckinsale, R.D., 1979. Granite magmatism in the tin belt of southeast Asia. in Origin of Granite Batholiths: Geochemical Evidence., eds. M.P. Atherton and J. Tarney. Shiva Publishing Ltd., Orpington, England. pp. 34-44.

Bell, T.H., and Etheridge, 1973. Microstructures of mylonites and their descriptive terminology. Lithos, vol. 6, pp. 337-348.

Best, M.G., 1982. Igneous and Metamorphic Petrology. San Francisco, Freeman, Cooper, and Co., 397p.

Brooks, C., 1979. Report on geochronology of Labrador. Unpub. report to NDME., 45 p.

Burns, J.G., 1980. Reconnaissance geology, Kaipokok West area, Labrador. Unpub. report Placer Devlopment Ltd., 6 p.

Burt, D.M., and Sheridan, M.F., 1981. Model for the formation of uranium/lithophile element deposits in fluorine-rich volcanic rocks. American Assoc. of Petrol. Geol. Special Publication, pp. 99-109.

Candela, P.A., and Holland, H.D., 1984. The partitioning of copper and molybdenum between silicate melts and aqueous fluids. Geochim. et Cosmo.

Acta, vol. 48, pp. 373-380.

Cathelineau, M., 1982. Signification de la fluorine dans la chaine hercynienne. (in French), Bull. du BRGM (2) sect. II, no. 4, pp. 407-413.

Chappell, B.W., and White, A.J.R, 1974. Two contrasting granite types. Pacific Geology, vol. 8, pp. 173-174.

Chatterjee, A.K., Strong, D.F., and Muecke, G.K., 1983. A multivariate approach to geochemical distinction between tin-specialized and uranium-specialized granites of southern Nova Scotia. Can. Jour. of Earth Sciences, vol. 20, pp. 420-430.

Chatterjee, A.K., and Strong, D.F., 1984. Rare earth and other element variations in greisens and granites associated with East Kemptville tin deposit, Nova Scotia, Canada. Ext. from Trans./Sect. B of the Inst. of Min. and Metal., vol. 93, pp. B 59-70.

Christie, A.M., Roscoe, S.M., and Fahrig, W.F., 1953. Central Labrador coast, Newfoundland, (descriptive notes). Geol. Sur. of Canada, paper 53-14, 3 p. (Preliminary Map).

Clark, A.M.S., 1970. A structural reinterpretation of the Aillik series, Labrador. Unpub. M.Sc. thesis, Memorial University of Nfld., St. John's, Nfld. 76 P.

Clark, A.M.S., 1973. A reinterpretation of the stratigraphy and deformation of the Aillik Group, Makkovik, Labrador. Unpub. Ph.D. thesis, Memorial University of Nfld., St. John's, Nfld. 346 p.

Clark, A.M.S., 1979. Proterozoic deformation and igneous intrusions in part of the Makkovik subprovince, Labrador. Precambrian Research, vol. 10, pp. 96-114.

Collerson, K.D., Jesseau, C.W., Ryan, A.B., and Hawkins, D.W., 1974. Mineral potential evaluation in the Makkovik and Hopedale areas, Labrador. NDME Report of Activities for 1973, Mineral Development Division, pp. 24-31.

Collins, W.J., Beans, S.D., White, A.J.R., and Chappell, B.W., 1982. Nature and origin of A-type granites with particular reference to southeastern Australia. Cont. to Mineral. and Pet., vol. 80. pp. 189-200.

Cooper, G.E., 1951. The petrology of some syenites and granites in Labrador. Unpub. M.Sc. thesis, McGill University, Montreal. 54 p.

Cullers, R.L., and Graf, J.L., 1984. Rare earth elements in igneous rocks of the continental crust: intermediate and silicic rocks - ore petrogenesis. in Rare Earth Element Geochemistry, ed. P.Henderson, Elsevier, New York. pp. 237-274.

Curtis, L., 1981. Uranium in volcanic and volcaniclastic rocks - examples from Canada, Australia, and Italy. American Assoc. of Petrol. Geol. Special Publication. pp. 37-53.

Daly, R.A., 1902. The geology of the northwest coast of Labrador. Bull. of the Museum of Comparitive Zoology, Harvard, vol. 38, Geological Series, vol. 5, No. 5, pp. 205-269.

Deer, W.A., Howie, R.A., Zussman, J., 1962. Rock-forming minerals. London, Longman (5 volumes).

Douglas, G.V., 1953. Notes on localities visited on the Labrador coast in 1946 and 1947. Geol. Sur. of Canada, paper 53-1, 67 p.

Du Bray, E.A., 1986. Specialized granitoids in the southeastern Arabian Shield - case history of regional assessment. Jour. of African Earth Sci., vol. 4, pp. 169-176.

Einaudi, M.T., Mein, L.D., and Newberry, R.J., 1981. Skarn deposits. Econ. Geol. 75th Anniversary vol., pp. 317-391.

Evans, D., 1980. Geology and petrochemistry of the Kitts and Michelin uranium deposits, and related prospects, Central Mineral Belt, Labrador. Unpub. Ph.D. thesis, Queen's University, Kingston, Ont., 311 p.

Ewart, A., Brothers, R.N., and Mateen, A., 1977. An outline of the geology and geochemistry, and the possible petrogenetic evolution of the volcanic rocks of the Tonga-Kermadec-New Zealand island arc. Jour. of Volcan. and Geotherm. Res., vol. 2, pp. 205-250.

Floyd, P.A., and Winchester, J.A., 1975. Magma type and tectonic setting discrimination using immobile elements. Earth Planet. Sci. Let., vol. 27, pp. 211-218.

Flynn, R.T., and Burnham, C.W., 1978. An experimental determination of rare earth partition coefficients between a chloride-containing vapour phase and silicate melts. Geochemica et Cosmochimica Acta, vol. 42, pp 685-701.

Foley, S.F., 1982. Mineralogy, petrology, petrogenesis and structural relationships of the Aillik Bay alkaline intrusive suite, Labrador, Canada. Unpub. M.Sc. thesis, Memorial University of Nfld., St. John's, Nfld. 140 p.

Fourcade, S. and Allegre, C.J., 1981. Trace element behaviour in granite genesis: a case study: the calc-alkaline plutonic association from the Querigut Complex, (Pyrenees, France). Cont. to Mineral. and Pet., vol. 76, pp. 177-195.

Fryer, B.J., 1977. Rare earth evidence in iron formation for changing oxidation states. Geochim. et Cosmo. Acta, vol. 41, pp. 361-367.

Fulton, R.J., Hodgson, D.A., and Minning, G.V., 1975. Inventory of Quaternary geology, southern Labrador: an example of Quaternary geology - terrain studies in undeveloped areas. Geol. Sur. of Canada, paper 74-46, 13 p.

Gale, G.H., and Pearce, J.A., 1982. Geochemical patterns in Norwegian greenstones. Can. Jour. of Earth Sci., Vol. 19, pp. 385-397.

Gandhi, S.S., 1968. Report on exploration in Aillik-Makkovik area, Labrador, during 1967, Brinex/Cominco joint venture. Unpub. Brinex Report G68009, 30 p.

Gandhi, S.S., 1968. General geological observations on the Aillik-Makkovik area, Labrador. Unpub. Brinex Report G68009, Appendix 1, 12 p.

Gandhi, S.S., 1970. Exploration in Kaipokok Bar - Big River area, Labrador. Unpub. Brinex Report G70004, 33 p.

Gandhi, S.S., 1978. Geological setting and genetic aspects of uranium occurrences in the Kaipokok Bay - Big River area, Labrador. Economic Geology, vol. 73, pp. 1492-1522.

Gandhi, S.S., 1984. Uranium in early Proterozoic Aillik Group, Labrador. In Proterozoic unconformity and stratabound uranium deposits. ed. Ferguson, J., IAEA, Vienna, Tech. Doc. 315. pp. 35-68.

Gandhi, S.S., 1986. Uranium in early Proterozoic Aillik Group, Labrador. Institute of Min. and Metal., Special vol. 33, pp. 70-82.

Gandhi, S.S., Grasty, R.L., and Grieve, R.A.F., 1969. The geology and geochronology of the Makkovik Bay area, Labrador. Canadian Jour. of Earth Science, vol. 6, pp 1019- 1034.

Gill, F.D., 1966. Petrology of molybdenite-bearing gneisses, Makkovik area, Labrador (abstract). Canadian Mineral. Journal, vol. 89, pp. 100-101.

Goodwin, A.M., 1977. Archean volcanism in the Superior Province, Canadian Shield. in Volcanic Regimes in Canada, eds. W.R.A. Barager, L.C. Coleman, and J.M. Hall, Geol. Ass. of Canada Spec. Paper 16, pp. 169-192.

Gower, C.F., Ryan, A.B., Bailey, D.G., and Thomas, A., 1980. The position of the Grenville Front in eastern and central Labrador. Can. Jour. of Earth Sci., vol. 17, pp. 748-788.

Gower, C.F., Flanagan, M.J., Kerr, A., and Bailey, D.G., 1982. Geology of the Kaipokok Bay-Big River area, Central Mineral Belt, Labrador. NDME report 82-7, 77 p.

Gower, C.F., and Owen, V., 1984. Pre-Grenvillian and Grenvillian lithotectonic domains in eastern Labrador - Correlation with the Sveconorwegian orogenic belt in Sweden. Can. Jour. of Earth Sciences, vol. 21, pp. 678-693.

Gower, C.F., and Ryan, A,B., 1986. Proterozoic evolution of the Grenville Province and adjacent Makkovik Province in eastern-central Labrador. in The Grenville Province. Geol. Assoc. of Canada Spec. Paper 33, pp. 281-296.

Gower, C.F., and Ryan, A.B., (in prep.) Two stage Felsic volcanism in the Lower Proterozoic Upper Aillik Group, Labrador, Canada: Its relationship to syn- and post-kinematic plutonism.

Greene, B.A., 1972. Geological map of Labrdor. NDME. Mineral Resources Division.

Greene, B.A., 1974. An outline of the geology of Labrador. NDME Inf. Cir. No. 15, 64 p.

Groves, D.I., and McCarthy, T.S., 1978. Fractional Crystallization and the origin of tin deposits in granitoids. Mineral. Deposita, vol. 13, pp 11-26.

Haffty, J. and Noble, C., 1972. Release and migration of molybdenum during the Primary crystallization of Peralkaline Silicic Volcanic Rocks. Econ. Geol. Vol.67, pp 768-775.

Hanson, G.N., 1980. Rare earth elements in petrogenetic studies of igneous systems. Ann. Rev. Earth Planet. Sci. Let., vol. 8, pp. 371-406.

Hansuld, J., 1959. Geochemical exploration, 1959, Anglo American joint venture area, Shoal Lake - Labrador. Unpub. Report, 18 p.

Hawkins, D.W., 1976. Emplacement, petrology, and geochemistry of ultrabasic to basic intrusives at Ailik Bay, Labrador. Unpub. M.Sc. thesis, Memorial University of NFLD, St. John's, Nfld., 236 p.

Hellingwerf, R.H., and Baker, J.H, 1985. Wall-rock alteration and tungsten and molybdenum mineralizations associated with older granites in western Bergslagen, Sweden. Econ. Geol., vol. 80, pp. 479-487.

Henderson, P., 1984. General geochemical properties and abundances of the rare earth elements. in Rare Earth Geochemistry., ed. P. Henderson, Elsevier Pub., Oxford, pp. 1-32.

Herrero, J.N., 1970. An intergrated exploration program for disseminated sulphides at Round Pond and Retreat Lake areas, Labrador. M.Sc. thesis, Queen's University, Kingston, Ontario. 85 p.

Hildreth, E.W., 1979. The Bishop Tuff: evidence of the origin of compositional zonation in silicic magma chambers. in Ash-flow Tuffs, eds. C.E. Chapin and W.E. Elston. Geol. Soc. of America, Spec. Paper 180, pp. 43-76.

Hildreth, E.W., 1981. Gradients in silicic magma chambers: implications for lithostatic magmatism. Jour. of Geophy. Research, vol. 86, pp. 10 153- 10 192.

Hobbs, B.E., Means, W.D., and Williams, P.F., 1976. An Outline of Structural Geology. John Wiley and Sons Inc., Toronto, 571 p.

Hoffman, P.F., and McGlynn, J.C., 1977. Great Bear Batholith: a volcano-plutonic depression. in Volcanic Regimes in Canada, eds. W.R.A. Barager, L.C. Coleman, and J.M. Hall. Geol. Assoc. of Canada Spec. Paper 16, pp. 169-192.

Hughes, C.J., 1973. Spilites, keratophyres, and the igneous spectrum. Geol. Magazine, vol. 109, pp. 513-527.

Hulen, J.B., Neilson, D.I., Goff, F., Gardner, J.N., and Charles, R.W., 1987.

Molybdenum mineralization in an active geothermal system Valles Caldera, New Mexico. Geology, vol. 15, pp. 748-752.

Imeokparia, E.G., 1985. Rare-metal mineralization in granitic rocks of the Tongolo Anorogenic Complex - northern Nigeria. Mineral. Deposita, vol. 20, pp. 81-88.

Isuk, E.E., and Carman, J.H., 1981. The system Na2SiO5 - K2SiO5 - MoS2 - H2O with implications for molybdenum transport in silicate melts. Econ. Geol., vol. 76, pp. 2222-2235.

Jakes, P., and White, A.J.R., 1971. Composition of island arcs and continental growth. Earth Planet. Sci. Let., vol. 12, pp. 224- 230.

Jakes, P., and White, A.J.R., 1972. Major and trace element abundance in volcanic rocks of orogenic areas. Geol. Soc. of America Bull., vol. 83, pp 29-40.

Jensen, L.S., 1977. A new cation plot for classifying subalkaline rocks. Ontario Division of Mines, Misc. Papre 66, 22 p.

Kerr, A., 1986. Plutonic rocks of the Eastern Central Mineral Belt, Labrador: general geology and description of regional granitoid units. Current Research, 1986, NDME Report 86-1, pp. 86-100.

Kerr, A., 1987. Plutonic rocks of the Eastern Central Mineral Belt: lithogeochemical patterns and identification of potential specialized granitoids. Current Research, 1987, NDME Report 87-1, pp. 161-181.

Kerr, A., 1988. Geochemical characteristics and mineral potential of specialized granitoid plutons in the Trans-Labrador Batholith, Eastern Labrador. in Current Research (1088) NDM, Mineral Development Division, Report 88-1, pp 15-36.

King, A.F., 1963. Geology of the Cape Makkovik peninsula, Aillik, Labrador. Unpub. M.Sc. thesis, Memorial University of NFLD, St. John's, Nfld. 411 p.

Kish, L. and Cuney, M., 1981. Uraninite-albite veins from the Mistamisk Valley of the Labrador Trough, Quebec. Minerological Mag. Vol. 44, pp 47-83.

Kontak, D.J., 1978. Preliminary report on four uranium showings in the Central Mineral Belt, Labrador. Report of Activities for 1977, NDME Report 78-1, pp. 27-43.

Kontak, D.J., 1979. Report on Rb/Sr and U/Pb dating in the Central Mineral Belt, Labrador. Unpub. NDME Report, Miner Development Division, 39 p.

Kontak, D.J., 1980. Geology, geochronology and uranium mineralization in the Central Mineral Belt of Labrador, Canada. Unpub. M.Sc. thesis, University of Alberta, Edmonton, Alberta. 378 p.

Kranck, E.H., 1939. Bedrock geology of the seaboard region of Newfoundland and Labrador. Geol. Sur. of NFLD, Bulletin 19, 44 p.

Kranck, E.H., 1953. Bedrock geology of the seaboard of Labrador between Domino Run and Hopedale, Newfoundland. Geol. Sur. of Canada, Bulletin 26, 41 p.

Lennon, I.G., 1963. A report on the geology of the Makkovik area, Labrador. Unpub. report Brinex Doc. G63008.

Leech, G.B., Lowdon, J.A., Stockwell, C.H., and Wanless, R.K., 1963. Age determinations and geological studies, K-Ar isotopic ages, Report 4. Geol. Sur. of Canada, Paper 63-17, pp. 114-117.

Leiber, O.M., 1860. Notes on the geology of the coast of Labrador. Report of the United States Coast Survey for 1860.

Loisselle, M.C., and Wones, D.R., 1979. Characteristics and origin of anorogenic granites. Geol. Soc. of America, Abs. with Prog., vol. 11, p. 468.

Lowdon, J.A., Stockwell, C.H., Tipper, H.W., and Wanless, R.K., 1962. Age determinations and geological studies (including isotopic ages - Report 3). Geol. Sur. of Canada, Paper 62- 17, pp. 115-116.

MacDougall, C.S., and Wilton, D.H.C., 1987a. Middle Proterozoic granite-related mineralization, in the Round Pond area, Labrador. Geol. Sur. of Canada, Current Research, Paper 87-1, pp. 457-466.

MacDougall, C.S., and Wilton, D.H.C., 1987b. A new sphalerite-galena showing with associated precious metals, in the Round Pond area, near Makkovik, Labrador. NDME Open File Report Lab, 13O/3 (110), p 9.

MacDougall, C.S., and Wilton, D.H.C., 1988. Geology of radioactive zones in the Round pond area, Labrador. in Current Research, Part C, Geol. Surv. of Canada Paper 88-1C, pp. 271-275.

MacKenzie, L.M., and Wilton, D.H.C., 1987. Uranium, molybdenum, and base metal mineralization: three different styles of ore formation in the Burnt Lake area, central Labrador. Geol. Sur. of Canada, Current Research, Paper 87-1, pp. 167-176.

Malpas, J., Foley, S.F., and King, A.F., 1986. Alkaline mafic and ultramafic lamprophyres from the Aillik Bay area, Labrador. Can. Jour. of Ear. Sci., vol. 23, pp. 1902-18.

Marten, B.E., 1977. The relationship between the Aillik Group and the Hopedale gneiss, Kaipokok Bay, Labrador. Unpub. Ph.D. thesis, Memorial University of Nfld., St. John's, Nfld., 389 p.

McBirney, A.R., 1970. Some current aspects of volcanology. Earth Sci. Rev., vol. 6, pp. 337-352.

McLennon, S.M., and Taylor, S.R., 1979. Rare earth element mobility associated with uranium mineralization. Nature, vol. 282, pp. 247-250.

McMillan, W.J., and Panteleyev, A., 1980. Ore deposits models - 1) Porphyry copper deposits. Geosci. Canada, vol. 7, pp. 52-63.

Meschede, M., 1986. A method of discrimination between different types of mid-ocean basalts and continental tholeiites with with the Nb-Zr-Y diagram. Chem. Geol. Vol. 56, pp 207-218.

Miller, C.F., and Mittlefehldt, D.W., 1982. Depletion of light rare earth elements in felsic magams. Geology, vol. 10, pp. 129-133.

Miller, C.F., and Mittlefehldt, D.W., 1984. Extreme fractionation in felsic magma chambers: a product of liquid-state diffusion or fractional crystallization? Earth Planet. Sci. Let., vol. 68, pp. 151-158.

Minatidis, D.G., 1976. A comparitive study of trace element geochemistry and mineralogy of some uranium deposits of Labrador, and evaluation of some uranium exploration techniques in a glacial terrain. Unpub. M.Sc. thesis, Memorial University of Nfld., St. John's, Nfld.

Moore, T.H., 1951. Igneous dike rocks of the Aillik-Makkovik area, Labrador. Unpub. M.Sc. thesis, McGill University, Montreal, 61 p.

Morse, S.A., 1961. Sodic rocks of the Falls Lake - Winter Lake area. Unpub. Brinex Report Sam-61-3, 11 p.

Muecke, G.K., and Clarke, D.B., 1981. Geochemical Evolution of the South Mountain Bathoilth, Nova Scotia: rare earth element evidence. Can. Mineral., vol. 19, pp. 133-145.

Mutschler, F.E., Wright, E.G., Ludington, S., and Abbott, J.T., 1981. Granite molybdenite systems. Econ. Geol., vol. 76, pp. 874-897.

Mysen, B.O., 1979. Trace element partitioning between garnet peridotite minerals and water-rich vapour: Experimental data from 5 to 30 kbars. American Mineralogist, vol. 64, pp. 274-287.

Newham, D.W., 1964. Report on prospecting in the Aillik-Makkovik area, Labrador. Unpub. Brinex Report G64013, Appendix iv, 36 p.

Newham, D.W., 1964. Geochemistry report, Aillik-Makkovik area, Labrador. Unpub. Brinex Report G64013, appendix ii, 24 p.

Ohlander, B., 1985. Geochemical characteristics of granites associated with Proterozoic molybdenite mineralization in northern Sweden. Chem. Geol., vol. 51, pp. 247-263.

Packard, A.S., 1891. The Labrador Coast. New York, N.D.C. Hodges (publisher), 513 p.

Payette, C., and Martin, R.F., 1986. The glass inclusions and mineralogy of rhyolites, Upper Aillik Group, Labrador. Unpub. Report, Geol. Sur. of Canada, Project 27 st23233-5-0058, 98 p.

Pearce, J.A., and Cann, J.R., 1973. Tectonic setting of basic volcanic rocks investigated using trace element analyses. Earth Planet. Sci. Let., vol. 19, pp. 290-300.

Pearce, J.A., Harris, N.B.W, and Tindle, A.G., 1984. Trace element discrimination diagrams for the tectonic interpretation of granitic rocks. Jour. of Pet., vol. 25, pp. 956-983.

Piloski, M.J., 1956. Geological report on the Aillik-Shoal Lake area. Unpub. Brinex Report G55015, 35 p.

Piloski, M.J., 1957. Geological report on Showings 16 and 17, Falls Lake area, Labrador. Unpub. Brinex Report G56016, Appendix 1, 9 p.

Piloski, M.J., 1960. Report on exploration in the Southwest Potash-Brinex joint venture area, Aillik Bay, Labrador. Unpub, Brinex Report, 23 p.

Pitcher, W.S., 1983. Granite: typology, geological environment, and melting relationships. in Migmatites, Melting, and Metamorphism, eds. M.P. Atherton and C.D. Gribble. Nantwich:Shiva Publications. pp. 277-87.

Ramsay, C., 1986. Specialized felsic plutonic rocks of the Arabian Shield and their precursors. Jour. of African Earth Sci., vol. 4, pp. 153-168.

Ramsay, J.G., 1967. Folding and fracturing of rocks. McGraw-Hill, New York, 568 p.

Rice, C.M., Harmon, R.S., and Shepherd, T.J., 1985. Central City, Colorado: the upper part of an alkaline porphyry molybdenum system. Econ. Geol., vol. 80, pp. 1769-1796.

Riley, G.S., 1951. The bedrock of Makkovik and its relations to the Aillik and Kaipokok Series. Unpub. M.Sc. thesis, McGill University, Montreal, 59 p.

Romberger, S.B., 1984. Transport and deposition of uranium at temperatures up to 300 C: geological implications. in Uranium Geochemisty, Mineralogy, Geology, Exploration, and Resources., eds. B. DeVivo, F. Ippolito, G. Capaldi, and P.R. Simpson. Inst. of Min. and Metall., pp. 12-17.

Rosen, P.S., 1980. Coastal environments of the Makkovik region, Labrador. In The Coastline of Canada., Ed. S.B. McCann. Geol. Sur. of Canada, Paper 80-10, pp. 267-280.

Rub, M.G., 1972. The role of the gaseous phase during the formation of ore-bearing magmatic complexes. Chem. Geol., pp. 89-98.

Ryan, A.B., 1977. Molybdenite: some background information and a review of mineralization on the Aillik Peninsula, Labrador. Unpub. Report, NDME. 14 p.

Ryan, A.B., 1984. Regional geology of the Central part of the Central Mineral Belt, Labrador. NDME Memoir 3, 185 p.

Ryan, A.B., Baragar, W.R.A., and Kontak, D.J., 1986. Geochemistry, tectonic setting, and mineralization of high-potassium Middle Proterozoic rocks in central Labrador, Canada. (in press), IGCP 217 Symposium Vol. 15p.

Sampson, G.J., 1966. The geology of the Round Pond-Cross Lake area, Labrador. Unpub. thesis, Imperial College of London, 65 p.

Scharer, U., Wardle, R.J., Ryan, A.B., and Gandhi, S.S., (in prep.). Uranium and lead ages of Lower to Middle Proterozoic volcanism in the Makkovik Province, Labrador.

Sillitoe, R.H., and Bonham (Jr.), H.F., 1984. Volcanic landforms and ore deposits. Econ. Geol., vol. 79, pp. 1286-1298.

Simmons, E.C., and Hedge, C.E., 1978. Minor-element and Sr-isotope geochemistry of Tertiary stocks, Colorado Mineral Belt. Cont. to Mineralogy and Petrology, vol. 67, pp. 379-396.

Smellie, J.A.T. and Laurikko, J., 1984. Skuppesavon, northern Sweden: A uranium mineralization associated with alkali metasomatism. Mineral. Deposita, vol. 19, pp. 183-192.

Soregaroa, A.E. 1975. The geology of molybdenum and copper deposits of Canada. Geol. Surv. of Canada Paper 75-1, pp. 243-244.

Steinhauer, H., 1814. Notes on the geology of the Labrador coast. Transactions of the Geological Society, II, pp. 486-491.

Stemprok, M., 1980. Differentiation of some elements by ore-bearing granites. in Metallization Associated with Acid Magmatism, vol. 3, pp. 393-403.

Stevenson, I.M., 1970. Rigolet and Groswater Bay map areas, Newfoundland (Labrador). Geol. Sur. of Canada, Paper 69-48, 21 p.

Stockwell, C.H., 1973. Revised Precambrian time-scale for the Canadian Shield. Geol. Sur. of Canada, Paper 75-52, 4 p.

Stoeterau, W.W., 1970. Geology of the Round Pond east area, Makkovik, Labrador. Unpub. B.Sc. thesis, Memorial University of Nfld., St. John's, Nfld.

Streckeisen, A., 1976. To each plutonic rock its proper name. Earth Sci. Rev., vol. 12, pp. 1-33.

Strong, D.F., 1980. Granitoid rocks and associated mineral deposits of eastern Canada and western Europe. in The Continental Crust and Its Mineral Deposits, ed. D. Strangway, Geol. Assoc. of Canada Spec. Paper 22, pp. 741-769.

Strong, D.F., 1981. Ore deposit models - 5: A model for granophile mineral deposits. Geoscience Canada, vol. 8, pp. 155-161.

Strong, D.F., Fryer, B.J., and Kerrich, R., 1984. Genesis of the St. Lawrence fluorspar deposit as indicated by fluid inclusion, rare earth element, and

isotopic data. Econ. Geol., vol. 79, pp. 1142-1158.

Sutton, J.S., Marten, B.E., and Clark, A.M.S., 1971. Structural history of the Kaipokok Bay area, Labrador, Newfoundland. Proc. of the Geol. Assoc. of Canada, vol. 24, pp. 103-106.

Sutton, W.R., 1964. Report on exploration in the Aillik-Makkovik area, Labrador. Unpub. Brinex Report G64013, 11 p., plus drill core logs.

Taylor, F.C., 1971. A revision of Precambrian structural provinces in northeastern Quebec and northern Labrador. Canadian Jour. of Earth Sciences, Vol. 8, pp. 579-584.

Taylor, F.C., 1972. Reconnaissance geology of a part of the Precambrian Shield, northeastern Quebec and northern Labrador. Part III, Geol. Sur. of Canada, Paper 71-48.

Taylor, F.C., 1975. Geology - Makkovik area, Labrador. Geol. Sur. of Canada, Map 1444A.

Taylor, R.P., Strong, D.F., and Fryer, B.J., 1981. Volatile control of contrasting trace element distributions in peralkaline granitic and volcanic rocks. Cont. to Mineral. and Pet., vol. 77, pp. 267-271.

Taylor, R.P., and Fryer, B.J., 1982. Rare earth element geochemistry as an aid to interpreting hydrothermal ore deposits. Metallization associated with acid magmatism, vol. 6

Taylor, R.P., and Fryer, B.J., 1983. Rare earth element lithogeochemistry of granitoid mineral deposits. Can. Min. Metall. Bull., vol. 76, No. 850, pp. 74-84.

Tayyar, J.A., Jackson, N.J., and Yazidi, S.A., 1986. Geology and mineralization of the Jabalat alkali-feldspar granite, northern Asir region, Kingdom of Saudi Arabia. Jour. of African Earth Sci., vol. 4, pp. 183-188.

Tingle, T.N., and Fenn, P.M., 1984. Transport and concentration of molybdenum in granite molybdenite systems: effects of fluorine and sulphur. Geology, vol. 12, pp. 156-158.

Tischendorf, G. 1977. Geochemical and petrographic characteristics of silicic magmatic rocks associated with rare-element mineralization. in Mineralization Associated with Acid Magmatism, vol. 2, pp. 41-96.

Tuach, J., Davenport, P.H., Dickson, W.L., and Strong, D.F., 1986. Geochemical trends in the Ackley Granite, southeast Newfoundland; their relevance to magmatic-metallogenic processes in high-silica granitoid systems. Can. Jour. of Earth Sciences, vol. 23, pp. 747-765.

Turekian, K.K., and Wedepohl, K.H., 1961. Distribution of the elements in the earth's crust. Geol. Soc. of America Bull., vol. 72, pp. 175-192.

Wanless, R.K., Stevens, R.D., Lachance, G.R., and Delabio, R.N., 1970. Age

determinations and geological studies, K-Ar isotopic ages, Report 9. Geol. Sur. of Canada, Paper 69-2A, pp. 73-74.

Wanless, R.K., Stevens, R.D., Lachance, G.R., and Delabio, R.N., 1972. Age determinations and geological studies, K-Ar isotopic ages, Report 10. Geol. Sur. of Canada, Paper 71-2, PP. 86-89.

Wanless, R.K., Stevens, R.D., Lachance, G.R., and Delabio, R.N., 1973. Age determinations and geological studies, K-Ar isotopic ages, Report 11. Geol. Sur. of Canada, Paper 73-2, pp. 90-104.

Wanless, R.K., Stevens, R.D., Lachance, G.R., and Delabio, R.N., 1974. Age determinations and geological studies, K-Ar isotopic ages, Report 12. Geol. Sur. of Canada, Paper 74-2, pp. 55-60.

Wanless, R.K., Stevens, R.D., Lachance, G.R., and Delabio, R.N., 1979. Age determinations and geological studies, K-Ar isotopic ages, Report 14. Geol. Sur. of Canada, Paper 79-2, pp. 59-61.

Wardle, R.J., and Bailey, D.G., 1981. Early Proterozoic sequences in Labrador. in Proterozoic Basins of Canada. Geol. Surv. of Canada, Paper 81-10, pp. 73-74.

Wardle, R.J., and Wilton, D.H.C., 1985. Reconnaissance sampling for precious metals in the Kaipokok Bay-Big River area, Labrador. NDME Open File Report, Lab 1679, 17 p.

Wardle, R.J., Rivers, T., Gower, C.F., Nunn, G.A.G., and Thomas, A., 1986. The northeastern Grenville Province: new insights. in The Grenville Province. Geol. Assoc. of Canada Spec. Paper 33, pp. 13-29.

Wendlandt, R.F., and Harrison, W.J., 1979. Rare earth partitioning between immiscible carbonate and silicate liquids and $CO_2$ vapour: Results and implications for the formation of light rare earth-enriched rocks. Cont. to Mineral. and Petrology, vol. 69, pp. 409-419.

Westra, G., and Keith, S.B., 1981. Classification and genesis of stockwork molybdenum deposits. Econ. Geol., vol. 76, pp. 844-873.

Whalen, J.B., 1986. A-type granites in New Brunswick. in Current Research, Part A, Geol. Sur. of Canada Paper 86-1A, pp. 297-300.

White, A.J.R., and Chappell, B.W., 1983. Granitoid types and their distribution in the Lachlan fold belt, southeastern Australia. in Circum-Pacific Pluton Terranes, ed. J.A.Roddick. Geol. Soc. of America Mem. 159, pp. 21-34.

White, M.V.W., 1976. A petrologicalstudy of acid volcanic rocks of the Aillik Series, Labrador. Unpub. M.Sc. thesis, McGill University, Montreal, 92 p.

White, M.V.W., and Marten, R.F., 1980. The metasomatic changes that accompany uranium mineralization in the nonorogenic rhyolites of the Upper Aillik Group, Labrador. Canadian Mineralogist, vol. 18, pp. 459-479.

White, W.H., Bookstrom, A.A., Kamilli, R.I., Ganster, M.W., Smith, R.P., Ranta, D.E., and Steinner, R.C., 1981. Character and origin of Climax-type molybdenum deposits. Econ. Geol., 75th Anniversary Vol., pp. 270-316.

Williams, H., and McBirney, A.R., 1979. Volcanology. San Fransico, W.H. Freeman and Co., 379 p.

Wilson, M.R., and Akerblom, G.V., 1982. Geological setting and geochemistry of uranium rich granites in the Proterozoic of Sweden. Mineral. Mag., vol. 46, pp. 233-245.

Wilton, D.H.C., MacDougall, C.S., and MacKenzie, L.M., 1986. Final report on the 1985 field work in the Central Mineral Belt, Labrador, for ERDA Agreement II-2, Metallogeny of the Central Mineral Belt. Unpub. Report to Geol. Sur. of Canada, 149 p.

Wilton, D.H.C., MacDougall, C.S., MacKenzie, L.M., and North, J., 1987a. Final report on the 1986 field work in the Central Mineral Belt, Labrador, for ERDA Agreement II-2, Metallogeny of the Central Mineral Belt. Unpub. Report to Geol Sur. of Canada, 121p.

Wilton, D.H.C., MacDougall, C.S., MacKenzie, L.M., and North, J., 1987b. Precious metal contents in samples from the eastern Central Mineral Belt, Labrador. NDME Open File Report Lab 724, 39 p.

Wilton, D.H.C., and Wardle, R.J., 1987. Two contrasting metallogenic styles in the Early Proterozoic Upper Aillik Group, Central Mineral Belt, Labrador, Canada. Vol. 22, pp 198-206.

Winchester, J.A., and Floyd, P.A., 1977. Geochemical discrimination of different magma series and their differentiation products using immobile elements. Chem. Geol., vol. 20, pp. 325-343.

Zielinski, R.A., 1979. Uranium mobility during interaction of rhyolitic obsidian, perlite and felsite with alkaline carbonate solutions. $T=120$ C, $P=210$ Kg/cm$^2$. Chem. Geol. Vol. 14.

# Appendix I

## Geochemical Methods

### I.1 Sample Preparation

Samples were 1-2 kg bulk chip or grab samples collected at unmineralized lithologic, or mineralized outcrop sites within the study area. Samples were collected so as to represent dominant lithologies ( ie. map units), or various features of the mineralization .

Samples were broken into coarse (1-2 inch) chips by crushing with a hammer on a steel plate. Fragments with visible steel chips were rejected. The chips were then run through a steel jaw crusher, followed by a tungsten-carbide bowl and puck assembly, producing a -100 mesh whole-rock powder. An internal standard of silica sand was crushed using the same procedure.

### I.2 Major Element Analyses

Major element oxides (except those described below) were determined by atomic absorption spectrometry. Sample preparation followed the methods of Langmhyr and Paus (1968). Table 1 lists precision of the method. Analyses were carried out on a Perkin-Elmer Model 370 atomic absorption spectrometer with digital readout. Occassionally aqua-regia dissolution was required for sulphide-rich samples. Major element analyses were not completed on all samples, and such a case is indicated by blanks in the major element column, or by its ommission. Fe is reported as total $Fe_2O_3$. Loss on ignition (LOI), which reflects volatile content of the sample, was determined by weighing (accurately to $10^{-4}$ gms) an amount of sample into a porcelain crucible, heating the crucible to 1050° C for at least two hours, cooling in a desicator, and then weighing the de-volatized sample to determine the percent loss of volatiles.

P205 was determined colourimetrically with a Baush and Lomb Spectronic 20 Colourimeter, based on a modification of the method outlined by Shapiro and Brannock (1962).

**Table 1:** Precision of major element analyses based on four analyses of standard G-2. (Published value from Flanagan (1970)).

|  | Published |  |  | Range |  |
| --- | --- | --- | --- | --- | --- |
| Element | Value | Mean | S.D. | Low | High |
| SiO2 | 69.11 | 69.70 | 0.57 | 68.2 | 69.96 |
| Al2O3 | 15.40 | 15.10 | 0.24 | 14.75 | 15.60 |
| Fe2O3 | 2.65 | 2.60 | 0.02 | 2.61 | 2.74 |
| MgO | 0.76 | 0.80 | 0.005 | 0.75 | 0.82 |
| CaO | 1.94 | 2.00 | 0.10 | 1.92 | 2.14 |
| Na2O | 4.07 | 4.30 | 0.02 | 4.07 | 4.21 |
| K2O | 4.51 | 4.56 | 0.02 | 4.50 | 4.57 |
| TiO2 | 0.50 | 0.50 | 0.01 | 0.47 | 0.51 |
| MnO | 0.03 | 0.03 | 0.00 | - | - |

### 1.3 Trace Element Analyses

The trace elements were determined by X-Ray Fluorescence techniques on pressed, whole rock powder pellets using a Phillips 1450 automatic X-Ray fluorescence spectrometer with a rhodium tube. The pellets were made from a homogenized powder containing 10, g sample and 1-1.5 gm binding material (Union Carbide Phenolic Resin TR-16933). The powder was pressed at 30 tons psi for a minute, and then baked for ten minutes at 200° C. Data reduction was done with a Hewlett-Packard 9845B mini-computer.

Precision and accuracy for the trace element analyses are given in Table 2 using the standards as listed.

Table 2: Precision and Accuracy of trace element analyses (from Longerich and Veinott, 1986).

| Standard<br>G-2 | Determined | Accepted | %RSD | N |
|---|---|---|---|---|
| TiO2 | 0.49 | 0.48 | 1 | 10 |
| V | 36 | 36 | 10.9 | 10 |
| Cr | 10 | 8 | 28.3 | 10 |
| Ni | 8 | 4 | 17.9 | 10 |
| Cu | 25 | 10 | 4.1 | 10 |
| Zn | 88 | 84 | 2.6 | 10 |
| Ga | 23 | 23 | 6.8 | 10 |
| Rb | 171 | 170 | 0.6 | 10 |
| Sr | 459 | 480 | 1.4 | 10 |
| Y | 15 | 11 | 12.4 | 10 |
| Zr | 304 | 300 | 1.0 | 10 |
| Nb | 13 | 13 | 9.3 | 10 |
| Ba | 1864 | 1900 | 1.7 | 10 |
| La | 130 | 92 | 3.7 | 10 |
| Ce | 155 | 160 | 23.7 | 10 |
| Pb | 35 | 30 | 15.4 | 10 |
| Th | 20 | 25 | 34.8 | 10 |
| U | 0 | 2 | 300.0 | 10 |

Analyses for Mo and Ag were performed by Chemex Labs Ltd. of Vancouver, using a semi-quantitative, multi-element ICP analyses. The analytical technique involves digestion of 0.5 gm of material in nitric acid - aqua regia followed by ICP analysis. Since digestion is incomplete for many minerals, values reported for Al, Sb, Ba, Be, Ca, Cr, Ga, La, Mg, K, Na, Sr, Tl, Ti, W, and V can only be considered as semiquantitative. In the case of elements which have been duplicated by both XRF and ICP analysis, the XRF values are used. ICP detection limits are listed in Table A-3.

**Table 3:** ICP trace element analysis detection limits
(from Chemex Ltd).

| | | | | | |
|-----|----------|-----|---------|-----|-------|
| Ag | 0.2 ppm | Cu | 1 ppm | K | 0.01% |
| Al | 0.01% | Fe | 0.01% | Sb | 5 ppm |
| As | 5 ppm | Ga | 10 ppm | Sr | 1 ppm |
| Ba | 1 ppm | La | 10 ppm | Tl | 10 ppm |
| Be | 0.5 ppm | Pb | 2 ppm | Ti | 0.01% |
| Bi | 2 ppm | Mg | 0.01% | W | 10 ppm |
| Cd | 0.5 ppm | Mn | 1 ppm | U | 10 pmm |
| Ca | 0.01% | Mo | 1 ppm | V | 1 ppm |
| Cr | 1 ppm | Ni | 1 ppm | Zn | 10 ppm |
| Co | 1 ppm | P | 10 ppm | | |

Analysis for Au were also performed by Chemex Labs Ltd. using fire assay preconcentration of 10 gm of samples followed by atomic absorption spectrometry. Detection limit for gold is quoted as 5 ppb.

1.4 Rare Earth Element Analyses

The rare earth element analyses were carried out using thin film X-Ray fluoresence techniques as outlined by Fryer (1977). A 1-2 gram sample size was dissolved by HF, and the resultant solution put through columns containing ion exchange resin. Calibrated elutions of 2N HCL concentrated the REE's into a final solution. $H_2SO_4$ was added to remove Ba, and the solution was dried on ion filter paper. The paper was then analysed by X-Ray Fluorescence spectrometry (see above).

The data are assumed to be accurate to $\pm$ 5-10%, or $\pm$ 0.1 ppm, whichever is greater.

Selected samples were re-analyzed by neutron activation techniques carried out by Chemex Labs of Vancouver. Detection limits are given as follows: Yb 1 ppm, Eu 1 ppm, Sm 0.1 ppm, Nd 5 ppm, Ce 2 ppm, La 1 ppm. Results indicate lower overall concentrations, but similar chondrite normalized profiles when compared to XRF produced data. Table 4 compares XRF versus Neutron activation derived data.

**Table 4:** Comparison between XRF and neutron activation derived rare earth element data.

### Monkey Hill Granite

| No. | CM-121 | | CM-122 | | CM-171 | | CM-181 | |
| ppm | XRF | NAA | XRF | NAA | XRF | NAA | XRF | NAA |
|-----|-----|-----|-----|-----|-----|-----|-----|-----|
| Yb | 1.6 | 2.1 | 2.4 | 3.2 | 2.1 | 3.4 | 0.9 | 1.8 |
| Eu | 0.0 | <0.5 | 0.2 | 0.6 | 0.6 | 0.5 | 0.0 | <0.5 |
| Sm | 0.0 | 0.9 | 4.0 | 3.4 | 6.4 | 3.5 | 1.2 | 1.1 |
| Nd | 6.5 | <5 | 37.3 | 22.0 | 39.4 | 23.0 | 9.6 | 6.0 |
| Ce | 22.0 | 12.0 | 98.8 | 55.0 | 99.4 | 56.0 | 32.9 | 22.0 |
| La | 8.2 | 4.0 | 48.6 | 32.0 | 50.1 | 31 | 18.7 | 13.0 |

## Upper Aillik Group

### Major Elements (wt.%)

| Unit: | 1 | 1 | 1 | 2 | 2 | 2 | 2 |
|-------|------|-------|-------|-------|-------|-------|-------|
| No. | CM-11 | CM-170 | CM-131 | CM-115 | CM-174 | CM-114 | CM-178 |
| $SiO_2$ | 77.20 | 73.30 | 75.40 | 60.80 | 59.90 | 69.10 | 65.90 |
| $TiO_2$ | 0.20 | 0.32 | 0.36 | 0.28 | 0.60 | 0.56 | 0.36 |
| $Al_2O_3$ | 11.90 | 11.90 | 11.70 | 18.50 | 18.90 | 18.70 | 13.20 |
| $Fe_2O_3$ | 2.36 | 4.45 | 4.69 | 2.36 | 4.98 | 4.88 | 3.80 |
| $MnO$ | 0.10 | 0.09 | 0.11 | 0.21 | 0.06 | 0.15 | 0.20 |
| $MgO$ | 0.12 | 0.13 | 0.02 | 1.23 | 1.43 | 0.24 | 2.18 |
| $CaO$ | 0.56 | 0.68 | 0.84 | 2.62 | 1.78 | 1.18 | 4.38 |
| $Na_2O$ | 7.28 | 6.80 | 6.88 | 7.88 | 7.84 | 3.36 | 5.88 |
| $K_2O$ | 0.24 | 0.15 | 0.21 | 4.38 | 4.35 | 6.49 | 3.37 |
| $P_2O_5$ | 0.00 | 0.00 | 0.01 | 0.08 | 0.14 | 0.04 | 0.11 |
| LOI | 0.14 | 0.22 | 0.15 | 2.31 | 0.41 | 0.45 | 0.21 |
| Total | 100.10 | 98.04 | 100.37 | 100.65 | 100.39 | 99.65 | 100.58 |

### Trace Elements (ppm)

| | | | | | | | |
|-----|-----|-----|-----|------|------|------|------|
| Pb | 16 | 18 | 17 | 35 | 20 | 21 | 21 |
| U | 0 | 0 | 3 | 0 | 1 | 3 | 0 |
| Th | 13 | 16 | 16 | 5 | 13 | 2 | 37 |
| Rb | 0 | 0 | 3 | 81 | 172 | 163 | 166 |
| Sr | 28 | 45 | 57 | 239 | 480 | 105 | 167 |
| Y | 41 | 75 | 76 | 15 | 20 | 18 | 73 |
| Zr | 239 | 359 | 420 | 41 | 125 | 468 | 197 |
| Nb | 18 | 24 | 24 | 3 | 7 | 21 | 16 |
| Ga | 22 | 27 | 24 | 18 | 23 | 20 | 16 |
| Zn | 168 | 30 | 164 | 78 | 66 | 58 | 266 |
| Cu | 6 | 4 | 5 | 8 | 6 | 13 | 5 |
| Ni | 0 | 0 | 0 | 0 | 0 | 0 | 17 |
| La | 26 | 79 | 112 | 0 | 13 | 7 | 107 |
| Ti | .12 | .27 | .26 | .26 | .58 | .45 | .35 |
| Ba | 216 | 101 | 39 | 1818 | 2241 | 2624 | 601 |
| V | 0 | 0 | 0 | 52 | 169 | 0 | 29 |
| Ce | 76 | 137 | 197 | 0 | 79 | 70 | 148 |
| Cr | 0 | 0 | 0 | 6 | 28 | 0 | 26 |

## Major Elements ((wt.%)

| Unit: | 3 | 3 | 3 | 3 | 3 | 4 | 4 |
|---|---|---|---|---|---|---|---|
| No. | CM-13 | CM-50 | CM-119 | CM-127 | CM-138 | CM-2 | CM-48 |
| SiO2 | 71.70 | 71.60 | 73.90 | 77.30 | 66.70 | 47.20 | .49.20 |
| TiO2 | 0.44 | 0.36 | 0.48 | 0.36 | 0.48 | 0.80 | 0.80 |
| Al2O3 | 12.10 | 11.80 | 11.20 | 11.70 | 14.60 | 18.50 | 16.50 |
| Fe2O3 | 3.74 | 3.09 | 3.38 | 2.16 | 4.94 | 11.95 | 11.33 |
| MnO | 0.12 | 0.24 | 0.15 | 0.03 | 0.10 | 0.17 | 0.16 |
| MgO | 1.06 | 1.53 | 0.80 | 0.60 | 2.46 | 5.80 | 8.04 |
| CaO | 3.46 | 3.28 | 3.00 | 0.68 | 3.00 | 6.26 | 9.64 |
| Na2O | 6.71 | 7.16 | 4.39 | 6.98 | 6.74 | 5.91 | 3.96 |
| K2O | 0.96 | 0.32 | 3.18 | 0.34 | 0.95 | 1.66 | 0.34 |
| P2O5 | 0.00 | 0.00 | 0.00 | 0.00 | 0.00 | 0.00 | 0.00 |
| LOI | 0.57 | 0.30 | 0.31 | 0.38 | 0.49 | 0.66 | 0.61 |
| Total | 100.86 | 99.68 | 100.79 | 100.45 | 100.46 | 98.91 | 100.88 |

## Trace Elements (ppm)

| | | | | | | | |
|---|---|---|---|---|---|---|---|
| Pb | 22 | 34 | 20 | 32 | 31 | 88 | 29 |
| U | 0 | 5 | 0 | 0 | 1 | 0 | 0 |
| Th | 20 | 29 | 21 | 23 | 16 | 0 | 3 |
| Rb | 30 | 11 | 77 | 23 | 34 | 93 | 8 |
| Sr | 89 | 65 | 78 | 27 | 291 | 530 | 446 |
| Y | 52 | 33 | 21 | 30 | 44 | 20 | 24 |
| Zr | 266 | 192 | 202 | 247 | 294 | 46 | 43 |
| Nb | 27 | 14 | 16 | 16 | 24 | 5 | 5 |
| Ga | 20 | 17 | 18 | 18 | 27 | 20 | 17 |
| Zn | 90 | 551 | 38 | 37 | 189 | 277 | 123 |
| Cu | 2 | 4 | 4 | 5 | 1 | 2 | 0 |
| Ni | 0 | 0 | 0 | 0 | 0 | 66 | 57 |
| La | 43 | 13 | 0 | 51 | 30 | 0 | 0 |
| Ti | .56 | .33 | .41 | .25 | .61 | .74 | .77 |
| Ba | 192 | 873 | 390 | 26 | 323 | 514 | 131 |
| V | 21 | 16 | 39 | 19 | 50 | 204 | 192 |
| Ce | 5 | 56 | 17 | 84 | 73 | 10 | 36 |
| Cr | 0 | 0 | 0 | 12 | 15 | 44 | 41 |

## Major Elements (wt.%)

| Unit: | 4 | 4 | 4 | 4 | 4 | 4 | 4 |
|---|---|---|---|---|---|---|---|
| No. | CM-57 | CM-71 | CM-112 | CM-142 | CM-163 | CM-166 | CM-105 |
| SiO2 | 48.00 | 46.20 | 47.70 | 48.80 | 50.30 | 49.60 | 48.30 |
| TiO2 | 0.84 | 1.00 | 0.88 | 0.72 | 0.76 | 0.72 | 2.52 |
| Al2O3 | 16.80 | 16.00 | 17.10 | 17.70 | 16.60 | 17.10 | 13.70 |
| Fe2O3 | 10.08 | 13.08 | 10.94 | 10.85 | 11.95 | 9.94 | 17.04 |
| MnO | 0.22 | 0.19 | 0.19 | 0.20 | 0.16 | 0.19 | 0.26 |
| MgO | 7.91 | 8.00 | 8.99 | 8.47 | 7.32 | 7.84 | 3.93 |
| CaO | 8.40 | 8.88 | 6.08 | 7.94 | 5.88 | 9.30 | 6.74 |
| Na2O | 4.48 | 2.95 | 4.41 | 4.22 | 4.56 | 4.93 | 5.30 |
| K2O | 2.57 | 1.05 | 1.63 | 1.16 | 1.86 | 0.54 | 1.06 |
| P2O5 | 0.00 | 0.00 | 0.00 | 0.00 | 0.00 | 0.00 | 0.30 |
| LOI | 0.91 | 2.07 | 1.67 | 0.70 | 1.45 | 0.64 | 0.19 |
| Total | 100.21 | 99.42 | 99.59 | 100.76 | 100.74 | 100.80 | 99.34 |

## Trace Elements (ppm)

| | | | | | | | |
|---|---|---|---|---|---|---|---|
| Pb | 89 | 10 | 7 | 40 | 49 | 30 | 31 |
| U | 0 | 0 | 0 | 0 | 0 | 0 | 10 |
| Th | 2 | 0 | 0 | 6 | 2 | 0 | 8 |
| Rb | 159 | 76 | 80 | 60 | 88 | 8 | 46 |
| Sr | 375 | 404 | 567 | 542 | 431 | 524 | 532 |
| Y | 22 | 22 | 28 | 25 | 26 | 22 | 61 |
| Zr | 49 | 44 | 43 | 42 | 65 | 54 | 221 |
| Nb | 6 | 4 | 5 | 4 | 5 | 5 | 16 |
| Ga | 19 | 19 | 20 | 14 | 20 | 17 | 20 |
| Zn | 629 | 142 | 232 | 331 | 206 | 151 | 436 |
| Cu | 38 | 36 | 1 | 0 | 8 | 0 | 0 |
| Ni | 37 | 71 | 65 | 64 | 43 | 53 | 0 |
| La | 0 | 0 | 0 | 0 | 0 | 0 | 22 |
| Ti | .69 | 1.04 | .87 | .78 | 1.03 | .74 | 2.39 |
| Ba | 639 | 311 | 666 | 514 | 2563 | 143 | 1432 |
| V | 193 | 247 | 203 | 182 | 210 | 184 | 167 |
| Ce | 80 | 0 | 0 | -0 | 23 | 81 | 95 |
| Cr | 46 | 42 | 48 | 43 | 27 | 40 | 0 |

## Major Elements (wt.%)

| Unit: | 5 | 5 | 5 | 5 | 5 | 5 | 5 |
|-------|---|---|---|---|---|---|---|
| No. | CM-16 | CM-83 | CM-102 | CM-40 | CM-46 | CM-47 | CM-80 |
| SiO2 | 72.00 | 75.50 | 71.40 | 76.60 | 74.00 | 76.10 | 75.80 |
| TiO2 | 0.44 | 0.08 | 0.32 | 0.12 | 0.20 | 0.16 | 0.16 |
| Al2O3 | 12.70 | 11.10 | 13.40 | 12.00 | 12.30 | 11.90 | 11.60 |
| Fe2O3 | 2.27 | 2.69 | 3.44 | 2.87 | 2.28 | 3.06 | 3.09 |
| MnO | 0.14 | 0.01 | 0.01 | 0.03 | 0.14 | 0.06 | 0.30 |
| MgO | 0.95 | 0.08 | 0.05 | 0.12 | 1.12 | 0.36 | 0.38 |
| CaO | 0.86 | 0.18 | 0.56 | 0.12 | 1.92 | 0.22 | 0.90 |
| Na2O | 3.15 | 3.31 | 4.88 | 6.03 | 5.88 | 6.26 | 6.26 |
| K2O | 6.48 | 5.12 | 4.54 | 1.49 | 2.20 | 1.17 | 0.27 |
| P2O5 | 0.12 | 0.00 | 0.03 | 0.05 | 0.00 | 0.02 | 0.01 |
| LOI | 0.86 | 0.31 | 0.47 | 0.18 | 0.24 | 0.18 | 0.36 |
| Total | 99.97 | 98.38 | 99.10 | 99.56 | 100.30 | 99.48 | 99.13 |

## Trace Elements (ppm)

| | | | | | | | |
|-----|-----|-----|-----|-----|-----|-----|-----|
| Pb | 34 | 28 | 14 | 27 | 20 | 25 | 28 |
| U | 16 | 0 | 0 | 12 | 0 | 0 | 0 |
| Th | 26 | 13 | 7 | 24 | 12 | 22 | 12 |
| Rb | 188 | 115 | 100 | 32 | 50 | 36 | 5 |
| Sr | 104 | 17 | 56 | 28 | 60 | 45 | 62 |
| Y | 36 | 54 | 29 | 92 | 72 | 74 | 34 |
| Zr | 231 | 418 | 578 | 555 | 484 | 555 | 279 |
| Nb | 20 | 22 | 31 | 25 | 23 | 28 | 18 |
| Ga | 16 | 26 | 20 | 28 | 26 | 33 | 20 |
| Zn | 34 | 4 | 0 | 0 | 16 | 34 | 44 |
| Cu | 18 | 5 | 4 | 4 | 5 | 9 | 6 |
| Ni | 0 | 0 | 0 | 0 | 0 | 0 | 0 |
| La | 0 | 60 | 38 | 44 | 61 | 105 | 19 |
| Ti | .43 | .10 | .32 | .17 | .18 | .18 | .19 |
| Ba | 2695 | 67 | 1671 | 37 | 360 | 327 | 0 |
| V | 60 | 0 | 12 | 0 | 14 | 0 | 5 |
| Ce | 197 | 111 | 0 | 41 | 53 | 45 | 50 |
| Cr | 7 | 0 | 0 | 0 | 0 | 0 | 0 |

## Major Elements (wt.%)

| Unit: | 5 | 5 | 6 | 6 | 6 | 6 | 6 |
|---|---|---|---|---|---|---|---|
| No. | CM-91 | CM-179 | CM-31 | CM-33 | CM-35 | CM-36 | CM-37 |
| SiO2 | 75.20 | 69.10 | 77.70 | 70.20 | 72.00 | 70.30 | 74.40 |
| TiO2 | 0.16 | 0.48 | 0.12 | 0.52 | 0.32 | 0.40 | 0.34 |
| Al2O3 | 11.50 | 13.70 | 11.50 | 13.00 | 12.20 | 12.80 | 11.90 |
| Fe2O3 | 1.61 | 5.89 | 1.04 | 5.59 | 5.74 | 5.75 | 2.59 |
| MnO | 0.09 | 0.15 | 0.00 | 0.04 | 0.02 | 0.07 | 0.04 |
| MgO | 0.46 | 0.14 | 0.01 | 0.03 | 0.05 | 0.29 | 0.19 |
| CaO | 1.76 | 2.22 | 0.12 | 0.66 | 0.24 | 0.36 | 0.80 |
| Na2O | 6.68 | 7.40 | 2.64 | 4.07 | 4.94 | 3.95 | 3.99 |
| K2O | 0.20 | 0.24 | 6.38 | 5.71 | 3.34 | 5.61 | 4.59 |
| P2O5 | 0.00 | 0.09 | 0.00 | 0.05 | 0.04 | 0.07 | 0.03 |
| LOI | 1.53 | 0.44 | 0.21 | 0.35 | 0.32 | 0.26 | 0.53 |
| Total | 99.19 | 99.85 | 99.52 | 100.22 | 99.21 | 99.86 | 99.40 |

## Trace Elements (ppm)

| | | | | | | | |
|---|---|---|---|---|---|---|---|
| Pb | 32 | 28 | 47 | 42 | 74 | 49 | 33 |
| U | 18 | 4 | 2 | 0 | 1 | 3 | 9 |
| Th | 4 | 23 | 12 | 2 | 21 | 9 | 26 |
| Rb | 15 | 3 | 152 | 169 | 92 | 155 | 128 |
| Sr | 138 | 160 | 25 | 38 | 72 | 37 | 30 |
| Y | 41 | 77 | 65 | 56 | 43 | 84 | 91 |
| Zr | 123 | 523 | 448 | 468 | 497 | 570 | 701 |
| Nb | 15 | 22 | 26 | 24 | 23 | 20 | 20 |
| Ga | 19 | 27 | 23 | 24 | 26 | 24 | 22 |
| Zn | 191 | 24 | 156 | 67 | 125 | 133 | 88 |
| Cu | 4 | 5 | 2 | 4 | 2 | 4 | 4 |
| Ni | 0 | 0 | 0 | 0 | 0 | 0 | 0 |
| La | 34 | 77 | 58 | 50 | 64 | 63 | 100 |
| Ti | .10 | .48 | .13 | .59 | .38 | .50 | .29 |
| Ba | 0 | 48 | 153 | 981 | 435 | 552 | 406 |
| V | 0 | 0 | 0 | 1 | 0 | 0 | 1 |
| Ce | 41 | 154 | 0 | 0 | 19 | 60 | 78 |
| Cr | 2 | 0 | 0 | 0 | 0 | 0 | 0 |

## Major Elements (wt.%)

| Unit: | 6 | 6 | 6 | 6 | 6 | 6 | 6 |
|---|---|---|---|---|---|---|---|
| No. | CM-38 | CM-75 | CM-83 | CM-85 | CM-86 | CM-88 | CM-93 |
| SiO2 | 68.30 | 73.30 | 75.50 | 76.50 | 76.50 | 70.80 | 75.40 |
| TiO2 | 0.40 | 0.12 | 0.08 | 0.12 | 0.12 | 0.16 | 0.16 |
| Al2O3 | 13.00 | 12.10 | 11.10 | 11.10 | 11.80 | 14.70 | 11.80 |
| Fe2O3 | 5.93 | 2.32 | 2.69 | 2.35 | 1.67 | 2.57 | 2.10 |
| MnO | 0.03 | 0.06 | 0.01 | 0.01 | 0.02 | 0.02 | 0.05 |
| MgO | 0.08 | 0.15 | 0.08 | 0.02 | 0.06 | 0.16 | 0.08 |
| CaO | 0.26 | 0.44 | 0.18 | 0.16 | 0.26 | 0.64 | 0.38 |
| Na2O | 2.01 | 3.31 | 3.31 | 3.05 | 5.15 | 5.07 | 3.47 |
| K2O | 8.86 | 6.03 | 5.12 | 5.81 | 3.23 | 4.13 | 5.45 |
| P2O5 | 0.02 | 0.00 | 0.00 | 0.08 | 0.09 | 0.03 | 0.00 |
| LOI | 0.35 | 0.43 | 0.31 | 0.24 | 0.29 | 0.45 | 0.47 |
| Total | 99.24 | 98.26 | 98.38 | 99.44 | 99.19 | 99.73 | 99.36 |

## Trace Elements (ppm)

| | | | | | | | |
|---|---|---|---|---|---|---|---|
| Pb | 19 | 54 | 28 | 23 | 43 | 37 | 26 |
| U | 5 | 0 | 0 | 0 | 0 | 0 | 10 |
| Th | 12 | 21 | 13 | 19 | 10 | 9 | 21 |
| Rb | 263 | 120 | 115 | 135 | 67 | 67 | 126 |
| Sr | 29 | 57 | 17 | 22 | 28 | 121 | 26 |
| Y | 58 | 51 | 54 | 77 | 68 | 31 | 78 |
| Zr | 475 | 271 | 418 | 429 | 408 | 316 | 413 |
| Nb | 21 | 23 | 22 | 21 | 24 | 15 | 25 |
| Ga | 19 | 24 | 26 | 22 | 24 | 23 | 27 |
| Zn | 22 | 672 | 4 | 0 | 96 | 22 | 178 |
| Cu | 3 | 26 | 5 | 6 | 5 | 6 | 4 |
| Ni | 0 | 0 | 0 | 0 | 0 | 0 | 0 |
| La | 57 | 92 | 60 | 91 | 112 | 0 | 127 |
| Ti | .50 | .18 | .10 | .13 | .11 | .25 | .12 |
| Ba | 2701 | 358 | 67 | 589 | 74 | 1768 | 268 |
| V | 0 | 4 | 0 | 0 | 0 | 0 | 0 |
| Ce | 87 | 82 | 111 | 58 | 126 | 0 | 136 |
| Cr | 0 | 0 | 0 | 0 | 0 | 0 | 0 |

## Major Elements (wt.%)

| Unit: | 6 | 6 | 6 | 6 | 7 | 7 |
|-------|------|------|--------|--------|--------|--------|
| No. | CM-94 | CM-97 | CM-157 | CM-87 | CM-140 | CM-195 |
| SiO2 | 76.60 | 76.30 | 74.90 | 74.90 | 77.10 | 74.00 |
| TiO2 | 0.12 | 0.20 | 0.12 | 0.24 | 0.20 | 0.36 |
| Al2O3 | 11.40 | 11.60 | 11.80 | 12.80 | 11.60 | 12.50 |
| Fe2O3 | 2.64 | 2.41 | 2.30 | 2.36 | 2.79 | 3.05 |
| MnO | 0.03 | 0.02 | 0.00 | 0.03 | 0.04 | 0.03 |
| MgO | 0.07 | 0.13 | 0.02 | 0.36 | 0.05 | 0.34 |
| CaO | 0.16 | 0.62 | 0.10 | 0.26 | 0.42 | 0.44 |
| Na2O | 3.30 | 3.59 | 3.86 | 4.80 | 2.99 | 3.43 |
| K2O | 4.93 | 4.10 | 4.89 | 4.38 | 5.39 | 5.90 |
| P2O5 | 0.00 | 0.00 | 0.00 | 0.00 | 0.00 | 0.35 |
| LOI | 0.41 | 0.36 | 0.21 | 0.25 | 0.22 | 0.35 |
| Total | 99.66 | 99.33 | 98.20 | 100.38 | 100.80 | 100.40 |

## Trace Elements (ppm)

| | | | | | | |
|-----|-----|-----|-----|-----|-----|-----|
| Pb | 23 | 31 | 60 | 62 | 34 | 23 |
| U | 0 | 0 | 1 | 0 | 17 | 0 |
| Th | 17 | 33 | 8 | 24 | 25 | 24 |
| Rb | 174 | 113 | 117 | 81 | 125 | 175 |
| Sr | 36 | 91 | 26 | 43 | 62 | 118 |
| Y | 108 | 118 | 51 | 77 | 69 | 64 |
| Zr | 528 | 498 | 385 | 319 | 500 | 490 |
| Nb | 50 | 45 | 22 | 18 | 35 | 37 |
| Ga | 33 | 27 | 22 | 24 | 28 | 27 |
| Zn | 13 | 22 | 62 | 123 | 7 | 19 |
| Cu | 4 | 24 | 3 | 2 | 7 | 5 |
| Ni | 0 | 0 | 0 | 0 | 0 | 0 |
| La | 50 | 183 | 50 | 108 | 76 | 27 |
| Ti | .18 | .16 | .10 | .17 | .17 | .36 |
| Ba | 40 | 138 | 387 | 411 | 342 | 827 |
| V | 0 | 0 | 0 | 8 | 0 | 4 |
| Ce | 74 | 253 | 63 | 93 | 119 | 14 |
| Cr | 0 | 0 | 0 | 0 | 0 | 0 |

## Monkey Hill Granite

### Major Elements (wt.%)

| No. | CM-18 | CM-19 | CM-28 | CM-29 | CM-53 | CM-56 | CM-121 |
|-----|-------|-------|-------|-------|-------|-------|--------|
| SiO2 | 76.40 | 76.40 | 73.50 | 75.40 | 77.40 | 76.10 | 77.80 |
| TiO2 | 0.08 | 0.08 | 0.12 | 0.04 | 0.00 | 0.04 | 0.00 |
| Al2O3 | 12.80 | 12.50 | 13.60 | 13.20 | 12.50 | 13.30 | 12.70 |
| Fe2O3 | 0.58 | 0.67 | 1.53 | 0.95 | 0.63 | 0.71 | 0.39 |
| MnO | 0.01 | 0.01 | 0.04 | 0.01 | 0.00 | 0.01 | 0.01 |
| MgO | 0.05 | 0.04 | 0.36 | 0.21 | 0.04 | 0.08 | 0.04 |
| CaO | 0.38 | 0.18 | 0.82 | 0.64 | 0.32 | 0.54 | 0.34 |
| Na2O | 3.96 | 3.80 | 4.39 | 3.88 | 4.19 | 4.16 | 4.34 |
| K2O | 4.79 | 5.06 | 4.58 | 5.20 | 4.40 | 4.50 | 4.20 |
| P2O5 | 0.01 | 0.02 | 0.03 | 0.02 | 0.00 | 0.00 | 0.00 |
| LOI | 0.41 | 0.53 | 0.76 | 0.66 | 0.42 | 0.39 | 0.32 |
| Total | 99.47 | 99.29 | 99.73 | 100.21 | 99.90 | 99.83 | 100.22 |

### Trace Elements (ppm)

| | CM-18 | CM-19 | CM-28 | CM-29 | CM-53 | CM-56 | CM-121 |
|-----|-------|-------|-------|-------|-------|-------|--------|
| F | 90 | 140 | 500 | 610 | 400 | 160 | 540 |
| Pb | 20 | 24 | 22 | 22 | 68 | 39 | 34 |
| U | 9 | 7 | 1 | 1 | 4 | 10 | 11 |
| Th | 22 | 9 | 17 | 15 | 32 | 16 | 19 |
| Rb | 175 | 177 | 184 | 184 | 200 | 176 | 214 |
| Sr | 53 | 103 | 197 | 136 | 22 | 87 | 17 |
| Y | 11 | 12 | 22 | 15 | 17 | 15 | 16 |
| Zr | 71 | 92 | 121 | 101 | 82 | 68 | 86 |
| Nb | 15 | 12 | 16 | 13 | 19 | 12 | 18 |
| Ga | 19 | 17 | 21 | 19 | 22 | 20 | 22 |
| Zn | 0 | 0 | 8 | 0 | 59 | 0 | 0 |
| Cu | 6 | 11 | 5 | 27 | 38 | 12 | 12 |
| La | 0 | 0 | 2 | 7 | 0 | 0 | 0 |
| Ti | 0.02 | 0.08 | 0.13 | 0.09 | 0.00 | 0.05 | 0.00 |
| Ba | 66 | 333 | 438 | 307 | 0 | 185 | 0 |
| V | 0 | 0 | 1 | 0 | 0 | 0 | 0 |
| Ce | 38 | 0 | 63 | 36 | 65 | 16 | 48 |
| Mo | 2 | 2 | 2 | 2 | ? | 4 | 2 |
| Li | 6 | 3 | 18 | 8 | 4 | 9 | 8 |

## Major Elements (wt.%)

| No. | CM-122 | CM-171 | CM-171 A | CM-180 | CM-181 | RP-4G | RP-6 |
|-----|--------|--------|----------|--------|--------|-------|------|
| SiO2  | 73.80  | 72.40  | 75.80 | 76.60  | 76.80 | 76.90 | 76.70 |
| TiO2  | 0.08   | 0.08   | 0.04  | 0.04   | 0.04  | 0.08  | 0.08  |
| AL2O3 | 14.10  | 14.10  | 13.10 | 12.70  | 13.00 | 12.80 | 12.60 |
| Fe2O3 | 1.65   | 1.60   | 0.81  | 0.61   | 0.53  | 0.44  | 0.71  |
| MnO   | 0.06   | 0.06   | 0.02  | 0.01   | 0.01  | 0.00  | 0.00  |
| MgO   | 0.04   | 0.04   | 0.14  | 0.06   | 0.05  | 0.03  | 0.06  |
| CaO   | 0.84   | 1.08   | 0.52  | 0.40   | 0.46  | 0.38  | 0.38  |
| Na2O  | 4.39   | 4.34   | 3.99  | 3.98   | 4.30  | 4.10  | 4.26  |
| K2O   | 4.49   | 4.56   | 4.87  | 4.63   | 4.25  | 4.77  | 4.80  |
| P2O5  | 0.03   | 0.02   | 0.01  | -0.00  | 0.00  | 0.01  | 0.01  |
| LOI   | 0.44   | -0.90  | 0.54  | 0.30   | 0.11  | 0.40  | 0.30  |
| Total | 100.28 | 99.54  | 99.84 | 99.33  | 99.55 | 99.91 | 99.90 |

## Trace Elements (ppm)

| | CM-122 | CM-171 | CM-171 A | CM-180 | CM-181 | RP-4G | RP-6 |
|-----|------|------|------|------|------|------|------|
| F   | 540  | 750  | 970  | 110  | 140  | NA   | NA   |
| Pb  | 30   | 33   | 23   | 28   | 30   | 13   | 10   |
| U   | 7    | 8    | 4    | 0    | 3    | 3    | 1    |
| Th  | 10   | 24   | 22   | 14   | 16   | 2    | 0    |
| Rb  | 174  | 183  | 188  | 175  | 178  | 179  | 229  |
| Sr  | 227  | 212  | 62   | 73   | 62   | 38   | 12   |
| Y   | 29   | 29   | 23   | 11   | 17   | 22   | 28   |
| Zr  | 124  | 132  | 88   | 77   | 56   | 78   | 102  |
| Nb  | 18   | 20   | 12   | 12   | 8    | 17   | 23   |
| Ga  | 20   | 19   | 19   | 19   | 19   | 21   | 23   |
| Zn  | 34   | 11   | 0    | 0    | 0    | 0    | 33   |
| Cu  | 5    | 6    | 17   | 6    | 5    | 6    | 6    |
| La  | 23   | 20   | 2    | 0    | 0    | 0    | 0    |
| Ti  | 0.13 | 0.13 | 0.05 | 0.02 | 0.01 | 0.02 | 0.00 |
| Ba  | 482  | 466  | 133  | 75   | 48   | 40   | 0    |
| V   | 0    | 3    | 0    | 0    | 0    | 0    | 0    |
| Ce  | 99   | 31   | 84   | 50   | 74   | 63   | 89   |
| Mo  | 2    | 2    | 3    | 2    | 2    | NA   | NA   |
| Li  | 33   | 27   | 7    | 9    | 8    | NA   | NA   |

## Major Elements (wt.%)

No.     RP-7

| | |
|---|---|
| SiO2 | 77.40 |
| TiO2 | 0.04 |
| AL2O3 | 12.70 |
| Fe2O3 | 0.62 |
| MnO | 0.00 |
| MgO | 0.03 |
| CaO | 0.36 |
| NaO2 | 4.36 |
| K2O | 4.40 |
| P2O5 | 0.00 |
| LOI | 0.02 |

Total   100.19

## Trace Elements (ppm)

| | |
|---|---|
| F | NA |
| Pb | 16 |
| U | 6 |
| Th | 9 |
| Rb | 225 |
| Sr | 18 |
| Y | 32 |
| Zr | 103 |
| Nb | 32 |
| Ga | 23 |
| Zn | 0 |
| Cu | 1 |
| La | 0 |
| Ti | 0.00 |
| Ba | 0 |
| V | 0 |
| Ce | 38 |
| Mo | NA |
| Li | NA |

Pyritiferous Gossans and
Calcsilicate Altered Wall Rock

## Major Elements (wt.%)

| No. | CM-5 | CM-14 | CM-24 | CM-26 | CM-54B | CM-65 | CM-70 |
|---|---|---|---|---|---|---|---|
| SiO2 | 56.00 | 74.00 | 63.50 | 65.00 | 40.20 | 58.80 | 53.50 |
| TiO2 | 0.32 | 0.32 | 0.42 | 0.44 | 0.00 | 0.42 | 1.00 |
| Al2O3 | 10.80 | 12.40 | 17.30 | 17.10 | 4.72 | 13.50 | 15.10 |
| Fe2O3 | 3.21 | 2.27 | 5.22 | 4.84 | 28.30 | 5.66 | 11.45 |
| MnO | 0.36 | 0.01 | 0.04 | 0.03 | 0.07 | 0.19 | 0.31 |
| MgO | 0.37 | 0.23 | 0.08 | 0.32 | 1.04 | 2.31 | 3.49 |
| CaO | 12.08 | 0.56 | 0.54 | 0.92 | 8.06 | 5.44 | 5.40 |
| Na2O | 2.66 | 3.73 | 10.75 | 9.60 | 0.79 | 4.19 | 7.02 |
| K2O | 5.62 | 5.47 | 0.39 | 0.15 | 3.11 | 5.95 | 0.88 |
| P2O5 | 0.00 | 0.13 | 0.07 | 0.02 | 0.04 | 0.12 | 0.24 |
| LOI | 6.84 | 1.23 | 2.07 | 1.93 | 12.24 | 2.31 | 1.65 |
| Total | 98.26 | 100.35 | 100.38 | 100.35 | 98.57 | 98.89 | 100.01 |

## Trace Elements (ppm)

| | CM-5 | CM-14 | CM-24 | CM-26 | CM-54B | CM-65 | CM-70 |
|---|---|---|---|---|---|---|---|
| Pb | 24 | 19 | 20 | 22 | 35 | 49 | 27 |
| U | 0 | 0 | 0 | 5 | 0 | 2 | 6 |
| Th | 18 | 17 | 21 | 16 | 11 | 80 | 3 |
| Rb | 150 | 145 | 4 | 2 | 138 | 133 | 50 |
| Sr | 218 | 53 | 84 | 108 | 52 | 222 | 570 |
| Y | 40 | 15 | 72 | 14 | 11 | 69 | 44 |
| Zr | 231 | 232 | 1049 | 681 | 33 | 790 | 44 |
| Nb | 18 | 18 | 54 | 35 | 5 | 26 | 9 |
| Ga | 15 | 12 | 40 | 33 | 0 | 23 | 18 |
| Zn | 301 | 0 | 0 | 7 | 26 | 564 | 1177 |
| Cu | 9 | 42 | 24 | 14 | 1490 | 81 | 69 |
| Ni | 0 | 0 | 0 | 0 | 6 | 1 | 27 |
| La | 67 | 8 | 23 | 0 | 0 | 75 | 0 |
| Ti | 0.19 | 0.35 | 0.51 | 0.58 | 0.05 | 0.38 | 0.87 |
| Ba | 424 | 358 | 162 | 95 | 1290 | 1070 | 394 |
| V | 7 | 22 | 6 | 7 | 20 | 22 | 248 |
| Ce | 140 | 57 | 0 | 140 | 227 | 1205 | 29 |
| Cr | 0 | 5 | 0 | 0 | 0 | 0 | 38 |

## Major Elements (wt.%)

| No. | CM-125 | CM-139 B | CM-145 | CM-147 | CM-148 | CM-151 | CM-155 |
|-----|--------|----------|--------|--------|--------|--------|--------|
| SiO2 | 70.30 | 81.20 | 71.40 | 78.30 | 70.20 | 46.10 | 78.30 |
| TiO2 | 0.36 | 0.16 | 0.28 | 0.28 | 0.44 | 0.44 | 0.24 |
| Al2O3 | 9.80 | 7.08 | 11.70 | 8.60 | 12.30 | 12.20 | 11.60 |
| Fe2O3 | 3.10 | 2.98 | 4.86 | 3.04 | 4.13 | 23.43 | 1.57 |
| MnO | 0.14 | 0.04 | 0.06 | 0.03 | 0.04 | 0.05 | 0.04 |
| MgO | 1.67 | 0.91 | 0.73 | 0.44 | 0.21 | 0.13 | 0.28 |
| CaO | 6.12 | 0.92 | 1.12 | 0.54 | 0.36 | 1.96 | 0.40 |
| Na2O | 5.45 | 3.82 | 6.52 | 5.05 | 4.63 | 6.38 | 6.75 |
| K2O | 0.45 | 0.36 | 0.39 | 0.14 | 4.03 | 0.51 | 0.07 |
| P2O5 | 0.09 | 0.03 | 0.08 | 0.08 | 0.07 | 0.08 | 0.00 |
| LOI | 2.82 | 1.17 | 1.49 | 1.24 | 2.04 | 7.46 | 0.64 |
| Total | 100.30 | 98.67 | 98.63 | 97.74 | 98.72 | 98.21 | 99.89 |

## Trace Elements (ppm)

| | | | | | | | |
|-----|--------|----------|--------|--------|--------|--------|--------|
| Pb | 15 | 74 | 48 | 39 | 47 | 0 | 103 |
| U | 3 | 43 | 20 | 42 | 0 | 5 | 0 |
| Th | 47 | 48 | 64 | 81 | 7 | 0 | 18 |
| Rb | 14 | 34 | 13 | 13 | 113 | 111 | 3 |
| Sr | 154 | 41 | 63 | 29 | 69 | 121 | 43 |
| Y | 33 | 20 | 14 | 57 | 58 | 13 | 63 |
| Zr | 175 | 332 | 416 | 345 | 346 | 437 | 401 |
| Nb | 17 | 12 | 24 | 25 | 23 | 15 | 20 |
| Ga | 12 | 15 | 18 | 14 | 21 | 12 | 25 |
| Zn | 107 | 152 | 108 | 84 | 755 | 61 | 513 |
| Cu | 248 | 195 | 24 | 11 | 197 | 413 | 11 |
| Ni | 12 | 0 | 0 | 0 | 33 | 17 | 0 |
| La | 16 | 0 | 0 | 0 | 26 | 5 | 0 |
| Ti | .25 | .14 | .42 | .28 | .46 | .52 | .12 |
| Ba | 79 | 2 | 114 | 33 | 1653 | 153 | 0 |
| V | 24 | 17 | 22 | 0 | 73 | 53 | 4 |
| Ce | 793 | 870 | 1045 | 1150 | 70 | 0 | 153 |
| Cr | 0 | 0 | 0 | 0 | 4 | 72 | 0 |

## Major Elements (wt.%)

| No. | CM-176 | T-1-1 | T-1-2 | T-1-3 | T-1-4 | T-1-6 | T-2-4 |
|-----|--------|-------|-------|-------|-------|-------|-------|
| $SiO_2$ | 72.00 | 64.20 | 78.80 | 76.30 | 55.50 | 68.90 | 46.20 |
| $TiO_2$ | 0.40 | 0.12 | 0.28 | 0.28 | 0.56 | 0.24 | 0.24 |
| $Al_2O_3$ | 11.70 | 4.18 | 10.00 | 8.45 | 12.80 | 10.40 | 8.09 |
| $Fe_2O_3$ | 6.58 | 13.04 | 1.06 | 3.37 | 4.48 | 6.01 | 19.17 |
| $MnO$ | 0.02 | 0.16 | 0.05 | 0.10 | 0.12 | 0.11 | 0.09 |
| $MgO$ | 0.04 | 2.32 | 0.44 | 1.19 | 1.19 | 1.80 | 1.99 |
| $CaO$ | 0.46 | 5.46 | 0.92 | 3.36 | 10.38 | 3.62 | 2.96 |
| $Na_2O$ | 6.59 | 0.92 | 5.50 | 3.80 | 7.08 | 5.20 | 4.16 |
| $K_2O$ | 0.33 | 2.14 | 0.29 | 1.65 | 0.69 | 1.02 | 0.80 |
| $P_2O_5$ | 0.02 | 0.03 | 0.05 | 0.17 | 0.18 | 0.05 | 0.07 |
| LOI | 0.91 | 5.65 | 0.05 | 0.17 | 0.18 | 0.05 | 0.07 |
| Total | 99.05 | 98.25 | 98.23 | 99.87 | 97.59 | 99.45 | 98.49 |

## Trace Elements (ppm)

| | | | | | | |
|-----|------|------|-----|------|-----|------|
| Pb | 11 | 24 | 8 | 31 | 32 | 21 |
| U | 0 | 0 | 4 | 0 | 4 | 1 |
| Th | 1 | 117 | 12 | 89 | 7 | 24 |
| Rb | 10 | 96 | 12 | 65 | 26 | 39 |
| Sr | 46 | 26 | 80 | 84 | 206 | 100 |
| Y | 53 | 10 | 19 | 24 | 44 | 19 |
| Zr | 386 | 50 | 175 | 151 | 303 | 187 |
| Nb | 25 | 14 | 12 | 23 | 17 | 11 |
| Ga | 24 | 0 | 12 | 7 | 23 | 16 |
| Zn | 289 | 253 | 0 | 118 | 131 | 56 |
| Cu | 164 | 3167 | 56 | 489 | 794 | 1758 |
| Ni | 0 | 39 | 0 | 0 | 3 | 0 |
| La | 30 | 0 | 19 | 0 | 96 | 0 |
| Ti | .30 | .04 | .21 | .27 | .37 | .26 |
| Ba | 39 | 564 | 1 | 341 | 72 | 220 |
| V | 0 | 21 | 8 | 15 | 46 | 33 |
| Ce | 16 | 1946 | 67 | 1652 | 189 | 298 |
| Cr | 0 | 0 | 14 | 0 | 27 | 1 |

## Major Elements (wt.%)

| No. | T-3-4 | T-3-2 | T-5-1 | T-5-2 | T-7-1 | T-8-1 | T-8A-1 |
|-----|-------|-------|-------|-------|-------|-------|--------|
| SiO2 | 71.80 | 59.90 | 73.70 | 66.10 | 68.50 | 63.50 | 66.10 |
| TiO2 | 0.16 | 0.56 | 0.52 | 0.40 | 0.20 | 0.44 | 0.32 |
| Al2O3 | 3.58 | 11.80 | 13.30 | 10.40 | 11.60 | 12.20 | 9.36 |
| Fe2O3 | 11.27 | 6.62 | 0.84 | 4.41 | 6.28 | 6.02 | 8.05 |
| MnO | 0.18 | 0.28 | 0.03 | 0.05 | 0.13 | 0.26 | 0.08 |
| MgO | 1.83 | 3.39 | 0.32 | 0.17 | 0.44 | 0.68 | 0.74 |
| CaO | 5.30 | 9.44 | 0.94 | 1.34 | 3.54 | 6.14 | 3.68 |
| Na2O | 1.11 | 5.76 | 3.83 | 1.84 | 6.28 | 4.18 | 4.73 |
| K2O | 1.52 | 2.21 | 6.17 | 6.20 | 0.70 | 5.08 | 0.80 |
| P2O5 | 0.04 | 0.00 | 0.20 | 0.10 | 0.07 | 0.00 | 0.08 |
| LOI | 2.45 | 0.53 | 0.49 | 8.55 | 1.50 | 0.34 | 4.57 |
| Total | 99.20 | 100.49 | 100.34 | 99.56 | 99.24 | 99.84 | 98.51 |

## Trace Elements (ppm)

| | T-3-4 | T-3-2 | T-5-1 | T-5-2 | T-7-1 | T-8-1 | T-8A-1 |
|-----|-------|-------|-------|-------|-------|-------|--------|
| Pb | 29 | 38 | 20 | 18 | 22 | 22 | 30 |
| U | 0 | 0 | 1 | 6 | 8 | 14 | 6 |
| Th | 0 | 31 | 48 | 16 | 53 | 14 | 19 |
| Rb | 72 | 97 | 228 | 240 | 19 | 196 | 31 |
| Sr | 43 | 107 | 104 | 59 | 161 | 117 | 81 |
| Y | 21 | 40 | 45 | 44 | 41 | 40 | 42 |
| Zr | 57 | 176 | 261 | 223 | 381 | 263 | 252 |
| Nb | 8 | 23 | 32 | 22 | 15 | 20 | 17 |
| Ga | 0 | 14 | 18 | 12 | 16 | 16 | 13 |
| Zn | 74 | 149 | 33 | 81 | 79 | 106 | 70 |
| Cu | 1409 | 84 | 13 | 1339 | 208 | 7 | 766 |
| Ni | 32 | 0 | 0 | 4 | 0 | 0 | 0 |
| La | 0 | 26 | 9 | 77 | 0 | 57 | 47 |
| Ti | .11 | .54 | .41 | .24 | .13 | .43 | .25 |
| Ba | 441 | 560 | 1108 | 1660 | 92 | 1546 | 437 |
| V | 24 | 58 | 16 | 13 | 2 | 27 | 19 |
| Ce | 15 | 212 | 766 | 163 | 637 | 109 | 140 |
| Cr | 4 | 19 | 0 | 0 | 0 | 0 | 0 |

Trace Elements (ppm)

| No. | CM-10 | CM-22 | CM-45 | CM-54A | CM-55 | CM-64 | CM-65 |
|-----|-------|-------|-------|--------|-------|-------|-------|
| Pb | 30 | 18 | 20 | 24 | 13 | 33 | 49 |
| U | 0 | 2 | 0 | 0 | 0 | 6 | 2 |
| Th | 17 | 0 | 13 | 130 | 27 | 3 | 80 |
| Rb | 2 | 0 | 90 | 106 | 66 | 11 | 133 |
| Sr | 18 | 1619 | 12 | 19 | 40 | 696 | 222 |
| Y | 23 | 23 | 66 | 4 | 21 | 31 | 69 |
| Zr | 285 | 602 | 518 | 18 | 108 | 45 | 790 |
| Nb | 17 | 20 | 30 | 19 | 9 | 9 | 26 |
| Ga | 22 | 28 | 22 | 4 | 9 | 18 | 23 |
| Zn | 0 | 3 | 0 | 160 | 7 | 227 | 564 |
| Cu | 7 | 24 | 2 | 18 | 402 | 537 | 81 |
| Ni | 0 | 0 | 0 | 0 | 0 | 56 | 1 |
| La | 7 | 0 | 45 | 0 | 0 | 0 | 75 |
| Ti | .18 | 1.60 | .14 | .00 | .19 | .80 | .38 |
| Ba | 0 | 31747 | 132 | 568 | 793 | 191 | 1070 |
| V | 0 | 10 | 0 | 0 | 2 | 95 | 22 |
| Ce | 61 | 150 | 59 | 1977 | 25 | 20 | 1205 |
| Cr | 0 | 0 | 0 | 0 | 8 | 53 | |

| No. | CM-67 | CM-69 | CM-124 | CM-124 Q | CM-123 | CM-125 Q | CM-135 |
|-----|-------|-------|--------|----------|--------|----------|--------|
| Pb | 36 | 61 | 0 | 5 | 33 | 6 | 22 |
| U | 2 | 2 | 2 | 0 | 106 | 0 | 21 |
| Th | 4 | 15 | 25 | 0 | 27 | 11 | 21 |
| Rb | 133 | 19 | 47 | 9 | 31 | 4 | 324 |
| Sr | 165 | 662 | 70 | 16 | 75 | 77 | 23 |
| Y | 69 | 23 | 10 | 10 | 25 | 10 | 52 |
| Zr | 689 | 279 | 110 | 23 | 133 | 7 | 18 |
| Nb | 27 | 11 | 10 | 4 | 10 | 4 | 62 |
| Ga | 25 | 21 | 0 | 0 | 0 | 0 | 41 |
| Zn | 124 | 104 | 36 | 1 | 219 | 28 | 0 |
| Cu | 47 | 556 | 1084 | 1251 | 3846 | 51 | 8 |
| Ni | 1 | 17 | 25 | 19 | 5 | 0 | 0 |
| La | 85 | 0 | 7 | 0 | 9 | 0 | 0 |
| Ti | .46 | .43 | .15 | .00 | .06 | .00 | .00 |
| Ba | 908 | 562 | 596 | 168 | 1188 | 0 | 331 |
| V | 23 | 100 | 7 | 0 | 6 | 0 | 0 |
| Ce | 331 | 266 | 385 | 17 | 530 | 14 | 65 |
| Cr | 0 | 7 | 12 | 15 | 0 | 0 | 0 |

Trace Elements (ppm)

| No. | CM-150 | CM-153 Q | CM-160 | CM-167 A | CM-167 B | CM-173 | CM-176 |
|-----|--------|----------|--------|----------|----------|--------|--------|
| Pb | 24 | 16 | 57 | 112 | 13 | 26 | 11 |
| U | 3 | 0 | 18 | 37 | 0 | 1 | 0 |
| Th | 17 | 11 | 12 | 0 | 0 | 22 | 1 |
| Rb | 5 | 3 | 26 | 10 | 88 | 260 | 10 |
| Sr | 29 | 6 | 398 | 64 | 96 | 119 | 46 |
| Y | 12 | 6 | 84 | 29 | 9 | 29 | 53 |
| Zr | 262 | 4 | 352 | 316 | 231 | 230 | 386 |
| Nb | 16 | 2 | 18 | 7 | 5 | 16 | 25 |
| Ga | 12 | 2 | 11 | 5 | 8 | 14 | 24 |
| Zn | 0 | 0 | 227 | 607 | 57 | 16 | 289 |
| Cu | 72 | 120 | 1161 | 28 | 1 | 12 | 164 |
| Ni | 0 | 0 | 15 | 0 | 0 | 0 | 0 |
| La | 0 | 0 | 38 | 100 | 0 | 15 | 30 |
| Ti | .10 | .00 | 1.56 | .07 | .44 | .51 | .30 |
| Ba | 0 | 0 | 251 | 653 | 9257 | 1737 | 39 |
| V | 0 | 0 | 285 | 0 | 91 | 30 | 0 |
| Ce | 172 | 54 | 73 | 167 | 0 | 66 | 16 |
| Cr | 0 | 0 | 0 | 0 | 9 | 28 | 0 |

| No. | T-1-M | T-2-3 | T-3-1 | T-4-1 | T-5-4 | T-6A-1 | T-7-3 | T-8-3 |
|-----|-------|-------|-------|-------|-------|--------|-------|-------|
| Pb | .1 | 107 | 12 | 28 | 40 | 17 | 23 | 8 |
| U | 0 | 7 | 1 | 19 | 0 | 2 | 0 | 5 |
| Th | 0 | 6 | 8 | 20 | 582 | 9 | 15 | 10 |
| Rb | 74 | 3 | 99 | 11 | 215 | 22 | 155 | 78 |
| Sr | 11 | 29 | 79 | 93 | 4 | 104 | 70 | 57 |
| Y | 15 | 28 | 22 | 35 | 11 | 24 | 25 | 32 |
| Zr | 64 | 62 | 157 | 168 | 144 | 237 | 251 | 173 |
| Nb | 11 | 10 | 10 | 17 | 71 | 15 | 19 | 14 |
| Ga | 0 | 0 | 11 | 0 | 0 | 4 | 10 | 0 |
| Zn | 0 | 0 | 38 | 6 | 632 | 5 | 4 | 23 |
| Cu | 4894 | 1248 | 1254 | 619 | 0 | 1819 | 151 | 4694 |
| Ni | 0 | 9 | 7 | 28 | 0 | 0 | 3 | 11 |
| La | 18 | 145 | 42 | 11 | 0 | 10 | 16 | 2 |
| Ti | .05 | .05 | .30 | .20 | .14 | .17 | .18 | .14 |
| Ba | 553 | 67 | 437 | 391 | 829 | 252 | 641 | 1655 |
| V | 12 | 51 | 13 | 15 | 0 | 7 | 0 | 1 |
| Ce | 37 | 332 | 151 | 288 | 2641 | 62 | 85 | 282 |
| Cr | 14 | 0 | 16 | 0 | 0 | 0 | 0 | 0 |

Trace Elements (ppm)

| No. | T-8B-2 | T-8B-2A | RP-17 | RP-18 |
|-----|--------|---------|-------|-------|
| Pb  | 84     | 0       | 0     | 13    |
| U   | 17     | 13      | 7     | 13    |
| Th  | 19     | 1       | 2     | 18    |
| Rb  | 15     | 27      | 123   | 6     |
| Sr  | 71     | 84      | 79    | 219   |
| Y   | 40     | 28      | 40    | 74    |
| Zr  | 97     | 73      | 217   | 514   |
| Nb  | 13     | 15      | 21    | 26    |
| Ga  | 0      | 0       | 2     | 19    |
| Zn  | 24     | 3       | 59    | 85    |
| Cu  | 326    | 371     | 405   | 187   |
| Ni  | 11     | 14      | 27    | 0     |
| La  | 12     | 0       | 26    | 48    |
| Ti  | .03    | .12     | .23   | .27   |
| Ba  | 641    | 3812    | 746   | 179   |
| V   | 9      | 7       | 14    | 15    |
| Ce  | 180    | 61      | 67    | 94    |
| Cr  | 0      | 0       | 0     | 0     |

## Radioactive Mineral Occurrences

### Major Elements (wt.%)

| No. | RP-1 | RP-2 | RP-3A | RP-8 | RP-10A | RP-10B | RP-10C |
|---|---|---|---|---|---|---|---|
| SiO2 | 62.10 | 63.50 | 60.20 | 75.70 | 51.10 | 49.10 | 49.30 |
| TiO2 | 0.48 | 0.68 | 0.56 | 0.24 | 2.32 | 1.28 | 2.16 |
| Al2O3 | 16.40 | 17.60 | 15.40 | 10.60 | 14.10 | 13.80 | 13.00 |
| Fe2O3 | 6.45 | 5.33 | 4.82 | 3.14 | 12.61 | 11.12 | 15.88 |
| MnO | 0.09 | 0.14 | 0.11 | 0.09 | 0.29 | 0.24 | 0.24 |
| MgO | 1.23 | 0.85 | 0.93 | 0.08 | 3.78 | 4.26 | 4.08 |
| CaO | 3.14 | 0.90 | 3.40 | 1.86 | 7.66 | 6.58 | 7.06 |
| Na2O | 9.10 | 10.20 | 8.30 | 6.25 | 5.01 | 4.81 | 4.94 |
| K2O | 0.36 | 0.22 | 0.80 | 0.12 | 1.77 | 2.11 | 1.08 |
| P2O5 | 0.03 | 0.08 | 0.14 | 0.02 | 1.27 | 0.62 | 1.10 |
| LOI | 0.69 | 0.71 | 1.63 | 1.69 | 0.63 | 2.03 | 0.94 |
| Total | 100.07 | 100.21 | 96.29 | 99.97 | 100.54 | 95.55 | 99.78 |

### Trace Elements (ppm)

| | | | | | | | |
|---|---|---|---|---|---|---|---|
| Pb | 385 | 504 | 762 | 1386 | 144 | 9463 | 8565 |
| U | 218 | 218 | 2816 | 726 | 100 | 33298 | 28832 |
| Th | 1 | 0 | 209 | 1 | 0 | 0 | 0 |
| Rb | 8 | 14 | 55 | 11 | 110 | 446 | 396 |
| Sr | 333 | 224 | 212 | 67 | 786 | 786 | 485 |
| Y | 45 | 44 | 124 | 75 | 76 | 172 | 126 |
| Zr | 747 | 566 | 1438 | 479 | 277 | 2193 | 5471 |
| Nb | 24 | 14 | 57 | 31 | 18 | 34 | 44 |
| Ga | 40 | 33 | 18 | 30 | 24 | 83 | 78 |
| Zn | 271 | 591 | 484 | 164 | 866 | 1594 | 3371 |
| Cu | 44 | 71 | 238 | 606 | 744 | 0 | 1773 |
| Ni | 0 | 0 | 2 | 0 | 0 | 0 | 0 |
| La | 63 | 72 | 27 | 102 | 6 | 9 | 16 |
| Ti | .46 | .84 | .43 | .16 | 2.19 | 1.10 | 1.17 |
| Ba | 183 | 307 | 318 | 16 | 1411 | 1156 | 1151 |
| V | 108 | 75 | 32 | 9 | 208 | 320 | 623 |
| Ce | 112 | 86 | 1626 | 199 | 125 | 453 | 2 |
| Cr | 0 | 0 | 0 | 0 | 0 | 0 | 0 |

## Major Elements (wt.%)

| No. | RP-11A | RP-11B | RP-13A | CM-59 | CM-99 | CM-100 | CM-100A |
|-----|--------|--------|--------|-------|-------|--------|---------|
| SiO2  | 50.00 | 48.50 | 46.10 | 57.90 | 75.40 | 55.50 | 47.30 |
| TiO2  | 2.16  | 2.12  | 3.36  | 0.48  | 0.08  | 2.08  | 2.28  |
| Al2O3 | 12.60 | 11.80 | 12.30 | 14.90 | 10.90 | 14.80 | 15.50 |
| Fe2O3 | 15.24 | 16.75 | 13.12 | 6.72  | 2.66  | 10.05 | 14.21 |
| MnO   | 0.27  | 0.28  | 0.56  | 0.45  | 0.04  | 0.32  | 0.36  |
| MgO   | 3.59  | 3.73  | 4.55  | 1.81  | 0.05  | 1.96  | 4.29  |
| CaO   | 7.66  | 8.60  | 9.56  | 5.20  | 2.46  | 4.38  | 5.44  |
| Na2O  | 4.94  | 4.81  | 4.58  | 8.02  | 6.05  | 7.64  | 5.28  |
| K2O   | 1.29  | 0.62  | 1.37  | 0.14  | 0.16  | 0.33  | 2.48  |
| P2O5  | 0.92  | 0.92  | 1.00  | 1.24  | 0.03  | 0.48  | 0.66  |
| LOI   | 0.26  | 1.26  | 2.08  | 2.31  | 1.14  | 0.62  | 0.68  |
| Total | 98.93 | 99.39 | 98.61 | 99.17 | 98.97 | 98.16 | 98.48 |

## Trace Elements (ppm)

| | RP-11A | RP-11B | RP-13A | CM-59 | CM-99 | CM-100 | CM-100A |
|-----|--------|--------|--------|-------|-------|--------|---------|
| Pb | 1754 | 406  | 557  | 131   | 303 | 164   | 87   |
| U  | 6041 | 1039 | 227  | 229   | 301 | 520   | 12   |
| Th | 0    | 0    | 31   | 37    | 17  | 11    | 0    |
| Rb | 106  | 14   | 83   | 2     | 5   | 10    | 144  |
| Sr | 480  | 439  | 604  | 474   | 75  | 424   | 958  |
| Y  | 105  | 73   | 294  | 241   | 35  | 139   | 76   |
| Zr | 767  | 388  | 2190 | 982   | 436 | 2263  | 258  |
| Nb | 20   | 21   | 31   | 20    | 19  | 24    | 17   |
| Ga | 23   | 17   | 22   | 33    | 28  | 34    | 27   |
| Zn | 499  | 555  | 6275 | 19171 | 20  | 11802 | 1553 |
| Cu | 0    | 940  | 654  | 258   | 33  | 1012  | 217  |
| Ni | 0    | 0    | 20   | 10    | 0   | 5     | 1    |
| La | 18   | 19   | 6    | 4     | 66  | 0     | 0    |
| Ti | 2.06 | 2.13 | 3.10 | 0.42  | 0.10| 1.89  | 2.18 |
| Ba | 1111 | 256  | 3898 | 233   | 0   | 560   | 4378 |
| V  | 158  | 100  | 137  | 27    | 6   | 194   | 106  |
| Ce | 123  | 100  | 0    | 82    | 131 | 0     | 95   |
| Cr | 0    | 0    | 0    | 0     | 0   | 2     | 0    |

## Major Elements (wt.%)

| No. | CM-139B | CM-146 | CM-58 |
|-----|---------|--------|-------|
| SiO2 | 57.00 | 59.00 | |
| TiO2 | 0.48 | 0.68 | |
| Al2O3 | 11.10 | 15.70 | |
| Fe2O3 | 10.70 | 7.75 | |
| MnO | 0.13 | 0.09 | |
| MgO | 2.28 | 1.64 | |
| CaO | 6.26 | 1.58 | |
| Na2O | 5.48 | 8.33 | |
| K2O | 0.58 | 1.02 | |
| P2O5 | 0.15 | 0.27 | |
| LOI | 4.65 | 2.38 | |
| Total | 98.81 | 98.44 | |

## Trace Elements (ppm)

| | CM-139B | CM-146 | CM-58 |
|-----|---------|--------|-------|
| Pb | 424 | 284 | 1379 |
| U | 481 | 154 | 5131 |
| Th | 28 | 163 | 339 |
| Rb | 38 | 116 | 197 |
| Sr | 154 | 176 | 638 |
| Y | 103 | 45 | 5868 |
| Zr | 1531 | 1787 | 2789 |
| Nb | 21 | 46 | 83 |
| Ga | 6 | 22 | 0 |
| Zn | 1404 | 237 | 859 |
| Cu | 22723 | 10 | 2255 |
| Ni | 1 | 3 | 413 |
| La | 23 | 0 | 59 |
| Ti | .38 | .89 | .90 |
| Ba | 124 | 725 | 6873 |
| V | 33 | 21 | 20 |
| Ce | 0 | 1513 | 164 |
| Cr | 13 | 0 | 0 |

Carbonate Vein

## Major Elements (wt.%)

| No. | CM-78 | CM-79 | RP-4A | RP-4B | RP-4C | RP-4D | RP-16C | RP-16CF |
|-----|-------|-------|-------|-------|-------|-------|--------|---------|
| SiO2 | 70.10 | | | | | | | |
| TiO2 | 0.16 | | | | | | | |
| Al2O3 | 11.60 | | | | | | | |
| Fe2O3 | 0.62 | | | | | | | |
| MnO | 0.06 | | | | | | | |
| MgO | 0.63 | | | | | | | |
| CaO | 3.52 | | | | | | | |
| Na2O | 2.39 | | | | | | | |
| K2O | 7.07 | | | | | | | |
| P2O5 | 0.06 | | | | | | | |
| LOI | 3.09 | | | | | | | |

Total  99.30

## Trace Elements (ppm)

| | | | | | | | | |
|-----|-------|-------|-------|-------|-------|-------|--------|---------|
| Pb | 546 | 1461 | 184 | 316 | 154 | 73 | 73 | |
| U | 44 | 19 | 46 | 42 | 162 | 11 | 6 | |
| Th | 13 | 0 | 0 | 54 | 0 | 6 | 3 | |
| Rb | 2 | 1 | 24 | 11 | 26 | 23 | 22 | |
| Sr | 253 | 212 | 218 | 57 | 433 | 96 | 127 | |
| Y | 46 | 38 | 60 | 75 | 41 | 38 | 44 | |
| Zr | 214 | 56 | 179 | 248 | 227 | 155 | 137 | |
| Nb | 6 | 3 | 5 | 3 | 11 | 12 | 12 | |
| Ga | 11 | 20 | 17 | 15 | 23 | 13 | 8 | |
| Zn | 39370 | 36604 | 63533 | 74151 | 40939 | 249 | 232 | |
| Cu | 376 | 192 | 341 | 1302 | 311 | 4183 | 4692 | |
| Ni | 0 | 0 | 0 | 15 | 0 | 0 | 0 | |
| La | 0 | 0 | 0 | 0 | 0 | 8 | 31 | |
| Ti | .00 | .00 | .00 | .04 | .24 | .19 | .13 | |
| Ba | 44 | 58 | 173 | 51 | 153 | 118 | 93 | |
| V | 14 | 19 | 12 | 234 | 104 | 38 | 28 | |
| Ce | 45 | 85 | 55 | 320 | 104 | 224 | 103 | |
| Cr | 0 | 0 | 0 | 47 | 0 | 0 | 0 | |

Fluorite Veins

---

Trace Elements

---

| No. | CM-123F | CM-153 | CM-169 | T-8B-1 | T-8F | T-8-5F | T-8M |
|-----|---------|--------|--------|--------|------|--------|------|
| Pb | 144 | 189 | 40 | 353 | 39 | 141 | 271 |
| U | 689 | 292 | 1 | 129 | 152 | 592 | 978 |
| Th | 4 | 365 | 7 | 233 | 0 | 0 | 147 |
| Rb | 7 | 50 | 27 | 13 | 56 | 16 | 19 |
| Sr | 125 | 42 | 97 | 195 | 131 | 99 | 196 |
| Y | 59 | 133 | 19 | 104 | 49 | 43 | 97 |
| Zr | 124 | 150 | 21 | 333 | 229 | 118 | 268 |
| Nb | 14 | 35 | 2 | 33 | 15 | 12 | 34 |
| Ga | 0 | 0 | 2 | 8 | 5 | 0 | 2 |
| Zn | 1236 | 553 | 13 | 299 | 7 | 960 | 299 |
| Cu | 684 | 34 | 25 | 183 | 166 | 741 | 182 |
| Ni | 40 | 0 | 0 | 0 | 1 | 56 | 0 |
| La | 17 | 88 | 0 | 23 | 0 | 15 | 5 |
| Ti | .05 | .07 | .00 | .12 | .21 | .03 | .09 |
| Ba | 98 | 485 | 1478 | 471 | 3035 | 124 | 422 |
| V | 12 | 12 | 0 | 13 | 13 | 9 | 11 |
| Ce | 58 | 2202 | 34 | 2077 | 127 | 0 | 1577 |
| Cr | 0 | 0 | 0 | 0 | 27 | 0 | 0 |

| SAMPLE NO. | DESCRIPTIONS |
|---|---|
| CM-5 | Pyritiferous, rusty felsic volcanic conglomerate. |
| CM-10 | Pyritiferous, rusty felsic volcanic rock. |
| CM-14 | Pyritiferous, rusty felsic volcanic conglomerate. |
| CM-22 | Pyritiferous, rusty felsic rhyolite volcanic rock with rare molybdenite. |
| CM-24 | Pyritiferous, rusty felsic rhyolite volcanic rock. |
| CM-26 | Pyritiferous, rusty felsic rhyolite volcanic rock with minor molybdenite. |
| CM-45 | Pyritiferous, rusty felsic rhyolite volcanic rock. |
| CM-54A | Molybdenite-bearing quartz vein in felsic volcanic conglomerate. |
| CM-54B | Intense calsilicate-fluorite altered rusty felsic volcanic conglomerate. |
| CM-55 | Pyritiferous rusty felsic volcanic conglomerate, with minor chalcopyrite. |
| CM-58 | Radioactive hornblende-fluorite vein, with minor chalcopyrite, molybdenite and galena. |
| CM-59 | Red hematized, radioactive rhyolite with minor sphalerite. |
| CM-64 | Rusty, pyritiferous metabasalt. |
| CM-65 | Silicified stockwork-style molybdenite mineralization in metabasalt. |
| CM-67 | Pyrite-molybdenite mineralized stockwork in metabasalt. |
| CM-69 | Pyrite-molybdenite mineralized stockwork in metabasalt. |

CM-70      Sheared, rusty metabasalt with abundant coarse hornblende and minor molybdenite.

CM-79      White to pale pink calcite vein with abundant dark grey sphalerite, and minor pyrite.

CM-99      Red hematized, radioactive rhyolite, with minor chalcopyrite, molybdenite, and fluorite (Showing # 18).

CM-100      Red hematized, radioactive rhyolite, at contact with amphibolite; minor galena, sphalerite, fluorite, and chalcopyrite (Showing # 16).

CM-100A      Amphibolite with abundant amphibole and calcite veinlets.

CM-123      Massive coarse sulphide with pyrite, chalcopyrite, and minor molybdenite.

CM-123F      Radioactive fluorite vein with massive pyrite-pyrrhotite.

CM-124      Sulphide-rich, molybdenite-bearing, rusty felsic volcanic conglomerate.

CM-124Q      Quartz vein with pyrite, chalcopyrite (above).

CM-125      Pyritiferous, rusty felsic tuff, with minor molybdenite.

CM-125 Q      Quartz vein (above).

CM-132      Pyritiferous, rusty felsic tuff, at contact with mafic dyke.

CM-139A      Pyritiferous, rusty felsic volcanic conglomerate, with minor molybdenite.

CM-139B      Red hematized radioactive felsic volcanic conglomerate, with abundant chalcopyrite, minor molybdenite, and fluorite (Showing #19).

CM-145      Rusty, pyritiferous felsic volcanic with minor molybdenite.

CM-146      Slightly radioactive, rusty pyritiferous felsic volcanic, with molybdenite.

| | |
|---|---|
| CM-147 | Rusty, pyritiferous felsic volcanic with minor molybdenite. |
| CM-148 | Rusty, pyritiferous felsic volcanic conglomerate. |
| CM-150 | Rusty, pyritiferous felsic volcanic tuff. |
| CM-151 | Rusty, pyritiferous felsic volcanic tuff, with abundant magnetite. |
| CM-153 | Radioactive fluorite-adularia vein with extensive molybdenite. |
| CM-153Q | Pyrite-pyrrhotite bearing quartz vein (above). |
| CM-155 | Rusty pyritiferous rhyolite. |
| CM-160 | Sulphide-rich volcanic conglomerate at contact with mafic dyke. |
| CM-167A | Quartz-fluorite vein with disseminated pyrite. |
| CM-167B | Quartz vein with minor magnetite. |
| CM-169 | Quartz-fluorite vein with rare molybdenite. |
| CM-173 | Rusty felsic conglomerate intruded by pegmatite. |
| CM-176 | Rusty felsic tuff intruded by pegmatite. |
| T-1-M | Massive coarse pyrite, chalcopyrite in gossan, with minor scheelite. |
| T-1-1 | Rusty felsic volcanic conglomerate with massive pyrite, minor chalcopyrite, and molybdenite. |
| T-1-2 | Silicified felsic volcanic with disseminated pyrite. |
| T-1-3 | Calcsilicate altered felsic volcanic conglomerate with pyrite and molybdenite bearing quartz veins. |
| T-1-4 | Rusty felsic conglomerate with disseminated pyrite. |

T-1-6        Rusty felsic conglomerate with minor disseminated pyrite and molybdenite.

T-2-3        Rusty felsic conglomerate with disseminated pyrite and chalcopyrite.

T-2-4        Rusty felsic volcanic with pyrite, chalcopyrite and molybdenite.

T-3-1        Felsic tuff transected by quartz stringers with minor pyrite and chalcopyrite.

T-3-4        Rusty sheared felsic tuff with minor pyrite.

T-4-1        Rusty felsic tuff with pods of massive pyrite and minor chalcopyrite and molybdenite.

T-5-1        Felsic tuff with disseminated molybdenite.

T-5-2        Rusty volcanic conglomerate, with minor pyrite, chalcopyrite.

T-5-4        Quartz-molybdenite veins from T-5-2.

T-6A-1        Rusty felsic conglomerate with stringers of massive pyrite-chalcopyite at dyke contact.

T-7-1        Rusty felsic tuff with pyrite and minor molybdenite.

T-7-3        Rusty pyritiferous felsic conglomerate.

T-8-3        Quartz stockwork in felsic conglomerate with extensive pyrite, chalcopyrite, and minor molybdenite.

T-8A-1        Rusty pyritiferous felsic tuff.

T-8B-1        Radioactive fluorite vein with extensive molybdenite mineralization.

T-8B-2        Massive pyrite-pyrrhotite-magnetite-fluorite zone.

T-8B-2A        Quartz-fluorite zone with massive pyrite-magnetite.

| | |
|---|---|
| RP-1 | Red hematized radioactive rhyolite (Round Pond radioactive zone). |
| RP-2 | Radioactive intermediate volcanic tuff (?) (above). |
| RP-3A | Red hematized radioactive felsic volcanic boulder with extensive molybdenite mineralization (Showing # 19). |
| RP-3B | Resample (1986) of CM-139B locale. |
| RP-4A | White to pale pink calcite hosting sphalerite, and minor galena mineralization (CM-79). |
| RP-4B | White to pale pink calcite hosting rich sphalerite mineralization, with minor pyrite and chalcopyrite. |
| RP-4C | White to brown weathered calcite, with abundant sphalerite, and minor deep purple fluorite. |
| RP-4D | Red brown carbonate-rich rock with disseminated sphalerite and anomalous radioactivity. |
| RP-10A | Red hematized radioactive rhyolite at contact with amphibolite (Showing #16N). |
| RP-10B | Radioactive amphibolite (above). |
| RP-10C | Amphibolite (above). |
| RP-10D | Radioactive amphibolite with minor galena, and sphalerite. |
| RP-11A | Radioactive amphibolite (Showing #17). |
| RP-11B | Rusty radioactive amphibolite, with minor chalcopyrite (Showing #17). |
| RP-13A | Resample (1986) of sample CM-100 locale. |
| RP-13B | Resample (1986) of sample CM-100 locale. |

RP-16C

Sheared carbonate-rich conglomerate with disseminated pyrite, chalcopyrite, molybdenite, and fluorite.

RP-16CF

Sheared carbonate-rich conglomerate with disseminated pyrite, chalcopyrite, molybdenite, and fluorite.

RP-17

Rusty pyritiferous felsic conglomerate.

# Chemex Labs Ltd.

*Analytical Chemists* • *Geochemists* • *Registered Assayers*

212 Brooksbank Ave.
North Vancouver, B.C.
Canada      V7J 2C1

Telephone (604) 984-0221
Telex:      04352597

CERTIFICATE OF ANALYSIS

TO : MEMORIAL UNIVERSITY OF NEWFOUNDLAND

DEPT. OF EARTH SCIENCES
ST. JOHN'S, NFLD.
A1B 3X5

CERT. #   : A8611115-001-A
INVOICE # : 18611115
DATE      : 17-MAR-86
P.O. #    : NONE

Semi-quantitative multi element ICP analysis

Nitric-Aqua-Regia digestion of 0.5 gm of material followed by ICP analysis. Since this digestion is incomplete for many minerals, values reported for Al, Sb, Ba, Be, Ca, Cr, Ga, La, Mg, K, Na, Sr, Ti, Ti, W and V can only be considered as semi-quantitative.

COMMENTS :
ATTN: DR. DEREK WILTON ( SOME SAMPLES BROKEN IN

SHIPMENT.

| Sample description | Au ppb FA+AA | Al % | Ag ppm | As ppm | Ba ppm | Be ppm | Bi ppm | Ca % | Cd ppm | Co ppm | Cr ppm | Cu ppm | Fe % | Ga ppm | K % | La ppm | Mg % | Mn ppm | Mo ppm | Na % | Ni ppm | P ppm | Pb ppm | Sb ppm | Sr ppm | Ti % | Tl ppm | U ppm | V ppm | W ppm | Zn ppm |
|---|---|---|---|---|---|---|---|---|---|---|---|---|---|---|---|---|---|---|---|---|---|---|---|---|---|---|---|---|---|---|---|
| CA-10 | — | 0.17 | 0.4 | 28 | 10 | <0.5 | 2 | 0.06 | <0.5 | 75 | 2 | 6 | 1.71 | <10 | 0.04 | 20 | 0.07 | 75 | 33 | 0.16 | 1 | 160 | 18 | <10 | 1 | 0.07 | <10 | <10 | 2 | 550 | 18 |
| CA-14 | — | 0.26 | 4.2 | 10 | 30 | <0.5 | 4 | 0.04 | <0.5 | 59 | 10 | 48 | 1.87 | <10 | 0.31 | 10 | 0.10 | 39 | 34 | 0.12 | 4 | 770 | 12 | <10 | 10 | 0.11 | <10 | <10 | 17 | 410 | <10 |
| CA-22 | 5 | 0.17 | 0.8 | 10 | 410 | <0.5 | 2 | 0.19 | <0.5 | 18 | 1 | 12 | 2.13 | <10 | 0.02 | <10 | 0.01 | 160 | 262 | 0.16 | 1 | 60 | 18 | <10 | 417 | 0.10 | <10 | <10 | 1 | 80 | <10 |
| CA-24 | — | 0.18 | 0.2 | 10 | 110 | <0.5 | <2 | 0.25 | <0.5 | 24 | 2 | 29 | 4.01 | <10 | 0.01 | 20 | 0.02 | 299 | 25 | 0.17 | 3 | 220 | 10 | <10 | 8 | 0.24 | <10 | <10 | 5 | 129 | <10 |
| CA-25 | — | 0.16 | 0.6 | 10 | 50 | <0.5 | 2 | 0.12 | <0.5 | <2 | 2 | 20 | 4.75 | <10 | 0.02 | <10 | 0.02 | 64 | 225 | 0.19 | 1 | 160 | 6 | <10 | 5 | 0.24 | <10 | <10 | 4 | 40 | <10 |
| CA-45 | — | 0.12 | 0.2 | 10 | 20 | <0.5 | <2 | 0.04 | <0.5 | 40 | <1 | <1 | 2.34 | <10 | 0.09 | 20 | <0.01 | 90 | 4 | 0.06 | <1 | 110 | 4 | <10 | 2 | 0.06 | <10 | <10 | <1 | 230 | <10 |
| CA-54 A | — | 0.12 | 0.2 | <10 | 50 | <0.5 | <2 | 0.08 | <0.5 | 122 | <1 | 77 | 0.44 | <10 | 0.11 | <10 | 0.02 | 122 | 7523 | 0.03 | 2 | 110 | 8 | 40 | 11 | 0.01 | <10 | <10 | 5 | 1000 | <10 |
| CA-54 B | — | 1.57 | 0.4 | 10 | 20 | <0.5 | <2 | 5.48 | <0.5 | 871 | 5 | 1499 | 19.99 | 10 | 1.79 | <10 | 0.50 | 481 | 380 | 0.22 | 18 | <10 | 3 | <10 | 42 | 0.02 | <10 | <10 | 10 | 150 | 30 |
| CA-55 | — | 0.15 | 1.2 | 20 | 250 | <0.5 | 62 | 0.22 | <0.5 | 114 | 11 | 522 | 2.60 | <10 | 0.06 | 10 | 0.02 | 111 | 5 | 0.05 | 4 | 340 | 18 | <10 | 7 | 0.11 | <10 | <10 | 10 | 710 | 28 |
| CA-58 | — | 2.69 | 10.6 | 70 | 4100 | <0.5 | <2 | 15.03 | 5.0 | 16 | 23 | 2282 | 7.03 | 110 | 2.74 | <10 | 2.36 | 2529 | 394 | 0.30 | 8 | 4790 | 1259 | 28 | 452 | 0.58 | 1000 | 4360 | 54 | 360 | 620 |
| CA-59 | — | 0.22 | 3.2 | 40 | 120 | <0.5 | <2 | 0.22 | 84.5 | 24 | <1 | 282 | 3.67 | 20 | <0.01 | 60 | 0.29 | 1547 | 40 | 0.12 | 2 | 4860 | 126 | 20 | 36 | 0.21 | 10 | 160 | 12 | 60 | 39999 |
| CA-64 | — | 0.48 | 3.4 | 10 | 20 | <0.5 | <2 | 1.02 | 1.3 | 138 | 22 | 623 | 4.34 | 20 | <0.01 | <10 | 0.28 | 184 | 3 | 0.12 | 72 | 580 | 20 | <10 | 47 | 0.45 | <10 | <10 | 53 | 160 | 190 |
| CA-65 | 15 | 0.25 | 2.0 | 20 | 50 | <0.5 | <2 | 2.76 | 2.5 | 24 | 3 | 106 | 3.63 | 20 | 0.12 | 50 | 0.42 | 818 | 3746 | 0.10 | 7 | 530 | 34 | 20 | 14 | 0.31 | <10 | <10 | 25 | 100 | 360 |
| CA-67 | — | 0.30 | 1.8 | 10 | 50 | <0.5 | <2 | 0.96 | <0.5 | 28 | <1 | 59 | 3.60 | 10 | 0.21 | 40 | 0.28 | 200 | 529 | 0.04 | 5 | 750 | 34 | <10 | 29 | 0.32 | <10 | <10 | 17 | 110 | 70 |
| CA-69 | — | 0.32 | 2.0 | <10 | 20 | <0.5 | <2 | 0.65 | <0.5 | 56 | 7 | 660 | 4.22 | <10 | 0.04 | <10 | 0.13 | 122 | 599 | 0.10 | 25 | 280 | 40 | <10 | 14 | 0.35 | <10 | <10 | 58 | 140 | 10 |
| CA-70 | — | 1.04 | 0.2 | 10 | 240 | <0.5 | <2 | 1.50 | 2.5 | 22 | 4 | 73 | 6.03 | 20 | 0.32 | <10 | 1.24 | 1749 | 52 | 0.25 | 30 | 840 | 4 | <10 | 29 | 0.47 | <10 | <10 | 298 | 30 | 840 |
| CA-73 | — | 0.33 | 0.2 | <10 | 40 | <0.5 | <2 | 2.21 | 4.5 | 33 | 2 | 42 | 9.47 | <10 | 0.15 | <30 | 0.31 | 459 | 7 | 0.04 | 4 | 360 | 4 | <10 | 26 | 0.01 | <10 | <10 | 14 | 290 | 18 |
| CA-74 | — | 0.21 | 2.0 | 40 | 20 | <0.5 | 8 | 30.02 | 999.9 | 27 | <1 | 665 | 1.15 | 50 | <0.01 | <10 | 0.92 | 5854 | 21 | <0.01 | 30 | 230 | 690 | 70 | 104 | <0.01 | <10 | <10 | 20 | 30 | 39999 |
| CA-99 | — | 0.53 | 0.4 | <10 | 10 | 3.0 | <2 | 1.75 | <0.5 | 24 | 1 | 27 | 1.92 | 10 | 0.02 | 40 | 0.02 | 257 | 11 | 0.78 | 1 | 40 | 320 | <10 | 12 | 0.04 | <10 | 200 | 8 | 250 | 40 |
| CA-100 | 20 | 0.67 | 4.4 | 10 | 420 | <0.5 | <2 | 2.11 | 50.5 | 27 | 9 | 1024 | 5.49 | 50 | 0.15 | 10 | 0.29 | 1254 | 5 | 0.23 | 4 | 1270 | 282 | 10 | 44 | 0.85 | <10 | 460 | 142 | <10 | 8610 |
| CA-122 | 25 | 0.29 | 10.2 | 100 | 10 | <0.5 | <2 | 1.64 | 1.5 | 2622 | 2 | 2225 | 27.11 | <10 | 0.06 | <10 | 9.09 | 1600 | 1263 | 0.12 | 19 | <10 | 4 | <10 | 40 | 0.05 | <10 | 40 | <1 | <10 | 150 |
| CA/122 F | — | 1.17 | 2.0 | <10 | 20 | <0.5 | <2 | 14.00 | 4.5 | 45 | <1 | 692 | 20.62 | 30 | 30.01 | <10 | 0.02 | 179 | 100 | 0.24 | 37 | 220 | 122 | <10 | 47 | <0.01 | <10 | 390 | <1 | <10 | 820 |
| CA-124 | — | 1.04 | 7.0 | 20 | 10 | <0.5 | <2 | 4.15 | <0.5 | 1035 | 9 | 756 | 10.53 | 30 | 0.21 | <10 | 0.21 | 234 | 433 | 0.12 | 43 | 70 | <2 | <10 | 16 | 0.68 | <10 | <10 | 2 | 70 | 20 |
| CA-124 Q | 15 | 0.06 | 1.8 | 10 | 20 | <0.5 | <2 | 0.25 | <0.5 | 667 | <1 | 1275 | 11.61 | <10 | <0.01 | <10 | 0.06 | 37 | 36 | 0.01 | 43 | <10 | 6 | <10 | 2 | 0.02 | <10 | <10 | <1 | 600 | 10 |
| CA-125 | — | 0.16 | 0.2 | 10 | 107 | <0.5 | <2 | 3.06 | <0.5 | 62 | 17 | 314 | 1.79 | 10 | 0.01 | 10 | 0.22 | 467 | 1694 | 0.09 | 22 | 250 | 6 | 10 | 27 | 0.28 | <10 | <10 | 20 | 230 | 30 |
| CA-125 Q | 5 | 0.18 | 0.2 | 10 | 10 | <0.5 | <2 | 0.54 | <0.5 | 123 | <1 | 62 | 1.69 | 10 | <0.01 | <10 | 0.29 | 378 | 7 | 0.25 | 8 | 60 | 8 | <10 | 30 | <0.01 | <10 | <10 | 8 | 550 | 40 |
| CA-132 | — | 0.11 | 1.2 | <10 | 420 | <0.5 | <2 | 2.10 | <0.5 | 64 | <1 | 124 | 2.5 | <10 | <0.01 | <10 | 0.02 | 12 | 89 | 0.11 | <1 | 90 | 28 | <10 | 6 | 0.11 | <10 | <10 | <1 | 230 | 50 |
| CA-135 | — | 0.21 | 0.2 | <10 | 20 | 2.5 | <2 | 0.39 | <0.5 | 87 | <1 | 1 | 0.21 | 50 | <0.01 | 20 | <0.01 | 29 | 1 | 0.01 | <1 | <10 | 16 | <10 | 3 | 0.01 | <10 | <10 | <1 | 230 | <10 |
| CA-137 A | 10 | 0.22 | 0.4 | <10 | 20 | <0.5 | <2 | 0.21 | <0.5 | 102 | 5 | 247 | 2.06 | <10 | 0.15 | <10 | 0.27 | 123 | 2072 | 0.08 | 1 | 160 | 44 | 10 | 2 | 0.09 | <10 | <10 | 19 | 620 | 80 |
| CA-137 B | 1250 | 0.72 | 68.0 | 50 | 20 | <0.5 | <2 | 2.05 | 82.5 | 111 | 77 | 9999 | 6.04 | 20 | 0.11 | 20 | 0.71 | 539 | 164 | 0.09 | 40 | 730 | 452 | 10 | 22 | 0.26 | <10 | 390 | 30 | 60 | 1100 |
| CA-145 | — | 0.17 | 0.4 | 20 | 40 | <0.5 | <2 | 0.29 | <0.5 | 40 | 10 | 50 | 2.42 | <10 | 0.04 | <10 | 0.12 | 128 | 2971 | 0.21 | 2 | 690 | 40 | 10 | 4 | 0.21 | <10 | <10 | 18 | 200 | 20 |
| CA-146 | 35 | 0.50 | 2.0 | 50 | 250 | <0.5 | <2 | 0.54 | <0.5 | 43 | 14 | 30 | 5.30 | 20 | 0.42 | <10 | 0.43 | 383 | 7760 | 0.14 | 12 | 1040 | 280 | 40 | 19 | 0.68 | <10 | 80 | 19 | 80 | 50 |
| CA-147 | — | 0.12 | 1.0 | 20 | 62 | <0.5 | <2 | 6.22 | <0.5 | 171 | 4 | 18 | 2.12 | <10 | 0.02 | 10 | 0.12 | 34 | 2272 | 0.28 | 4 | 370 | 34 | 20 | 2 | 0.13 | <10 | <10 | 4 | 580 | 10 |
| CA-148 | 20 | 0.34 | 0.2 | 190 | 160 | <0.5 | <2 | 0.17 | 1.5 | 60 | 15 | 261 | 2.24 | <10 | 0.29 | 30 | 0.10 | 174 | <2 | 0.08 | 43 | 230 | 40 | <10 | 10 | 0.17 | <10 | <10 | 62 | 210 | 770 |
| CA-150 | — | 0.10 | 0.4 | <10 | <10 | <0.5 | <2 | <0.01 | <0.5 | 113 | <1 | 92 | 2.24 | <10 | <0.01 | <10 | 0.01 | 23 | 251 | 0.06 | <1 | <10 | 10 | <10 | 1 | 0.05 | <10 | <10 | 1 | 620 | <10 |
| CA-151 | 10 | 0.22 | 2.0 | <10 | 10 | <0.5 | <2 | 1.09 | 4.5 | 169 | 57 | 290 | 16.99 | 10 | <0.01 | <10 | 0.03 | 290 | 40 | 0.07 | 27 | 230 | <2 | <10 | 6 | 0.22 | <10 | <10 | 31 | 50 | 50 |
| CA-153 | — | 1.34 | 1.2 | 20 | 260 | 3.0 | <2 | 11.27 | <0.5 | 20 | 4 | 84 | 4.27 | 30 | 0.78 | <10 | 0.17 | 2502 | 9999 | 0.44 | 4 | 1090 | 182 | 100 | 3 | 0.07 | 10 | 90 | 24 | 210 | 170 |
| CA-153 B | <2 | 0.01 | 0.2 | <10 | 10 | <0.5 | <2 | 0.26 | <0.5 | 223 | <1 | 175 | 0.79 | <10 | <0.01 | <10 | <0.01 | 23 | 11 | <0.01 | 1 | <10 | <2 | <10 | <1 | <0.01 | <10 | <10 | <1 | 160 | <10 |
| CA-155 | — | 0.09 | 2.0 | 10 | 10 | <0.5 | <2 | 3.09 | 1.5 | 40 | 3 | 10 | 1.40 | <10 | <0.01 | <10 | 0.02 | 42 | 131 | 0.09 | <1 | <10 | 88 | <10 | 1 | 0.06 | <10 | <10 | 4 | 290 | 640 |
| CA-167 A | — | 0.12 | 0.2 | <10 | 470 | <0.5 | <2 | 1.07 | 2.0 | 156 | 3 | 34 | 0.89 | <10 | 0.02 | 20 | 1.04 | 494 | 10 | 0.02 | 5 | 110 | 124 | <10 | 44 | <0.01 | <10 | <10 | 12 | 250 | 640 |

Certified by ................

# Chemex Labs Ltd.

*Analytical Chemists — Geochemists — Registered Assayers*

212 Brooksbank Ave
North Vancouver, B.C.
Canada   V7J 2C1

Phone  (604) 984-0221
Telex  043-52597

**CERTIFICATE OF ANALYSIS**

TO : MEMORIAL UNIVERSITY OF NEWFOUNDLAND

DEPT. OF EARTH SCIENCES
ST. JOHN'S, NFLD.
A1B 3X5

CERT. # : A8619986-001-A
INVOICE # : 18618986
DATE : 13-OCT-86
P.O. # : NONE
N

Semi quantitative multi element ICP analysis

Nitric-Aqua-Regia digestion of 0.5 gm of material followed by ICP analysis. Since this digestion is incomplete for many minerals, values reported for Al, Sb, Ba, Be, Ca, Cr, Ga, La, Mg, K, Na, Sr, Tl, Ti, W and V can only be considered as semi-quantitative.

COMMENTS :
ATTN: DREIK WILTON

| Sample description | Au ppb FA+AA | Al % | Ag ppm | As ppm | Bi ppm | Be ppm | Bi ppm | Ca % | Cd ppm | Co ppm | Cr ppm | Cu ppm | Fe % | Ga ppm | K % | La ppm | Mg % | Mn ppm | Mo ppm | Na % | Ni ppm | P ppm | Pb ppm | Sb ppm | Sr ppm | Ti % | Tl ppm | U ppm | V ppm | W ppm | Zn ppm |
|---|---|---|---|---|---|---|---|---|---|---|---|---|---|---|---|---|---|---|---|---|---|---|---|---|---|---|---|---|---|---|---|
| CX-100A | <5 | 2.53 | 1.0 | <5 | 3990 | <0.5 | <2 | 2.38 | 4.0 | 41 | <1 | 261 | 7.8 | <10 | 1.85 | 30 | 1.64 | 2045 | <1 | 0.27 | 1 | 1320 | 102 | <5 | 29 | 0.85 | <10 | <10 | 95 | 30 | 1310 |
| CX-129 II | 690 | 0.32 | 52.0 | 18 | 10 | <0.5 | <2 | 2.50 | 6.5 | 45 | 4 | >9999 | 5.23 | 100 | 0.01 | 40 | 0.04 | 488 | 85 | 0.06 | 10 | 150 | 842 | <5 | 26 | 0.17 | <10 | 2264 | 5 | 125 | 688 |
| CX-160 | 5 | 1.25 | 2.2 | 15 | 40 | <0.5 | <2 | 2.93 | 1.0 | 62 | 4 | 1468 | 6.53 | <10 | 0.12 | 20 | 0.84 | 1139 | <1 | 0.15 | 26 | 2200 | 76 | <5 | 30 | 0.67 | <10 | <10 | 240 | 15 | 164 |
| LX-143 | <5 | 1.49 | 2.0 | <2 | 150 | 1.0 | <2 | 4.84 | 20.0 | 34 | 13 | 358 | 5.59 | 110 | 0.78 | 66 | 1.18 | 2827 | <1 | 0.40 | 8 | 200 | 536 | <5 | 273 | 0.15 | <10 | 1190 | 91 | 70 | 6754 |
| XP-1 | <5 | 0.24 | 0.6 | 5 | 30 | <0.5 | 2 | 1.50 | 1.5 | 18 | 1 | 62 | 3.49 | 20 | 0.04 | 70 | 0.21 | 419 | <1 | 0.09 | <1 | 90 | 390 | <5 | 5 | 0.23 | <10 | 150 | 98 | 50 | 212 |
| XP-2 | <5 | 0.29 | 0.4 | <5 | 280 | <0.5 | <2 | 0.49 | <0.5 | 28 | 1 | 89 | 3.61 | 10 | 0.15 | 60 | 0.33 | 813 | 7 | 0.10 | 3 | 320 | 500 | <5 | 53 | 0.25 | <10 | 150 | 64 | 65 | 568 |
| XP-3A | <5 | 0.40 | 3.0 | 20 | 120 | <0.5 | 12 | 0.99 | <0.5 | 69 | 9 | 339 | 2.42 | 170 | 0.04 | 40 | 0.14 | 259 | >9799 | 0.10 | 7 | 780 | 680 | 65 | 31 | 0.31 | 30 | 2450 | <1 | 125 | 90 |
| XP-3B | 400 | 0.46 | 42.0 | 25 | 30 | <0.5 | <2 | 2.70 | 9.0 | 53 | 10 | >9999 | 5.16 | 60 | 0.11 | 30 | 0.25 | 600 | 242 | 0.07 | 3 | 110 | 618 | <5 | 35 | 0.16 | <10 | 600 | 9 | 115 | 846 |
| XP-4A | 55 | 0.09 | 3.2 | <5 | 20 | <0.5 | 8 | 27.14 | 99.9 | 21 | 6 | 252 | 0.68 | 60 | <0.01 | <10 | 0.96 | 5899 | 7 | <0.01 | 2 | 230 | 1664 | <5 | <1 | <0.01 | <10 | <10 | 22 | 45 | >9999 |
| XP-4B | 20 | 0.25 | 2.4 | 10 | 100 | <0.5 | 8 | 25.86 | 99.9 | 31 | 2 | 401 | 1.24 | 70 | 0.11 | <10 | 1.34 | 5219 | 3 | 0.01 | <1 | 310 | 232 | <5 | <1 | <0.01 | <10 | 10 | 7 | 63 | >9999 |
| XP-4C | 50 | 0.55 | 6.6 | 15 | 80 | 2.0 | 20 | 24.71 | 99.9 | 51 | 68 | 1197 | 1.66 | 70 | 0.26 | <10 | 0.51 | 6273 | 6 | 0.03 | 6 | 410 | 318 | <5 | <1 | 0.02 | <10 | <10 | 252 | 110 | >9999 |
| XP-4B | 30 | 0.97 | 6.2 | 5 | 30 | 0.5 | 10 | 15.22 | 99.9 | 74 | 22 | 375 | 2.38 | 50 | 0.01 | <10 | 1.76 | 3223 | 3 | 0.02 | 5 | 630 | 164 | <5 | <1 | <0.01 | <10 | 110 | 91 | 60 | >9999 |
| XP-8 | <5 | 0.16 | 4.0 | 10 | 30 | <0.5 | 2 | 1.29 | <0.5 | 20 | 6 | 804 | 2.22 | 60 | <0.01 | 70 | 0.04 | 607 | 30 | 0.07 | 5 | 120 | 1506 | <5 | 15 | 0.04 | <10 | 680 | 9 | 165 | 208 |
| XP-10A | 30 | 1.94 | 6.0 | 5 | 760 | 2.5 | <2 | 3.37 | 0.5 | 31 | 3 | 862 | 5.31 | 10 | 1.08 | 30 | 1.34 | 1303 | 22 | 0.31 | 6 | 1450 | 152 | <5 | 28 | 1.75 | <10 | 40 | 141 | 5 | 610 |
| XP-10B | <5 | 2.04 | 0.3 | 75 | 830 | 4.5 | 40 | 3.25 | <0.5 | 32 | 40 | 42 | 5.53 | 2210 | 1.41 | 90 | 1.73 | 1293 | <1 | 0.27 | 3 | 900 | 8798 | <5 | 35 | 0.23 | <10 | >9999 | 62 | <5 | 884 |
| XP-10C | <5 | 1.54 | 0.7 | 5 | 560 | <0.5 | <2 | 2.10 | <0.5 | 28 | 6 | 36 | 4.13 | 20 | 0.49 | 20 | 1.15 | 951 | 5 | 0.22 | 6 | 2680 | 34 | <5 | 36 | 0.23 | <10 | 10 | 88 | 10 | 348 |
| XP-10D | 30 | 3.05 | 3.4 | 70 | 840 | 10.0 | 22 | 3.68 | <0.5 | 39 | 34 | 1667 | 3.89 | 1820 | 1.63 | 80 | 2.24 | 2078 | <1 | 0.51 | 5 | 330 | 7314 | <5 | 22 | 0.63 | <10 | >9999 | 227 | <5 | 2044 |
| XP-11A | <5 | 1.84 | 0.2 | 15 | 850 | <0.5 | 6 | 2.10 | <0.5 | 31 | 16 | 34 | 4.56 | 450 | 0.73 | 40 | 0.87 | 734 | <1 | 0.23 | 4 | 1160 | 1586 | <5 | 42 | 0.48 | <10 | 6720 | 52 | 10 | 226 |
| XP-11B | 30 | 0.93 | 1.6 | <5 | 70 | <0.5 | <2 | 2.51 | 1.5 | 66 | 3 | 1002 | 4.40 | 70 | 0.18 | 30 | 0.53 | 391 | 6 | 0.29 | 2 | 1710 | 386 | <5 | 22 | 0.49 | <10 | 990 | 32 | 25 | 258 |
| XP-15A | 25 | 1.93 | 2.6 | <5 | 3420 | 0.5 | <5 | 5.06 | 29.0 | 36 | 4 | 681 | 5.7 | 10 | 1.04 | 40 | 1.60 | 2248 | 4 | 0.36 | 5 | 740 | 524 | <5 | 113 | 1.16 | <10 | 200 | 99 | 90 | 6802 |
| XP-13B | <5 | 1.90 | 1.2 | <5 | 4020 | <0.5 | <2 | 4.69 | 9.0 | 36 | <1 | 56 | 4.77 | 60 | 1.11 | 30 | 1.54 | 2230 | <1 | 0.34 | 2 | 1360 | 930 | <5 | 179 | 0.72 | <10 | 800 | 70 | 40 | 1634 |
| XP016C | 790 | 0.66 | 3.0 | <5 | 30 | <0.5 | <2 | 4.57 | 0.5 | 73 | <1 | 5310 | 1.21 | 20 | 0.16 | <10 | 0.50 | 930 | <15 | 0.23 | 3 | 290 | 86 | <5 | 11 | 0.01 | <10 | <10 | 30 | 215 | 274 |
| XP-16CI | 570 | 1.23 | 2.4 | 5 | 50 | <0.5 | <2 | 8.71 | 0.5 | 74 | 5 | 5896 | 1.63 | 30 | 0.45 | <10 | 0.59 | 1124 | 175 | 0.50 | 6 | 290 | 76 | <5 | 13 | 0.01 | <10 | <10 | 28 | 310 | 322 |
| XP-17 | 30 | 0.17 | 2.6 | 10 | 10 | <0.5 | <2 | 0.10 | <0.5 | 564 | 2 | 476 | 20.59 | 20 | 0.05 | 30 | 0.07 | 204 | 2 | 0.02 | <1 | 450 | 22 | <5 | 6 | 0.33 | <10 | <10 | 16 | 175 | 38 |
| XP-18 | <5 | 0.25 | 0.2 | 5 | 30 | <0.5 | <2 | 3.99 | <0.5 | 64 | 2 | 241 | 1.96 | 10 | <0.01 | 30 | 0.66 | 617 | 2 | 0.04 | 3 | 440 | 16 | <5 | 10 | 0.11 | <10 | <10 | 16 | 100 | 80 |
| STD | <5 | 0.03 | 0.2 | <5 | 10 | <0.5 | <2 | 0.01 | <0.5 | 84 | <1 | <1 | 0.05 | <10 | <0.01 | 20 | <0.01 | 40 | <1 | <0.01 | <1 | 40 | <2 | <5 | 1 | 0.01 | <10 | <10 | 2 | 285 | <2 |
| T-1-2 | <5 | 0.22 | 0.2 | <5 | 20 | <0.5 | 2 | 0.07 | <0.5 | 83 | 9 | 70 | 0.75 | <10 | 0.15 | 30 | 0.17 | 289 | 29 | 0.11 | 4 | 260 | 2 | <5 | 2 | 0.11 | <10 | <10 | 13 | 525 | 2 |
| T-1-4 | <5 | 0.15 | 0.2 | <5 | <10 | <0.5 | <2 | 6.54 | <0.5 | 64 | 40 | 938 | 2.42 | 20 | 0.01 | 40 | 0.23 | 494 | 1 | 0.09 | 13 | 730 | 6 | <5 | 31 | 0.30 | <10 | <10 | 46 | 240 | 24 |
| T-9-E | 10 | 0.72 | 1.6 | <5 | 60 | <0.5 | 2 | 5.07 | <0.5 | 150 | 2 | 193 | 9.55 | 40 | 0.46 | <10 | 0.10 | 289 | 331 | 0.29 | 11 | 340 | 22 | <5 | 19 | 0.09 | <10 | 120 | 17 | 375 | 18 |
| T-8-A | 10 | 2.04 | 3.6 | 10 | 370 | <0.5 | 14 | 18.08 | <0.3 | 74 | 3 | 264 | 0.91 | 110 | 0.17 | <10 | 0.05 | 217 | >9999 | 1.65 | 1 | 560 | 244 | 25 | <1 | 0.06 | 10 | 860 | <1 | 220 | 22 |
| T-8-SF | 5 | 1.02 | 3.6 | <5 | 60 | <0.5 | <2 | 9.73 | 5.0 | 41 | 2 | 730 | 32.21 | 120 | 0.03 | <10 | 0.09 | 251 | 164 | 0.47 | 56 | 300 | 146 | <5 | <1 | <0.01 | <10 | 560 | 15 | <5 | 790 |

certified by ................

# Chemex Labs Ltd.

*Analytical Chemists*  *Geochemists*  *Registered Assayers*

212 Brookbank Ave.
North Vancouver, B.C.
Canada          V7J 2C1
Telephone: (604) 984-0221
Telex:        043 52597

## CERTIFICATE OF ANALYSIS

TO : MEMORIAL UNIVERSITY OF NEWFOUNDLAND

DEPT. OF EARTH SCIENCES
ST. JOHN'S, NFLD.
A1B 3X5

CERT. #   : A8611115-003-A
INVOICE # : I8611115
DATE      : 17-MAR-86
P.O. #    : NONE

Semi quantitative multi element ICP analysis

Nitric-Aqua-Regia digestion of 0.5 gm of
material followed by ICP analysis. Since this
digestion is incomplete for many minerals,
values reported for Al, Sb, Ba, Be, Ca, Cr,
Ga, La, Mg, K, Na, Sr, Ti, Tl, W and V can
only be considered as semi-quantitative.

COMMENTS :
ATTN: DR. DEREK WILTON ( SOME SAMPLES BROKEN IN

# Chemex Labs Ltd. [231]

Analytical Chemists • Geochemists • Registered Assayers

212 Brooksbank Ave.
North Vancouver, B.C.
Canada    V7J 2C1

Phone:    (604) 984-0221
Telex:    043-52597

## CERTIFICATE OF ANALYSIS

TO : MEMORIAL UNIVERSITY OF NEWFOUNDLAND

DEPT. OF EARTH SCIENCES
ST. JOHN'S, NFLD.
A1B 3X5

ATTN: DEREK WILTON

CERT. #   : A8618987-001-A
INVOICE # : 18618987
DATE      : 9-OCT-86
P.O. #    : NONE

| Sample description | Prep code | Au ppb FA+AA | | | | | |
|---|---|---|---|---|---|---|---|
| CM-10 | 214 | <5 | -- | -- | -- | -- | -- |
| CM-14 | 214 | <5 | -- | -- | -- | -- | -- |
| CM-22 | 214 | <5 | <5 -- | -- | -- | -- | -- |
| CM-24 | 214 | 10 | -- | -- | -- | -- | -- |
| CM-26 | 214 | 10 | -- | -- | -- | -- | -- |
| CM-45 | 214 | <5 | -- | -- | -- | -- | -- |
| CM-54A | 214 | <5 | -- | -- | -- | -- | -- |
| CM-54B | 214 | 45 | -- | -- | -- | -- | -- |
| CM-55 | 214 | 30 | -- | -- | -- | -- | -- |
| CM-58 | 214 | 10 | -- | -- | -- | -- | -- |
| CM-59 | 214 | 15 | -- | -- | -- | -- | -- |
| CM-64 | 214 | 10 | -- | -- | -- | -- | -- |
| CM-67 | 214 | 5 | -- | -- | -- | -- | -- |
| CM-69 | 214 | 15 | -- | -- | -- | -- | -- |
| CM-70 | 214 | <5 | -- | -- | -- | -- | -- |
| CM-78 | 214 | 25 | -- | -- | -- | -- | -- |
| CM-79 | 214 | 40 | -- | -- | -- | -- | -- |
| CM-99 | 214 | <5 | -- | -- | -- | -- | -- |
| CM-100 | 214 | 15 | 20 -- | -- | -- | -- | -- |
| CM-123 | 214 | 30 | 35 -- | -- | -- | -- | -- |
| CM-123F | 214 | 15 | -- | -- | -- | -- | -- |
| CM-124 | 214 | 85 | -- | -- | -- | -- | -- |
| CM-125 | 214 | <5 | -- | -- | -- | -- | -- |
| CM-132 | 214 | <5 | -- | -- | -- | -- | -- |
| CM-139A | 214 | 30 | 10 -- | -- | -- | -- | -- |
| CM-139B | 214 | 1600 | 1250 -- | -- | -- | -- | -- |
| CM-145 | 214 | 15 | -- | -- | -- | -- | -- |
| CM-146 | 214 | 40 | 35 -- | -- | -- | -- | -- |
| CM-147 | 214 | 15 | -- | -- | -- | -- | -- |
| CM-148 | 214 | 25 | 20 -- | -- | -- | -- | -- |
| CM-150 | 214 | <5 | -- | -- | -- | -- | -- |
| CM-153 | 214 | <5 | -- | -- | -- | -- | -- |
| CM-155 | 214 | 10 | -- | -- | -- | -- | -- |
| CM-167A | 214 | 35 | -- | -- | -- | -- | -- |
| CM-167B | 214 | 5 | -- | -- ?? | -- | -- | -- |
| CM-169 | 214 | <5 | -- | -- | -- | -- | -- |
| CM-173 | 214 | <5 | -- | -- | -- | -- | -- |
| CM-176 | 214 | <5 | -- | -- | -- | -- | -- |
| T-1-H | 214 | 10 | 20 -- | -- | -- | -- | -- |
| T-1-1 | 214 | 10 | -- | -- | -- | -- | -- |

VOI rev. 4/85

Certified by .../Hart Buchler.........

# Chemex Labs Ltd.

232.

212 Brooksbank Ave.
North Vancouver, B.C.
Canada        V7J 2C1

*Analytical Chemists* • *Geochemists* • *Registered Assayers*

Phone:   (604) 984-0221
Telex:    043-52597

**CERTIFICATE OF ANALYSIS**

TO : MEMORIAL UNIVERSITY OF NEWFOUNDLAND

DEPT. OF EARTH SCIENCES
ST. JOHN'S, NFLD.
A1B 3X5

CERT. #    : A8618987-002-A
INVOICE #  : 18618987
DATE       : 9-OCT-86
P.O. #     : NONE

ATTN: DEREK WILTON

| Sample description | Prep code | Au ppb FA+AA | | | | | |
|---|---|---|---|---|---|---|---|
| T-1-3 | 214 | <5 | 5 -- | -- | -- | -- | -- |
| T-1-6 | 214 | <5 | -- | -- | -- | -- | -- |
| T-2-3 | 214 | <5 | -- | -- | -- | -- | -- |
| T-2-4 | 214 | <5 | -- | -- | -- | -- | -- |
| T-3-1 | 214 | <5 | -- | -- | -- | -- | -- |
| T-3-4 | 214 | <5 | -- | -- | -- | -- | -- |
| T-4-1 | 214 | <5 | -- | -- | -- | -- | -- |
| T-5-1 | 214 | <5 | -- | -- | -- | -- | -- |
| T-5-2 | 214 | 30 | 30 -- | -- | -- | -- | -- |
| T-5-4 | 214 | <5 | -- | -- | -- | -- | -- |
| T-6A-1 | 214 | <5 | 10 -- | -- | -- | -- | -- |
| T-7-1 | 214 | <5 | -- | -- | -- | -- | -- |
| T-7-3 | 214 | <5 | -- | -- | -- | -- | -- |
| T-8-3 | 214 | 30 | 25 -- | -- | -- | -- | -- |
| T-8A-1 | 214 | <5 | -- | -- | -- | -- | -- |
| T-8B-1 | 214 | 20 | 50 -- | -- | -- | -- | -- |
| T-8B-2 | 214 | 60 | 50 -- | -- | -- | -- | -- |
| T-8B-2A | 214 | 15 | -- | -- | -- | -- | -- |
| W84-9A | 214 | <5 | -- | -- | -- | -- | -- |
| W84-9B | 214 | <5 | -- | -- | -- | -- | -- |
| W84-9C | 214 | <5 | -- | -- | -- | -- | -- |
| W84-9D | 214 | <5 | -- | -- | -- | -- | -- |
| W84-9D1 | 214 | <5 | -- | -- | -- | -- | -- |
| W84-9E | 214 | <5 | -- | -- | -- | -- | -- |
| W84-12A | 214 | <5 | -- | -- | -- | -- | -- |
| W84-16 | 214 | <5 | -- | -- | -- | -- | -- |
| W84-17C | 214 | <5 | -- | -- | -- | -- | -- |
| W84-18 | 214 | 25 | -- | -- | -- | -- | -- |
| W84-20C | 214 | <5 | -- | -- | -- | -- | -- |
| W84-21A | 214 | <5 | -- | -- | -- | -- | -- |
| W84-23B | 214 | <5 | -- | -- | -- | -- | -- |
| W84-24A | 214 | 35 | -- | -- | -- | -- | -- |
| W84-24A.1 | 214 | <5 | -- | -- | -- | -- | -- |
| W84-24B.2 | 214 | <5 | -- | -- | -- | -- | -- |
| W84-24C | 214 | <5 | -- | -- | -- | -- | -- |
| W84-24D | 214 | <5 | -- | -- | -- | -- | -- |
| W84-29D | 214 | MISSING | -- | -- | -- | -- | -- |
| W84-33 | 214 | <5 | -- | -- | -- | -- | -- |
| W84-33DUP | 214 | <5 | -- | -- | -- | -- | -- |
| W84-33.1 | 214 | 45 | -- | -- | -- | -- | -- |

VOI rev. 4/85

Certified by *Hart Buchler*

## Rare Earth Elements

## Monkey Hill Granite

| | CM-19 | | CM-28 | | CM-53 | |
|------|-------|---------|-------|---------|------|---------|
| | ppm | x chond. | ppm | x chond. | ppm | x chond. |
| Yb | 1.6 | 7.5 | 3.1 | 14.7 | 1.6 | 7.6 |
| Er | 2.1 | 10.0 | 3.0 | 13.9 | 2.2 | 10.4 |
| Dy | 2.7 | 8.5 | 4.2 | 13.1 | 1.7 | 5.3 |
| Gd | 1.1 | 4.3 | 2.7 | 10.3 | 0.7 | 2.7 |
| Eu | 0.4 | 5.7 | 0.4 | 5.3 | 0.0 | 0.0 |
| Sm | 1.0 | 5.1 | 2.4 | 12.2 | 0.2 | 1.2 |
| Nd | 7.3 | 12.2 | 31.0 | 52.0 | 6.9 | 11.6 |
| Pr | 1.1 | 9.7 | 9.7 | 83.3 | 1.9 | 16.2 |
| Ce | 33.6 | 41.3 | 114.2 | 140.4 | 21.8 | 26.8 |
| La | 11.2 | 35.6 | 57.4 | 182.3 | 10.5 | 33.3 |

| | CM-56 | | CM-121 | | CM-122 | |
|------|-------|---------|-------|---------|------|---------|
| | ppm | x chond. | ppm | x chond. | ppm | x chond. |
| Yb | 1.1 | 5.2 | 1.6 | 7.6 | 2.4 | 11.3 |
| Er | 1.4 | 6.6 | 1.8 | 8.4 | 2.7 | 12.5 |
| Dy | 1.7 | 5.1 | 2.1 | 6.6 | 4.6 | 14.2 |
| Gd | 1.2 | 4.8 | 1.5 | 6.0 | 3.5 | 13.4 |
| Eu | 0.0 | 0.0 | 0.0 | 0.0 | 0.2 | 2.5 |
| Sm | 0.8 | 4.0 | 0.0 | 0.0 | 4.0 | 20.5 |
| Nd | 4.6 | 7.7 | 6.5 | 10.8 | 37.3 | 62.5 |
| Pr | 0.7 | 6.3 | 1.2 | 10.5 | 9.0 | 77.4 |
| Ce | 16.9 | 20.8 | 22.0 | 27.1 | 98.8 | 121.6 |
| La | 6.4 | 20.3 | 8.2 | 26.2 | 48.6 | 154.3 |

| | CM-171 | | CM-171A | | CM-180 | |
|------|--------|---------|---------|---------|------|---------|
| | ppm | x chond. | ppm | x chond. | ppm | x chond. |
| Yb | 2.1 | 10.1 | 2.0 | 9.8 | 0.8 | 4.1 |
| Er | 2.2 | 10.2 | 2.1 | 9.9 | 1.8 | 8.5 |
| Dy | 4.9 | 15.0 | 2.6 | 8.1 | 1.5 | 4.6 |
| Gd | 5.1 | 19.6 | 1.1 | 4.4 | 0.3 | 1.0 |
| Eu | 0.6 | 8.4 | 0.1 | 2.1 | 0.1 | 2.0 |
| Sm | 6.4 | 32.3 | 0.9 | 4.4 | 0.3 | 1.3 |
| Nd | 39.4 | 66.0 | 15.5 | 25.9 | 7.8 | 13.0 |
| Pr | 9.4 | 81.0 | 4.6 | 39.3 | 2.6 | 22.3 |
| Ce | 99.4 | 122.2 | 46.3 | 57.0 | 25.7 | 31.6 |
| La | 50.1 | 159.0 | 26.0 | 82.6 | 14.1 | 44.7 |

234

CM-181

|     | ppm  | x chond. |
|-----|------|----------|
| Yb  | 0.9  | 4.4      |
| Er  | 2.0  | 9.3      |
| Dy  | 2.0  | 6.2      |
| Gd  | 0.9  | 3.4      |
| Eu  | 0.0  | 0.0      |
| Sm  | 1.2  | 6.1      |
| Nd  | 9.6  | 16.1     |
| Pr  | 3.2  | 27.2     |
| Ce  | 32.9 | 40.5     |
| La  | 18.7 | 59.4     |

## Upper Aillik Group Rhyolites

| | CM-75 | | CM-97 | |
|---|---|---|---|---|
| | ppm | x chond. | ppm | x chond. |
| Yb | 2.2 | 10.6 | 12.6 | 57.2 |
| Er | 2.9 | 13.5 | 13.4 | 59.7 |
| Dy | 4.6 | 14.3 | 20.5 | 59.9 |
| Gd | 5.4 | 21.0 | 23.8 | 86.1 |
| Eu | 0.2 | 3.0 | 0.3 | 4.0 |
| Sm | 7.0 | 35.3 | 24.4 | 120.1 |
| Nd | 41.0 | 68.7 | 130.3 | 206.9 |
| Pr | 10.4 | 90.0 | 34.1 | 262.2 |
| Ce | 94.7 | 116.5 | 343.0 | 397.4 |
| La | 50.6 | 160.6 | 185.0 | 562.4 |

## Gossans and Carbonate Vein-hosted
## Mineralization

| | CM-24 | | CM-65 | | CM-79 | |
|----|-------|----------|-------|----------|-------|----------|
| | ppm | x chond. | ppm | x chond. | ppm | x chond. |
| Yb | 6.8 | 30.8 | 2.1 | 10.1 | 7.0 | 33.7 |
| Er | 11.3 | 50.0 | 8.1 | 37.9 | 13.9 | 65.4 |
| Dy | 21.3 | 62.0 | 14.0 | 43.2 | 22.7 | 69.9 |
| Gd, | 24.2 | 87.6 | 16.9 | 65.3 | 20.3 | 78.3 |
| Eu | 3.5 | 45.6 | 3.6 | 50.3 | 4.3 | 59.3 |
| Sm | 28.7 | 141.3 | 17.5 | 89.0 | 21.7 | 110.0 |
| Nd | 102.5 | 162.7 | 121.8 | 204.0 | 148.9 | 249.4 |
| Pr | 21.6 | 165.8 | 28.3 | 244.0 | 36.7 | 316.2 |
| Ce | 153.0 | 176.9 | 254.5 | 313.0 | 369.4 | 454.4 |
| La | 64.0 | 194.4 | 110.9 | 352.0 | 172.8 | 548.7 |

| | T-1-3 | | T-3-2 | | T-5-1 | |
|----|-------|----------|-------|----------|-------|----------|
| | ppm | x chond. | ppm | x chond. | ppm | x chond. |
| Yb | 1.5 | 5.7 | 3.1 | 14.2 | 3.8 | 17.2 |
| Er | 2.8 | 13.4 | 6.0 | 26.9 | 6.8 | 30.3 |
| Dy | 5.9 | 18.3 | 14.7 | 42.9 | 14.3 | 41.7 |
| Gd | 4.6 | 17.9 | 20.7 | 75.1 | 16.0 | 58.1 |
| Eu | 1.3 | 17.8 | 3.3 | 43.2 | 2.3 | 30.2 |
| Sm | 5.4 | 27.5 | 30.3 | 148.9 | 19.6 | 96.7 |
| Nd | 34.0 | 56.9 | 149.0 | 236.9 | 90.1 | 143.0 |
| Pr | 5.1 | 43.6 | 38.3 | 294.9 | 24.4 | 187.0 |
| Ce | 41.6 | 51.1 | 274.6 | 317.4 | 153.2 | 177.1 |
| La | 10.3 | 32.6 | 87.4 | 265.6 | 53.9 | 164.0 |

| | T-8-1 | |
|----|-------|----------|
| | ppm | x chond. |
| Yb | 4.0 | 18.1 |
| Er | 6.2 | 27.4 |
| Dy | 12.3 | 35.9 |
| Gd | 14.0 | 50.8 |
| Eu | 3.5 | 45.4 |
| Sm | 19.1 | 93.9 |
| Nd | 92.2 | 146.3 |
| Pr | 24.1 | 185.3 |
| Ce | 227.7 | 262.4 |
| La | 110.0 | 334.5 |

## Radioactive Mineral Occurrences

| | RP-1 | | RP-3A | | RP-8 | |
|---|---|---|---|---|---|---|
| | ppm | x chond. | ppm | x chond. | ppm | x chond. |
| Yb | 6.5 | 29.6 | 12.7 | 57.6 | 9.5 | 43.4 |
| Er | 5.2 | 23.0 | 15.5 | 68.8 | 10.1 | 44.8 |
| Dy | 7.2 | 21.1 | 26.8 | 78.1 | 17.1 | 49.9 |
| Gd | 8.3 | 29.9 | 26.4 | 95.5 | 16.0 | 57.9 |
| Eu | 0.8 | 10.1 | 5.0 | 64.4 | 1.6 | 21.1 |
| Sm | 7.4 | 36.1 | 28.9 | 142.4 | 17.5 | 86.4 |
| Nd | 58.5 | 92.9 | 106.3 | 168.8 | 78.7 | 124.9 |
| Pr | 17.2 | 132.5 | 24.4 | 187.5 | 22.6 | 173.7 |
| Ce | 174.3 | 201.5 | 163.6 | 189.2 | 197.5 | 228.4 |
| La | 90.6 | 275.5 | 50.3 | 153.0 | 107.4 | 326.4 |

| | RP-10A | | RP-11 | | CM-58 | |
|---|---|---|---|---|---|---|
| | ppm | x chond. | ppm | x chond. | ppm | x chond. |
| Yb | 8.0 | 36.3 | 22.8 | 103.4 | 702.5 | 3377.4 |
| Er | 10.6 | 47.1 | 19.1 | 84.9 | 1013.6 | 4758.6 |
| Dy | 17.9 | 52.3 | 20.0 | 58.3 | 1210.9 | 3725.8 |
| Gd | 18.9 | 68.3 | 14.5 | 52.5 | 314.7 | 1215.2 |
| Eu | 5.5 | 71.7 | 5.5 | 71.4 | 29.5 | 408.2 |
| Sm | 19.5 | 96.3 | 13.7 | 67.7 | 126.5 | 642.4 |
| Nd | 95.2 | 151.1 | 64.1 | 101.8 | 328.5 | 550.2 |
| Pr | 23.4 | 180.0 | 14.9 | 114.8 | 61.6 | 527.8 |
| Ce | 185.3 | 214.2 | 111.2 | 128.6 | 590.6 | 726.4 |
| La | 88.2 | 268.1 | 54.1 | 164.4 | 205.5 | 652.3 |

| | CM-59 | | CM-100 | | CM-139B | |
|---|---|---|---|---|---|---|
| | ppm | x chond. | ppm | x chond. | ppm | x chond. |
| Yb | 43.1 | 195.9 | 19.4 | 88.1 | 5.9 | 28.5 |
| Er | 40.4 | 179.4 | 19.3 | 85.7 | 11.5 | 53.9 |
| Dy | 39.4 | 114.9 | 23.5 | 68.6 | 24.9 | 76.6 |
| Gd | 22.8 | 82.7 | 16.9 | 61.3 | 20.4 | 78.8 |
| Eu | 7.1 | 92.6 | 4.5 | 58.8 | 3.4 | 47.4 |
| Sm | 22.2 | 109.6 | 13.6 | 66.9 | 22.0 | 111.7 |
| Nd | 112.0 | 177.8 | 43.4 | 68.8 | 74.3 | 124.5 |
| Pr | 29.2 | 224.9 | 10.2 | 78.7 | 14.5 | 125.2 |
| Ce | 255.0 | 294.8 | 71.5 | 82.7 | 124.9 | 153.6 |
| La | 123.1 | 374.0 | 33.9 | 103.1 | 44.1 | 140.1 |

Fluorite Veins

| | CM-123F | | CM-153 | | 169 | |
|---|---|---|---|---|---|---|
| | ppm | x chond. | ppm | x chond. | ppm | x chond. |
| Yb | 1.9 | 9.0 | 6.9 | 31.2 | 2.4 | 11.5 |
| Er | 6.4 | 30.2 | 10.8 | 48.1 | 2.8 | 13.3 |
| Dy | 10.8 | 33.3 | 27.4 | 79.7 | 5.9 | 18.3 |
| Gd | 6.1 | 23.4 | 38.3 | 138.6 | 5.2 | 19.9 |
| Eu | 0.9 | 12.0 | 2.6 | 34.1 | 0.4 | 5.1 |
| Sm | 3.6 | 18.1 | 33.1 | 163.2 | 2.1 | 10.9 |
| Nd | 20.6 | 34.6 | 171.1 | 272.5 | 25.9 | 43.4 |
| Pr | 2.8 | 24.0 | 46.9 | 360.7 | 2.9 | 24.6 |
| Ce | 30.6 | 37.7 | 43.5 | 505.8 | 57.1 | 70.2 |
| La | 11.1 | 35.4 | 237.2 | 721.1 | 29.5 | 93.8 |

| | T-8-F | | T-8-M | | T-8B-1 | |
|---|---|---|---|---|---|---|
| | ppm | x chond. | ppm | x chond. | ppm | x chond. |
| Yb | 5.0 | 22.5 | 4.2 | 19.0 | 13.4 | 60.8 |
| Er | | | 12.6 | 55.9 | 19.4 | 86.3 |
| Dy | 11.2 | 32.8 | 35.4 | 103.3 | 36.2 | 105.5 |
| Gd | 7.8 | 28.2 | 37.8 | 137.1 | 29.7 | 107.6 |
| Eu | 1.2 | 15.7 | 3.2 | 41.2 | 0.0 | 0.0 |
| Sm | 8.5 | 41.8 | 32.7 | 161.0 | 13.1 | 64.5 |
| Nd | 30.4 | 48.2 | 162.6 | 258.0 | 92.4 | 146.5 |
| Pr | 7.3 | 56.4 | 38.3 | 294.3 | 18.9 | 145.6 |
| Ce | 54.0 | 62.4 | 305.4 | 353.1 | 186.5 | 215.6 |
| La | 20.5 | 62.2 | 88.6 | 269.3 | 74.9 | 227.6 |

# Appendix II

## Microprobe Techniques

Electron microprobe analyses were carried on various alteration mineral assemblages on the Jeo1 JXA-50A electron microanalyser with Krisel control by a PDP-11 mini-computer. Operating conditions were: accelerating voltage of 15 Kv, beam current approximately 0.22 microamps, beam size 1-2 micrometres, and a counting rate up to 60,000 with a default time of 30 seconds. The Alpha correction program was used for the silicate analyses. Analyses were considered acceptable if totals varied between 98 and 102%, except in the case of hydrous minerals.

## Hornblende

| Sample No. | CM-59 | CM-58 | CM-100 |
|---|---|---|---|
| Na | 2.15 | 2.05 | 1.80 |
| Mg | 13.00 | 10.76 | 9.29 |
| Al | 5.80 | 6.92 | 6.48 |
| Si | 48.93 | 45.11 | 46.50 |
| K | 0.66 | 1.17 | 0.71 |
| Ca | 10.90 | 10.55 | 10.71 |
| Ti | 0.21 | 0.64 | 0.37 |
| Cr | 0.01 | 0.00 | 0.02 |
| Mn | 1.72 | 1.07 | 1.06 |
| Fe(+2) | 14.56 | 18.33 | 20.95 |
| Ni | 0.03 | 0.01 | 0.02 |
| Total | 97.97 | 97.23 | 97.91 |
| n | 5 | 5 | 5 |

## Andradite Garnet

| Sample No. | T-8B-2 | CM-125 | T-1-1 | T-3-4 | CM-123 | T-4-1 |
|---|---|---|---|---|---|---|
| Na | 0.01 | 0.00 | 0.02 | 0.02 | 0.02 | 0.01 |
| Mg | 0.01 | 0.02 | 0.05 | 0.02 | 0.02 | 0.01 |
| Al | 1.34 | 0.91 | 4.63 | 3.87 | 4.15 | 1.09 |
| Si | 36.79 | 37.65 | 36.59 | 37.78 | 37.11 | 36.51 |
| K | 0.00 | 0.00 | 0.01 | 0.00 | 0.16 | 0.01 |
| Ca | 31.19 | 32.06 | 31.75 | 32.12 | 29.34 | 31.31 |
| Ti | 0.30 | 0.01 | 0.41 | 0.18 | 0.04 | 1.10 |
| Cr | 0.02 | 0.02 | 0.02 | 0.03 | 0.01 | 0.07 |
| Mn | 0.20 | 0.53 | 0.51 | 0.75 | 1.68 | 0.17 |
| Fe(+2) | 27.88 | 28.28 | 26.55 | 24.40 | 27.40 | 30.22 |
| Ni | 0.01 | 0.00 | 0.01 | 0.02 | 0.01 | 0.01 |
| Total | 101.09 | 99.49 | 100.58 | 99.15 | 99.90 | 100.45 |
| n | 5 | 5 | 5 | 5 | 5 | 5 |

## Diopside-Hedenbergite

| Sample No. | T-1-1 | T-3-4 | CM-125 | CM-24 | T-1-M | CM-139B | CM-59 |
|---|---|---|---|---|---|---|---|
| Na | 0.68 | 0.63 | 0.91 | 1.23 | 0.48 | 1.32 | 0.93 |
| Mg | 9.06 | 9.02 | 10.01 | 9.00 | 8.47 | 9.82 | 10.93 |
| Al | 0.52 | 0.23 | 0.47 | 0.95 | 0.92 | 0.60 | 0.72 |
| Si | 52.17 | 53.39 | 53.70 | 52.61 | 51.68 | 53.17 | 53.14 |
| K | 0.00 | 0.00 | 0.00 | 0.00 | 0.03 | 0.01 | 0.00 |
| Ca | 21.97 | 21.57 | 21.69 | 21.07 | 21.38 | 21.54 | 21.11 |
| Ti | 0.44 | 0.00 | 0.01 | 0.02 | 0.03 | 0.03 | 0.05 |
| Cr | 0.03 | 0.02 | 0.03 | 0.03 | 0.02 | 0.04 | 0.02 |
| Mn | 0.53 | 0.78 | 0.89 | 0.77 | 0.81 | 0.60 | 2.59 |
| Fe(+2) | 14.79 | 15.54 | 13.44 | 15.32 | 17.14 | 13.38 | 10.08 |
| Ni | 0.02 | 0.06 | 0.04 | 0.03 | 0.05 | 0.02 | 0.01 |
| Total | 100.22 | 101.26 | 101.21 | 101.04 | 101.02 | 100.52 | 99.60 |
| n | 5 | 5 | 5 | 5 | 5 | 5 | 5 |

## Appendix 3

### Scanning Electron Microscope Ore Mineral Identification

Polished, carbon-coated, thin sections were examined in Hitachi S570 scanning electron microscope at an accelerating voltage of 15 Kv. Backscattered electron imaging was obtained with a GW Electronic type 113 solid state Backscattered Electron Detector. X-ray analysis was performed on beam spot mode with a Tracer Northern 5500 Energy Dispersive X-ray Analyzer equipped with a spectral resolution of 145 eV. Detector/sample positioning was set at 30' take-off angle.

Backscattered electron images were recorded on Polaroid type 665 positive/negative film.
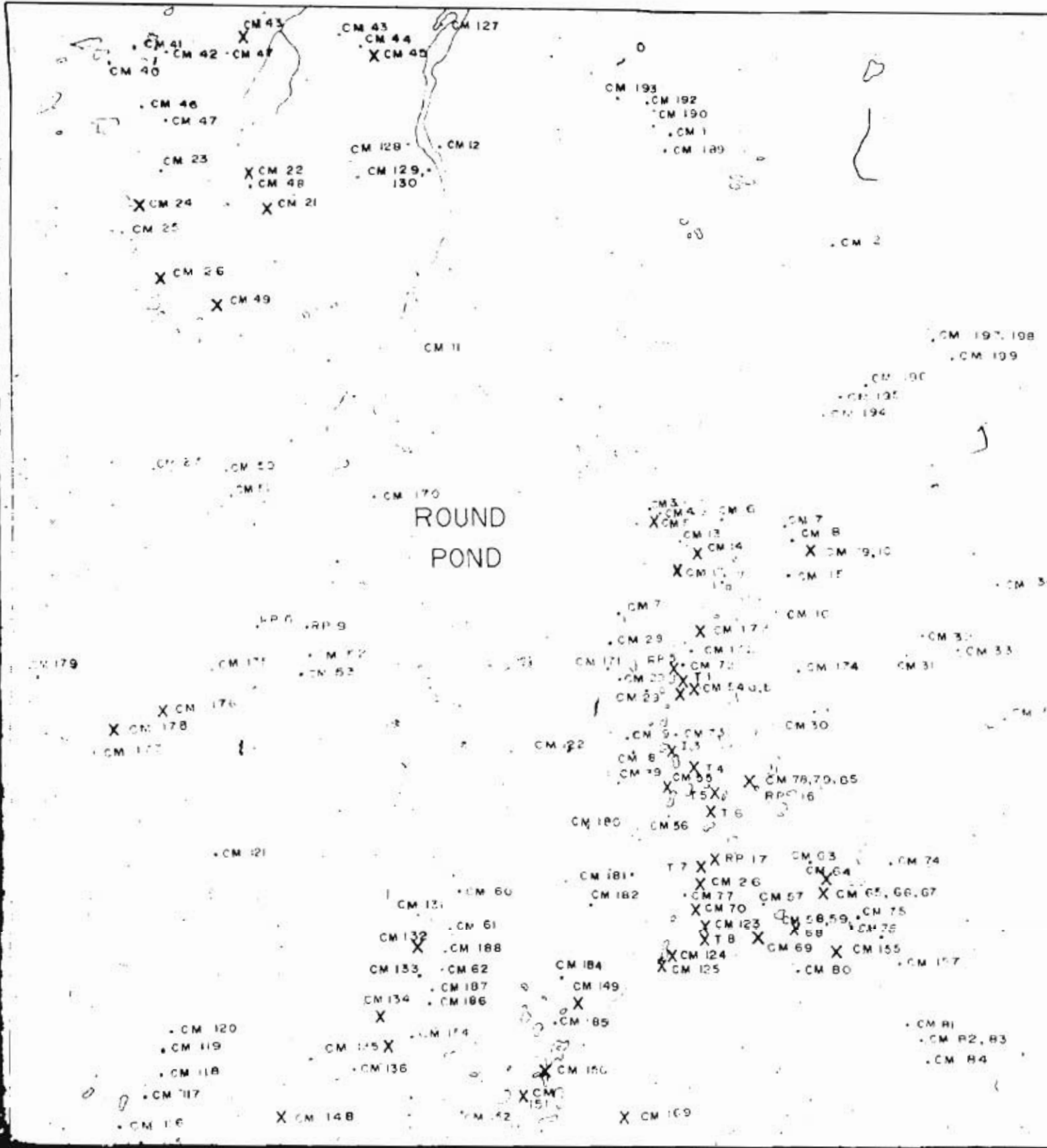
## Appendix IV

Ar/Ar age dating was performed for a fee at the University of Maine, under the supervision of Dr. D. Lux. Fresh hornblende mineral seperates were collected from mineralized samples for the analyses.

The technique involves irradiation of the sample by neutrons in a nuclear reactor. $^{39}$K is thus converted to $^{39}$Ar and the argon is then released from the sample fractionally by stepwise heating (See table 5).

The stepwise fractions of total $^{39}$Ar and radiogenic $^{40}$Ar were determined with a mass spectrometer and a plateau age was calculated.

**Table 5:**  Ar/Ar age dating data from stepwise temperatures

| Temp °C | 40Ar / 39Ar | 37Ar / 39Ar | 36Ar / 39Ar | Moles 39Ar | 40Ar %Total | %Ar40 Rad | K/Ca | Age (Ma) | |
|---|---|---|---|---|---|---|---|---|---|
| | | CM-58-B | | | | | J = .003917 | | |
| 925 | 1145.21 | 5.1500 | 0.7916 | 0.6 | 1.4 | 79.6 | 0.0948 | 2747 +/- | 89 |
| 1000 | 456.36 | 3.3922 | 0.1342 | 1.1 | 2.8 | 91.4 | 0.1441 | 1750 +/- | 21 |
| 1075 | 258.47 | 1.1709 | 0.0182 | 4.9 | 12.0 | 97.9 | 0.4181 | 1244 +/- | 11 |
| 1100 | 375.38 | 0.4058 | 0.0372 | 3.4 | 8.4 | 97.1 | 1.2072 | 1600 +/- | 21 |
| 1125 | 372.62 | 0.4722 | 0.0130 | 5.0 | 12.2 | 99.0 | 1.0373 | 1613 +/- | 14 |
| 1145 | 369.98 | 0.5495 | 0.0095 | 7.0 | 17.1 | 99.2 | 0.8913 | 1608 +/- | 12 |
| FUSE | 363.71 | 0.7597 | 0.0084 | 18.9 | 46.2 | 99.3 | 0.6446 | 1591 +/- | 12 |
| TOTAL | | | | 41.0 | 100.0 | | | 1576 | |
| PLATEAU AGE | | | | | | | | 1603 +/- | 27 |
| | | CM-70-B | | | | | J = .003921 | | |
| 825 | 2218.48 | 2.4180 | 1.4179 | 0.6 | 4.0 | 81.1 | 0.2023 | 3767 +/- | 158 |
| 940 | 821.06 | 1.7601 | 0.6458 | 0.5 | 3.2 | 76.8 | 0.2780 | 2247 +/- | 169 |
| 1000 | 694.90 | 0.7268 | 0.3420 | 0.4 | 2.8 | 85.5 | 0.6738 | 2170 +/- | 120 |
| 1045 | 532.49 | 0.9038 | 0.1260 | 0.9 | 5.6 | 93.0 | 0.5418 | 1948 +/- | 40 |
| 1080 | 426.34 | 0.5964 | 0.0741 | 1.2 | 8.0 | 94.9 | 0.8212 | 1714 +/- | 63 |
| 1115 | 360.05 | 0.4466 | 0.0315 | 2.2 | 13.9 | 97.4 | 1.0968 | 1561 +/- | 29 |
| FUSE | 356.62 | 1.0776 | 0.0145 | 9.7 | 62.5 | 98.8 | 0.4543 | 1566 +/- | 12 |
| TOTAL | | | | 15.5 | 100.0 | | | 1725 | |
| PLATEAU AGE | | | | | | | | 1564 +/- | 15 |

## References Cited in Appendices

Fryer, B.J., 1977. Rare earth evidence in iron formation for changing oxidation states. Geochim. Cosmochim. Acta, vol. 41, pp 361-367.

Flanagan, F.J., 1070. Sources of geochemical standards - II. Geochim. Cosmochim. Acta, vol. 34, pp 121-125.

Langmhyr, F.J., and Paus, P.E., 1968. The analysis of inorganic siliceous materials by atomic absorption spectrophotometry and the hydrofluoric acid decomposition technique. Pt. I. The analysis of silicate rocks. Anal. Chimica Acta, vol. 43, pp. 397-408.

Longerich, H.P., and Veinott, G., 1986. Study of precision and accuracy of XRF data obtained in the Department of Earth Sciences and Center for Earth Resources Research at Memorial University of Newfoundland. Unpub. Report, Dept. of Earth Sciences, Memorial University of Newfoundland, 20 p.

Shapiro, L., and Brannock, W.W., 1962. Rapid analysis of silicate, carbonate, and phosphate rocks. U.S. Geol. Sur. Bull., 1144A, pp. 31-33.

N

.CM 197, 198
.CM 199
190

CM 10
.CM 17

.CM 34

CM 3.
.CM 33
CM 51

CM 18

M 74
6, 67

CM 1:7

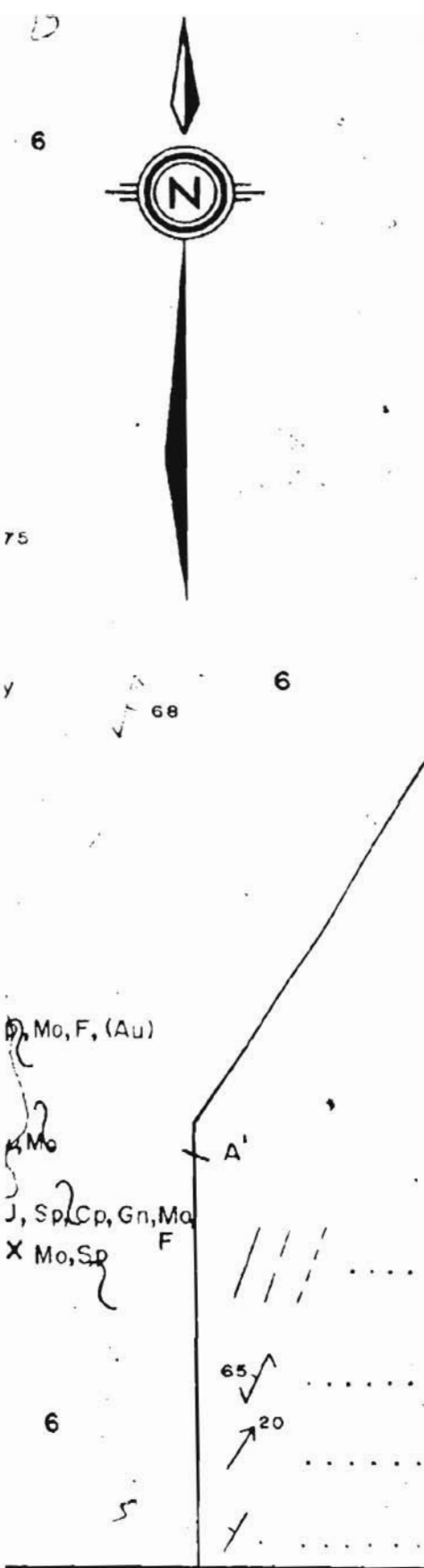CM 81
.CM 82, 83
.CM 84

LABRADOR

Location
of
Study Area

Grenville Province

Central Mineral Belt

ROUND POND
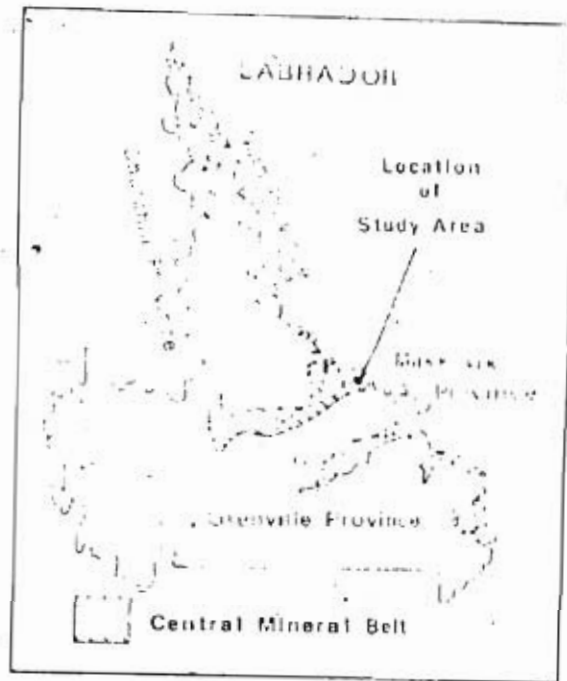
## HELIKIAN

8    Monkey Hill Granite : quartz – feldspar leucocratic monzogranite.

## APHEBIAN

# UPPER AILLIK GROUP

7    Subvolcanic Quartz-feldspar Porphyritic Rhyolite.

6    Quartz-porphyritic, banded rhyolitic flows, tuffs and ignimbrites.

5    Banded rhyolitic flows and pyroclastic tuffs.

4    Metabasalt flows and related subvolcanic amphibolitic sills.

3    Felsic volcanic conglomerate agglomerate, with minor intermixed felsic tuffs.
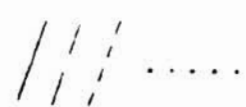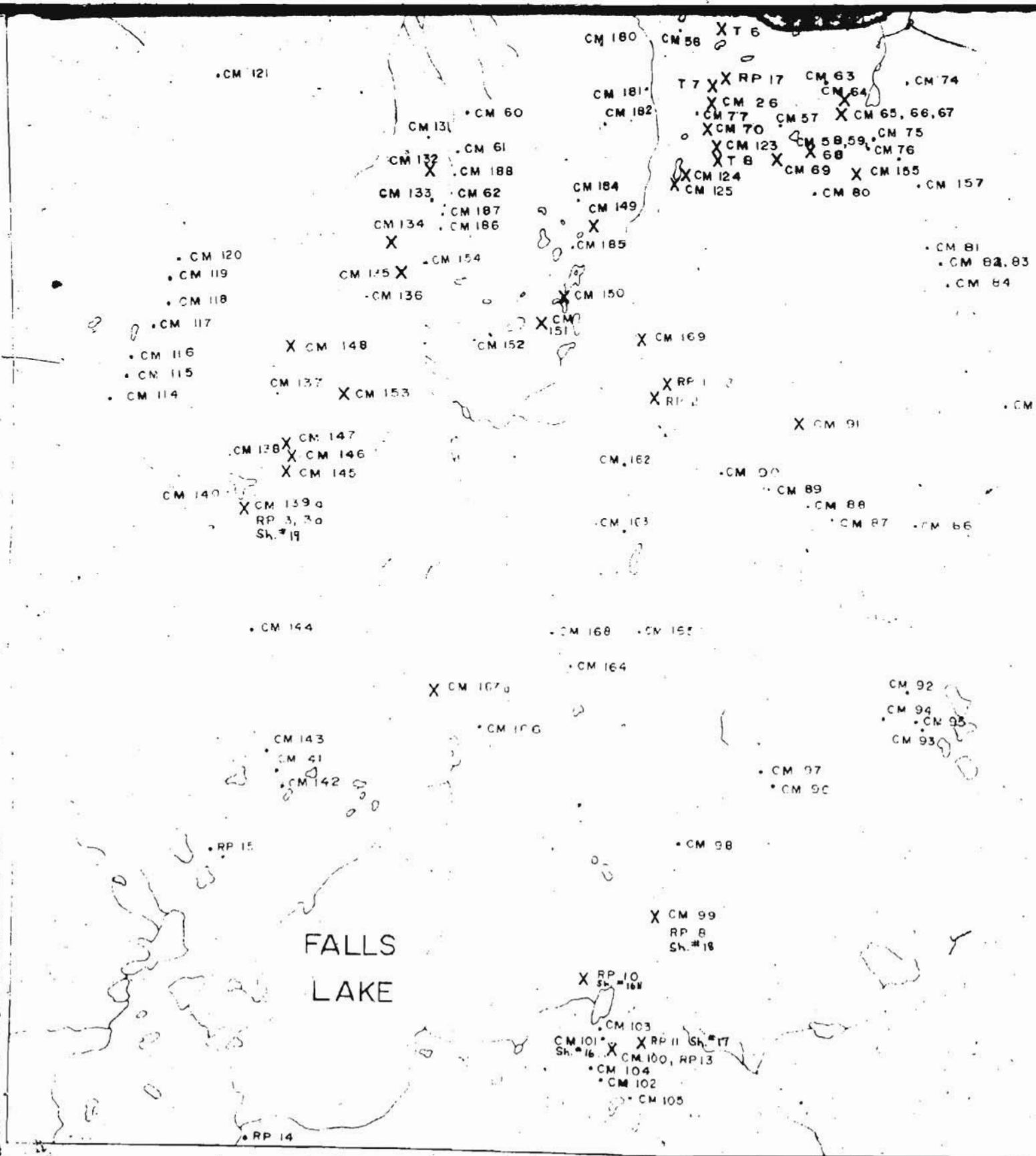
2    Volcanoclastic sediments, minor rhyolitic and dacitic flows.

1    Recrystallized felsic tuffs.

## SYMBOLS

///  ..... Geological Contact
(defined, approximate, assumed)

65 ⋮ ....... S type fabric (D₁) (inclined)

⤴20 ....... Clast Lineation (inclined)

／ ....... Attitude volcanic strata (inclined)

## ABBREVIATIONS

Ag — Silver
Au — Gold
Cp — Chalcopyrite
F — Flourite
Gn — Galena
Mo — Molybdenite
Py — Pyrite
Sc — Scheelite

Mo, F, (Au)

Mo

J, Sp, Cp, Gn, Mo
X Mo, Sp   F

A'

6

75

68

6

6

6

Grenville Province

Central Mineral Belt

83

CM 85
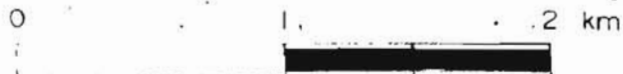
## SYMBOLS

•    Outcrop Sample
     (Sample No.)

✳    Mineralized Sample (grab)
     (Sample No.; Trench No.)

## SAMPLE LOCATION MAP
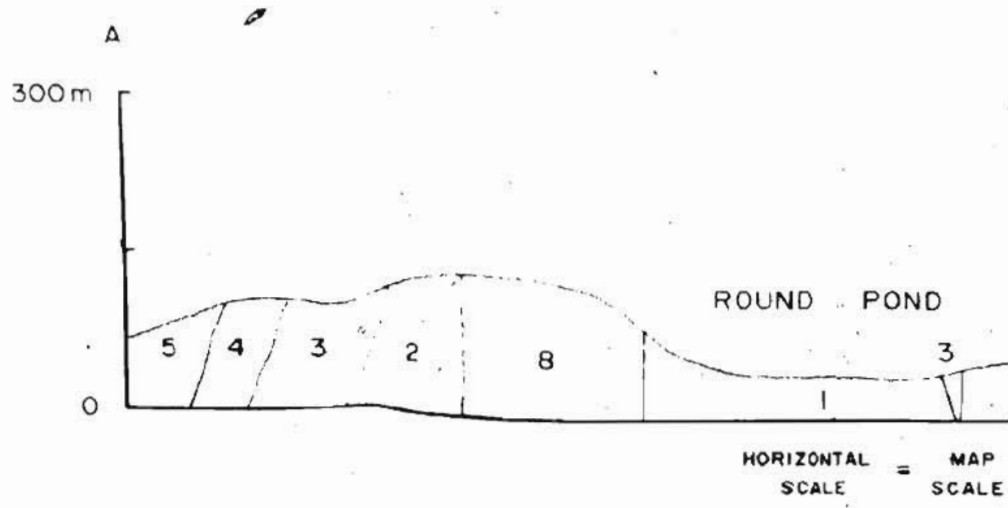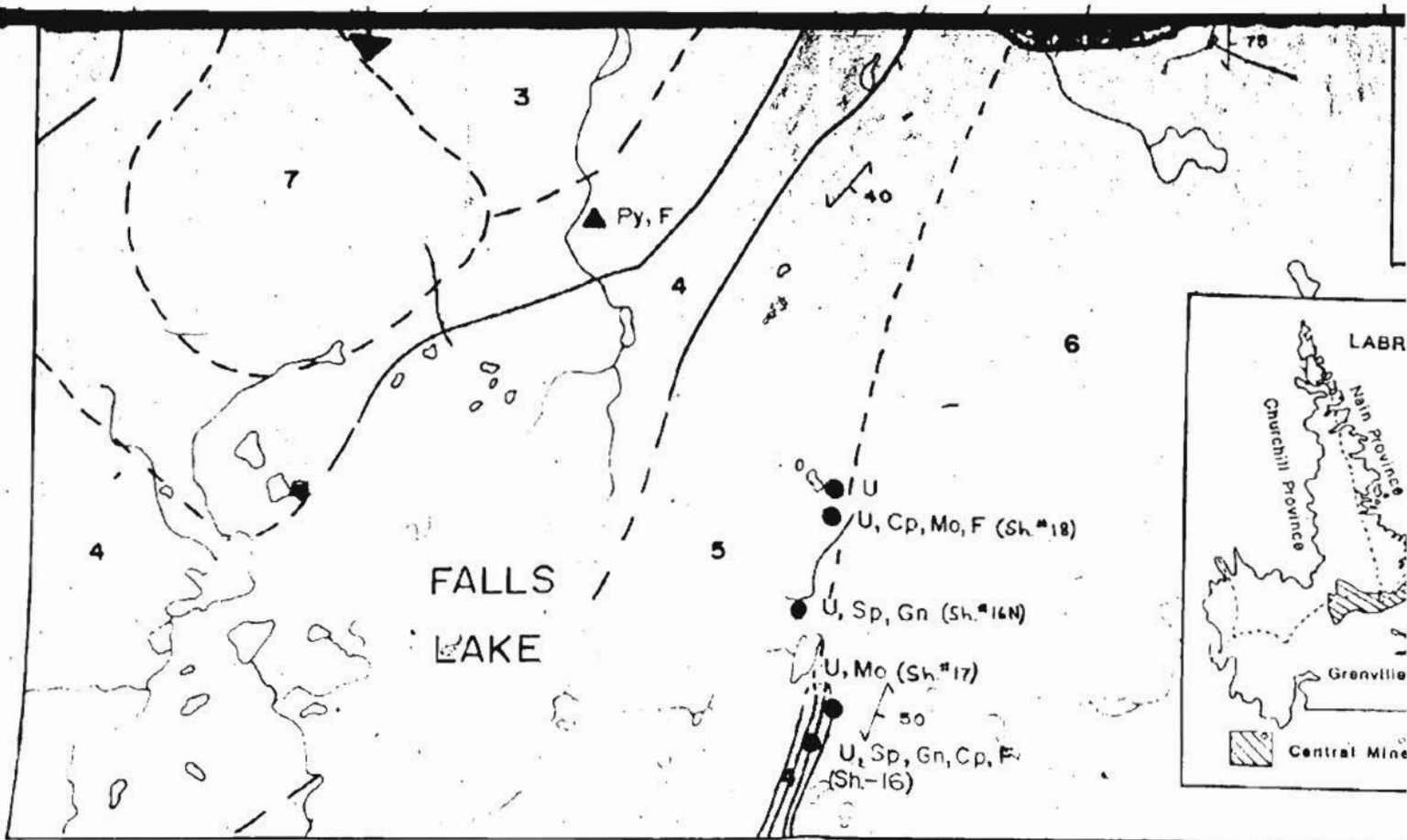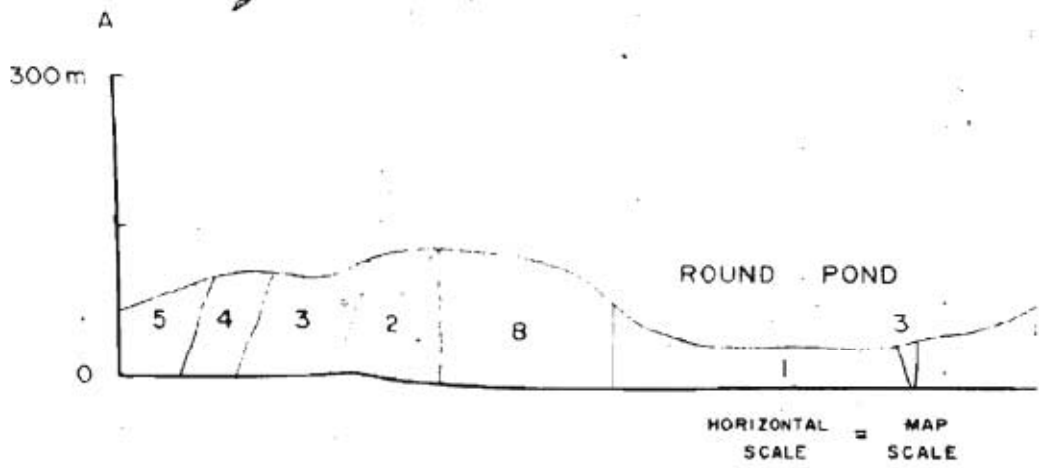
### ROUND POND AREA
### LABRADOR.

0         1.        .2 km

Scale: 1:25,000

Date: March, 1988      By: C.S. Mac Dougall

MAP 2

3

7

4

▲ Py, F

4

6

● U

● U, Cp, Mo, F (Sh.#18)

5

● U, Sp, Gn (Sh.#16N)

FALLS
LAKE

U, Mo (Sh.#17)

● ↙ 50

● U, Sp, Gn, Cp, F
(Sh-16)

A

LABR

Churchill Province

Nain Province

Grenville

Central Mine

A

300 m

ROUND POND

5  4  3  2  8  3

0  1

HORIZONTAL = MAP
SCALE    SCALE

GEOLOGICAL CROSS—SECTION OF THE

FALLS LAKE

U
U, Cp, Mo, F (Sh.#18)
U, Sp, Gn (Sh.#16N)
U, Mo (Sh#17)
U, Sp, Gn, Cp, F (Sh-16)

Py, F

LABRADOR

Churchill Province
Nain Province
Granville Province

Central Mineral Belt
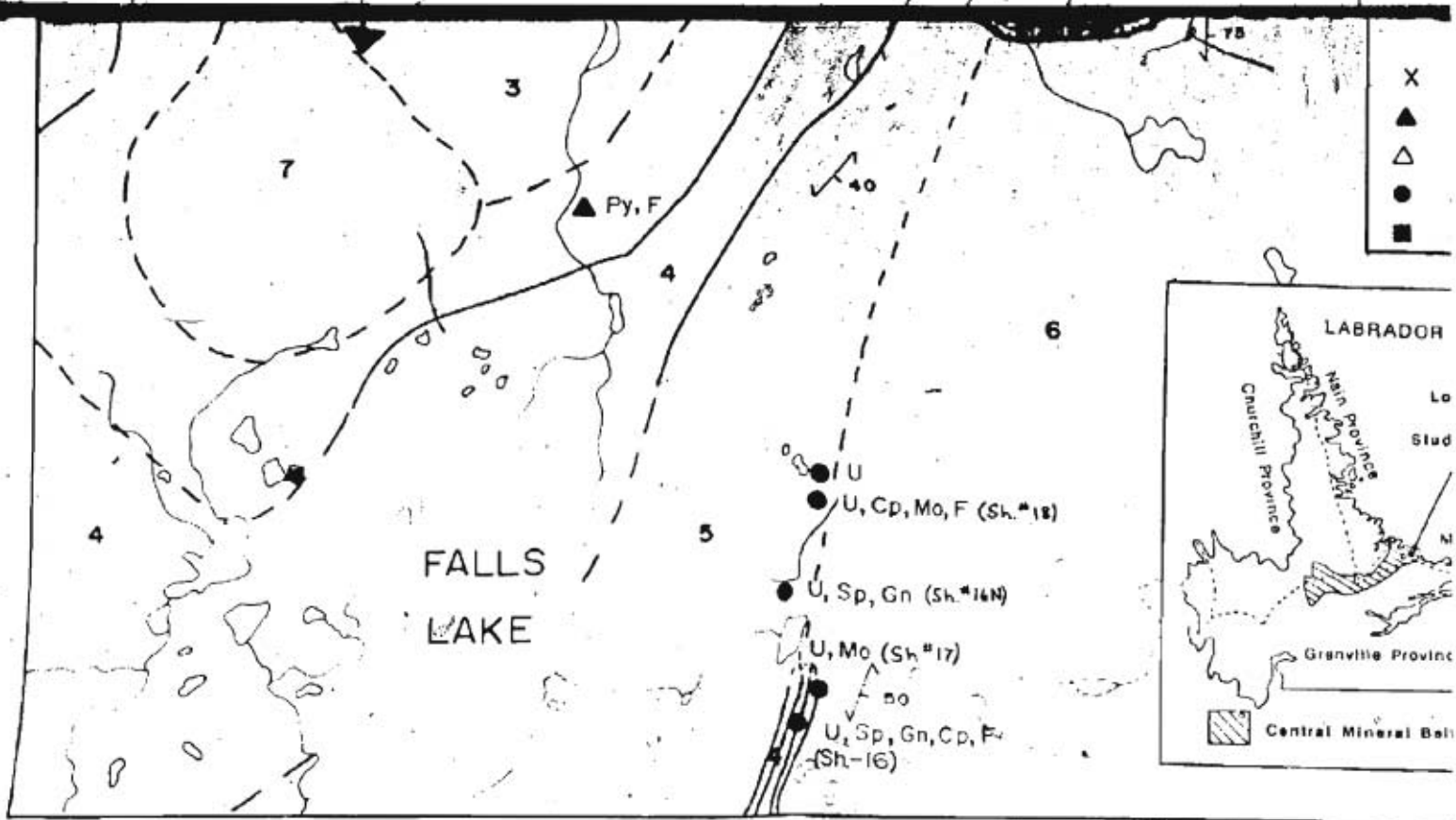
GEOLOGICAL CROSS—SECTION OF THE ROU

300 m

ROUND POND

HORIZONTAL SCALE = MAP SCALE

## MINERAL OCCURRENCE TYPES

| | | |
|---|---|---|
| X | . . . . . . . . | pyritiferous gossan |
| ▲ | . . . . . . . . | hydrothermal vein |
| △ | . . . . . . . | pegmatitic, aplitic, granitic veins |
| ● | . . . . . . . | hematized radioactive zone |
| ■ | . . . . . . . | carbonate vein-hosted |

64-5    Site and number

RADOR

Location of Study Area

Makkovik Province

e Province

neral Belt

# GEOLOGICAL MAP
# OF THE ROUND POND AREA,
# MAKKOVIK, LABRADOR

Scale        1:25,000

0        1        2        3 km

DATE : March, 1988        BY: C. S. MacDOUGALL

## MAP I

A'

300 m

8        3        2  4        6

5

O

E

ROUND POND AREA